



Publicly Accessible Penn Dissertations


Summer 8-13-2010

The Role of 15-Lipoxygenase-1- and Cyclooxygenase-2-Derived Lipid Mediators in Endothelial Cell Proliferation

Cong Wei

University of Pennsylvania, congwei@mail.med.upenn.edu

Follow this and additional works at: <http://repository.upenn.edu/edissertations>

 Part of the [Medicinal Chemistry and Pharmaceutics Commons](#), and the [Pharmacology Commons](#)

Recommended Citation

Wei, Cong, "The Role of 15-Lipoxygenase-1- and Cyclooxygenase-2-Derived Lipid Mediators in Endothelial Cell Proliferation" (2010). *Publicly Accessible Penn Dissertations*. 219.
<http://repository.upenn.edu/edissertations/219>

This paper is posted at ScholarlyCommons. <http://repository.upenn.edu/edissertations/219>
For more information, please contact libraryrepository@pobox.upenn.edu.

The Role of 15-Lipoxygenase-1- and Cyclooxygenase-2-Derived Lipid Mediators in Endothelial Cell Proliferation

Abstract

It is a generally accepted paradigm that there is a direct link between inflammation and tumor progression. During inflammation, there is increased formation of lipid hydroperoxides, mediated either non-enzymatically by reactive oxygen species or enzymatically by lipoxygenases (LOs) or cyclooxygenases (COXs). Lipid hydroperoxides undergo further oxidation into oxo-eicosatetraenoic acids (oxo-ETEs), which are produced and released by cells including macrophages and epithelial cells. Therefore, these oxo-ETEs could potentially mediate biological effects in an autocrine and/or a paracrine manner. In addition, oxo-ETEs conjugate intracellular glutathione (GSH) to form adducts which could serve as biomarkers of oxo-ETE formation.

In this study, a targeted lipidomics approach combined with stable isotope dilution methodology was employed to identify and quantify lipid hydroperoxides and their metabolites formed in 15-LO-expressing mouse macrophage cell line (R15L cells) and COX-2 expressing cell models (RIES cells and Caco-2 cells) as well as in mouse hematocytes and primary human monocytes. 15-Oxo-5,8,11,13-(Z,Z,Z,E)-ETE (15-oxo-ETE) was identified and characterized as a major eicosanoid produced in both mouse and human macrophage 15-LO pathway. 15-Oxo-ETE was shown to be a metabolite of arachidonic acid (AA)-derived 15(S)-hydroxyeicosatetraenoic acid (15(S)-HETE) by 15-hydroxyprostaglandin dehydrogenase (15-PGDH). A novel biological activity of 15-oxo-ETE was revealed, which involved inhibition of human umbilical vein endothelial cell (HUVEC) proliferation by suppressing DNA synthesis, implicating a potential anti-angiogenic role of 15-oxo-ETE.

In addition to 15-oxo-ETE, another AA-derived eicosanoid 11-oxo-5,8,12,14-(Z,Z,E,Z)-eicosatetraenoic acid (11-oxo-ETE), was identified as a major metabolite arising from COX-2-derived from 11(R)-hydroxyl-5,8,12,14-(Z,Z,E,Z)-eicosatetraenoic acid (11(R)-HETE) in both rat (RIES) and human (Caco-2) epithelial cell lines. A specific liquid chromatography-multiple reaction monitoring mass spectrometry (LC-MRM/MS) method revealed that both 11-oxo-ETE and 15-oxo-ETE were secreted in nM concentrations when AA was added to RIES and human Caco-2 cells. Surprisingly, 11(R)-HETE was an excellent substrate for 15-PGDH, with a catalytic efficiency similar to that found for 15(S)-HETE. In addition, it was demonstrated that aspirin significantly stimulated the production of 15(R)-HETE, which was then converted to 15-oxo-ETE by an unknown dehydrogenase (DH). These findings could have significant clinical implications since 15-PGDH is down-regulated during carcinogenesis, which in addition to increasing the pro-proliferative activity of PGE₂ would prevent the formation of anti-proliferative 15-oxo-ETE from 15(S)-HETE. However, the formation of 15-oxo-ETE from 15(R)-HETE after aspirin treatment, through a pathway that does not involve 15-PGDH, could help counteract the increased pro-proliferative activity of PGE₂.

Degree Type

Dissertation

Degree Name

Doctor of Philosophy (PhD)

First Advisor

Dr. Ian A. Blair

Keywords

LIPID MEDIATORS, 15-LIPOXYGENASE-1, CYCLOOXYGENASE-2, ENDOTHELIAL CELL
PROLIFERATION, 15-OXO-EETE, 11-OXO-EETE

Subject Categories

Medicinal Chemistry and Pharmaceutics | Pharmacology

**THE ROLE OF 15-LIPOXYGENASE-1- AND
CYCLOOXYGENASE-2-DERIVED LIPID MEDIATORS IN
ENDOTHELIAL CELL PROLIFERATION**

Cong Wei

A DISSERTATION

In

Pharmacological Sciences

Presented to the Faculties of the University of Pennsylvania

In

Partial Fulfillment of the Requirements for the

Degree of Doctor of Philosophy

2010

Supervisor of Dissertation

Ian A. Blair, Ph.D.
A. N. Richards Professor of Pharmacology

Graduate Group Chairperson

Vladimir R. Muzykantov, M.D., Ph.D.
Associate Professor of Pharmacology and Medicine

Dissertation Committee

Harry Ischiropoulos, Ph.D., Research Professor of Pediatrics and Pharmacology
Ellen Puré, Ph.D., Professor of Pharmacology
George H. Rothblat, Ph.D., Professor of Pediatrics
Alexander Steven Whitehead, Ph.D., Professor of Pharmacology

DEDICATION

On the last day before I came to the United States for my Ph.D. study,

I learned the names of my grandparents.

This thesis is dedicated to them and my beloved parents

Ziqing Wei & Shuzhen Li

Lianren He & Weiben Zhou

and

Ruidong Wei & Xinglin He

ACKNOWLEDGMENTS

I give endless thanks to my thesis advisor and mentor Dr. Ian A. Blair, who has provided me with tremendous inspiration, guidance, and support. His wisdom, generosity and scientific knowledge have been instilled into my Ph.D. journey to make it an extremely great experience, and will continuously boost my motivation in my future career.

I would like to thank all the past and current members of Blair lab for their advice, support and friendship over the years. I owe particular thanks to Drs. Wenying Jian, Seon Hwa Lee, and Peijuan Zhu who have brought me and trained me in the field of biomarkers and LC-MS since the very beginning. I am especially grateful to Drs. Suhong Zhang and Jasbir Arora who have generously provided their expertise to help with my studies. I am also grateful to Dr. Clementina Mesaros, with whom I shared with a lot of trouble-shooting on the instruments. I would like to give special thanks to Xiaojing Liu and Catherine Huang who provided generous assistance on the completion of my work. Without all the help and support, my thesis work would not be possible.

I am particularly grateful to my dissertation committee chair Dr. Harry Ischiropoulos, who has provided me with his invaluable insight, suggestions and support since before my preliminary exam. I would like to thank Dr. Ellen Puré and Dr. George Rothblat for being my committee members giving constructive advice and the pleasant research collaborations. I would also like to thank Dr. Steve Whitehead for his time and support through my studies.

I am so grateful to Dr. Tian J. Yang for his generous support to my thesis studies during my internship at Hoffman-La Roche. I would like to thank Dr. Vladimir Muzykantov and Dr. Vladimir Shuvaev for providing important materials as well as their inspiring suggestions for my studies. I would also like to thank Dr. Klaus Kaestner for his training during my laboratory rotation and the ongoing support.

I would like to thank Christine Shwed, Linda LeRoy, Mary Scott and Sarah Squire for their help throughout the years in the Pharmacology Program at Penn.

I have been graced with incredible friendships during my time here, and I am very grateful to all my friends and relatives during my Ph.D. journey. Special thanks go to Dr. Diana Ye and her husband Bruce Au, Dr. Michael Pollack and his wife Judith, Jie Gao and his wife Mei Long, Jiansheng Huang and his wife Qi Wu, Minhao Xue and her husband John McGurk, Stefanie Khartulyari, Dr. Arnaldo Diaz, Dr. Xuan Dai, Dr. Ginny Weibel, Michelle Joshi, Dr. Michelle Kinder, Zhuo Ye, Jing Hu, Yun Wang, Michelle Chang, Hongmei Li, and Mei Liu. Their help, caring about me, sharing ups and downs with me as well as all the fun time together have helped me go through the graduate life more easily.

Last but not least, I am deeply indebted to my parents Ruidong Wei and Xinglin He. Their unconditional love and always being there supporting have led me to the science palace, and made my Ph.D. journey much more meaningful.

ABSTRACT

THE ROLE OF 15-LIPOXYGENASE-1- AND CYCLOOXYGENASE-2-DERIVED LIPID MEDIATORS IN ENDOTHELIAL CELL PROLIFERATION

Cong Wei

Ian A. Blair, Ph.D.

Supervisor of Dissertation

It is a generally accepted paradigm that there is a direct link between inflammation and tumor progression. During inflammation, there is increased formation of lipid hydroperoxides, mediated either non-enzymatically by reactive oxygen species or enzymatically by lipoxygenases (LOs) or cyclooxygenases (COXs). Lipid hydroperoxides undergo further oxidation into oxo-eicosatetraenoic acids (oxo-ETEs), which are produced and released by cells including macrophages and epithelial cells. Therefore, these oxo-ETEs could potentially mediate biological effects in an autocrine and/or a paracrine manner. In addition, oxo-ETEs conjugate intracellular glutathione (GSH) to form adducts which could serve as biomarkers of oxo-ETE formation.

In this study, a targeted lipidomics approach combined with stable isotope dilution methodology was employed to identify and quantify lipid hydroperoxides and their metabolites formed in 15-LO-expressing mouse macrophage cell line (R15L cells) and COX-2 expressing cell models (RIES cells and Caco-2 cells) as well as in mouse hematocytes and primary human monocytes. 15-Oxo-5,8,11,13-(Z,Z,Z,E)-ETE (15-oxo-ETE) was identified and characterized as a major eicosanoid produced in both mouse and

human macrophage 15-LO pathway. 15-Oxo-ETE was shown to be a metabolite of arachidonic acid (AA)-derived 15(*S*)-hydroxyeicosatetraenoic acid (15(*S*)-HETE) by 15-hydroxyprostaglandin dehydrogenase (15-PGDH). A novel biological activity of 15-oxo-ETE was revealed, which involved inhibition of human umbilical vein endothelial cell (HUVEC) proliferation by suppressing DNA synthesis, implicating a potential anti-angiogenic role of 15-oxo-ETE.

In addition to 15-oxo-ETE, another AA-derived eicosanoid 11-oxo-5,8,12,14-(*Z,Z,E,Z*)-eicosatetraenoic acid (11-oxo-ETE), was identified as a major metabolite arising from COX-2-derived from 11(*R*)-hydroxyl-5,8,12,14-(*Z,Z,E,Z*)-eicosatetraenoic acid (11(*R*)-HETE) in both rat (RIES) and human (Caco-2) epithelial cell lines. A specific liquid chromatography-multiple reaction monitoring mass spectrometry (LC-MRM/MS) method revealed that both 11-oxo-ETE and 15-oxo-ETE were secreted in nM concentrations when AA was added to RIES and human Caco-2 cells. Surprisingly, 11(*R*)-HETE was an excellent substrate for 15-PGDH, with a catalytic efficiency similar to that found for 15(*S*)-HETE. In addition, it was demonstrated that aspirin significantly stimulated the production of 15(*R*)-HETE, which was then converted to 15-oxo-ETE by an unknown dehydrogenase (DH). These findings could have significant clinical implications since 15-PGDH is down-regulated during carcinogenesis, which in addition to increasing the pro-proliferative activity of PGE₂ would prevent the formation of anti-proliferative 15-oxo-ETE from 15(*S*)-HETE. However, the formation of 15-oxo-ETE from 15(*R*)-HETE after aspirin treatment, through a pathway that does not involve 15-PGDH, could help counteract the increased pro-proliferative activity of PGE₂.

TABLE OF CONTENTS

Title page.....	i
Dedication.....	ii
Acknowledgment.....	iii
Abstract.....	v
Table of Contents	vii
List of Figures	xiv
List of Schemes	xvii
Abbreviations.....	xviii
Chapter 1. General Introduction	
1.1 Lipid Peroxidation.....	1
1.1.1 LO–Mediated Lipid Peroxidation.....	1
1.1.2 COX–Mediated Lipid Peroxidation.....	4
1.1.3 ROS-Mediated Lipid Peroxidation.....	5
1.2 Eicosanoid Formation.....	6
1.2.1 Biosynthesis and Metabolism of Eicosanoids.....	7
1.2.2 Eicosanoids as Mediators of Cell Signaling.....	10
1.2.2.1 Modulation of Cell Proliferation by Eicosanoids.....	12
1.2.2.2 Modulation Mechanisms of Cell Proliferation by Eicosanoids.....	13
1.3 GSH and Lipid Peroxidation-Derived Eicosanoids.....	17
1.3.1 GSH Homeostasis.....	17
1.3.2 GSTs and Other GSH-adducts Metabolizing Enzymes	22
1.3.3 GSH-adducts Transporters.....	23

1.3.4 Biological Effect of GSH-adducts.....	24
1.4. Lipid Peroxidation-Derived Eicosanoids and Disease.....	26
1.4.1 Cancer Angiogenesis.....	26
1.4.2 Cancer.....	28
1.4.3 Cardiovascular Disease	30
1.5 Lipid Peroxidation Products as Biomarkers of Oxidative Stress.....	32
1.6 Scope of Thesis Research	35
Chapter 2. 15-Oxo-Eicosatetraenoic Acid, a Metabolite of Macrophage 15-	
 Hydroxyprostaglandin Dehydrogenase That Inhibits Endothelial Cell	
 Proliferation	
2.1 Abstract.....	37
2.2 Introduction.....	38
2.3 Materials and Methods	41
2.3.1 Materials	41
2.3.2 Mass Spectrometry.....	42
2.3.3 Liquid Chromatography.....	43
2.3.4 Cell Culture	43
2.3.5 AA or CI Treatment of Primary Human Monocyte.....	44
2.3.6 AA Treatment of R15L and RMock Cells.....	45
2.3.7 CI Treatment of R15L Cells	45
2.3.8 Quantitative Analyses of Eicosanoids from AA or CI Treated Primary Human Monocytes	46

2.3.9 Quantitative Analyses of Eicosanoids from Ionomycin- or AA-Treated Whole Bone Marrow (WBM) from 12/15-LO Deficient Mice and Wild-Type Mice ..46	46
2.3.10 AA or CI Treatment of R15L Cells with LO Inhibitor CDC ..46	46
2.3.11 15(<i>S</i>)-HETE or AA Treatment of R15L Cells with 15-PGDH Inhibitor CAY10397.....47	47
2.3.12 Cell Proliferation 5-Bromo-2'-Deoxyuridine (BrdU) Assay.....47	47
2.3.13 Extraction of Intracellular Eicosanoids in HUVECs after Incubation with 15-oxo-EETE 48	48
2.4 Results.....48	48
2.4.1 AA- or CI-Mediated Production of 15(<i>R,S</i>)-HETEs and 15-oxo-EETE in Primary Human Monocytes.....48	48
2.4.2 AA-Mediated Production of 15(<i>R,S</i>)-HETEs and 15-oxo-EETE in R15L Cells.49	49
2.4.3 CI-Mediated Production of 15(<i>R,S</i>)-HETEs and 15-oxo-EETE in R15L Cells...52	52
2.4.4 Effect of CDC on 15-oxo-EETE Production in R15L Cells 52	52
2.4.5 Quantitative Analyses of 15(<i>S</i>)-HETEs and 15-oxo-EETE from Mice Whole Bone Marrow (WBM) by LC-ECAPCI/MS.....53	53
2.4.6 Kinetics of 15(<i>S</i>)-HETE Metabolism to 15-oxo-EETE by R15L Cells.....58	58
2.4.7 Effect of CAY10397 on 15-oxo-EETE and 15(<i>S</i>)-HETE in R15L Cells.....60	60
2.4.8 Effect of 15-oxo-EETE on Proliferation on HUVECs.....61	61
2.4.9 15-oxo-EETE Uptake into HUVECs61	61
2.5 Discussion..... 64	64

Chapter 3. 11-Oxo-Eicosatetraenoic Acid is a Novel Cyclooxygenase-2/15-Hydroxyprostaglandin Dehydrogenase-Derived Endogenous Arachidonic Acid Metabolite

3.1 Abstract.....	73
3.2 Introduction.....	74
3.3 Materials and Methods.....	77
3.3.1 Materials.....	77
3.3.2 Mass Spectrometry.....	78
3.3.3 Liquid Chromatography.....	79
3.3.4 Eicosanoid Analyses.....	81
3.3.5 Synthesis and Purification of 11-oxo-ETE.....	82
3.3.6 Preparation and Purification of 15(<i>S</i>)-HETE and 11(<i>R</i>)-HETE.....	83
3.3.7 Preparation of [¹³ C ₂₀]-15-oxo-ETE.....	84
3.3.8 Preparation of 11-Oxo-ETE-Glutathione-Adduct (OEG).....	84
3.3.9 Cell Culture.....	85
3.3.10 Metabolism of Arachidonic Acid by RIES Cells.....	85
3.3.11 Inhibition of RIES Cell 15-PGDH with CAY10397.....	85
3.3.12 Western Blot Analysis of Caco-2 Cells and HCT-116 cells.....	86
3.3.13 Metabolism of Arachidonic Acid by Caco-2 Cells.....	86
3.3.14 Analysis of 11-Oxo-ETE-Glutathione-Adduct (OEG) and its Cysteinylglycine Metabolite in 11(<i>R,S</i>)-HETE-Treated-RIES Cells.....	87
3.3.15 Incubation of 11(<i>R</i>)-HETE and 15(<i>S</i>)-HETE with 15-PGDH.....	87
3.3.16 Statistical Analyses.....	88

3.4 Results.....	88
3.4.1 LC-MS and MS/MS Analysis of 11-oxo-ETE and 15-oxo-ETE.....	88
3.4.2 Arachidonic Acid-Mediated Formation of HETEs in RIES Cells.....	90
3.4.3 Dose-dependent Effect of CAY10397 on 11-oxo-ETE and 11(<i>R</i>)-HETE in RIES Cells.....	96
3.4.4 Formation of 11-OEG in RIES Cell Culture.....	98
3.4.5 Arachidonic acid-Mediated Formation of HETEs in Caco-2 Cells Analysis.....	99
3.4.6 15-PGDH-Mediated Formation of 11-oxo-ETE and 15-oxo-ETE	102
3.5 Discussion.....	102
 Chapter 4. Novel Aspirin Effect on COX-2-Mediated Formation of 15-Oxo- Eicosatetraenoic Acid and 11-Oxo-Eicosatetraenoic Acid	
4.1 Abstract.....	109
4.2 Introduction.....	110
4.3 Materials and Methods	112
4.3.1 Materials	112
4.3.2 LC-MS Analysis of Eicosanoids.....	113
4.3.3 Cell Culture and Treatment.....	113
4.3.4 AA Treatment of RIES Cells.....	113
4.3.5 AA Treatment of RIES Cells with Aspirin.....	113
4.3.6 15(<i>R</i>)-HETE Treatment of RIES Cells.....	114
4.3.7 15(<i>R</i>)-HETE Treatment of RIES Cells with 11-HSD Inhibitor Carbenoxolone.....	114

4.3.8 AA or 11(<i>R</i>)-HETE Treatment of Caco-2 Cells.....	114
4.4 Results.....	115
4.4.1 Effect of Aspirin on AA-mediated Production of HETEs in RIES Cells.....	115
4.4.2 Kinetics of 15(<i>R, S</i>)-HETE and 15-oxo-ETE Metabolism by RIES Cells and Aspirin-Treated RIES Cells.....	117
4.4.3 Kinetics of 11(<i>R</i>)-HETE and 11-oxo-ETE Metabolism by RIES Cells and Aspirin-Treated RIES Cells.....	119
4.4.4 Kinetics of 15(<i>R</i>)-HETE to 15-oxo-ETE Metabolism by RIES Cells.....	120
4.4.5 Effect of Carbenoxolone on 15(<i>R</i>)-HETE and 15-oxo-ETE in RIES Cells...	122
4.4.6 AA-mediated Production of HETEs in Caco-2 cells.....	123
4.4.7 Kinetic Analysis of 11(<i>R</i>)-HETE to 11-oxo-ETE Metabolism by Caco-2 Cells.....	124
4.5 Discussion	128
Chapter 5. General Discussion and Conclusions	
5.1 Conclusions	134
5.2 Discussion and Future Directions.....	135
Appendix. HPETE-Mediated DNA Damage by Forming DNA-Adducts	
A.1 Background	141
A.2 Experimental Procedure.....	142
A.2.1 Vitamin C-Mediated Decomposition of 11-HPETE, 12-HPETE, and 15-HPETE in the Presence of Calf Thymus DNA.....	142
A.2.2 LC-MS Analysis of HPETE-Mediated DNA-adducts.....	144
A.3 Result and Discussion	145

Bibliography150

LIST OF FIGURES

Figure 2.1	Chemical structures of AA metabolites with similar structural features..	39
Figure 2.2	LC-MRM/MS analysis of 15-LO-derived eicosanoids from primary human monocytes treated with AA and CI.....	50
Figure 2.3	Quantitative analyses of 15-LO-derived eicosanoids from primary human monocytes treated with AA and CI.....	51
Figure 2.4	LC-MRM/MS analysis and quantitation of 15-LO-derived eicosanoids from R15L cells and RMock cells treated with AA.....	54
Figure 2.5	LC-MRM/MS analysis and quantitation of 15-LO-derived eicosanoids from R15L cells treated with CI.....	55
Figure 2.6	Effect of LO inhibitor (CDC) on formation of 15-oxo-ETE and 15(S)-HETE by R15L cells.....	56
Figure 2.7	Quantitative analyses of 15(S)-HETE and 15-oxo-ETE released from ionomycin- or AA-treated whole bone marrow (WBM) from 12/15-LO deficient mice and wild-type mice by LC-ECAPCI/MS	57
Figure 2.8	Kinetics of 15(S)-HETE metabolism by R15L cells.....	59
Figure 2.9	Dose-dependent effects of CAY10397 on the levels of 15-oxo-ETE and 15(S)-HETE released by R15L cells.....	62
Figure 2.10	Effect of 15-oxo-ETE on cell proliferation of HUVECs.....	63
Figure 2.11	15-oxo-ETE uptake into HUVECs.....	64
Figure 2.12	LC-MRM/MS analysis of GSH and cysteinylglycine adducts after incubation of R15L cells with 15-oxo-ETE (30 μ M)	68

Figure 2.13	Formation and action of 15-LO-1-derived eicosanoids in a monocyte/macrophage cell model.....	72
Figure 3.1	The formation of 15-oxo-PGE ₂ from PGE ₂ , 15-oxo-PGD ₂ and 15d-PGJ ₂ from PGD ₂ , and 11-oxo-ETE from 11(<i>R</i>)-HETE.....	75
Figure 3.2	¹ H NMR spectrum for 11-oxo-ETE.....	83
Figure 3.3	MS/MS analyses of 11-oxo-ETE and 15-oxo-ETE.....	89
Figure 3.4	Targeted chiral lipidomics analysis of COX-2 derived AA metabolites from RIES and Caco-2 cells.....	91
Figure 3.5	Kinetics of 11(<i>R</i>)-HETE and 11-oxo-ETE by RIES cells.....	92
Figure 3.6	Western blot analysis of COX-2 in human epithelial colorectal adenocarcinoma cells (HCT-116 and Caco-2).....	93
Figure 3.7	Inhibition of 15-HETE metabolism to 15-oxo-ETE by 15-PGDH inhibitor CAY 10397.....	94
Figure 3.8	Inhibition of 11-HETE metabolism to 11-oxo-ETE by 15-PGDH inhibitor CAY 10397.....	95
Figure 3.9	Dose-dependent effects of CAY 10397 on the levels of 11-oxo-ETE and 11-HETEs released by RIES cells.....	97
Figure 3.10	LC-MS analysis and MS/MS spectrums of the formation of 11-oxo-ETE-GSH adduct (11-OEG).....	100
Figure 3.11	Kinetic plot of the formation of 11-oxo-ETE and 15-oxo-ETE by 15-PGDH.....	101
Figure 3.12	Formation and action of COX-2-derived eicosanoids in epithelial cell models.....	107

Figure 4.1	LC-MRM/MS analysis of 15(<i>R,S</i>)-HETE and 15-oxo-ETE derived from AA in RIES cells.....	116
Figure 4.2	Kinetics of 15(<i>R, S</i>)-HETE and 15-oxo-ETE by RIES cells.....	118
Figure 4.3	Kinetics of 11(<i>R</i>)-HETE and 11-oxo-ETE by RIES cells	121
Figure 4.4	Metabolism of 15(<i>R</i>)-HETE to 15-oxo-ETE by RIES cells.....	122
Figure 4.5	Inhibition of 15(<i>R</i>)-HETE metabolism to 15-oxo-ETE by 11-HSD inhibitor carbenoxolone (CBX) in RIES cells.....	125
Figure 4.6	Metabolism of AA to 11(<i>R,S</i>)-HETE and 11-oxo-ETE by Caco-2 cells.....	127
Figure 4.7	Kinetics of 11(<i>R, S</i>)-HETE and 11-oxo-ETE by Caco-2 cells	128
Figure 4.8	Formation of eicosanoids and inhibition of endothelial proliferation by aspirin-treated COX-2 in epithelial cell models.....	132
Figure A.1	HPETE-mediated DNA damage... ..	141
Figure A.2	LC-MS analysis of HPETE-mediated DNA-adducts	142
Figure A.3	Quantitative analysis of DNA-adducts formed from 11-, 12- and 15-HPETE	145
Figure A.4	The potential role of COX-2-derived eicosanoids in mutagenesis and proliferation.....	149

LIST OF SCHEMES

Scheme 1.1	Lipid peroxidation pathways.....	2
Scheme 1.2	Formation of lipid peroxidation-mediated endogenous DNA adducts....	11
Scheme 1.3	Action of 15d-PGJ2 on receptor-dependent and receptor-independent targets.....	16
Scheme 1.4	Metabolism of 15-oxo-ETE to 15-oxo-ETE-GSH (OEG) and 15-oxo-ETE–cysteinylglycine adducts.....	18
Scheme 1.5	GSH/GSSG homeostasis.....	19
Scheme 1.6	Cellular GSH-adduct transport and metabolism	22
Scheme 1.7	Formation of eicosanoids and eicosanoid-derived GSH-adducts.....	25
Scheme 5.1	Further proposed mechanisms of oxo-ETEs on the inhibition of EC proliferation	139
Scheme 5.2	Oxo-ETE family and their GSH-adducts.....	140

ABBREVIATIONS

5-LO	5-lipoxygenase
5-oxo-ETE	5-oxo-eicosatetraenoic acid
5(<i>S</i>)-HPETE	5(<i>S</i>)-hydroperoxy-6,8,11,14-(<i>E,Z,Z,Z</i>)-eicosatetraenoic acid
9(<i>R</i>)-HPODE	9(<i>R</i>)-hydroperoxy-10, 12-(<i>E,Z</i>)-octadecadienoic acid
11-HETE	11-hydroxy-5,8,12,13-(<i>Z,Z,E,Z</i>)-eicosatetraenoic acid
11-HPETE	11-hydroperoxy-5,8,12,13-(<i>Z,Z,E,Z</i>)-eicosatetraenoic acid
11-oxo-ETE	11-oxo-5,8,12,13-(<i>Z,Z,E,Z</i>)-eicosatetraenoic acid
12-LO	12-lipoxygenase
12(<i>S</i>)-HPETE	12(<i>S</i>)-hydroperoxy-5,8,10,13-(<i>Z,Z,Z,Z</i>)-eicosatetraenoic acid
13(<i>S</i>)-HPODE	13(<i>S</i>)-hydroperoxy-9,11-(<i>Z,E</i>)-octadecadienoic acid
15d-PGJ ₂	15-deoxy- $\Delta^{12,14}$ -prostaglandin J ₂
15-HETE	15-hydroxy-5,8,11,13-(<i>Z,Z,Z,E</i>)-eicosatetraenoic acid
15-HPETE	15-hydroperoxy-5,8,11,13-(<i>Z,Z,Z,E</i>)-eicosatetraenoic acid
15-LO-1	15-lipoxygenase-1
15-oxo-ETE	15-oxo-5,8,11,13-(<i>Z,Z,Z,E</i>)-eicosatetraenoic acid
A-23187	calcimycin
AA	arachidonic acid
ABC	ATP-binding cassette
ACN	acetonitrile
ADH	alcohol dehydrogenase
AKR	aldo-keto reductase
ALDH	aldehyde dehydrogenase

APCI	atmospheric pressure chemical ionization
ARE	antioxidant response element
ATCC	American Type Culture Collection
ATP	adenosine triphosphate
AUC	area under the concentration-time curve
BrdU	5-bromo-2-deoxyuridine
CAY10397	5-[[4-(ethoxycarbonyl)phenyl]azo]-2-hydroxy-benzeneacetic acid
CBX	carbenoxolone
CDC	cinnamyl-3,4-dihydroxy- α -cyanocinnamate
CFTR	cystic fibrosis transmembrane conductance regulator
CI	calcium ionophore
CID	Collision-induced dissociation
COX	cyclooxygenase
cPLA ₂	cytosolic phospholipase A ₂
Cys	cysteine
CysLTs	cysteinyl leukotrienes
d	doublet
DH	dehydrogenase
DIPE	diisopropylethylamine
DMEM	Dulbecco's minimal essential medium
DP	dipeptidase
EC	endothelial cells
ECAPCI	electron capture atmospheric pressure chemical ionization

EDE	4,5-epoxy-2(<i>E</i>)-decenal
EDTA	ethylenediaminetetraacetic acid
EGF	epidermal growth factor
EGFR	epidermal growth factor receptor
ELISA	enzyme-linked immunosorbent assay
EMEM	Eagle's minimal essential medium
ESI	electrospray
FBS	fetal bovine serum
FLAP	5-lipoxygenase activating protein
GC	gas chromatography
GCL	glutamate-cysteine ligase
GGT	γ -glutamyltranspeptidase
GR	glutathione reductase
GS	glutathione synthetase
GSH	glutathione
GSHPx	glutathione peroxidase
GSSG	glutathione disulfide
GST	glutathione-S-transferases
GSX	glutathione conjugate
H- ϵ dAdo	heptanone-1, <i>N</i> ⁶ -etheno-2'-deoxyadenosine
H- ϵ dCyd	heptanone-3, <i>N</i> ⁴ -etheno-2'-deoxycytidine
H- ϵ dGuo	heptanone-1, <i>N</i> ² -etheno-2'-deoxyguanosine
HETE	hydroxy-eicosatetraenoic acid

HNE	4-hydroxy-2(<i>E</i>)-nonenal
¹ H NMR	proton nuclear magnetic resonance
HODE	hydroxyl-octadecadenoic acid
HPETE	hydroperoxy-eicosatetraenoic acid
HPLC	high performance liquid chromatography
HPNE	4-hydroperoxy-2-nonenal
HRMS	high-resolution mass spectrometry
HUVEC	human umbilical vein endothelial cell
ICAM-1	intercellular adhesion molecule-1
IKK	I κ B kinase
IL	interleukin
IsoPs	isoprostanes
JNK	c-Jun N-terminal kinases
k	pseudo-first order rate constant
LA	linoleic acid
LC	liquid chromatography
LDL	low-density lipoprotein
LO	lipoxygenase
LT	leukotriene
LTA ₄	leukotriene A ₄
LTB ₄	leukotriene B ₄
LTC ₄	leukotriene C ₄
MALDI	matrix-assisted laser desorption ionization

MAPEG	membrane-associated proteins in eicosanoid and glutathione
MAPK	mitogen-activated protein kinase
MDA	malondialdehyde
MH ⁺	protonated molecule
MOPS	morpholinopropanesulfonic acid
MRM	multiple reaction monitoring
MRP	multidrug resistance protein
MS	mass spectrometry
MS ⁿ	multiple tandem mass spectrometry
NAC	<i>N</i> -Acetyl-cysteine
NAD ⁺	β-nicotinamide adenine dinucleotide hydrate
NAT	<i>N</i> -acetyl transferase
NF-κB	nuclear-factor kappaB
NMR	nuclear magnetic resonance
NSAID	non-steroid anti-inflammatory drug
OEC	oxo-ETE-cysteinylglycine-adduct
OEG	oxo-ETE-glutathione adduct
ONA	4-oxononanal
ONE	4-oxo-2(<i>E</i>)-nonenal
OATP	organic anion transporter polypeptide
oxLDL	oxidized low-density lipoprotein
PARP	poly(ADP-ribose) polymerase
PBS	phosphate buffered saline

PDGF	platelet-derived growth factor
PFB	2,3,4,5,6-pentafluorobenzyl
PFB-Br	2,3,4,5,6-pentafluorobenzyl bromide
PG	prostaglandin
PGDH	hydroxyprostaglandin dehydrogenase
Pgp	P-glycoprotein
PLA ₂	phospholipase A ₂
PPAR	peroxisome proliferator-activated receptor
PUFA	polyunsaturated fatty acid
R15L	mouse macrophage RAW cells stably expressing human 15-LO-1
RIES cells	rat intestinal epithelial cells stably expressing COX-2
RMock	mouse macrophage RAW cells transfected with the pcDNA3 plasmid
ROS	reactive oxygen species
rt	retention time
s	singlet
SRM	selected reaction monitoring
Stat	signal transducer and activator of transcription
t _{1/2}	half-life
TFA	trifluoroacetic acid
TGF-β	transforming growth factor β
TIC	total ion current
TXA ₂	thromboxane A ₂

VCAM-1

vascular cell adhesion molecule-1

CHAPTER 1

General Introduction

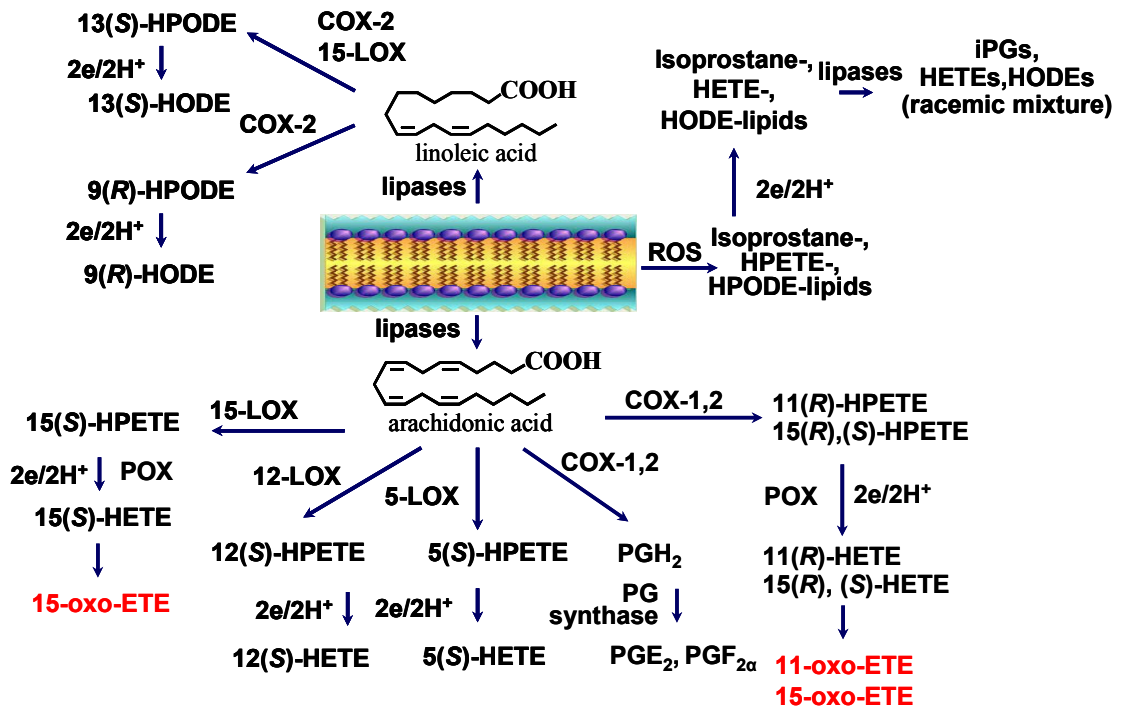
1.1 Lipid Peroxidation

Many diseases such as cancer, cardiovascular diseases, diabetes and neurodegenerative diseases are associated with cellular oxidative stress as an important pathological process (Ames et al., 1993). During oxidative stress, there is increased production of reactive oxygen species (ROS). Up-regulation of cyclooxygenases (COXs) and lipoxygenases (LOs) is also observed (Farrow and Evers, 2002; Tanabe and Tohnai, 2002; Jang and Surh, 2005; Pathak et al., 2005). All of these three pathways are involved in the formation of lipid hydroperoxides that play pivotal roles in pathological processes.

Polyunsaturated fatty acid (PUFAs) such as AA and linonic acid (LA) are present in many esterified lipid classes. Free AA and LA can be released from esterified lipid pools by the action of specific lipases. AA and LA, as free fatty acids or as esterified lipids, can be oxidized to lipid hydroperoxides either enzymatically by COXs (Blair, 2008) and LOs (Jian et al., 2009) or non-enzymatically by the action of ROS (Porter et al., 1995) (Scheme 1.1).

1.1.1 LO-Mediated Lipid Peroxidation

LOs are non-heme iron-containing enzymes that catalyze the stereospecific insertion of molecular oxygen into PUFAs to form lipid hydroperoxides (Brash, 1999). In the case of mammals, the preferred substrate is most often AA, and the product is hydroperoxyeicosatetraenoic acid (HPETE). HPETEs are subsequently reduced by glutathione peroxidase (GSH POX) and/or glutathione-*S*-transferases (GSTs) into the



Scheme 1.1 Lipid peroxidation pathways.

corresponding HETEs (Cohen and Hochstein, 1963). The LOs are classified with respect to their positional specificity of AA oxygenation into 5-, 12- and 15-LOs (Bryant et al., 1982; Brash, 1999).

5-LO is the enzyme responsible for converting AA into leukotrienes (LTs), which are potent inflammatory mediators (Chen and Funk, 2001). It is expressed mainly in inflammatory cells such as polymorphonuclear leukocytes, macrophages and mast cells (Werz, 2002). In resting cells, 5-LO is localized in the cytoplasm and upon stimulation of the cells (e.g. by increases in calcium concentration), 5-LO translocates to the outside of the nuclear envelope (Woods et al., 1993). Meanwhile cytosolic phospholipase A₂ (cPLA₂) releases AA from phospholipids on the membrane (Six and Dennis, 2000). 5-LO activating protein (FLAP), which located on the nuclear envelope serves as a substrate presenter to provide the AA to 5-LO. 5-LO stereoselectively converts AA into 5(*S*)-hydroperoxy-6,8,11,14-(*E,Z,Z,Z*)-eicosatetraenoic acid [5(*S*)-HPETE], which is further metabolized into LTA₄ and other LTs.

In contrast to 5-LOs, which strongly prefer free AA as substrate (Jian et al., 2009), mammalian 15-LOs are capable of oxygenating both free and esterified PUFAs (Chaitidis et al., 1998; Kuhn et al., 2002; Kuhn and O'Donnell, 2006). 15-LO can also oxygenate even more complex lipid protein assemblies such as biomembranes (Kuhn and Borchert, 2002) and lipoproteins (Belkner et al., 1993; Brinckmann et al., 1998). Type 1 human 15-LO (15-LO-1), mainly expressed by reticulocytes, eosinophils and macrophages, is the enzyme responsible for converting AA to 15(*S*)-hydroperoxy-5,8,11,13-(*Z,Z,Z,E*)-eicosatetraenoic acid [15(*S*)-HPETE] and a small amount of 12(*S*)-hydroperoxy-5,8,10,13-(*Z,Z,E,Z*)-eicosatetraenoic acid [12(*S*)-HPETE] (Bryant et al.,

1982). Type 2 15-LO (15-LO-2), which is mainly expressed in prostate, lung, skin and cornea, converts AA into 15(*S*)-HPETE (Hsi et al., 2002), which is subsequently reduced into the corresponding alcohol, 15(*S*)-HETE. LA can also serve as a substrate for 15-LO to produce 13(*S*)-hydroperoxy-9,11-(*Z,E*)-octadecadienoic acid [13(*S*)-HPODE] (Kamitani et al., 1998; Blair, 2008), which is subsequently reduced to the corresponding hydroxyoctadecadenoic acid [13(*S*)-HODE].

Several isoforms of 12-LOs have been characterized, including human platelet-type 12-LO, human leukocyte-type 12-LO and epithelial type 12-LO, all of which produce 12(*S*)-HPETE, which is subsequently reduced to 12(*S*)-HETE (Shannon et al., 1993; Rioux and Castonguay, 1998; Raso et al., 2004; Kinder et al., 2010).

1.1.2 COX–Mediated Lipid Peroxidation

There are three COX isoforms: COX-1, 2 and 3. COX-1 is constitutively expressed in nearly all tissues in the body and plays a housekeeping role in normal physiological process by producing prostaglandins (PGs) and thromboxane A₂ (TXA₂). Besides PGs and TXA₂, it also produces 11(*R*)-hydroperoxy-5,8,12,13-(*Z,Z,E,Z*)-eicosatetraenoic acid [11(*R*)-HPETE], 15(*R*)-HPETE (30 %) and 15(*S*)-HPETE (70 %) (Hecker et al., 1987). COX-2 is inducible by various cytokines, growth factors, shear stress, inflammation mediators and tumor promoters (Williams and DuBois, 1996; Smyth et al., 2009). It is the more important source of PG and other eicosanoid formation than COX-1 in inflammation and perhaps cancer (Smyth et al., 2009). AA is converted by COX-2 into PGs, 11(*R*)-HPETE and 15(*S*)-HPETE (Bonazzi et al., 2000; Thuresson et al., 2002; Lee et al., 2007). Recently, AA was shown to produce an enantiometric excess of 33% 15(*S*)-HETE by COX-2 compared with 15(*R*)-HETE (Lee et al., 2007). LA is

metabolized by COX-2 into 9(*R*)-hydroperoxy-10,12-(*E,Z*)-octadecadienoic acid [9(*R*)-HPODE] (52 %), 9(*S*)-HPODE (11 %), 13(*R*)-HPODE (35 %), and 13(*S*)-HPODE (2 %) (Hamberg, 1998). Bioactive lipid mediators are increasingly being recognized as important endogenous regulators of angiogenesis (Gonzalez-Periz and Claria, 2007; Marks et al., 2007; Kim and Surh, 2008). One of the major cascades of the bioactive lipid mediators production involves the release of AA from membrane phospholipids followed by COX-2-mediated formation of eicosanoids (Lee et al., 2007). COX-3 is an alternatively spliced variant of COX-1 found in canine cerebral cortex (Chandrasekharan et al., 2002). Its function is still unresolved.

1.1.3 ROS–Mediated Lipid Peroxidation

ROS, including superoxide radical anion ($\bullet\text{O}_2^-$), hydrogen peroxide and hydroxyl radical are generated constantly in biological processes, such as normal mitochondrial aerobic respiration, phagocytosis of bacteria or virus-infected cells, peroxisomal-mediated degradation of fatty acids and cytochrome P450-mediated metabolism (Ames et al., 1993). During mitochondria respiration, the free radical intermediate of coenzyme Q can transfer one electron to an oxygen molecule to produce $\bullet\text{O}_2^-$ (Turrens, 1997). Previous *in vitro* studies showed that 1-2% of total consumed oxygen is converted to $\bullet\text{O}_2^-$ by mitochondria (Boveris and Chance, 1973). The $\bullet\text{O}_2^-$ can undergo a 1-electron reduction to give rise to hydrogen peroxide (Boveris and Chance, 1973). Besides mitochondria, there are other sources of ROS (Forman and Torres, 2001). During phagocytosis of bacteria or virus-infected cells, nicotinamide adenine dinucleotide phosphate (NADPH) oxidase can catalyze the reduction of molecular oxygen to $\bullet\text{O}_2^-$ (Forman and Torres, 2001). A body of evidence has emerged to suggest that non-

phagocyte NADPH oxidase also produces ROS as second messengers to regulate cell signaling (Forman and Torres, 2001). In addition, myeloperoxidase converts hydrogen peroxide to hypochlorous acid during neutrophil phagocytosis to help kill bacteria (Hampton et al., 1998).

ROS are normally detoxified by antioxidant defense systems including enzymatic systems such as superoxide dismutase, catalase and GSH POX; and small molecule antioxidants such as vitamin E, β -carotene, and glutathione (GSH) (Di Mascio et al., 1991). Under pathological conditions such as inflammation, infection, radiation or metabolism of hormones (estrogens), drugs (etoposides) and environmental toxins (polycyclic aromatic hydrocarbons), increased production of ROS overwhelms the cellular protection systems and causes damage to cellular components such as lipids (Ischiropoulos et al., 1992; Stamler et al., 1992; McCoull et al., 1999; Bolton et al., 2000; Lovett et al., 2001). Fatty acids within phospholipids can be oxidized *in situ* into different regioisomers and enantiomers of HPETEs, HPODEs and isoprostanes (IsoPs), which are autooxidation products of AA (Morrow et al., 1992; Spiteller, 2001). These products are reduced and then released by lipases to give rise to a racemic mixture of HETEs, HODEs and IsoPs. In contrast to the LO and COX pathways, ROS-mediated lipid peroxidation has no stereoselectivity or enantioselectivity.

1.2 Eicosanoid Formation

PGs, prostacyclins, thromboxanes, LTs and HETEs are all considered to be eicosanoids. They are involved in complex signaling pathways involved in normal and pathophysiological biological processes including inflammation. Eicosanoids are derived from either omega-3 (ω -3) or omega-6 (ω -6) essential fatty acids. The amounts and

balance of these lipid derivatives will affect numerous signaling pathways *in vivo*. Anti-inflammatory drugs such as aspirin and other non-steroid anti-inflammatory drugs (NSAIDs) act by inhibiting eicosanoid synthesis.

1.2.1 Biosynthesis and Metabolism of Eicosanoids

Eicosanoids are not stored within cells, but are synthesized as required (Funk, 2001). They are derived from the fatty acids that make up the cell membrane and nuclear membrane (Funk, 2001). Increased intracellular calcium triggers the release of a phospholipase at the cell membrane. The phospholipase travels to the nuclear membrane or the nearby cell membrane where it catalyzes ester hydrolysis of the phospholipid (by cPLA₂) or diacylglycerol (by phospholipase C) (Funk, 2001). This releases a 20-carbon essential fatty acid such as AA, and this hydrolysis appears to be the rate-determining step for eicosanoid formation. The fatty acids may be released by any of several phospholipases, among which type IV cytosolic phospholipase A₂ (cPLA₂) is the key actor, as cells lacking cPLA₂ are generally devoid of eicosanoid synthesis (Funk, 2001). The phospholipase cPLA₂ is specific for phospholipids that contain AA, eicosapentaenoic acid (EPA, 20:5, ω -3) or dihomo-gamma-linolenic acid (DGLA, 20:3, ω -6) at the SN₂ position.

At the endoplasmic reticulum (ER) and nuclear membrane, arachidonic acid released by cPLA₂ is presented to prostaglandin H synthase (PGHS; referred to colloquially as COX for cyclooxygenase) and is then metabolized to an intermediate prostaglandin PGH₂. PGHS exists as two isoforms referred to as PGHS-1 (COX-1) and PGHS-2 (COX-2) (Smith et al., 2000). COX-1 is the enzyme responsible for basal, constitutive prostaglandin synthesis, whereas COX-2 is important in various

inflammatory and “induced” settings. The COX enzymes are monotonically inserted in the ER and nuclear membrane with the substrate binding pocket precisely orientated to take up released arachidonic acid. The crystal structures of COX-1 and COX-2 are remarkably similar, with one notable amino acid difference that leads to a larger “side-pocket” for substrate access in COX-2 (Smith et al., 2000). The coupling of PGH₂ synthesis to metabolism by downstream enzymes is intricately orchestrated in a cell-specific fashion. Thromboxane synthase is found in platelets and macrophages, prostacyclin synthase is found in endothelial cells and prostaglandin F (PGF) synthase in uterus, and two types of PGD synthase are found in brain and mast cells. Microsomal PGE synthase (mPGES), a member of the MAPEG (membrane-associated proteins in eicosanoid and glutathione metabolism) family, is responsible for prostaglandin E₂ (PGE₂) synthesis (Jakobsson et al., 1999). Coordinate induction of multiple enzymes in the prostanoid pathway, in particular mPGES and COX-2, in inflammatory settings is a current concept being developed (Mancini et al., 2001). In contrast to PGs, LTs are made predominantly by inflammatory cells like polymorphonuclear leukocytes, macrophages, and mast cells (Funk, 2001). Cellular activation by immune complexes, bacterial peptides, and other stimuli elicit a sequence of events that include cPLA₂ and 5-LO translocations to the nuclear envelope. 5-LO, a nonheme iron dioxygenase, is the key enzyme in this cascade and is located in the nucleus in some cell types and the cytosol of others (Peters-Golden and Brock, 2001). 5-LO possesses a NH₂-terminal domain that binds two calcium ions, similar to the β -sandwich C₂ domains of cPLA₂ and protein kinase C, and a large catalytic domain that binds iron (Hammarberg et al., 2000; Chen

and Funk, 2001). It transforms released arachidonic acid to the epoxide LTA₄ with the concerted efforts of 5-LO-activating protein (FLAP).

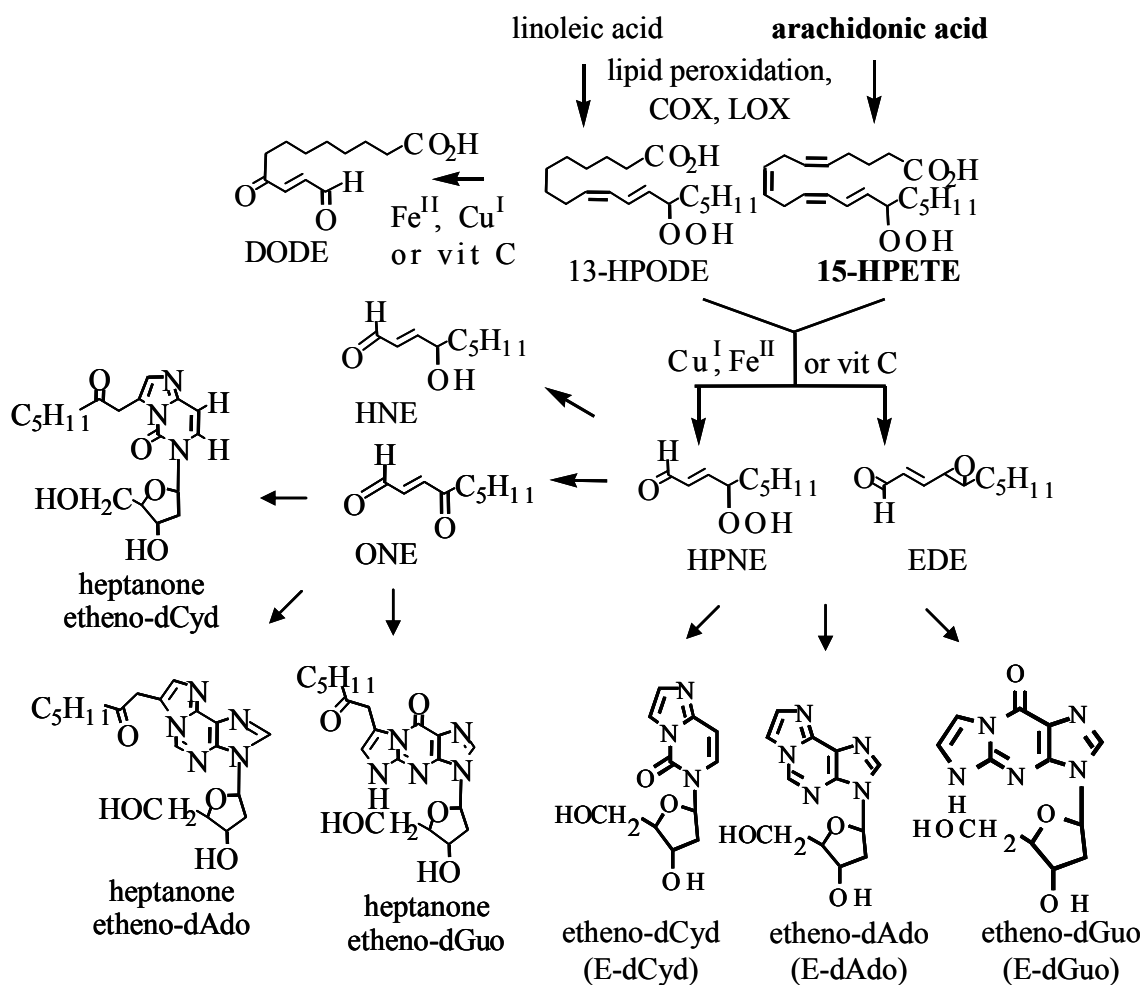
When intracellular calcium concentrations are elevated in macrophages, 15-LO-1 is recruited to the inner side of the plasma membrane of monocytes/macrophages where it converts esterified arachidonic acid to 15(*S*)-HPETE. Esterified 15(*S*)-HPETE is reduced to 15(*S*)-HETE and released as the free acid by cytoplasmic phospholipase A₂. 15(*S*)-HETE could potentially be further oxidized to form 15-oxo-eicosatetraenoic acid (15-oxo-ETE) at the C-15 position (Scheme 1.1). Furthermore, it was demonstrated that upon the action of COX-2, arachidonic acid was converted to 15(*S*)-HPETE and 11(*R*)-HPETE that were further reduced to 15(*S*)-HETE and 11(*R*)-HETE, respectively (Lee et al., 2007). Our group has recently identified 15-oxo-ETE as a metabolite of 15(*S*)-HETE from COX-2-mediated AA metabolism (Lee et al., 2007) (Scheme 1.1). 15-Oxo-ETE was shown to arise from rabbit lung 15-PGDH-mediated oxidation of 15(*S*)-HETE over twenty years ago (Bergholte et al., 1987). However, this interesting arachidonic acid metabolite has remained a pharmacological curiosity for many years.

In addition, lipid hydroperoxides such as 15(*S*)-HPETE also undergo homolytic decomposition that is mediated by one-electron reductants such as transition metal ions or vitamin C (Lee et al., 2001). 13-HPODE, the prototypic ω -6 PUFA-derived lipid hydroperoxide, gives rise to 4,5-epoxy-2(*E*)-decenal (EDE) and 4-hydroperoxy-2-nonenal (HPNE), which is not stable and is rapidly reduced to 4-hydroxy-2(*E*)-nonenal (HNE) or dehydrated to 4-oxo-2(*E*)-nonenal (ONE) (Lee et al., 2000) (Scheme 1.2). 13-HPODE also produces 9,12-dioxo-10(*E*)-decenoic acid (DODE), which unlike the other bifunctional electrophiles, is derived from the α -terminus of the lipid and therefore

contains a carboxyl group (Gallasch and Spiteller, 2000) (Scheme 1.2). They can form DNA-adducts by hydroxyl radical attack on the 2'-deoxyribose DNA backbone (Hecker and Ullrich, 1989; Rashid et al., 1999; Zhou et al., 2005). A recent study by Williams *et al.* on the decomposition of 15(*S*)-HPETE showed that it formed EDE, HPNE, HNE and ONE, but not DODE (Williams et al., 2005) (Scheme 1.2).

1.2.2 Eicosanoids as Mediators of Cell Signaling

Eicosanoids are involved in cell signaling cascades that modulate many cellular functions, such as cell proliferation, inflammation responses, stimulation of adhesion molecules, chemoattractant production, and cell death (Marra et al., 1999; Tanaka et al., 2000; Segui et al., 2004; Kabe et al., 2005; Le Bras et al., 2005). Hydroxyl lipids and oxidized lipids (e. g. oxo-EETE family) as well as some aldehydic decomposition products (e. g. HNE and ONE) are relatively stable and are able to diffuse into or out of cells (Rossi et al., 2000; Straus et al., 2000; Waku et al., 2009). The aldehydes exhibit facile reactivity towards cellular components, and can affect and modulate cellular functions at very low concentrations (Jian et al., 2005).



Scheme 1.2 Formation of lipid peroxidation-mediated endogenous DNA adducts.

1.2.2.1 Modulation of Cell Proliferation by Eicosanoids

Many studies have focused on the potential biological roles of the 15-LO-derived lipid mediators such as 15(*S*)-HPETE and 15(*S*)-HETE which promote recruitment of monocytes to endothelium, a key initial step in atherogenesis (Hedrick et al., 1999). 15(*S*)-HPETE and 15(*S*)-HETE were also shown to inhibit cell proliferation and induce apoptosis such as on chronic myeloid leukemia cell line (K-562) (Mahipal et al., 2007). However, it is not clear whether 15(*S*)-HPETE and 15(*S*)-HETE are the biologically important 15-LO-1 metabolites involved in modulating cell proliferation, monocyte differentiation and macrophage infiltration. One of the 15-oxo-ETE analogs, 5-oxo-ETE, generated by human monocytes, promotes cell survival and acts as a chemo-attractant (Sozzani et al., 1996). The PGD₂ decomposition product, 15-deoxy- $\Delta^{12,14}$ -PGJ₂ (15d-PGJ₂) has unusual properties for a PG – it has anti-inflammatory properties and inhibits cell proliferation, causes apoptosis and induces monocyte differentiation (O'Flaherty et al., 2005).

Biological activities of traditional COX-2-derived PGs have been studied extensively. PGE₂ is well-known for its pro-proliferation/tumorigenic activity, and it is the most abundant PG found in human colorectal cancer (Rigas et al., 1993; Wang et al., 2004). A recent study showed that PGE₂ treatment dramatically increased both small and large intestinal adenoma burden in Apc^{Min/+} mice and significantly enhanced colon carcinogen-induced colon tumor incidence and multiplicity (Kawamori et al., 2003; Wang et al., 2004). Furthermore, PGE₂ protects small intestinal adenomas from NSAID-induced regression in Apc^{Min/+} mice (Hansen-Petrik et al., 2002). The central role of PGE₂ in colorectal tumorigenesis has been further confirmed by evaluating mice with

homozygous deletion of PGE₂ receptors (Watanabe et al., 1999; Sonoshita et al., 2001; Mutoh et al., 2002).

1.2.2.2 Modulation Mechanisms of Cell Proliferation by Eicosanoids

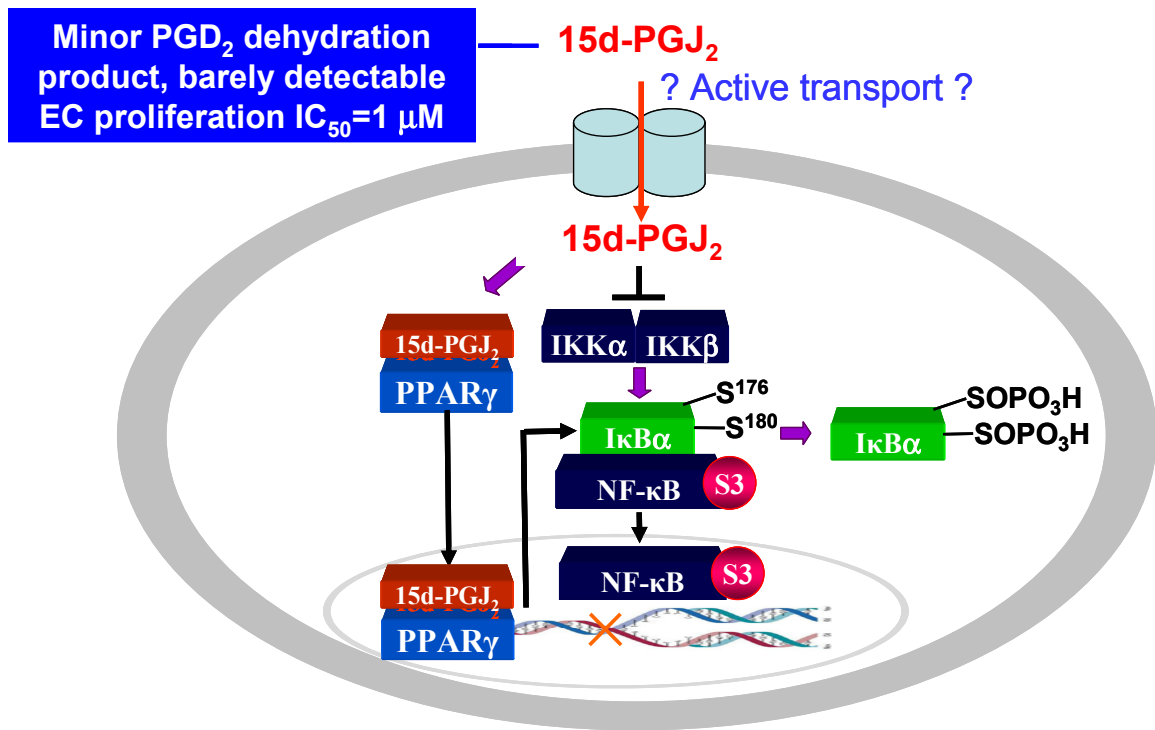
Peroxisomal proliferator-activating receptor- γ (PPAR γ) can be activated by several lipid metabolites, including PUFAs, oxidized fatty acids and nitrated fatty acids (Kliwer et al., 1999; Baker et al., 2005; Schopfer et al., 2005; Itoh et al., 2008; Li et al., 2008). PPAR γ is a member of the nuclear receptor family that has been implicated in cell differentiation and proliferation, glucose metabolism, macrophage development, and inflammatory responses (Limor et al., 2008). Both 5-oxo-ETE and 15d-PGJ₂ are PPAR γ agonists (O'Flaherty et al., 2005). In particular, 15d-PGJ₂ is more potent (Forman et al., 1995; Kliwer et al., 1995; Ricote et al., 1998). 15d-PGJ₂ inhibits cell proliferation and causes apoptosis, which has been ascribed to its ability to potently activate PPAR γ (Scheme 1.3) (O'Flaherty et al., 2005; Waku et al., 2009). Recently, spectroscopic analysis of the binding kinetics of 15d-PGJ₂ to PPAR γ revealed the activating process, which involves two distinct steps, termed “dock and lock”: 15d-PGJ₂ first enters the ligand binding pocket to form a non-covalent intermediate complex (docking step), and subsequently this endogenous fatty acid binds covalently to cysteine (Cys285) in the PPAR γ ligand binding domains (LBD) (Waku et al., 2009). PPAR γ agonists strongly inhibit experimental atherosclerosis and formation of macrophage foam cells (Li et al., 2004). Sharing the similar chemical structure features, the oxo-ETE family members (5, 8, 9, 11, 12 and 15-oxo-ETE) have been shown to exhibit transcriptional activity as covalent bound ligands to PPAR γ (Waku et al., 2009). Moreover, 15(*S*)-HETE (0.1 μ M)

increased the expression of PPAR γ messenger RNA (mRNA) by 50% in human vascular smooth muscle cells (Limor et al., 2008), which could potentially be ascribed to the activity of 15(*S*)-HETE metabolite 15-oxo-ETE.

Furthermore, the oxo-ETE moiety can potentially covalently modify cellular targets such as nuclear factor kappaB (NF- κ B) as well as form adducts with sulfhydryl nucleophiles such as glutathione (GSH) (O'Flaherty et al., 2005). It has been proposed that 15d-PGJ₂ is an endogenous inhibitor of NF- κ B activation, and inhibits cell proliferation by covalently binding in a Michael addition reaction to the thiol residues in I κ B kinase (IKK) or p50 subunit of NF- κ B to block the proteins from performing their survival function, using a PPAR γ independent mechanism (Scheme 1.3) (Rossi et al., 2000; Straus et al., 2000; Cernuda-Morollon et al., 2001; Ward et al., 2002; Scher and Pillinger, 2009). 15d-PGJ₂ modulates the NF- κ B pathway, which plays an important role in gene regulation during inflammation and immune responses. In endothelial cells, 15d-PGJ₂ inhibited CXC chemokine production, stimulates apoptosis and has variable effects on cellular adhesion molecules, such as intercellular adhesion molecule-1 (ICAM-1) (Bishop-Bailey and Hla, 1999; Marx et al., 2000; Chen and Han, 2001). Cellular proteolytic systems, such as the ubiquitin/proteasome system, play an important role in the stress response by removing abnormal proteins (Scher and Pillinger, 2009). 15d-PGJ₂ inhibits the proteasome pathway and causes dysregulation of cellular protein turnover, leading to cell death (Scheme 1.3) (Okada et al., 1999). The activation of NF- κ B, the predominant transcription factor responsible for immune responses, has also been increasingly recognized as the key coordinator of the link between the inflammation and

cancer. More specifically, the signal transduction activates IKK which binds to NF- κ B and keeps it in cytoplasm for not being activated. The α and/or β subunit of IKK complex (IKK α and/or IKK β) phosphorylates I κ B and thus NF- κ B is then released to nucleus for further gene activation. Despite the conflicting functions of NF- κ B in various cell types (either promote or inhibit carcinogenesis), the causative role of NF- κ B in tumorigenesis has been increasingly revealed by both genetic and biochemical evidence (Karin, 2006). NF- κ B is an activator of anti-apoptotic genes. Both in colitis-associated cancer and cholestatic liver cancer, the activation of NF- κ B within pre-neoplastic or progressing cancer cells is the rate-limiting event, which ensures their survival and prevents elimination by pro-apoptotic tumor-surveillance mechanisms.

The similarity in the structures of 5-oxo-EETE, 15d-PGJ₂ and 15-oxo-EETE raises the possibility that 15-oxo-EETE might be a PPAR γ ligand and so it could modulate cell proliferation and apoptosis in a PPAR γ -dependent and/or PPAR γ -independent mechanism (e. g. through NF- κ B pathway). In addition, activation of PPAR γ could lead to monocyte differentiation (Tontonoz et al., 1998). Thus if 15-oxo-EETE is a PPAR γ ligand or it indirectly activates PPAR γ , it might stimulate the differentiation of monocytes and/or other types of cells.



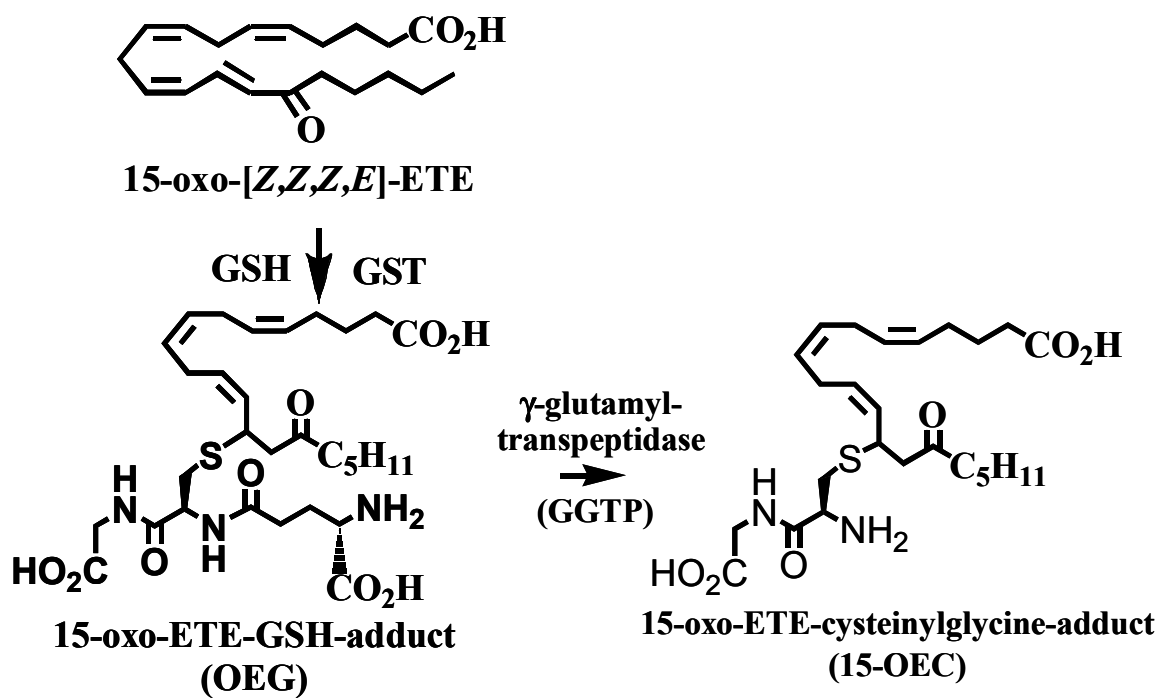
Scheme 1.3 Action of 15d-PGJ₂ on receptor-dependent and receptor-independent targets (modified from Scher JU and Pillinger MH. *J Investig Med.* 2009; 57:703).

1.3 GSH and Lipid Peroxidation-Derived Eicosanoids

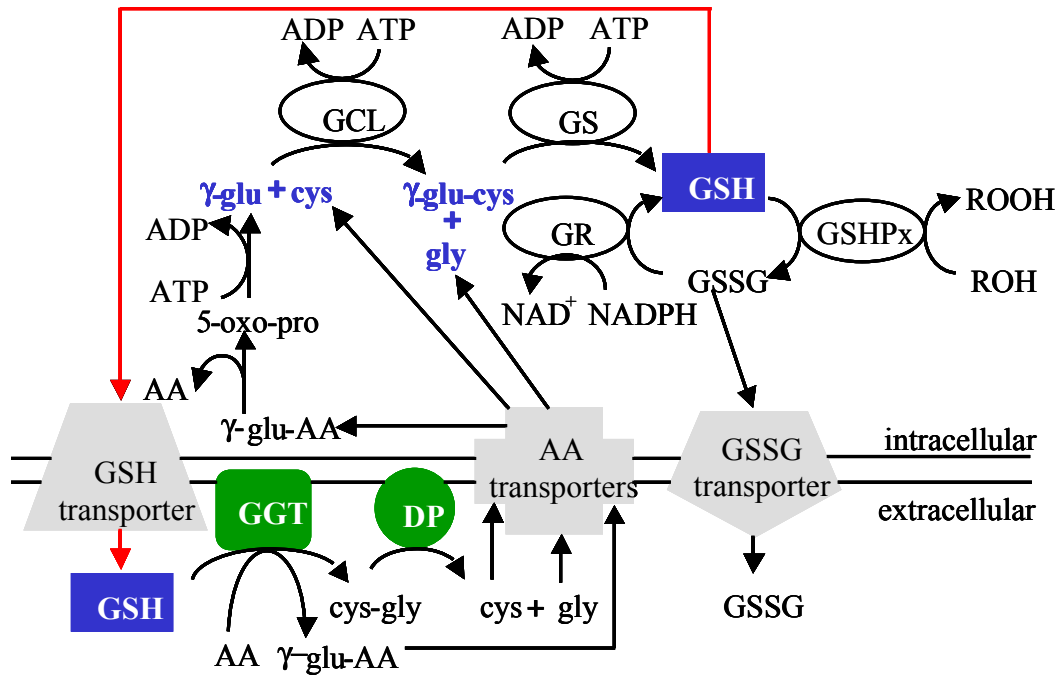
GSH is a tripeptide (γ -L-Glutamyl-L-cysteinylglycine) with the chemical structure (2*S*)-2-amino-5-[[*(2R)*-1-(carboxymethylamino)-1-oxo-3-sulfany]propan-2-yl]amino]-5-oxo-pentanoic acid, and is the most abundant small molecule thiol in cells with concentrations in the millimolar range (Blair, 2006). It plays an essential role in antioxidant defense and in the metabolism of both xenobiotics and endogenous toxins (Blair, 2010). Most of the intracellular GSH (85–90 %) is present in the cytosol at concentrations ranging from 3-4 mM, with the remainder being found in the mitochondria, nuclear matrix, and peroxisomes (Lu, 2000). Beside its role in detoxification, GSH-adducts may exhibit biological activity and/or provide specific biomarkers for specific oxidative stress pathways (Murphy and Zarini, 2002; Blair, 2010). The GSH conjugation pathway is the major route of 5-oxo-ETE and 15-oxo-ETE metabolism pathway in cells (Schemes 1.4 and 1.7) (Lee et al., 2007). Cellular GSH levels were also modulated during bifunctional electrophile administration and this process was involved in apoptosis and other signal transduction pathways (Liu et al., 2000; Ji et al., 2001; Awasthi et al., 2003; Awasthi et al., 2004).

1.3.1 GSH Homeostasis

GSH molecules are in dynamic equilibrium with the extracellular milieu and with cellular organelles (Scheme 1.5) (Dickinson and Forman, 2002). During oxidative stress, reduced GSH is converted to GSSG. In contrast, concentrations of GSSG in mammalian cells are usually two orders of magnitude lower (Schafer and Buettner, 2001). The high



Scheme 1.4 Metabolism of 15-oxo-ETE to 15-oxo-ETE-GSH (OEG) and 15-oxo-ETE-cysteinylglycine (15-OEC) adducts.



Scheme 1.5 GSH/GSSG homeostasis.

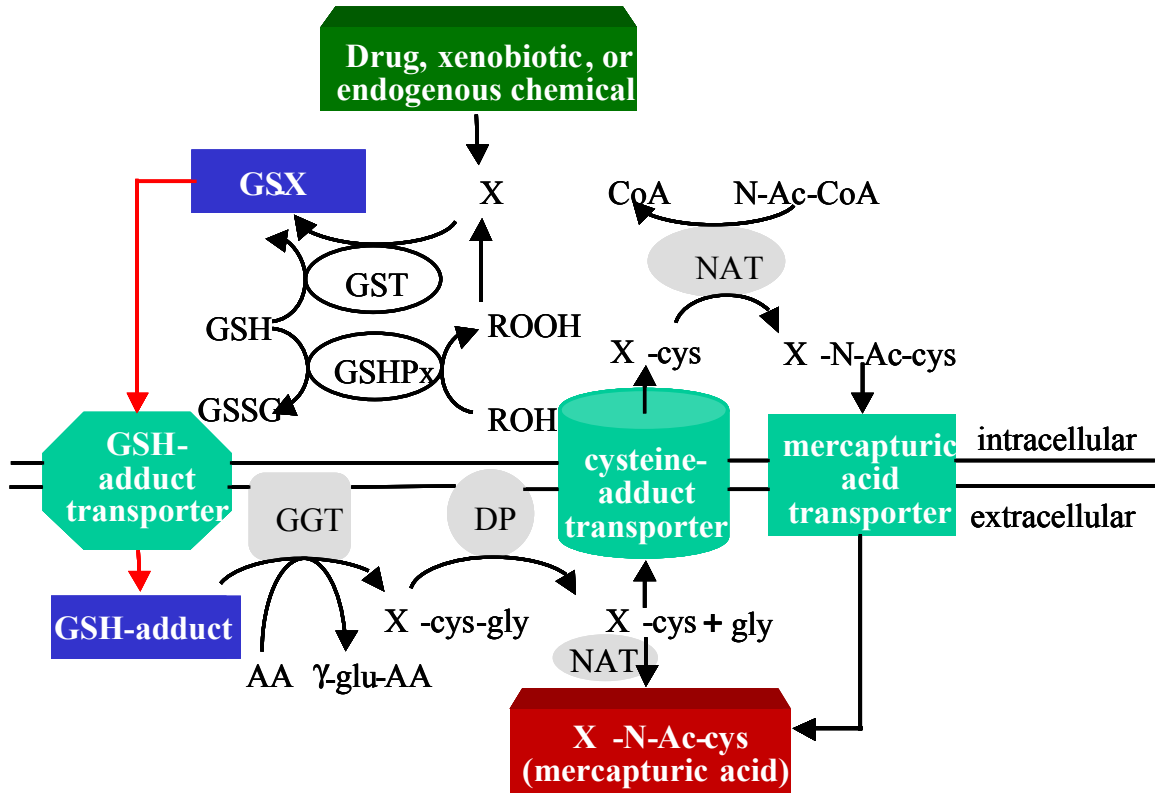
abundance of GSH and low abundance of GSSG helps to maintain cells under a reducing environment and prevents oxidative damage to cellular macromolecules. Hydrogen peroxide and lipid hydroperoxides undergo GSH POX-mediated reduction to water and lipid hydroxides, respectively with GSH providing the reducing equivalents (Arthur, 2000; Blair, 2010). GSH also readily forms adducts with a great variety of both exogenously- and endogenously-derived electrophilic reactive intermediates (Blair, 2006; Doss and Baillie, 2006). Formation of the GSH-adducts is generally facilitated by GSH *S*-transferases (GSTs) and is normally considered to represent a detoxification of the relevant reactive intermediate. GSH/GSSG homeostasis plays an important role in maintaining cellular redox status (Schafer and Buettner, 2001). Changes in the half-cell reduction potential of the 2GSH/GSSG couple correlate with the biological status of the cell (Zhu et al., 2008; Blair, 2010).

GSSG can either be reduced back to GSH at the expense of NADPH by GSH reductase (GR), or it can be excreted from cells by transmembrane multidrug resistance protein (MRP) (Suzuki and Sugiyama, 1998; Homolya et al., 2003). GSH itself can be transported out of cells through the transmembrane GSH transporter (Rappa et al., 1997; Ballatori et al., 2005). In particular, five of the twelve members of the MRP/cystic fibrosis transmembrane conductance regulator (CFTR) family appear to mediate GSH export from cells namely, MRP1, MRP2, MRP4, MRP5, and CFTR (Ballatori et al., 2005; Ritter et al., 2005). GSH can also be utilized to form adducts with various xenobiotics and with endogenous compounds to form mixed GSH-adducts, which are exported out of cells usually by MRPs (Scheme 1.6) (Borst et al., 2000; Kruh et al., 2001; Ritter et al., 2005). Once secreted from cells, GSH, GSSG, and GSH-adducts are partially degraded

by γ -glutamyltranspeptidase (GGT), an enzyme that resides on the extracellular surface of the cell membrane (Griffith et al., 1978; Lieberman et al., 1995; Dalton et al., 2004; Blair, 2010), to yield the γ -glutamyl moiety coupled to another amino acid (usually cystine) and a dipeptide, which is in turn broken down by external dipeptidase (DP) (Scheme 1.6). Different amino acid transporters bring the free amino acids and the γ -glutamyl-amino acid complex back to the cells (Dickinson and Forman, 2002). The γ -glutamyl-cystine is converted to 5-oxoproline, which is then converted to glutamine (Glu). Glu and Cys are conjugated by Glu-Cys ligase (GCL) to form γ -glutamyl-cysteine, which is then conjugated with glycine (Gly) by glutathione synthetase (GS) (Dickinson and Forman, 2002; Dalton et al., 2004). Both steps of the conjugation require ATP.

GGT plays an essential role in GSH metabolism. It is an extracellular enzyme that exists on the outside of the plasma membrane. It is the only enzyme that can break the γ -glutamyl amide bond in GSH, GSSG and GSH-adducts. The importance of GGT can be demonstrated by blocking its activity with an inhibitor such as acivicin. As GSH is normally rapidly recycled, acivicin prevents GSH hydrolysis effectively by trapping it in the extracellular milieu, which results in intracellular GSH depletion (Capraro and Hughey, 1985; Liu et al., 1996). A decrease in GSH content causes a transient increase in the activity of GCL because GCL is feedback inhibited by GSH (Richman and Meister, 1975). *De novo* GSH biosynthesis regulation is mediated by ARE on the *Gcl* gene (Mulcahy and Gipp, 1995). Numerous conditions can change intracellular GSH levels, including heavy metal or GSH-trapping xenobiotics treatment, high glucose

concentrations, and exposure to ROS or bifunctional electrophiles such as an α , β -unsaturated aldehyde genotoxin, HNE (Wild and Mulcahy, 2000).



Scheme 1.6 Cellular GSH-adduct transport and metabolism.

1.3.2 GSTs and Other GSH-adduct Metabolizing Enzymes

Cytosolic GSTs represent the largest family and comprise seven classes in mammalian species. Isoenzymes within a class typically share more than 40% identity in amino acid sequence, while those between classes share more than 25% identity (Hayes et al., 2005). GSTs catalyze the first of the four steps involved in the synthesis of

mercapturic acid derivatives of GSH-adducts. GGTs and DPs then remove the γ -glutamyl moiety and the Gly, followed by *N*-acetylation of the resulting Cys conjugate, which is catalyzed by the cytosolic enzyme *N*-acetyl transferase (NAT) (Hinchman and Ballatori, 1994) (Schemes 1.6 and 1.7). In a study of intracellular HNE metabolism, Gly-Cys-HNE, Cys-HNE and the mercapturic acid derivative from GSH-HNE were detected in specific cell types, including kidney cells and neutrophils (Siems and Grune, 2003).

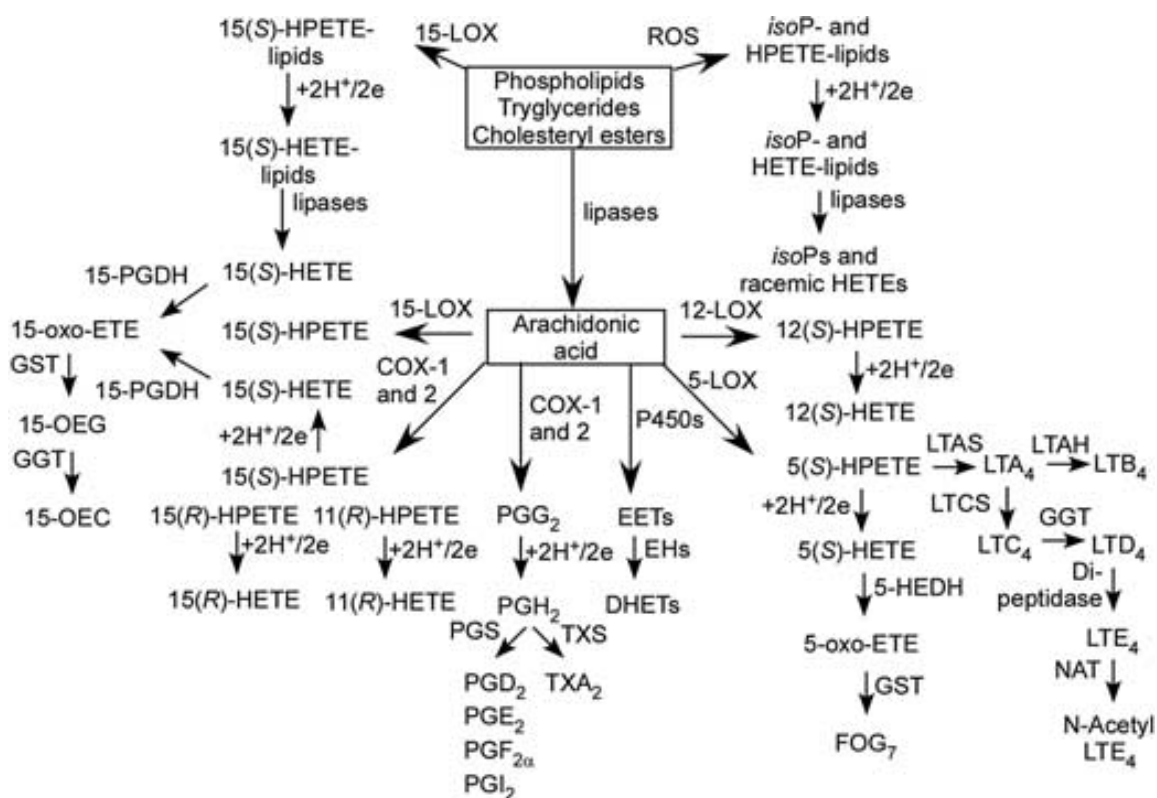
GSTs catalyze nucleophilic attack by GSH on electrophilic carbon, nitrogen or sulphur atoms. There are three families of GSTs. Two of these families, the cytosolic and mitochondrial GSTs are soluble enzymes and share some similarities in their three-dimensional folds (Ladner et al., 2004; Robinson et al., 2004). The third family comprises membrane-associated proteins that are involved in eicosanoid and GSH metabolism (MAPEG) and bear no structural resemblance to the other two families of enzymes (Jakobsson *et al.*, 2000; Lam and Austen, 2002; Murakami and Kudo, 2006). The MAPEG family includes six human proteins: 5-LO-activating protein (FLAP), LTC₄ synthase, MGST1, MGST2, MGST3 and PGE synthase, earlier known as microsomal glutathione transferase 1-like-1 (MGST1-L-1). MAPEGs play important roles in eicosanoid metabolism, and members of the MAPEG superfamily are involved in the transformation of reactive lipid intermediates to bioactive eicosanoids or un-reactive products such as lipid alcohols or GSH-adducts. MGSTs 2 and 3 have both been shown to act as GSH peroxidases as well as LTC₄ synthases (Jakobsson *et al.*, 2000) (Scheme 1.7).

1.3.3 GSH-adduct Transporters

GSH-adducts are exported from cells by ATP binding cassette (ABC) transporters and/or non-ATP binding cassette transporters (Awasthi *et al.*, 2007; Deeley *et al.*, 2006). MRP families are comprised of twelve related ABC proteins that transport structurally-diverse lipophilic anions and function as drug efflux pumps (Borst *et al.*, 2000; Kruh *et al.*, 2001). Among them, MRP1 functions as the most important and ubiquitous GSH-adduct pump, and confers drug resistance to anti-cancer drugs (Cole *et al.*, 1994; Chen *et al.*, 1999; Diestra *et al.*, 2003). In spite of the similarity in the resistance profiles of P-glycoprotein (Pgp) and MRP1, the substrate selectivities of these two kinds of pumps differ markedly. Pgp substrates are neutral or mildly positively charged compounds without conjugation, whereas MRP1 substrates include GSH, glucuronate and sulfate conjugates (Kruh *et al.*, 2001).

1.3.4 Biological Effect of GSH-adducts

Intracellular GSH provides one of the major defenses against oxidative stress in mammalian cells (Blair, 2010). GSH adducts are not merely inactivation products, but can also have biological activities. The best-known examples are the cysteinyl LTs that GSH-adducts (LTC₄) formed between LTA₄ and GSH and act as important inflammation mediators (Murphy *et al.*, 1979). By interacting with cysteinyl leukotriene receptors, LTC₄ can stimulate proinflammatory activities such as endothelial cell adherence and chemokine production (Murphy *et al.*, 1979). The GSH-adduct with the cyclopentenone PGA₁ showed a potent inhibitory effect on energy dependent, active export of cAMP (Cagen and Pisano, 1979). Hepoxilins are hydroxy epoxides derived from AA through 12-LO metabolism, and they induce release of insulin from pancreatic islet cells. Their GSH conjugates retain significant biological activity and can act as hepoxilins themselves



Scheme 1.7 Formation of eicosanoids and eicosanoid-derived GSH-adducts (adopted from Blair IA *Biomed Chromatogr.* 2010 Jan; 24(1):29-38). Abbreviations: 5-HEDH, 5-hydroxyeicosanoid dehydrogenase; EH, epoxide hydrolase; FLAP, 5-lipoxygenase activating protein; FOG-7, 5-oxo-eicosatetraenoic acid GSH-adduct, LTAH, leukotriene A₄ hydrolase; LTAS, leukotriene A₄ synthase; PGS, prostaglandin synthase; TX, thromboxane; TXS, thromboxane synthase.

(Pace-Asciak et al., 1989; Laneuville et al., 1990). A GSH adduct of 5-oxo-eicosatetraenoic acid (5-oxo-ETE) named as FOG₇ (Scheme 1.7) caused a potent chemotactic response in human eosinophils and neutrophils, and was also capable of initiating actin polymerization (Bowers et al., 2000). In addition, the GGT-derived cysteinylglycine-adduct (HNE-Cys-Gly) from its corresponding GSH-adduct exhibited cytotoxic properties in fibroblast cells (Enoiu et al., 2002).

1.4 Lipid Peroxidation-Derived Eicosanoids and Disease

Increased lipid peroxidation accompanied by decreased ability of the body to remove its products results in accumulation of lipid peroxidation-derived eicosanoids and their metabolites. The eicosanoids could potentially cause effects on cell proliferation, cell differentiation, and other biological effects. All these processes are thought to be involved in the etiology of diseases such as cancer, cancer angiogenesis, and cardiovascular diseases.

1.4.1 Cancer Angiogenesis

Pro-inflammatory PGs and LTs promote tumor growth by regulating tumor epithelial cells themselves and orchestrating the complex interactions between transformed epithelial cells and surrounding stromal cells to establish the tumor microenvironment that facilitates tumor-associated angiogenesis and evades attack by the immune system, while anti-inflammatory eicosanoids oppose this effect (Wang and Dubois, 2010). Among the enzymes known to have increased expression in diseases involving integrated action of macrophages and ECs, 15-LO, a cytoplasmic enzyme, appears to play a critical pathophysiological role. This is evidenced by the elevated expression of 15-LO-1 in atherosclerotic lesions and its localization at the sites of

macrophage accumulation (Yla-Herttuala et al., 1990; Kuhn and Chan, 1997; Kuhn et al., 1997). Studies of 15-LO-1 in hematopoietic cells have demonstrated that it is localized on the inner cell membrane and other non-nuclear membranes (e.g. sub-mitochondrial membranes) after stimulation with calcium (Brinckmann et al., 1997; Walther et al., 2004). In mice, endothelial cells are activated by macrophage 12/15-LO activity in the presence of low-density lipoprotein (Huo et al., 2004). It has also been suggested that 15-LO-1 plays an important role in angiogenesis and carcinogenesis (Harats et al., 2005; Furstenberger et al., 2006; Viita et al., 2008). Human 15-LO-1 is preferentially expressed in normal tissues and benign lesions, but not in carcinomas of bladder, breast, colon, lung, prostate and skin (Shureiqi et al., 1999). Angiogenesis and tumor formation in two xenograft models are inhibited in transgenic mice over-expressing 15-LO-1 in ECs (Harats et al., 2005). These effects may contribute to the known anti-tumorigenic activity of 15-LO-1. Interestingly, in contrast to inhibiting colorectal cancer cell growth (Shureiqi et al., 2003; Hsi et al., 2004), 15-LO-1 stimulates prostate cancer cell growth (Belkner et al., 1993; Kelavkar et al., 2001; Kelavkar et al., 2004). It has also been suggested that several possible pro- versus anti-angiogenesis functions are mediated by various products of 15-LO-mediated lipid oxidation (Zhang et al., 2005; Viita et al., 2008). This is because 15-LO-mediated lipid metabolic pathways have not been fully elucidated, and the exact biological role of each of the metabolites has not been completely investigated (Weibel et al., 2009). This is further complicated by the observations that 15-LO has pro-inflammatory and anti-inflammatory effects in cell cultures and primary cells and even opposite effects on atherosclerosis in two different animal species (Wittwer and Hersberger, 2007). There is also substantial evidence for a

pro-atherosclerotic effect of 15-LO including the direct contribution to LDL oxidation and to the recruitment of monocytes to the vessel wall, its role in angiotensin II mediated mechanisms and in vascular smooth muscle cell proliferation (Wittwer and Hersberger, 2007).

1.4.2 Cancer

Major causes of cancer are chronic infection or inflammation, accompanied by increases in lipid peroxidation mediated either by enzymes or ROS (Ames et al., 1993). There is increasing evidence that lipid peroxidation products are involved in DNA damage and mutagenesis in different cancers. Unsubstituted etheno-DNA-adducts and other DNA-adducts such as M₁G have been observed in human and animal tissues (Chaudhary et al., 1994; Chaudhary et al., 1994; Burcham, 1998). They are mutagenic in mammalian cells due to error-prone translesion DNA synthesis (Levine et al., 2000; Levine et al., 2001).

Pharmacological inhibition, or genetic deletion of COX-2, reduces tumor formation in experimental animal models of colon, breast, lung, and other cancers (Wang and Dubois, 2006; Wang et al., 2007). In mice, targeted overexpression of COX-2 in the mammary epithelium is sufficient to induce tumorigenesis (Smyth et al., 2009). Epidemiologic studies have shown that regular use of NSAIDs is associated with a reduction in the risk of cancers including colorectal cancer (Waddell et al., 1989; Thun, 1996; Harris et al., 2005). NSAIDs inhibit both COX-1 and COX-2 (Smith et al., 2000). COX inhibitors significantly decrease polyp formation, in patients with familial polyposis coli, while a polymorphism in COX-2 has been associated with increased risk of colon cancer (Smyth et al., 2009). Three randomized controlled trials, the Adenoma Prevention

with Celecoxib trial, the Prevention of Sporadic Adenomatous Polyps trial, and the Adenomatous Polyp Prevention on Vioxx trial, reported a significant reduction in the reoccurrence of adenomas in patients receiving either celecoxib or rofecoxib (Bertagnolli, 2007). However, this coincided with an increase in risk of cardiovascular events, undermining the risk-to-benefit ratio. Moreover, COX-2 is upregulated in colorectal tumor tissue (Eberhart et al., 1994; DuBois et al., 1996). Substantial evidence suggests that PGE₂ derived from COX-2 is a primary pro-oncogenic prostanoid, at least in part via transactivation of epidermal growth factor receptor (Wang and Dubois, 2006). PGE₂ facilitates tumor initiation, progression, and metastasis through multiple biological effects, including increased proliferation and angiogenesis, decreased apoptosis, augmented cellular invasiveness, and modified immunosuppression. Mice lacking the PGE₂ receptors (EP1, EP2, or EP4) display reduced disease in multiple carcinogenesis models. By contrast, the PGE₂ receptor EP3 may play a protective role in some cancers. The pro- and anti-oncogenic roles of other prostanoids/eicosanoids remain under investigation, with TxA₂ emerging as another likely COX-2-derived procarcinogenic mediator (Wang et al., 2007). Furthermore, COX-2 derived lipid peroxidation products such as 15(*S*)-HPETE, form heptanone-etheno-DNA-adducts and etheno-DNA-adducts (Williams et al., 2005). Heptanone-etheno-2'-deoxyguanosine (H- ϵ dGuo) was formed in rat intestinal epithelial cells that stably express COX-2 (Lee et al., 2005). In addition, there were statistically significant increased levels of H- ϵ dGuo and H- ϵ dCyd in a mouse model of colon cancer compared with control mice (Williams 2005). Another study showed that another DNA-adduct (M₁G) formation is correlated with COX-2 expression in human colon cells

(Sharma et al., 2001). These provide substantial evidence that COX-2 mediated DNA damage plays a role in carcinogenesis.

Moreover, significantly elevated levels of LO metabolites have been found in lung, prostate, breast, colon, and skin cancer cells, as well as in cells from patients with both acute and chronic leukemia (Steele et al., 1999). For example, 12-LO overexpression has been well documented in many types of solid tumor cells, including those of the prostate, colon, and epidermoid carcinoma (Chen et al., 1994; Honn et al., 1994). In one mouse model of skin cancer, increased etheno-DNA adduct formation was correlated to 12-LO-mediated lipid peroxidation (Nair et al., 2000). In addition, 12-LO inhibition was shown to significantly inhibit tumor development in skin (Huang et al., 1991; Minekura et al., 2001). Overexpression of 15-LO in human prostate cancer cells increases tumorigenesis (Kelavkar et al., 2001; Hsi et al., 2002). 5-LO is expressed in many cancer cells and overexpressed in human prostate or pancreatic cancer tissue (Goetzl et al., 1995; Gupta et al., 2001; Hennig et al., 2002). Inhibition of 5-LO activity has also been shown to have a chemopreventive effect (Steele et al., 1999; Li et al., 2005).

1.4.3 Cardiovascular Disease

Eicosanoids produced by COX-2 are thought to promote tumorigenesis by stimulating angiogenesis (Cha et al., 2006). However, in atherosclerotic lesions where macrophages and ECs are present, COX-2 and LOs can be found suggesting the LO-derived products might also be involved (Aviram, 1996; Feinmark and Cornicelli, 1997; Cornicelli and Trivedi, 1999; Mehrabian and Allayee, 2003; Nie, 2007). There is also an increased level of lipid peroxidation in atherosclerotic lesions as evidenced by the

presence of lipid hydroperoxide-derived bifunctional electrophiles such as malondialdehyde (Yla-Herttuala et al., 1989) and HNE (as a pyrrole derivative) (McGeer et al., 2002), and ROS-derived isoprostanes (IsoPs) (Pratico et al., 1997).

In atherosclerotic lesions, LOs and COXs are upregulated (Baker et al., 1999; Spanbroek et al., 2003). Lipids are accumulated in the foam cells and necrotic core, leading to increased levels of lipid peroxidation. Expression of 15-LO-1, as a cytoplasmic enzyme, is elevated in atherosclerotic lesions and is localized at the sites of macrophage accumulation (Yla-Herttuala et al., 1990; Kuhn and Chan, 1997; Kuhn et al., 1997; Tuomisto et al., 2003). Studies of 15-LO-1 in 15-LO-expressing mouse macrophage (RAW264.7) demonstrated that 15-LO-1 is localized on the inner side of the cell membrane and other nonnuclear membranes (e.g. submitochondrial membranes) after stimulation with calcium (Brinckmann et al., 1997; Walther et al., 2004). It has been proposed that low-density lipoprotein (LDL), the key component of fatty streak atherosclerotic lesion, undergoes modification by lipid peroxidation products before it is taken up by macrophages to form foam cells (Steinberg et al., 1989). The modified apoB on LDL gives rise to new epitopes that can be recognized by the scavenger receptor on macrophages which would then take away the LDL (Palinski et al., 1989; Rosenfeld et al., 1990). It has also been suggested that 15-LO-1 plays an important role in atherogenesis by oxidizing LDL (Feinmark and Cornicelli, 1997). In mice, endothelial cells are activated by macrophage 12/15-LO activity in the presence of LDL (Huo et al., 2004). Interestingly, in contrast to promoting atherosclerotic lesions in mice and human, macrophage-mediated 15-LO expression protects against atherosclerosis development in rabbits (Shen et al., 1996). It has also been suggested that several possible pro- versus

anti-atherogenic functions may be mediated by various products of 15-LO-mediated lipid oxidation (Cathcart and Folcik, 2000). Therefore, LO- and COX-mediated lipid hydroperoxide formation may provide a rich source of endogenous bifunctional electrophiles under atherogenic conditions.

Recently, it was observed that efflux of 15(*S*)-HETE from cholesteryl ester-enriched 15-LO-expressing RAW264.7 macrophages, when lipid droplets are present, was significantly reduced compared with that from cells enriched with free cholesterol (lipid droplets are absent) (Weibel et al., 2009). It was further proposed that 15-LO-1 is present and functional on cytoplasmic neutral lipid droplets in macrophage foam cells, and these droplets may act to accumulate the anti-inflammatory lipid mediator 15(*S*)-HETE (Weibel et al., 2009). Moreover, apoptosis may play important roles in different stages of cardiovascular disease, especially as apoptosis occur in a variety of cell types involved in atherosclerosis, including macrophages, vascular smooth muscle cells, and lymphocytes (Kockx and Herman, 2000).

In cardiovascular ischemia-reperfusion injuries, there is a cycle of ROS bursts and lipid peroxidation (Nita et al., 2001; Warner et al., 2004; Fukai et al., 2005; McCord and Edeas, 2005; Ozer et al., 2005). Lipid peroxidation products might also cause oxidative injury by inducing apoptosis in the vascular cells (Rittner et al., 1999; Ruef et al., 2001).

1.5 Lipid Peroxidation Products as Biomarkers of Oxidative Stress

Small-molecule biomarkers are derived from modifications to GSH, DNA and cellular metabolites, such as lipids and folates (Ciccimaro and Blair, 2010). Intensive efforts have been made to search for small-molecule biomarkers that are predictive of cancers, cardiovascular disease and neurodegenerative diseases (Blair, 2006; Lee and

Blair, 2009; Mesaros et al., 2009; Blair, 2010). By linking biomarker discovery and validation with known pathways of endogenous metabolism, it is possible to rationally approach the development of a biomarker for a specific disease (Ciccimaro and Blair, 2010).

The primary products in lipid peroxidation are lipid hydroperoxides as well as their metabolites. Lipid peroxidation products provide a rich source of biomarkers, including lipid hydroperoxides, hydroxy lipids, MDA, IsoPs, DNA-adducts, protein adducts, and GSH adducts (Abuja and Albertini, 2001; Blair, 2010). Lipid hydroperoxides contain a conjugated diene system and strongly absorb light at 234 nm. This characteristic absorbance has been employed for continuous monitoring of lipid peroxidation in lipoproteins and model membrane system (Esterbauer et al., 1989). The limitation of this method is that it is highly sensitive to UV-absorbing compounds. Most biological systems contain high concentration of such UV-absorbing compounds, which makes it almost impossible to monitor lipid peroxidation in biological fluids and tissues using this method. Gas chromatography (GC)-MS and LC-MS methods have also been developed to quantify IsoPs (Morrow et al., 1990; Morrow and Roberts, 1994; Pratico et al., 1998; Pratico et al., 2004). The drawback in using IsoPs as biomarkers of oxidative stress is that they only reflect the oxidation of AA.

Lipid hydroperoxides are rapidly reduced to hydroxy lipids in biological systems by GSH POX (Cohen and Hochstein, 1963). Highly specific and accurate stable isotope dilution LC-MS methodology has been developed that makes it possible to resolve and quantify different regioisomers and enantiomers of hydroxy-lipids that are formed in trace amounts in the medium of cultured cells (Lee et al., 2003). This method has

enabled us to elucidate lipid peroxidation mediated by different pathways. Tissue samples such as atherosclerotic plaques and bronchoalveolar lavage (BAL) fluid can also be analyzed by this method. Furthermore, routinely conduct LC-MS assays are being developed for analyzing multiple estrogen metabolites in serum and plasma at even lower concentrations than the current lower limit of quantitation of 0.4 pg/mL (1.6 pmol/L) (Blair, 2010).

In addition, highly sensitive and specific LC-electrospray ionization (ESI)/MRM/MS methodology has been developed to monitor a variety of etheno-DNA adducts, heptanone-etheno-DNA-adducts and other DNA adducts (e. g. 7,8-dihydro-8-oxo-2'-dGuo) which have been shown to be specifically derived from lipid hydroperoxides in human and mouse tissue (Lee et al., 2005; Williams et al., 2005; Williams et al., 2006; Mangal et al., 2009). In addition, an MS-based study showed that urinary etheno-dCyd was correlated with cigarette smoking (Chen et al., 2004).

In the last decade, there has been a fundamental improvement in the analysis of protein adducts by mass spectrometry, and in particular by matrix-assisted laser desorption ionization (MALDI) and ESI tandem MS. Until recently, MS approaches have been applied, with few exceptions, to characterize protein adducts in *in vitro* systems (incubation of the target peptide/protein with reactive intermediates in buffer), often forcing the reaction with large and non-physiological reactive intermediate concentrations. With MS techniques, the α,β -unsaturated aldehyde HNE mediated modification of several groups of proteins has been elucidated, including hemoproteins, lipoproteins, insulin, and different enzymes (Carini et al., 2004). Studies in our group have elucidated 4-oxo-2(*E*)-nonenal (ONE)-mediated modification on hemoglobin and

the histone H₄ protein (Oe et al., 2003; Yocum et al., 2005). MS methods have then been used to detect bifunctional electrophile-peptide adducts (such as HNE-GSH adducts and HNE-carnosine adducts) directly in biological matrices (Aldini et al., 2002; Aldini et al., 2002). In one study on oxidative stress-induced lipid peroxidation in rats, HNE-GSH levels measured by LC-MS analysis in hepatocytes were shown to be correlated with oxidative stress induced by iron nitrilotriacetate (Volkel et al., 2005). More recently, a novel GSH adduct derived from lipid peroxidation, thiadiazabicyclo-ONE-GSH-adduct (TOG), can provide a specific biomarker of lipid hydroperoxide-derived ONE formation (Blair, 2010).

1.6 Scope of Thesis Research

Studies on lipid hydroperoxide-mediated formation of eicosanoids have been primarily limited to PGs and the prototypic lipid hydroperoxides [e. g. 13(*S*)-HPODE and 15(*S*)-HPETE] and their corresponding alcohols such as 13(*S*)-HODE and 15(*S*)-HETE (Lee et al., 2001; Williams et al., 2005). Little is known about the roles of further metabolites of lipid hydroperoxides, which may have critical bioactivity and be important intermediates in cell signaling. Also, lack of sensitivity has greatly compromised the effectiveness of *in vivo* detection and analysis of lipid peroxidation products and their derivatives. Once highly sensitive and specific LC-MS methods have been developed, suitable cell models can be utilized to elucidate lipid peroxidation pathways in cells and to detect cellular components modified by further metabolites of hydroxyl-lipids. The purpose of this study is to identify the *in vitro* and *in vivo* metabolites of 15-LO-1- and COX-2-derived 15(*R,S*)-HETE, to examine the biological activity of 15-HETE metabolites, to characterize the metabolites of COX-2-derived 11(*R*)-HETE, and to

examine the effect of aspirin on the production and metabolism of COX-2-derived 15(*R,S*)-HETE, 11(*R*)-HETE and their metabolites.

The first specific aim was to elucidate the 15-LO-1-mediated formation of 15-oxo-EETE and 15-oxo-EETE-GSH adduct. A stable isotope dilution LC-MS method was established to quantify the formation of 15-oxo-EETE as a metabolite of 15-LO-1 and 15-PGDH in mouse macrophages and primary human monocytes from both exogenously and endogenously AA. 15-oxo-EETE-GSH adduct and γ -cysteinylglycine adduct formation were also monitored. The biological effect of 15-oxo-EETE on the proliferation of human HUVECs was examined.

The second specific aim was to study COX-2-mediated formation of 11-oxo-EETE and 11-oxo-EETE-GSH adduct. The biosynthesis of 11-oxo-EETE, a novel metabolite of COX-2 and 15-PGDH, was revealed in both mouse and human epithelial cell models (RIES and Caco-2 cell lines). The structure of 11-oxo-EETE as well as its GSH-adduct structure was confirmed by LC-MS analysis.

The third specific aim was to study the effect of aspirin on the formation and metabolism of 15-oxo-EETE and 11-oxo-EETE as well as their upstream 15(*R,S*)-HETE and 11(*R*)-HETE as COX-2-derived metabolites. The biosynthesis of 15-oxo-EETE from 15(*R*)-HETE was also studied.

CHAPTER 2

15-Oxo-Eicosatetraenoic Acid, a Metabolite of Macrophage 15-Hydroxyprostaglandin Dehydrogenase That Inhibits Endothelial Cell Proliferation

Published, *Molecular Pharmacology*, 2009; 76 (3):516-529

2.1 Abstract

The formation of 15-oxo-EETE as a product from rabbit lung 15-PGDH-mediated oxidation of 15(*S*)-HPETE was first reported over 20 years ago. However, the pharmacological significance of 15-oxo-EETE formation has never been established. We have now evaluated 15-LO-1-mediated arachidonic acid (AA) metabolism to 15-oxo-EETE in human monocytes and mouse RAW macrophages that stably express human 15-LO-1 (R15L cells). A targeted lipidomics approach was employed to identify and quantify the oxidized lipids that were formed. 15-oxo-EETE was found to be a major AA-derived 15-LO-1 metabolite when AA was given exogenously or released from endogenous esterified lipid stores by calcium ionophore A-23187 (CI). This established the R15L cells as a useful *in vitro* model system. Pre-treatment of the R15L cells with cinnamyl-3,4-dihydroxycinnamate (CDC), significantly inhibited AA- or CI-mediated production of 15(*S*)-HETE and 15-oxo-EETE, confirming the role of 15-LO-1 in mediating AA metabolite formation. Furthermore, 15(*S*)-HETE was metabolized primarily to 15-oxo-EETE. Pre-treatment of the R15L cells with the 15-PGDH inhibitor, 5-[[4-ethoxycarbonyl] phenyl]azo]-2-hydroxy-benzeneacetic acid (CAY10397), reduced AA- and 15(*S*)-HETE-mediated formation of 15-oxo-EETE in a dose-dependent manner. This confirmed that macrophage-derived 15-PGDH was responsible for catalyzing the conversion of 15(*S*)-HETE to 15-oxo-EETE. Finally, 15-oxo-EETE was shown to inhibit

the proliferation of human vascular vein endothelial cells (HUVECs) by suppressing DNA synthesis, implicating a potential anti-proliferative role. This is the first report describing the biosynthesis of 15-oxo-EETE by macrophage/monocytes and its ability to inhibit EC proliferation.

2.2 Introduction

15-oxo-EETE was originally shown to arise from rabbit lung 15-PGDH-mediated oxidation of 15(*S*)-HETE (Bergholte et al., 1987) (Fig. 2.1). More recently, 15-oxo-EETE was identified as a metabolite of COX-2-mediated-AA metabolism (Lee et al., 2007). It was also observed as an AA metabolite formed in human mast cells (Gulliksson et al., 2007). Unlike its 5-LO-derived isomer, 5-oxo-EETE, the pharmacology of 15-oxo-EETE has not been explored in detail (Murphy and Zarini, 2002; Powell and Rokach, 2005). Therefore, this interesting AA metabolite has remained a pharmacological curiosity for many years. AA is present in many esterified lipid classes and can be released by the action of specific lipases. It can then be oxidized to lipid hydroperoxides either enzymatically by COXs (Blair, 2008) and LOs (Jian et al., 2009) or non-enzymatically by the action of reactive oxygen species (Porter et al., 1995).

Bioactive lipid mediators are increasingly being recognized as important endogenous regulators of angiogenesis (Gonzalez-Periz and Claria, 2007). One of the major cascades of bioactive lipid mediator production involves the release of AA from

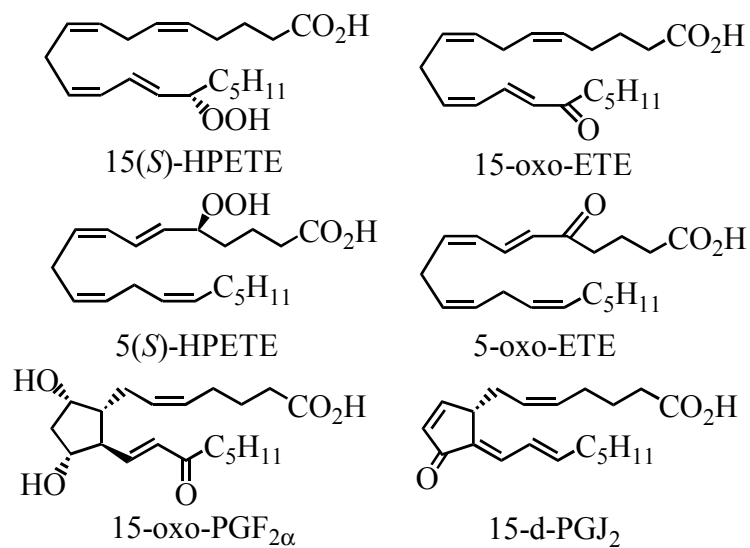


Figure 2.1 Chemical structures of AA metabolites with similar structural features.

membrane phospholipids followed by COX-2-mediated formation of eicosanoids (Lee et al., 2007). Eicosanoids produced by COX-2 are thought to promote tumorigenesis by stimulating angiogenesis (Cha et al., 2006). It is noteworthy that there is an increased level of lipid peroxidation in atherosclerotic lesions as evidenced by the presence of lipid hydroperoxide-derived bifunctional electrophiles such as 4-hydroxy-2-nonenal (HNE) (as a pyrrole derivative) (Salomon et al., 2000).

In contrast to 5-LOs, which strongly prefer free AA as substrate (Jian et al., 2009), mammalian 15-LOs are capable of oxygenating both free and esterified polyunsaturated fatty acids (Kuhn and O'Donnell, 2006). 15-LO can also oxygenate even more complex lipid-protein assemblies such as biomembranes (Kuhn and Borchert, 2002) and lipoproteins (Brinckmann et al., 1998). Type 1 human 15-LO (15-LO-1), mainly expressed by reticulocytes, eosinophils and macrophages, is the enzyme responsible for converting AA to 15(*S*)-HPETE and a small amount of 12(*S*)-hydroperoxy-5,8,10,14-(*Z,Z,E,Z*)-eicosatetraenoic acid (12(*S*)-HETE) (Bryant et al., 1982). 15-LO-1 is a cytoplasmic enzyme with up-regulated expression in atherosclerotic lesions and localization at sites of macrophage accumulation (Kuhn and Chan, 1997). Studies of 15-LO-1 in hematopoietic cells have demonstrated that it translocates to the inner plasma membrane and other non-nuclear membranes (e.g. sub-mitochondrial membranes) after stimulation with calcium (Walther et al., 2004).

Endothelial cells are activated by murine macrophage 12/15-LO activity in the presence of low-density lipoprotein (Huo et al., 2004). Furthermore, it has been suggested that 15-LO-1 plays an important role in angiogenesis and carcinogenesis (Viita et al., 2008). Both angiogenesis and tumor formation in two xenograft models were

inhibited in transgenic mice over-expressing 15-LO-1 in ECs (Harats et al., 2005). It has been suggested that several possible pro- versus anti-angiogenesis functions are mediated by metabolites derived from 15-LO-mediated lipid oxidation (Viita et al., 2008). These issues make it difficult to assess the precise contribution of the 15-LO pathway to angiogenesis, atherosclerosis, and tumorigenesis. For example, 15-LO has pro-inflammatory and anti-inflammatory effects in cell cultures and primary cells and opposite effects on atherosclerosis in two different animal species (Wittwer and Hersberger, 2007). There is also substantial evidence for a pro-atherosclerotic effect of 15-LO-1 including its direct contribution to LDL oxidation and to the recruitment of monocytes to the vessel wall (Wittwer and Hersberger, 2007). The explanation to these conflicting observations might reside in the different biological effects of many lipid mediators generated by 15-LO-1 pathway, which have not yet been fully elucidated (Weibel et al., 2009). The present study was designed to elucidate the biosynthesis of 15-oxo-ETE through the actions of 15-LO-1 and 15-PGDH and to explore its potential pharmacological role in angiogenesis, an important mediator of tumorigenesis (Folkman, 2007).

2.3 Materials and Methods

2.3.1 Materials – AA (peroxide-free), 15(*S*)-HETE, 15-oxo-ETE, [²H₈]-15(*S*)-HETE, [²H₆]-5-oxo-ETE, CAY10397 were purchased from Cayman Chemical Co. (Ann Arbor, MI). CDC was obtained from BioMol (Plymouth Meeting, PA). CI, diisopropylethylamine (DIPE), 2,3,4,5,6-pentafluorobenzyl bromide (PFB) bromide, fetal bovine serum (FBS) and heparin were purchased from Sigma-Aldrich. Dulbecco's Modified Eagle's Medium (DMEM), RPMI-1640 media, Medium 199 (M199), phosphate

buffered saline (PBS), D-glucose, L-glutamine, penicillin, streptomycin and geneticin were supplied by Invitrogen (Carlsbad, CA). EC growth supplement was purchased from Millipore (Temecula, CA). Collagen I-coated plates for HUVEC cell culture and recombinant human interleukin (IL)-4 was obtained from BD Biosciences (San Jose, CA). Nuclear Extract Kit and TransAMTM NF- κ B Family Transcription Factor ELISA Kit were purchased from Active Motif Co. (Carlsbad, CA). BCA protein assay reagent was obtained from Pierce Biotechnology (Rockford, IL). High performance LC grade water, hexane, methanol, and isopropanol were obtained from Fisher Scientific (Fair Lawn, NJ). Gases were supplied by BOC Gases (Lebanon, NJ).

2.3.2 Mass spectrometry (MS) - The quantitative targeted lipidomics profile was obtained on a triple-quadrupole Finnigan TSQ Quantum Ultra AM mass spectrometer (Thermo Scientific, San Jose, CA) equipped for electron capture negative atmospheric pressure chemical ionization (ECAPCI) (Lee and Blair, 2007; Mesaros et al., 2009). Operating conditions were as follows: spray voltage 4.5 kV, vaporizer temperature at 450 °C and heated capillary temperature was 350 °C with a discharge current of 30 μ A applied to the corona needle. A post column addition of 0.75 ml/min of methanol was used to prevent buildup of carbon in the source. Nitrogen was used as the sheath gas and auxiliary gas, set at 60 and 10 (in arbitrary units), respectively. Collision-induced dissociation was performed using argon as the collision gas at 1.5 mTorr in the second (rf-only) quadrupole and the collision energy was set at 18 eV. An additional dc offset voltage was applied to the region of the second multipole ion guide (Q₀) at 5 V to impart enough translational kinetic energy to the ions so that solvent adduct ions dissociate to form sample ions. For multiple reaction monitoring (MRM), unit resolution was

maintained for both parent and product ions. The following MRM transitions were monitored: 15-HETEs (m/z 319 \rightarrow 219), [$^2\text{H}_8$]-15(*S*)-HETE (m/z 327 \rightarrow 226), 15-oxo-ETE (m/z 317 \rightarrow 273) and [$^2\text{H}_6$]-5-oxo-ETE (m/z 323 \rightarrow 279).

2.3.3 Liquid Chromatography - Normal phase chiral LC-ECAPCI/MS analyses were conducted using a Waters Alliance 2690 high performance LC system (Waters Corp., Milford, MA). A Chiralpak AD-H column (250 x 4.6-mm inner diameter, 5 μm ; Daicel Chemical Industries, Ltd., West Chester, PA) was employed for gradient 1 with a flow rate of 1.0 ml/min. Solvent A was hexane, and solvent B was methanol/isopropanol (1:1, v/v). Gradient 1 was as follows: 2% B at 0 min, 2% B at 3 min, 3.6% B at 11 min, 8% B at 15 min, 8% B at 27 min, 50% B at 30 min, 50% B at 35 min, 2% B at 37 min and 2% B at 45 min. Separations were performed at 30 $^{\circ}\text{C}$ using a linear gradient.

2.3.4 Cell Culture – Murine macrophage RAW 264.7 cells (obtained from American Type Culture Collection, Manassas, VA) were stably transfected with the pcDNA3 plasmid containing the human 15-LO-1 gene (R15L cells) or an empty pcDNA3 plasmid (RMock cells) (Zhu et al., 2008). Cells were cultured in DMEM supplemented with 10% FBS, 4,500 mg/l D-glucose, and 0.5 g/l geneticin. Before the treatment for lipidomics analysis, the culture media was replaced with serum-free DMEM. HUVECs were a generous gift from Dr. Vladimir Muzykantov (University of Pennsylvania). HUVECs were cultured in Medium 199 supplemented with 15% (or 10%) FBS, 110 mg/l L-glutamine, 100 mg/l heparin, 15 mg/l EC growth supplement, 100,000 units/l penicillin and 100,000 $\mu\text{g/l}$ streptomycin. Primary human monocytes were isolated from the peripheral blood of healthy adult donors and purified by the Biomolecular and Cellular Resource Center, Department of Pathology and Laboratory Medicine, University of

Pennsylvania in accordance with human subject protocols approved by the Internal Review Board of the National Institutes of Health. Cells were cultured in RPMI 1640 media with 10% FBS, 2 mM L-glutamine, 100,000 units/l penicillin and 100,000 µg/l streptomycin for 2 h. Human IL-4 was added to the cell culture media to reach a final concentration of 1000 pM. Cells were cultured for 40 h at 37 °C. Before treatment, cell culture media were replaced with serum free RPMI 1640 media containing 2 mM L-glutamine. Extraction and incubations of Whole Bone Marrow (WBM) cells from 12/15-LO deficient mice and wild-type mice were conducted by Michelle Kinder in the laboratory of Dr. Ellen Puré at the Wistar Institute. Cells and media were then harvested for further analysis after treatment. Cell numbers were counted by a hemocytometer.

2.3.5 AA or CI Treatment of Primary Human Monocytes - Primary human monocytes were cultured as described above. The media was removed and replaced with serum-free RPMI-1640 media containing 2 mM L-glutamine. AA (50 µM final concentration) or CI (5 µM final concentration) was added to the media. The final concentration of ethanol in the culture media was less than 0.1%. Cells were then incubated for 40 min at 37 °C. A portion of cell supernatant (3 ml) was transferred into a glass tube and adjusted to pH 3 with 2.5 N hydrochloric acid (HCl). Lipids were extracted with diethyl ether (4 ml x 2) and the organic layer was then evaporated to dryness under nitrogen. 100 µl of acetonitrile, 100 µl of PFB bromide in acetonitrile (1:19, v/v) and 100 µl of DIPE in acetonitrile (1:9, v/v) were added to the residue and the solution was heated at 60 °C for 60 min. The solution was allowed to cool down, evaporated to dryness under nitrogen at room temperature, dissolved in 100 µl of hexane/ethanol (97:3, v/v) and an aliquot of 20

μl was used for normal-phase chiral LC-ECAPCI/MRM/MS analysis using gradient 1 as described above.

2.3.6 AA treatment of R15L and RMock Cells - R15L cells and RMock cells were cultured in DMEM supplemented with 10% FBS, 4,500 mg/l D-glucose, and 0.5 g/l geneticin. The media was removed and replaced with serum-free DMEM containing peroxide-free AA (10 μM final concentration). Cells were then incubated for 0 min, 1 min, 5 min, 10 min, 30 min, 40 min, 1 h, 2 h, 3 h and 24 h at 37 °C. After each incubation, a portion of cell supernatant (3 ml) was transferred into a glass tube and cell numbers were counted by a hemocytometer. Blank media standards (3 ml) were prepared, spiked with the following amounts of authentic lipid standards [15(*R,S*)-HETEs, 15-oxo-ETE]: 10, 20, 50, 100, 200, 500 and 1000 pg. A mixture of internal standards [$^2\text{H}_8$]-15(*S*)-HETE, [$^2\text{H}_6$]-5-oxo-ETE, 1 ng each was added to each cell supernatant sample and standard solution. The samples and standards were adjusted to pH 3 with 2.5 N HCl. Extraction of 15(*R,S*)-HETEs and 15-oxo-ETE from cell culture media and LC-ECAPCI/MRM/MS analyses were performed as described above. Calibration curves were obtained with linear regressions of analyte versus internal standard peak-area ratio 15(*R,S*)-HETEs/[$^2\text{H}_8$]-15(*S*)-HETE, 15-oxo-ETE/[$^2\text{H}_6$]-5-oxo-ETE against analyte concentrations. Concentrations of 15(*R,S*)-HETEs and 15-oxo-ETE in the media supernatants were calculated by interpolation from the calculated regression lines.

2.3.7 CI Treatment of R15L Cells - R15L cells were cultured as described above. The media was removed and replaced with serum-free DMEM containing CI (5 μM final concentration). Cells were then incubated for 0 min, 1 min, 5 min, 10 min, 30 min, 40

min, 1 h, 2 h, 3 h and 24 h at 37 °C. Extraction and quantitation of 15(*R,S*)-HETEs and 15-oxo-EETE from cell culture media (3 ml) were performed as described above.

2.3.8 Quantitative Analyses of Eicosanoids from AA or CI Treated Primary Human

Monocytes – Primary human monocytes were cultured and induced by IL-4 as described above. 10 µM of AA or 5 µM of CI in ethanol was added to the media and cells were incubated for 40 min at 37 °C. The final concentration of ethanol in the culture media was less than 0.1%. Cell media (3 ml) from each treatment were spiked with a mixture of internal standards described above. Extraction and quantitation of 15(*R,S*)-HETEs and 15-oxo-EETE from cell culture media were performed as described above.

2.3.9 Quantitative Analyses of Eicosanoids from Ionomycin- or AA-Treated WBM from 12/15-LO Deficient Mice and Wild-Type Mice

– WBM containing macrophages and hematocyte stem cells were extracted from wild-type (WT) mice and 12/15-LO-deficient (12/15-LO^{-/-}) mice, and cultured in serum-free RPMI-1640 media. The mice WBM were incubated with 10 µM AA or 5 µM ionomycin for 30 min at 37 °C. The culture media (3 ml) from each treatment were taken and spiked with a mixture of internal standards described above. Extraction and quantitation of 15(*R,S*)-HETEs and 15-oxo-EETE from culture media were performed with the same procedure as that of R15L cell media or primary human monocyte media as described above.

2.3.10 AA or CI Treatment of R15L Cells with LO inhibitor CDC

- R15L cells were cultured as described above. Cells were treated with either 10 µM AA for 10 min or 5 µM CI for 40 min with or without the pretreatment with 20 µM CDC for 40 min. Extraction and quantitation of 15-oxo-EETE from cell culture media (3 ml) were performed as described above.

2.3.11 15(*S*)-HETE or AA Treatment of R15L Cells with 15-PGDH Inhibitor

CAY10397 – R15L cells were cultured as described above until almost confluent. The media was removed and replaced with serum-free DMEM containing various doses of CAY10397 (0 μ M, 5 μ M, 10 μ M, 15 μ M, 25 μ M, 50 μ M, and 100 μ M final concentration). Cells were then incubated for 4 h at 37 °C followed by incubation with additional 15(*S*)-HETE (50 nM final concentration) or AA (10 μ M final concentration) for 10 min. Extraction and quantitation of 15(*S*)-HETE and 15-oxo-EETE from cell culture media (3 ml) were performed as described above. IC₅₀ and EC₅₀ values for CAY10397 were calculated from the equation of the non-linear regression dose-response curves assuming that the 15(*S*)-HETE bound to the enzyme following the laws of mass action.

2.3.12 Cell Proliferation 5-Bromo-2'-Deoxyuridine (BrdU) Assay – Equal numbers

(1000 cells/well) of HUVECs were plated as described above in 24-well collagen I-coated plates and allowed to attach overnight. Cells were then treated with 15-oxo-EETE dissolved in ethanol (0 μ M, 1 μ M, 5 μ M, 10 μ M or 20 μ M final concentrations). The final concentration of ethanol in the culture media was less than 0.1%. Cell proliferation was assessed for two days by a commercially available BrdU assay kit according to the manufacturer's protocol [Roche[®] Cell Proliferation Enzyme-linked immunosorbent assay (ELISA) BrdU (colorimetric)]. After the final step of development, the developed solution of each well was transferred to 96-well plates to read in a 96-well plate reader at the absorbance at 370 nm with 492 nm as reference. The absorbance at $\lambda = 370$ nm obtained from the assay was normalized to the cell numbers according to a standard curve which was conducted at the same time with various cell numbers (0, 250, 500, 1000,

2500 and 5000 cells/well). Each data point represents the mean value from triplicate wells.

2.3.13 Extraction of Intracellular Eicosanoids in HUVECs after Incubation with 15-

oxo-ETE – HUVECs were cultured as described above. The media was removed and replaced with the media containing 1 μ M or 10 μ M 15-oxo-ETE. Cells were then incubated for 30 min, 1 h, 4 h, 24 h and 48 h at 37 °C. After each incubation, cells were washed with PBS and re-suspended in 1 ml PBS. Blank PBS (1 ml) solutions were prepared, spiked with the following amounts of authentic lipid standards [15(*R,S*)-HETEs, 15-oxo-ETE]: 10, 20, 50, 100, 200, 500 and 1000 pg. A mixture of internal standards [$^2\text{H}_8$]-15(*S*)-HETE, [$^2\text{H}_6$]-5-oxo-ETE, 1 ng each was added to each analytical sample and standard solution. Lipids were extracted with chloroform/methanol (2:1, v/v, 5 ml x 2). The organic layer was then washed with 0.9% sodium chloride (1 ml x 2) and evaporated to dryness under nitrogen. Lipid samples were further derivatized with PFB bromide, reconstituted in hexane/ethanol and analyzed by LC-ECAPCI/MRM/MS as described above.

2.4 Results

2.4.1 AA- or CI-Mediated Production of 15(*R,S*)-HETEs and 15-oxo-ETE in

Primary Human Monocytes - The cytokine IL-4 induces 15-LO-1 expression in human monocytes. Primary human monocytes were incubated with AA (50 μ M) or CI (5 μ M) for 40 min in serum free RPMI-1640 media following 40 h pretreatment with IL-4 (1 nM). Compared to the non-treated IL-4 induced monocytes, the chromatograms from LC-ECAPCI/MRM/MS analyses demonstrated the formation of 15(*S*)-HETE [retention time (rt), 15.5 min] in IL-4-induced primary human monocytes treated with exogenous

AA or CI (Fig. 2.2A). There was very little 15(*R*)-HETE (rt, 15.4 min) compared with 15(*S*)-HETE (Fig. 2.2A). 15-oxo-EETE was also identified (rt, 8.10 min) in IL-4-induced primary human monocytes with either AA or CI treatment (Fig. 2.2B). The signal intensity of 15-oxo-EETE was approximately 3-fold lower (1.34×10^7) than the intensity of 15(*S*)-HETE (4.35×10^7) in AA-treated cells and approximately 10-fold lower (5.04×10^5) than the intensity of 15(*S*)-HETE (4.05×10^6) in CI-treated cells (Figs. 2.2A and 2.2B). Quantitative analyses further demonstrated that $303.22 (\pm 21.69)$ pmol/ 10^6 cells of 15(*S*)-HETE (Fig. 2.3A) and $55.61 (\pm 2.34)$ pmol/ 10^6 cells of 15-oxo-EETE (Fig. 2.3B) were produced by IL-4-induced primary human monocytes with AA treatment, and $17.46 (\pm 0.52)$ pmol/ 10^6 cells of 15(*S*)-HETE (Fig. 2.3A) with $4.98 (\pm 0.21)$ pmol/ 10^6 cells of 15-oxo-EETE (Fig. 2.3B) was formed by IL-4-induced cells treated with CI, while cells with no treatment (NT) or cells only induced with IL-4 did not produce AA-derived eicosanoids (Fig. 2.3).

2.4.2 AA-Mediated Production of 15(*R,S*)-HETEs and 15-oxo-EETE in R15L Cells -

R15L cells and RMock cells were incubated with 10 μ M AA for a time-course of 24 h. LC-ECAPCI/MRM/MS analyses of the R15L cell supernatants demonstrated the production of 15-oxo-EETE (rt, 8.67 min) and 15(*S*)-HETE (rt, 16.15 min) within 5 min treatment of AA (Fig. 2.4A). Extracted chromatograms for 15-oxo-EETE, [$^2\text{H}_6$]-5-oxo-EETE, 15(*R*)-HETE, 15(*S*)-HETE and [$^2\text{H}_8$]-15(*S*)-HETE are shown in Fig. 2.4A. [$^2\text{H}_6$]-5-oxo-EETE and [$^2\text{H}_8$]-15(*S*)-HETE were used as internal standards to quantify 15-oxo-EETE and 15(*R,S*)-HETEs, respectively. Fig. 2.4B displays the production of 15(*R*)- and 15(*S*)-HETE by R15L and RMock cells upon AA treatment. 15(*S*)-HETE was the predominant

eicosanoid isomer released by R15L cells, with negligible amounts of 15(*R*)-HETE produced in response to AA treatment. Furthermore, 15(*S*)-HETE level peaked within 5

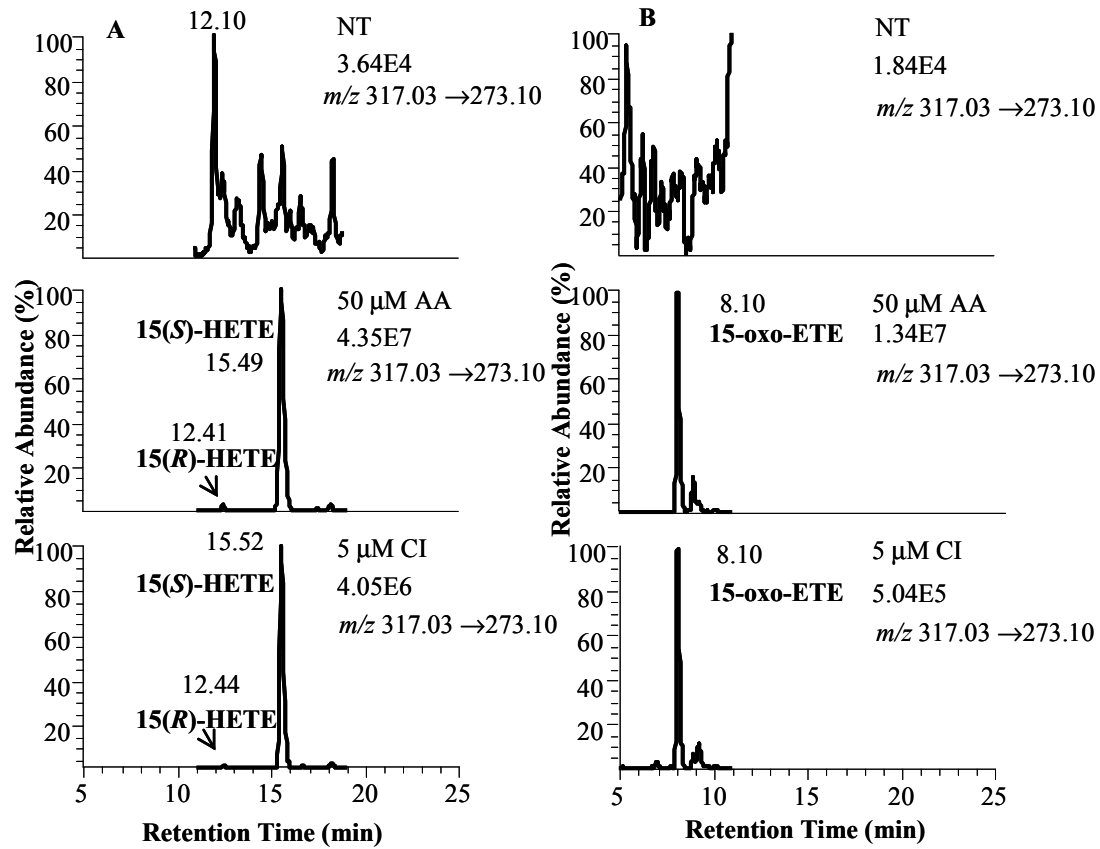


Figure 2.2 LC-MRM/MS analysis of 15-LO-derived eicosanoids from primary human monocytes treated with AA and CI. Primary human monocytes were isolated and stimulated with IL-4 for 40 h (NT) followed by 40 min treatment with 50 μM AA (AA) or 5 μM CI (CI A-23187). Cell supernatant in each treatment group was collected. Lipid metabolites in the cell supernatant were extracted, derivatized with PFB, and analyzed by stable isotope dilution LC-ECAPCI/MRM/MS analysis. MRM chromatograms are shown for (A) 15(*R,S*)-HETE-PFB (*m/z* 319 → 219) and (B) 15-oxo-ETE-PFB (*m/z* 317 → 273).

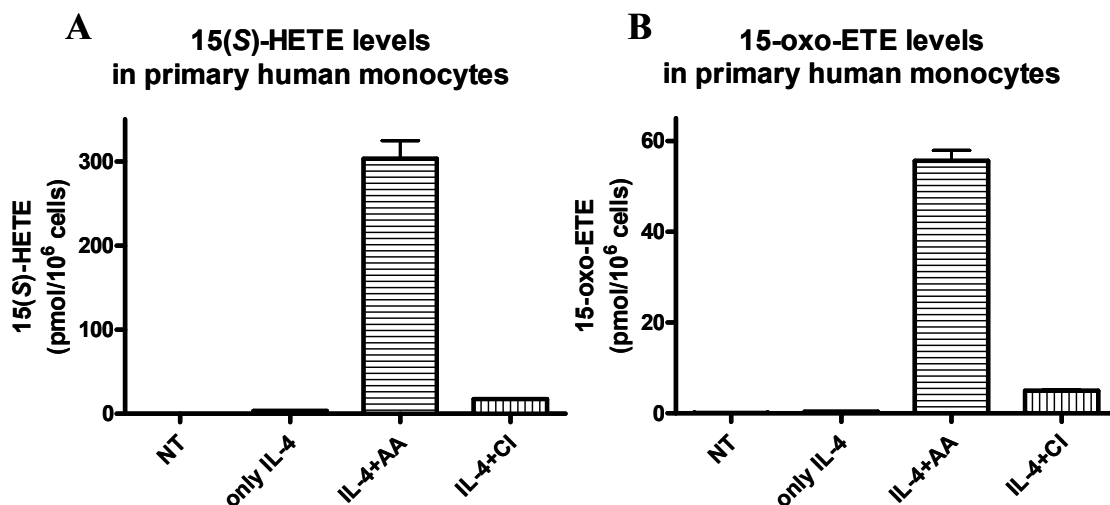


Figure 2.3 Quantitative analyses of 15-LO-derived eicosanoids from primary human monocytes treated with AA and CI. (A) 15(*S*)-HETE formation by primary human monocytes that were treated with 10 μ M AA or 5 μ M CI for 40 min following IL-4 (1 nM) stimulation. (B) 15-oxo-EETE formation by primary human monocytes that were treated with 10 μ M AA or 5 μ M CI for 40 min following IL-4 (1 nM) stimulation. Cells with no treatment (NT) or only IL-4 treatment were used as controls. Lipid metabolites in the cell media were extracted and derivatized with PFB. 15(*S*)-HETE and 15-oxo-EETE concentrations were determined in triplicate by stable isotope dilution by LC-ECAPCI/MRM/MS analysis of PFB derivatives. Values presented in bar graphs are means \pm S.E.M.

min treatment of AA (500 pmol/10⁶ cells) (Fig. 2.4B). In contrast, both 15(*R*)- and 15(*S*)-HETE production in RMock cells were close to limit of detection (Fig. 2.4B). The time course of 15-oxo-EETE produced in R15L cells upon AA treatment were similar to 15(*S*)-HETE with maximum level of 15-oxo-EETE observed (120 pmol/10⁶ cells) within 5 min of AA treatment, then continuing to diminish over the remainder of the 24 h treatment period (Fig. 2.4C). Again, there was very little production of 15-oxo-EETE in RMock cells (Fig. 2.4C).

2.4.3 CI-Mediated Production of 15(*R,S*)-HETEs and 15-oxo-EETE in R15L Cells - CI

increases the intracellular calcium concentration, which recruits 15-LO from the cytosol to the inner side of the plasma membrane, oxidizes AA to 15(*S*)-HPETE, which is subsequently reduced and released as 15(*S*)-HETE. The chromatograms of LC-ECAPCI/MRM/MS analyses demonstrated the production of the endogenous 15-oxo-EETE (rt, 8.31 min) and 15(*S*)-HETE (rt, 15.93 min) after 40 min treatment of 5 μM CI (Fig. 2.5A). Maximum synthesis of 15(*S*)-HETE was observed at 18 pmol/10⁶ cells within 1 h of the CI treatment, and decreased to limit of detection after 3 h, while there was very little production of 15(*R*)-HETE (rt, 12.60 min) throughout the time course of the treatment (Fig. 2.5B). Similarly, 15-oxo-EETE production peaked at 2 pmol/10⁶ cells after 40 min of the CI treatment, and declined to limit of detection after 3 h (Fig. 2.5C).

2.4.4 Effect of CDC on 15-oxo-EETE Production in R15L Cells - CDC is a LO inhibitor

that inhibits the production of 15-LO-mediated lipid metabolites (Cho et al., 1991). R15L cells were treated with 10 μM AA for 10 min or 5 μM CI for 40 min, with or without 40 min pretreatment with 20 μM CDC. AA treatment alone of R15L cells led to the production of 15-oxo-EETE (40 pmol/10⁶ cells) as well as 15(*S*)-HETE (420 pmol/10⁶

cells) (Fig. 2.6A and 2.6C, respectively). Pretreatment with CDC resulted in significant inhibition of 15-oxo-ETE production by almost 70% (12 pmol/10⁶ cells), and 15(*S*)-HETE production by almost 95% (20 pmol/10⁶ cells) (Figs. 2.6A and 2.6C, respectively). CDC treatment by itself did not lead to 15-oxo-ETE or 15(*S*)-HETE generation (Figs. 2.6A and 2.6C respectively). CI treatment generated 2 pmol/10⁶ cells of 15-oxo-ETE (Fig. 2.6B) and 35 pmol/10⁶ cells of 15(*S*)-HETE (Fig. 2.6D) in R15L cells. CDC pretreatment completely abolished both the CI-mediated 15-oxo-ETE and 15(*S*)-HETE production (Figs. 2.6B and 2.6D, respectively). CDC treatment alone had no effect on 15-oxo-ETE or 15(*S*)-HETE generation (Figs. 2.6B and 2.6D, respectively). These data further confirmed that both 15(*S*)-HETE and 15-oxo-ETE were 15-LO-derived metabolites of endogenous AA.

2.4.5 Quantitative Analyses of 15(*S*)-HETE and 15-oxo-ETE from Mice Whole Bone Marrow (WBM) by LC-ECAPCI/MS –WBM containing macrophages and hematocyte stem cells were extracted from wild-type (WT) mice and 12/15-LO-deficient (12/15-LO^{-/-}) mice. The mice WBM were incubated with 10 μM AA or 5 μM ionomycin for 30 min. AA led to the formation of 15(*S*)-HETE [224.90 (±4.35) pmol/10⁶] in WT mice while only 1.14 (±0.07) pmol/10⁶ in 12/15-LO^{-/-} mice (Fig. 2.7A). AA also generated 31.64 (±1.94) pmol/10⁶ of 15-oxo-ETE in WT mice and 0.07 (±0.00) pmol/10⁶ of 15-oxo-ETE in 12/15-LO^{-/-} mice (Fig. 2.7B). Ionomycin increased the intracellular Ca²⁺ level leading to the endogenous formation of 33.99 (±0.77) pmol/10⁶ 15(*S*)-HETE in WT mice while only 1.42 (±0.07) pmol/10⁶ in 12/15-LO^{-/-} mice (Fig. 2.7A). Endogenous 15-oxo-ETE in WBM induced by ionomycin was 7.70 (±0.34) pmol/10⁶ in WT mice and only 0.09 (±0.00) pmol/10⁶ which was under the limit of detection in 12/15-LO^{-/-} mice (Fig. 2.7B).

These data confirmed 15-oxo-EETE production *in vivo* with animal models and this production is through 15-LO pathway.

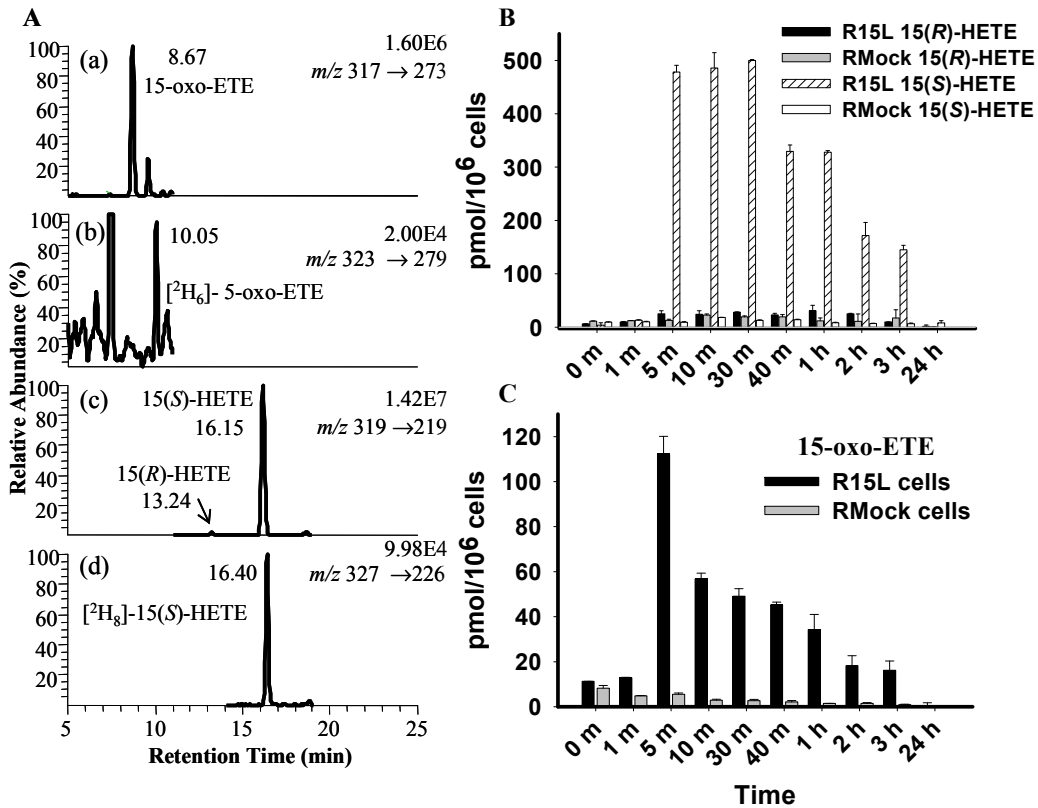


Figure 2.4 LC-MRM/MS analysis and quantitation of 15-LO-derived eicosanoids from R15L cells and RMock cells treated with AA. (A) Representative chromatograms of 15-LO-derived lipid metabolites released by R15L cells following 5 min treatment with 10 μM AA. MRM chromatograms are shown for (a) 15-oxo-EETE-PFB (m/z 317 \rightarrow 273), (b) [$^2\text{H}_6$]-5-oxo-EETE-PFB internal standard (m/z 326 \rightarrow 279), (c) 15-(R,S)-HETE-PFB (m/z 319 \rightarrow 219), and (d) [$^2\text{H}_8$]-15-(S)-HETE-PFB internal standard (m/z 327 \rightarrow 226); (B) Concentration-time graph of 15-HETE (R and S-form) released by R15L or RMock cells treated with 10 μM AA for 24 h; (C) Concentration-time graph of 15-oxo-EETE released by R15L or RMock cells treated with 10 μM AA for 24 h. Cell

supernatants were collected at each time point. Lipid metabolites in the cell supernatants were extracted and derivatized with PFB. Determinations were conducted in triplicate (means \pm S.E.M.) by stable isotope dilution chiral LC-ECAPCI/MRM/MS analyses of PFB derivatives.

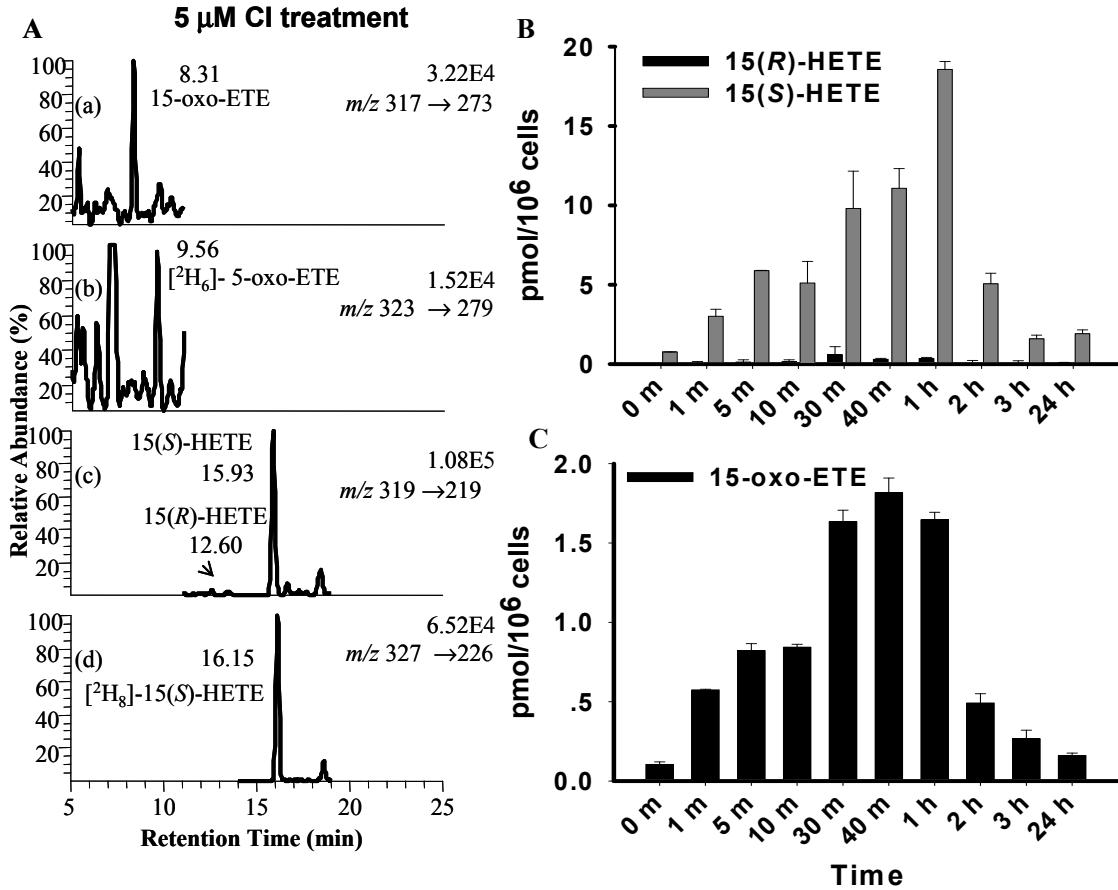


Figure 2.5 LC-MRM/MS analysis and quantitation of 15-LO-derived eicosanoids from R15L cells treated with CI. (A) Representative chromatograms of endogenous 15-LO-derived lipid metabolites released by R15L cells following 40 min treatment with 5 μ M CI. MRM chromatograms are shown for (a) 15-oxo-EETE-PFB (m/z 317 \rightarrow 273), (b) [$^2\text{H}_6$]-5-oxo-EETE-PFB internal standard (m/z 326 \rightarrow 279), (c) 15-(R,S)-HETE-PFB

(m/z 319 \rightarrow 219), and (d) [$^2\text{H}_8$]-15-(*S*)-HETE-PFB internal standard (m/z 327 \rightarrow 226); **(B)** Concentration-time graph of 15-HETE (*R* and *S*-form) released by R15L treated with 5 μM CI for 24 h; **(C)** Concentration-time graph of 15-oxo-EETE released by R15L cells treated with 5 μM CI for 24 h. Cell supernatants were collected at each time point. Lipid metabolites in the cell supernatants were extracted and derivatized with PFB. Determinations were conducted in triplicate (means \pm S.E.M.) by stable isotope dilution chiral LC-ECAPCI/MRM/MS analyses of PFB derivatives.

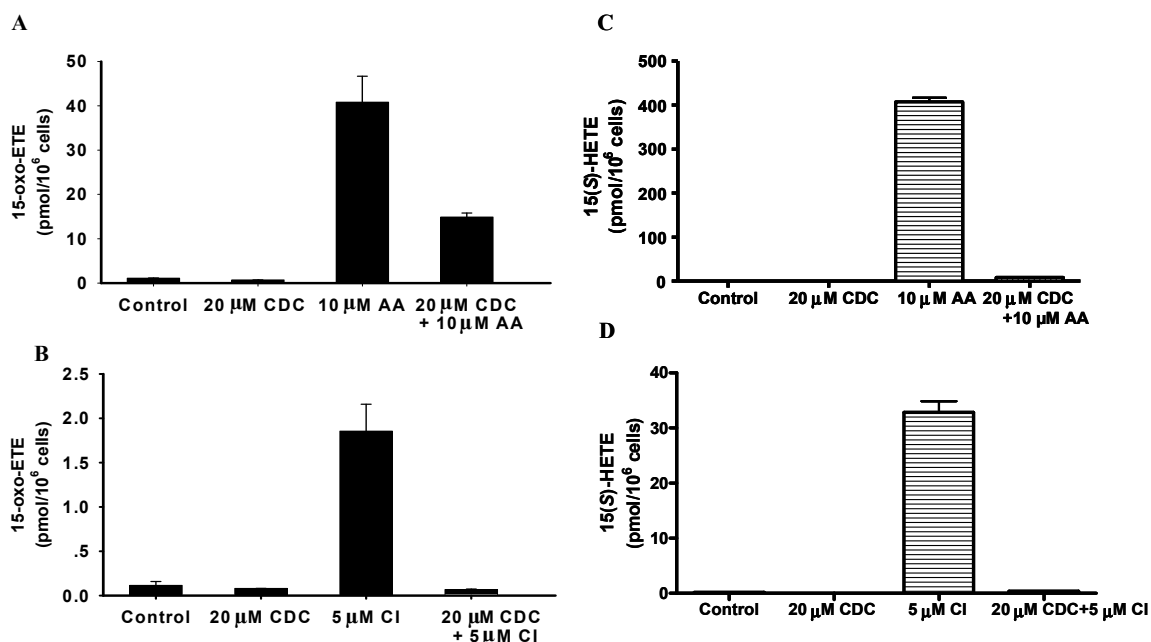


Figure 2.6 Effect of LO inhibitor (CDC) on formation of 15-oxo-EETE and 15(S)-HETE by R15L cells. **(A)** 15-Oxo-EETE formation by cells that were treated with 10 μM AA or pre-treated with 20 μM CDC for 40 min prior to vehicle or 10 μM AA treatment. **(B)** 15-Oxo-EETE formation by cells that were treated with 5 μM CI or pre-treated with 20 μM CDC for 40 min prior to vehicle or 5 μM CI treatment. **(C)** 15(*S*)-HETE formation

by cells that were treated with 10 μ M AA or pre-treated with 20 μ M CDC for 40 min prior to vehicle or 10 μ M AA treatment. **(D)** 15(*S*)-HETE formation by cells that were treated with 5 μ M CI or pre-treated with 20 μ M CDC for 40 min prior to vehicle or 5 μ M CI treatment. Lipid metabolites in the cell media were extracted and derivatized with PFB. 15-Oxo-ETE and 15(*S*)-HETE concentrations were determined in triplicate by stable isotope dilution LC-ECAPCI/MRM/MS analyses of PFB derivatives. Values presented in bar graphs are means \pm S.E.M.

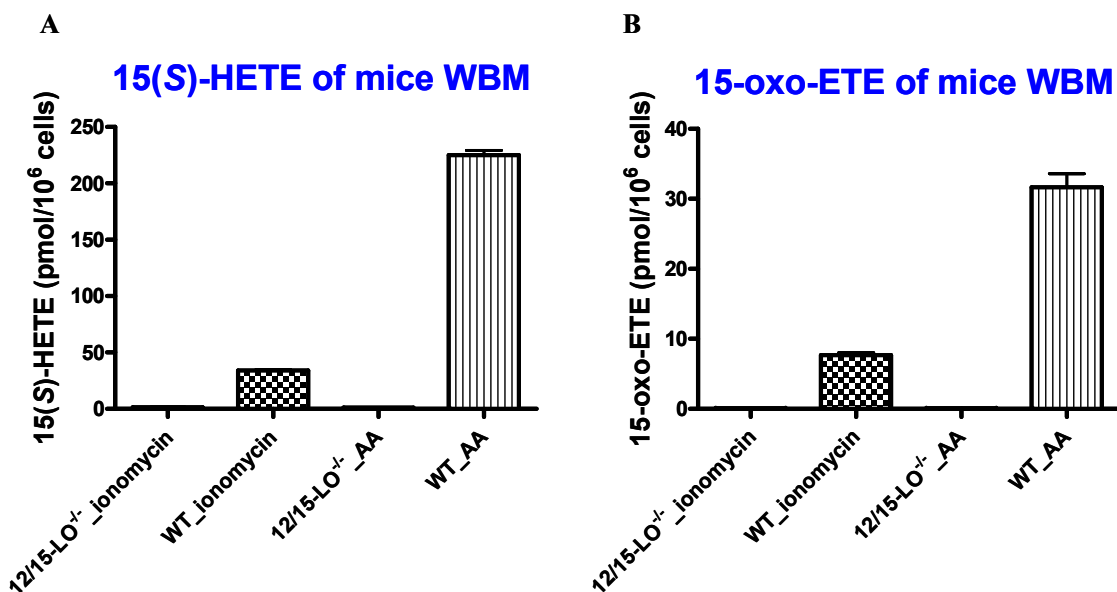


Figure 2.7 Quantitative analyses of 15(*S*)-HETE and 15-oxo-ETE released from ionomycin- or AA-treated whole bone marrow (WBM) from 12/15-LO deficient (12/15-LO^{-/-}) mice and wild-type (WT) mice by LC-ECAPCI/MS. **(A)** 15(*S*)-HETE formation by whole bone marrow from 12/15-LO^{-/-} mice and WT mice that were treated with 10 μ M AA or 5 μ M ionomycin for 30 min. **(B)** 15-oxo-ETE formation by whole

bone marrow from 12/15-LO^{-/-} mice and WT mice that were treated with 10 μM AA or 5 μM ionomycin for 30 min. Lipid metabolites in the cell media were extracted and derivatized with PFB. 15(*S*)-HETE and 15-oxo-ETE concentrations were determined in triplicate by stable isotope dilution by LC-ECAPCI/MRM/MS analysis of PFB derivatives. Values presented in bar graphs are means ± S.E.M.

2.4.6 Kinetics of 15(*S*)-HETE Metabolism to 15-oxo-ETE by R15L Cells – To study the kinetics of 15(*S*)-HETE metabolism in R15L cells, R15L cells were incubated with 15(*S*)-HETE (0.9 μM) for 3 h. The level of 15(*S*)-HETE in the cell media declined from 0.9 μM to being close to the limit of detection in 3 h (Fig. 2.8A). The half-life of 15(*S*)-HETE was determined to be 21 min and the pseudo first-order rate constant (*k*) was 0.0331 min⁻¹ (Fig. 2.8B). Concomitantly, the level of 15-oxo-ETE in the cell media was observed to peak within 5 min of 15(*S*)-HETE treatment with the concentration of 0.022 (± 0.002) μM, and declined to being close to the limit of detection in 3 h (Fig. 2.8C). The half-life of 15-oxo-ETE was determined to be 11 min and the pseudo first-order rate constant (*k*) was 0.0643 min⁻¹ (Fig. 2.8D).

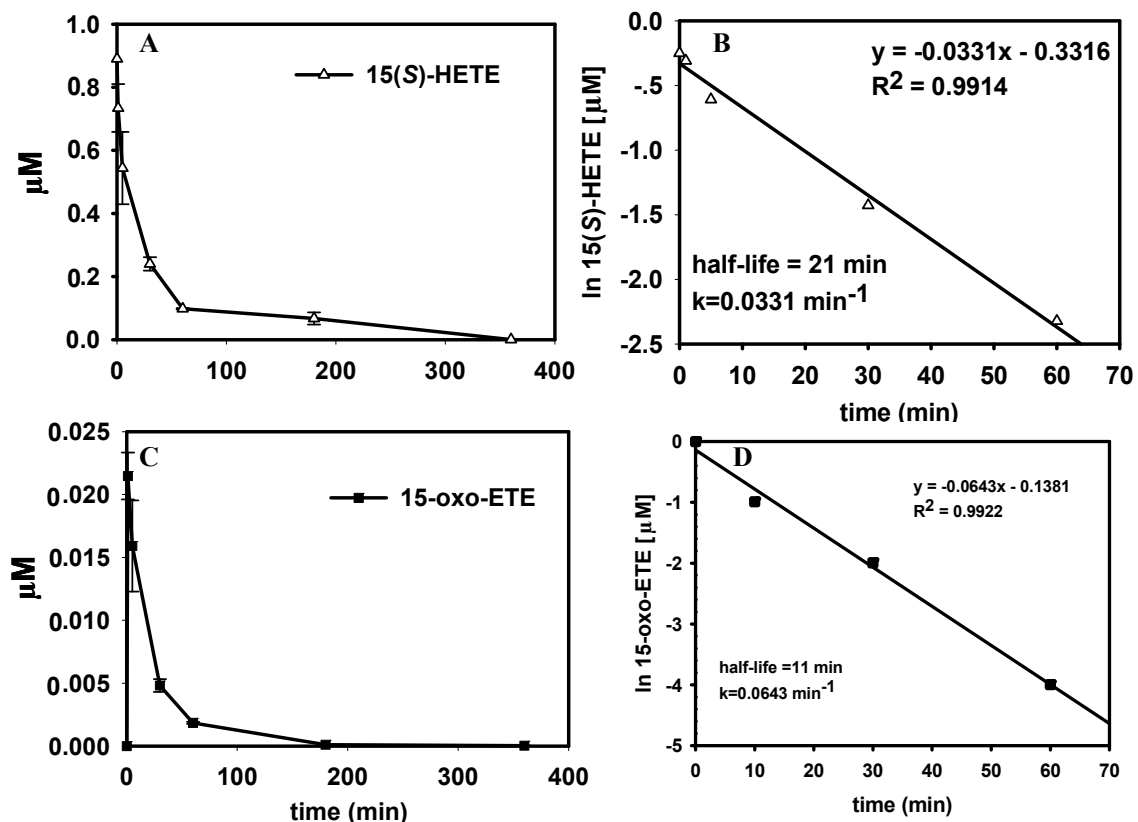


Figure 2.8 Kinetics of 15(S)-HETE metabolism by R15L cells. R15L cells were incubated with 15(S)-HETE (1 µM) for a period of 360 min. Supernatant was collected at different time points. Lipid metabolites [15(S)-HETE and 15-oxo-EETE] in the cell supernatant were extracted and derivatized with PFB and their concentrations were determined in triplicate (means \pm S.E.M.) by LC-ECAPCI/MRM/MS analysis. **(A)** Concentration-time plot of 15(S)-HETE (µM) remaining un-metabolized in R15L cell culture media; **(B)** Kinetic plot of 15(S)-HETE metabolism by R15L cells ($t_{1/2}$ =21 min and $k=0.0331 \text{ min}^{-1}$); **(C)** Concentration-time plot of 15-oxo-EETE (µM) produced in R15L cell culture media. **(D)** Kinetic plot of 15-oxo-EETE metabolism by R15L cells ($t_{1/2}$ =11 min and $k=0.0643 \text{ min}^{-1}$).

2.4.7 Effect of CAY10397 on 15-oxo-EETE and 15(*S*)-HETE in R15L Cells -

CAY10397 is a selective inhibitor of the 15-PGDH that oxidizes 15-hydroxyl group of prostaglandins (PGs) to a 15-oxo-group (Berry et al., 1983; Quidville et al., 2006). To determine the effect of CAY10397 on AA-derived 15(*S*)-HETE and 15-oxo-EETE, R15L cells were treated with 10 μ M AA for 10 min, with or without the pretreatment with various doses of CAY10397 (0-100 μ M) for 4 h. This resulted in a significant inhibition of the production of 15-oxo-EETE (Fig. 2.9A) and a simultaneous accumulation of 15(*S*)-HETE in a dose-dependent manner (Fig. 2.9B). To confirm that 15-PGDH was the enzyme that oxidized 15(*S*)-HETE to 15-oxo-EETE, R15L cells were treated with 50 nM 15(*S*)-HETE for 10 min, with or without the pretreatment with various doses of CAY10397 (0-100 μ M) for 4 h. 15(*S*)-HETE treatment alone gave rise to the production of 15-oxo-EETE (3 pmol/ 10^6 cells). CAY10397 pretreatment resulted in dose dependent inhibition of 15-oxo-EETE production. The inhibition reached 80% in the presence of 100 μ M CAY10397 (Fig. 2.9C). CAY10397 also caused a concomitant dose-dependent increase in 15(*S*)-HETE concentrations after the addition of exogenous 15(*S*)-HETE (Fig. 2.9D). CAY10397 treatment by itself in the absence of AA did not lead to 15-oxo-EETE generation (data not shown). The IC_{50} of CAY10397 on AA-mediated (Fig. 2.9A) or 15(*S*)-HETE-mediated (Fig. 2.9C) 15-oxo-EETE production were very similar at 17.3 μ M and 13.2 μ M, respectively. The Hill coefficient for the inhibition of 15(*S*)-HETE-derived 15-oxo-EETE was -1.2 indicating that the 15(*S*)-HETE and CAY10397 were binding at the same site (Fig. 2.9C). However, a Hill coefficient of -2.2 was obtained for the inhibition of AA-derived 15-oxo-EETE indicating that there was cooperativity in the inhibition of these more complex ligand/binding site interactions (Fig. 2.9A). The EC_{50} for

CAY10397-induced increase in AA-mediated 15(*S*)-HETE formation was 19.6 μM (Fig. 2.9B), which was similar to the IC_{50} of 17.3 μM for inhibition of AA-mediated 15-oxo-ETE formation (Fig. 2.9A). As expected, the Hill coefficient (-3.0) deviated from -1.0 because of cooperativity effects. The effect of CAY10397 on 15(*S*)-HETE concentrations after the addition of exogenous 15(*S*)-HETE was too complex to analyze using conventional non-linear binding models (Fig. 2.9D). This suggested that conversion of 15(*S*)-HETE to 15-oxo-ETE is more complex than simple 15-PGDH-mediated metabolism.

2.4.8 Effect of 15-oxo-ETE on Proliferation on HUVECs - In order to examine the effect of 15-oxo-ETE on cell proliferation, colorimetric BrdU ELISA assays were performed on HUVECs treated with different concentrations (1-20 μM) of 15-oxo-ETE for a 48 h period (Fig. 2.10A). BrdU incorporation was analyzed and the corresponding cell number was determined from a standard curve (Fig. 2.10B). DNA synthesis in the HUVECs (as measured by BrdU incorporation) was inhibited by 15-oxo-ETE (Fig. 2.10A). This resulted in a dose-dependent decrease in cellular proliferation as reflected by the cell count determined from the BrdU standard curve (Fig. 2.10C).

2.4.9 15-oxo-ETE Uptake into HUVECs - Cells were incubated with 1 μM or 10 μM of 15-oxo-ETE for 48 h. For 1 μM 15-oxo-ETE incubation, the intracellular concentrations of 15-oxo-ETE were measured during the time course. The intracellular concentrations of 15-oxo-ETE increased from below the limit of detection at 0 min to 408.08 (\pm 12.13) nM at 30 min, 154.18 (\pm 14.91) nM at 1 h, 70.18 (\pm 9.85) nM at 4 h and below the limit of detection after 24 h (Fig. 2.11A). In HUVECs incubated with 10 μM of 15-oxo-ETE, the intracellular concentrations of 15-oxo-ETE were measured at 3.19 (\pm 1.10) μM at 30

min, $2.48 (\pm 0.21) \mu\text{M}$ at 1 h, $2.42 (\pm 0.52) \mu\text{M}$ at 4 h and below the limit of detection after 24 h (Fig. 2.11B).

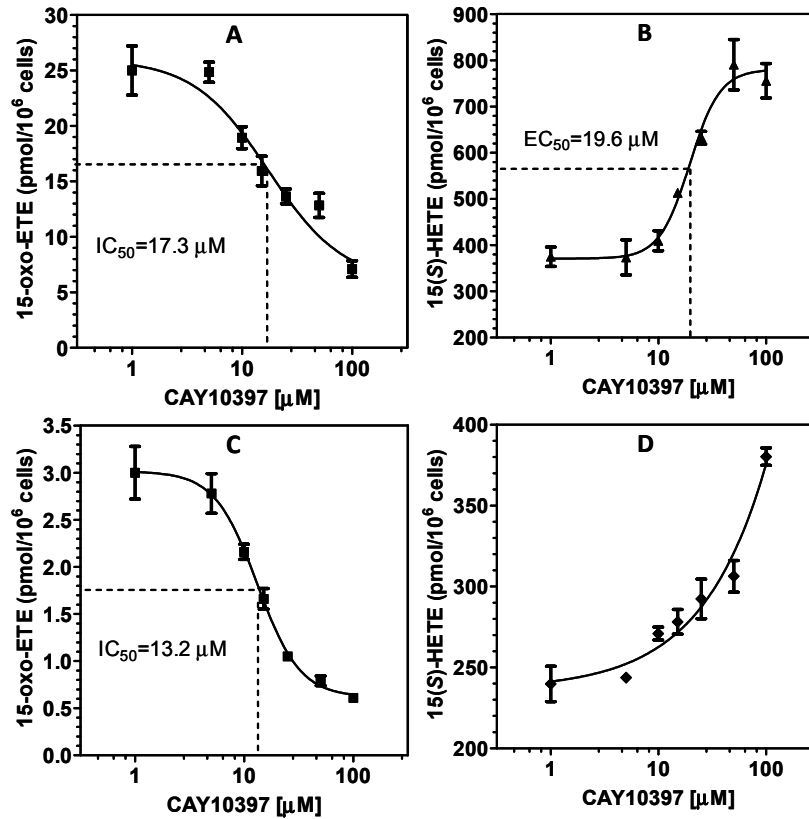


Figure 2.9 Dose-dependent effects of CAY10397 on the levels of 15-oxo-EETE and 15(S)-HETE released by R15L cells. (A) Dose-dependent inhibition curve of CAY10397 on 15-oxo-EETE released by R15L cells treated with $10 \mu\text{M}$ AA for 10 min following the pretreatment with CAY10397 for 4 h; (B) Dose-dependent curve of CAY10397 on 15(S)-HETE accumulation by R15L cells treated with $10 \mu\text{M}$ AA for 10 min following the pretreatment with CAY10397 for 4 h; (C) Dose-dependent inhibition curve of CAY10397 on 15-oxo-EETE released by R15L cells treated with 50 nM 15(S)-HETE for 10 min following the pretreatment with CAY10397 for 4 h; (D) Dose-dependent curve of CAY10397 on 15(S)-HETE accumulation by R15L cells treated with

50 nM 15(S)-HETE for 10 min following the pretreatment with CAY10397 for 4 h. Cell supernatants were collected at each time point. Lipid metabolites in the cell supernatants were extracted and derivatized with PFB. Determinations were conducted in triplicate (means \pm S EM) by stable isotope dilution chiral LC-ECAPCI/MRM/MS analyses of PFB derivatives.

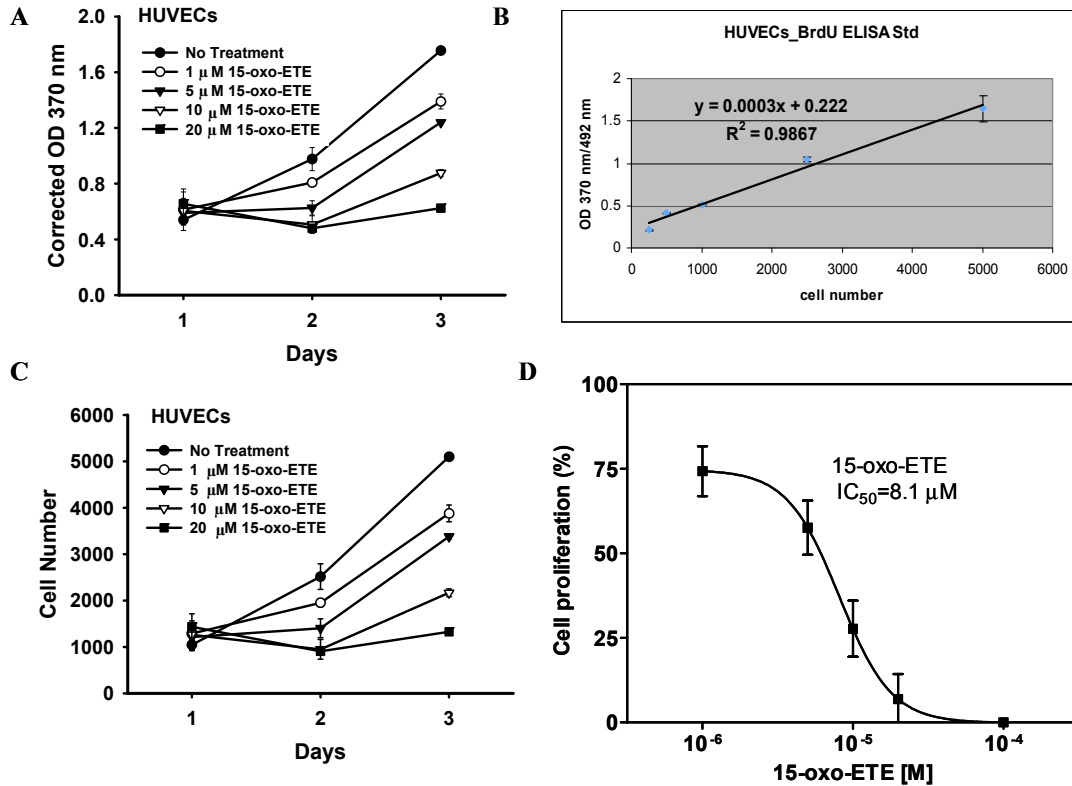


Figure 2.10 Effect of 15-oxo-EETE on cell proliferation of HUVECs. Determinations were conducted in triplicate (means \pm S.E.M.). Concentrations of 15-oxo-EETE were determined by LC-ECAPCI/MS. (A) HUVECs were treated with various doses (0-20 μ M) of 15-oxo-EETE for a period of 48 h. Cell proliferation in terms of DNA synthesis was determined by colorimetric BrdU ELISA assays. Absorbance was measured in triplicate at 370 nm with 492 nm as reference. (B) A standard curve of corrected OD370nm was determined with the various numbers of cells by the BrdU ELISA assay.

(C) The corresponding cell numbers with 15-oxo-EETE treatment were determined from the standard curve. (D) Inhibition constant of 15-oxo-EETE ($IC_{50}=8.1 \mu\text{M}$).

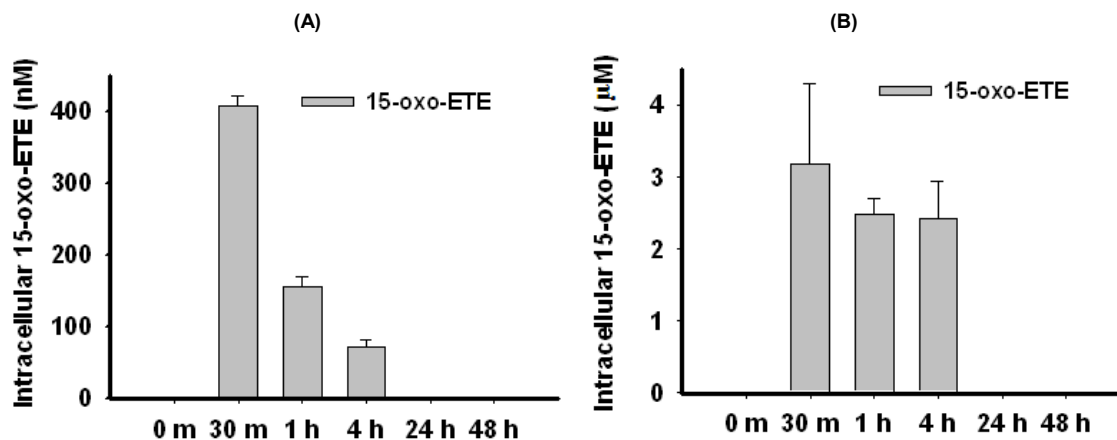


Figure 2.11 15-oxo-EETE uptake into HUVECs. (A) Intracellular levels of 15-oxo-EETE in HUVECs incubated with $1 \mu\text{M}$ 15-oxo-EETE for 48 h. (B) Intracellular levels of 15-oxo-EETE in HUVECs incubated with $10 \mu\text{M}$ 15-oxo-EETE for 48 h.

2.5 Discussion

IL-4 stimulated human monocytes were found to secrete primarily 15(S)-HETE and 15-oxo-EETE when treated with exogenous AA or with CI (Fig. 2.2). Brinckmann *et al.* reported that 15-LO-1 translocated to plasma membrane in a calcium-dependent manner in rabbit hematopoietic cells and that the translocation activated the oxygenase activity of the enzyme (Brinckmann *et al.*, 1998). It is known that 15-LO-1 has a broad substrate specificity so that it can oxidize esterified lipids as well as protein-lipid assemblies (Kuhn and O'Donnell, 2006). Furthermore, Maskrey *et al.* showed that when

IL-4-treated monocytes were stimulated with CI, they generated predominantly esterified 15-HETE; with many fold less free 15-HETE (Maskrey et al., 2007). These studies suggest that CI treatment of the monocytes resulted in translocation of 15-LO-1 to the plasma membrane so that it was no longer present in the cytosol. 15(*S*)-HPETE was then formed primarily on esterified AA rather than from free AA released by CI-mediated translocation of cytosolic phospholipase A₂ (cPLA₂) to the membrane. The resulting esterified 15(*S*)-HPETE was then reduced to 15(*S*)-HETE (Schnurr et al., 1999) and a significant amount then released by cPLA₂-mediated hydrolysis of the esterified 15(*S*)-HETE and released from the cells as suggested previously by Chaitidis *et al.* (Chaitidis et al., 1998). Indeed, CI or ionomycin treatment of R15L cells and mice WBM led to the production of 15(*S*)-HETE and 15-oxo-EETE (Figs. 2.2 and 2.7), confirming that they are metabolites of endogenously-derived AA. These data also suggest that 15(*S*)-HETE is the predominant precursor of 15-oxo-EETE in 15-LO-1 mediated metabolism of endogenously-derived AA. This contrasts with COX-2-mediated formation of 15-oxo-EETE, which could be derived from 15(*S*)-HPETE, 15(*S*)-HETE, or the corresponding 15(*R*)-enantiomers (Lee et al., 2007).

A targeted quantitative chiral lipidomics analysis showed that 15(*S*)-HETE and 15-oxo-EETE were also major metabolites derived from exogenous and endogenous AA in R15L cells (Figs. 2.4 and 2.5). Moreover, the RMock cells that do not express any human 15-LO-1 failed to generate these metabolites (Figs. 2.4 and 2.5). Pre-treatment of R15L cells with CDC, a LO inhibitor, led to a significant reduction in 15-oxo-EETE and 15(*S*)-HETE levels that were produced by AA treatment alone (Fig. 2.6A and 2.6C respectively). CDC pre-treatment also led to complete inhibition of 15-oxo-EETE and

15(*S*)-HETE production by CI treatment in R15L cells (Fig. 2.6B and 2.6D respectively). CDC treatment by itself did not generate any 15(*S*)-HETE and 15-oxo-EETE in R15L cells. Thus, these data provide further evidence that 15(*S*)-HETE and 15-oxo-EETE are 15-LO-specific metabolites of AA. 15(*S*)-HETE was found to be rapidly converted into 15-oxo-EETE, with approximately 90% conversion occurring within 3 h in the R15L cells (Fig. 2.8A). A kinetic plot (Fig. 2.8B) revealed that the half-life of 15(*S*)-HETE in R15L cells was 21 min with a pseudo first-order rate constant of 0.0331 min^{-1} . These data are consistent with findings from a similar study involving COX-2 expressing RIES cells (Lee et al., 2007).

15-PGDH catalyzes NAD^+ -mediated oxidation of 15(*S*)-hydroxyl group of PGs and lipoxins (Quidville et al., 2006; Tai et al., 2007). It is a key PG catabolism enzyme, converting (for example) $\text{PGF}_{2\alpha}$ to 15-oxo- $\text{PGF}_{2\alpha}$ (Fig. 2.1). Our previous studies had established 15-oxo-EETE as a downstream metabolite of 15(*S*)-HETE (Lee et al., 2007); however, the enzyme responsible for this oxidation was not identified. In the present study we have shown that the specific 15-PGDH inhibitor (CAY10397) significantly decreased the production of 15-oxo-EETE and the metabolism of 15(*S*)-HETE in the macrophages treated with either AA (Fig. 2.9A) or 15(*S*)-HETE (Fig. 2.9C). The IC_{50} values for CAY10397-mediated 15-oxo-EETE inhibition were determined to be 17.3 and 13.2 μM , respectively. There was a concomitant increase in 15(*S*)-HETE concentrations after inhibition of AA- (Fig. 2.9B) and 15(*S*)-HETE-mediated (Fig. 2.9D) 15-oxo-EETE formation. These data clearly show that 15-oxo-EETE arose through the oxidation of 15(*S*)-HETE by murine 15-PGDH. Mouse 12/15-LO, which is the counterpart of human 15-LO-1, produces both 12-LO- and 15-LO-derived lipid metabolites (Fig. 2.7) (Kuhn

and O'Donnell, 2006; Middleton et al., 2006). Mouse WBM were found to produce 15(*S*)-HETE, 15-oxo-EETE (Figure 2.7) and 12(*S*)-HETE (data not shown). Additional studies will be required to determine whether 12-oxo-EETE is also formed and the potential biological consequences. Thus, it is not clear that the phenotypes in 12/15-LO-deficient mice are due to lack of 12-LO- or 15-LO-derived lipid mediators. In this regard, the mouse R15L macrophage cell line, which expresses human 15-LO-1, provided an excellent model to identify 15-LO-derived lipid metabolites.

15-oxo-EETE was rapidly cleared from the R15L cells, with a half-life of only 11 min, indicating that it underwent further metabolism (Fig. 2.8D). We showed previously that 15-oxo-EETE forms a GSH-adduct through GSH *S*-transferase-mediated Michael addition (Lee et al., 2007). Other studies have shown that AA-derived metabolites such as leukotriene C₄ and 5-oxo-EETE can also form GSH-adducts (Murphy and Zarini, 2002; Blair, 2006). This suggests and indeed that 15-oxo-EETE is also metabolized to a GSH-adduct in the R15L cells (Fig. 2.12A) and the GSH-adduct is then cleaved by GGTP on the cell membrane to form a cysteinylglycine adduct extracellularly (Fig. 2.12B), which would account in part for its rapid clearance.

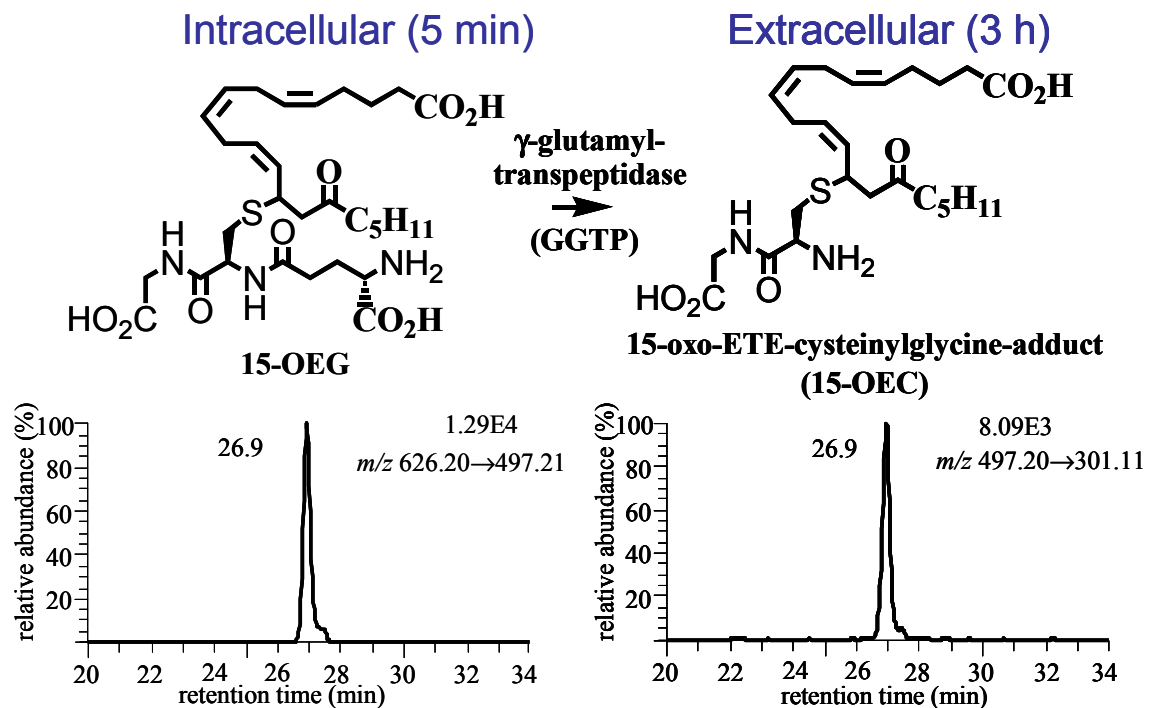


Figure 2.12 LC-MRM/MS analysis of GSH and cysteinylglycine adducts after incubation of R15L cells with 15-oxo-ETE (30 μ M). (A) Intracellular formation and the representative chromatogram of 15-oxo-ETE-GSH adducts (15-OEG) in R15L cells after incubated with 15-oxo-ETE for 5 min. (B) Formation and the representative chromatogram of 15-oxo-ETE-cysteinylglycine (15-OEC) adduct in the extracellular milieu of R15L cells after cells were incubated with 15-oxo-ETE for 3 h.

A previous study reported that 15-oxo-ETE has very low but detectable chemotactic activity in human monocytes *in vitro* (Sozzani et al., 1996). Another study reported that 15-oxo-ETE can inhibit proliferation in breast cancer cell lines, however, only at concentrations exceeding 100 μ M (O'Flaherty et al., 2005). The present study has shown that 15-oxo-ETE inhibits BrdU incorporation and HUVEC proliferation in a time-

dependent manner at much lower concentrations (down to 1 μM) than reported for breast cancer cells (Fig. 2.10). Rapid 15-oxo-EETE uptake in R15L cells was quantified in order to confirm that this pharmacological effect was in fact due to the presence of intracellular 15-oxo-EETE. Rapid uptake was observed at extra-cellular concentrations of 1 μM (Fig. 2.11A) and 10 μM (Fig. 2.11B) showing that 15-oxo-EETE can readily cross the plasma membrane.

The 15-oxo-EETE analogs, 5-oxo-EETE and 15d-PGJ₂, (15-deoxy- Δ 12,14-prostaglandin J₂, Fig. 2.1) modulate cell proliferation and apoptosis as peroxisome proliferator-activated receptor (PPAR) γ agonists (O'Flaherty et al., 2005). PPAR γ agonists inhibit experimental models of atherosclerosis and the formation of macrophage foam cells (Li et al., 2004). It has been proposed that 15d-PGJ₂ inhibits proliferation by covalently binding to the thiol residues in I κ B kinase or p50 subunit of NF- κ B through a Michael addition reaction to block the proteins from performing their survival function, using a PPAR γ independent mechanism (Cernuda-Morollon et al., 2001). The similar structural features present in 5-oxo-EETE, 15d-PGJ₂ and 15-oxo-EETE (Fig. 2.1) suggest that 15-oxo-EETE might also modulate cell proliferation and apoptosis through PPAR γ -dependent and/or PPAR γ -independent mechanism.

Our observation that 15-oxo-EETE can inhibit HUVEC proliferation provides a novel mechanism that could promote endothelial dysfunction (Carmeliet, 2005). It is interesting to note that 15-PGDH is down-regulated *in vivo* in colorectal cancer (Backlund et al., 2005). In view of our new findings, it is intriguing to speculate that down-regulation of 15-PGDH inhibits the production of 15-oxo-EETE and suppresses the

anti-proliferative effect of 15-oxo-EETE on ECs, thus potentially exacerbating colorectal cancer. Moreover, the capability of 15-oxo-EETE to inhibit EC proliferation suggests that it might be involved in other conditions where macrophage and/or endothelial cell dysfunction play a role such as in chronic inflammation, atherosclerosis, leukemia, and asthma. Chronic inflammation is known to be involved as a critical component in angiogenesis as well as cancer (Fierro et al., 2002). Therefore, depending on the location and the local environment *in vivo*, reduction of EC proliferation and migration in response to 15-oxo-EETE treatment might also be responsible for anti-inflammatory activity. Previous studies have demonstrated that overexpression of 15-LO-1 is associated with an anti-inflammatory response in both rabbit and murine models (Merched et al., 2008). Furthermore, aspirin-triggered 15-LO-1 metabolites of AA (lipoxins) have an anti-inflammatory activity through inhibition of EC proliferation (Fierro et al., 2002). Lipoxins have also been shown to promote resolution, a process known to involve active biochemical programs that enables inflamed tissues to return to homeostasis (Serhan et al., 2008). 15-LO-1 activation during the process of inflammation has also been correlated with switching the metabolism of AA and other ω -3 polyunsaturated fatty acids to produce pro-resolving lipid mediators such as resolvins and protectins. Taken together, 15-LO-1 up-regulation can result in the production of anti-inflammatory as well as pro-resolving activities (Serhan et al., 2008). Localized formation of 15-oxo-EETE production *in vivo* could be involved in both of these processes.

In summary, our studies have provided additional insight into IL-4-induced 15-LO-1 signaling in monocyte/macrophages and potential cell-cell interactions (Fig. 2.13). After IL-4 binds to its receptor, 15-LO-1 expression is induced via Janus kinase 1 (JAK1)

activation, followed by dimerization and nuclear trans-localization of signal transducer and activator of transcription 6 (Stat6) (Chatila, 2004). With elevated intracellular calcium concentrations, 15-LO-1 is recruited to the inner side of the plasma membrane where it converts esterified AA to 15(*S*)-HPETE. Esterified 15(*S*)-HPETE is reduced to 15(*S*)-HETE and released as the free acid by c-PLA₂. The 15(*S*)-HETE is then oxidized to 15-oxo-ETE by 15-PGDH, and 15-oxo-ETE is conjugated to form a 15-oxo-ETE-GSH-adduct (OEG), which is then hydrolyzed by γ -glutamyltranspeptidase (GGTP) to a 15-oxo-ETE-cysteinylglycine-adduct (OEC) by R15L cells (Figs. 2.12 and 2.13) (Lee et al., 2007). Released 15-oxo-ETE can inhibit EC proliferation which could further prevent EC growth and that in turn could lead to the inhibition of angiogenesis. In the absence of 15-PGDH (Backlund et al., 2005), no 15-oxo-ETE would be formed and therefore the anti-angiogenesis activity on ECs would be lost. This could then lead to increased tumor growth and metastasis. Therefore, these studies provide a pharmacological basis for the design of new targeted therapeutic strategies to inhibit angiogenesis.

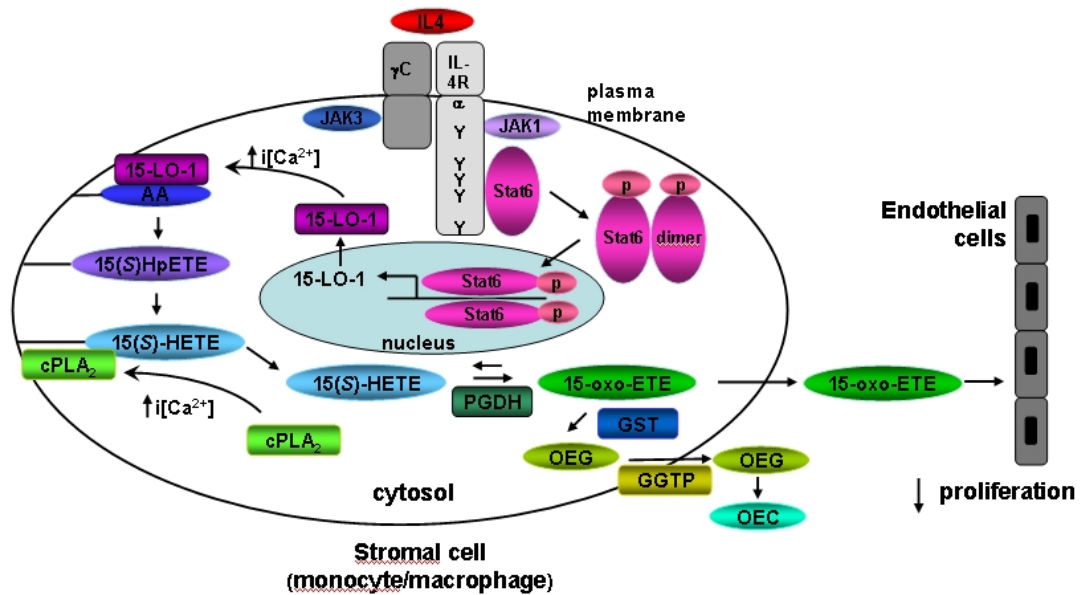


Figure 2.13 Formation and action of 15-LO-1-derived eicosanoids in a monocyte/macrophage cell model. IL-4 binds to its receptor, and activates JAK1, which causes dimerization and nuclear trans-localization of transcription 6 (Stat6). The dimerized Stat6 binds to DNA stimulating the production of 15-LO-1. When intracellular calcium concentrations increase, 15-LO-1 is recruited to the inner side of the cell membrane where it metabolizes AA to 15(S)-HPETE and 15(S)-HETE which is released by c-PLA₂ from the plasma membrane. 15(S)-HETE is then oxidized to 15-oxo-EETE by intracellular 15-PGDH and 15-oxo-EETE is conjugated to form OEG, which is released and hydrolyzed by GGTP to give OEC. Released intact 15-oxo-EETE can participate in cell-cell interactions such as with ECs to inhibit proliferation.

CHAPTER 3

11-Oxo-Eicosatetraenoic Acid is a Novel Cyclooxygenase-2/15-Hydroxyprostaglandin Dehydrogenase-Derived Endogenous Arachidonic Acid Metabolite

3.1 Abstract

Previous studies have shown that COX-2 is up-regulated during carcinogenesis while 15-PGDH is down-regulated. 11(*R*)-HETE is a major eicosanoid formed from arachidonic acid metabolism in both rat (RIES) and human (Caco-2) epithelial cell lines that express COX-2. 11(*R*)-HETE was metabolized primarily to 11-oxo-EETE. 11-oxo-EETE as well as 15-oxo-EETE was revealed by a specific LC-MRM/MS method to be secreted in nM concentrations when AA was added to RIES and Caco-2 cells. Pre-treatment of the RIES cells with the 15-PGDH inhibitor (CAY10397) decreased AA- and 11(*R*)-HETE-mediated formation of 11-oxo-EETE in a dose-dependent manner. We have also made the surprising observation that 11(*R*)-HETE is an excellent substrate for 15-PGDH, with a catalytic efficiency similar to that found for 15(*S*)-HETE. This confirmed that epithelial cell-derived 15-PGDH was responsible for catalyzing the conversion of 11(*R*)-HETE to 11-oxo-EETE. In comparison to the rat cell line (RIES cells), 11(*S*)-HETE and 15(*R*)-HETE were observed in the human cell line (Caco-2 cells), which was most likely due to the back reduction of 11-oxo-EETE and 15-oxo-EETE by aldo-keto reductases (AKRs) in the human Caco-2 cells with increased reductase activity when compared with the RIES cells. Furthermore, the formation of 11-oxo-EETE-GSH adduct (11-OEG) and its corresponding cysteinylglycine adduct were also identified in RIES cells by LC-MS.

3.2 Introduction

Endogenous factors such as COX-derived PGE₂ can increase the proliferation of tumor cells through multiple mechanisms including activation of plasma membrane G-protein-coupled receptors and nuclear PPAR γ receptors (Wang and Dubois, 2010) up to the point where they need a new blood supply (Folkman, 1995). Tumors accomplish this goal through the release of bioactive substances such as vascular endothelial growth factor (VEGF) that stimulate angiogenesis by increasing endothelial cell proliferation (Breen, 2007). The concept has evolved that there is an “angiogenic switch” from endogenous substances produced by normal physiological processes such as angiostatin (O'Reilly et al., 1994) that inhibit endothelial cell proliferation and so prevent the progression of cancer; and pro-proliferative substances such as VEGF produced by the tumor that aid in progression (Bergers and Benjamin, 2003). Some 27 different endogenous proteins and small molecules have been identified that can inhibit angiogenesis *in vitro* (Ribatti, 2009). As a result, numerous therapeutic strategies have been developed to inhibit angiogenesis and modulate tumor cell proliferation (Fujita et al., 2008).

COX-2, an immediate-early inducible gene that is involved in inflammation, mitogenesis, and signal transduction pathways is up-regulated in many tumor types (Wang and Dubois, 2010). Traditional non-steroidal anti-inflammatory drugs (NSAIDs), which inhibit both COX-1 and COX-2 were shown in an observational study to be associated with a decreased risk for colon cancer (Thun et al., 1991). A steady-state level of PGE₂ is maintained in tumors from PGE-synthase-mediated metabolism of COX-2-derived PGH₂ and a catabolic pathway involving 15-PGDH-mediated inactivation to the

15-oxo-PGE₂ metabolite (Fig. 3.1) (Tai et al., 2007; Hughes et al., 2008). The 15-oxo-PGE₂ is then converted to 15-oxo-13,14-dihydro-PGE₂ by 15-oxo-prostaglandin- Δ^{13} reductase (Chou et al., 2007). Loss of 15-PGDH expression correlates with tumor formation in bladder, breast, colon, intestine, kidney, lung, pancreas, stomach, and skin

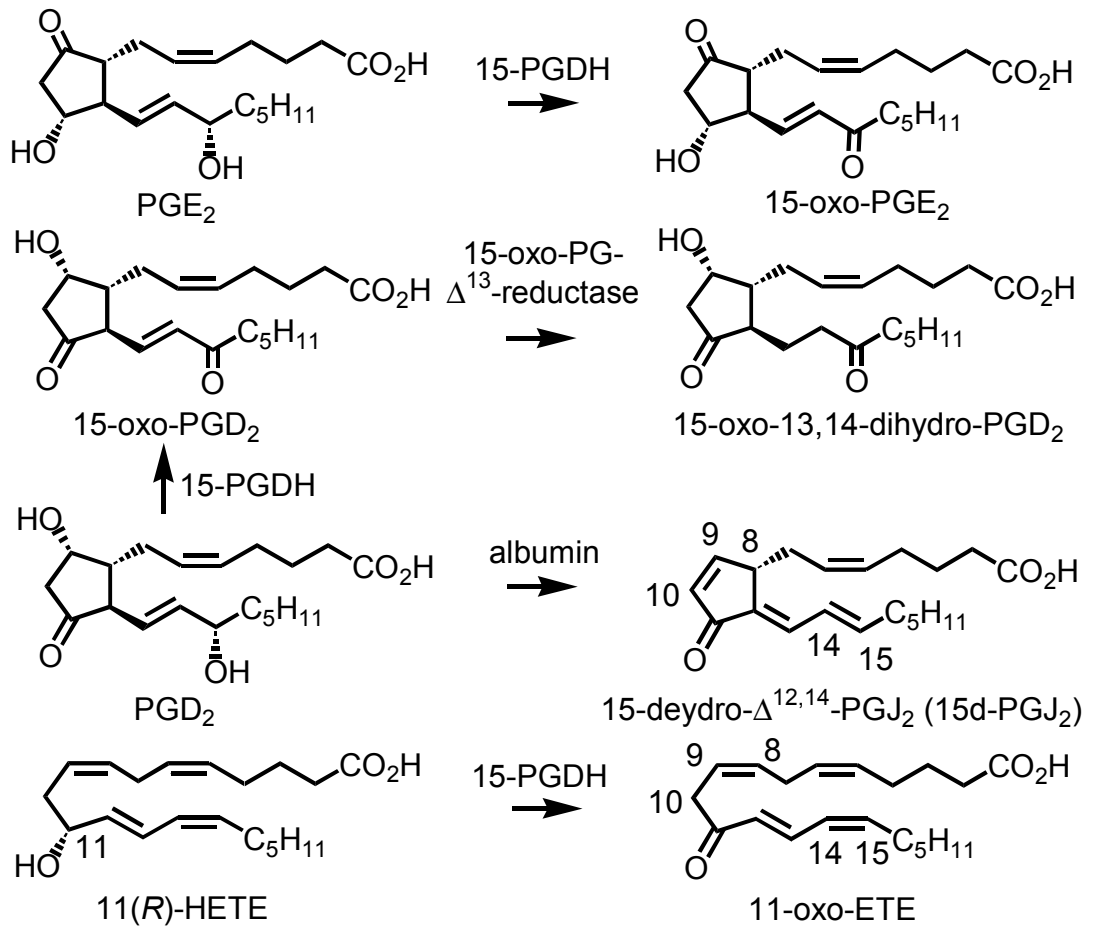


Figure 3.1 The formation of 15-oxo-PGE₂ from PGE₂, 15-oxo-PGD₂ and 15d-PGJ₂ from PGD₂, and 11-oxo-ETE from 11(R)-HETE.

cancer (Backlund et al., 2005; Tai et al., 2007; Celis et al., 2008; Hughes et al., 2008; Thiel et al., 2009; Pham et al., 2010; Tseng-Rogenski et al., 2010). Thus, up-regulation of COX-2 (Wang and Dubois, 2010) and down-regulation of PGDH (Backlund et al., 2005) provides endogenous oncogenic mediators that are significant contributors to cancer progression (Markowitz and Bertagnolli, 2009).

PGD₂, another COX-derived metabolite is also metabolized by 15-PGDH to form 15-oxo-PGD₂, which is then converted to the corresponding inactive 13,14-dihydro-derivative (Rangachari and Betti, 1993), most likely by a 15-oxo-prostaglandin- Δ^{13} reductase (Fig. 3.1) (Chou et al., 2007). Alternatively PGD₂ undergoes albumin-mediated dehydration to give PGJ₂, followed by a further dehydration to give 15d-PGJ₂ (Fig. 3.1) (Fitzpatrick and Wynalda, 1983). Previous studies have shown that 15d-PGJ₂ is a PPAR γ receptor agonist that induces adipogenesis (Forman et al., 1995) and inhibits the proliferation of HUVECs in culture (Xin et al., 1999). However, 15d-PGJ₂ is known to have multiple activities including its ability to induce endothelial cell apoptosis and inhibit the NF- κ B pathway (Bishop-Bailey and Hla, 1999; Scher and Pillinger, 2009). In contrast to the anti-proliferative macrophage/monocyte-derived 15-oxo-ETE that we identified recently (Wei et al., 2009) there is little evidence to show that 15d-PGJ₂ can be formed in concentrations commensurate with an *in vivo* anti-proliferative role (Ide et al., 2003).

There has been enormous interest in the potential activity of COX-derived PGs as mediators of cell proliferation and tumorigenesis (Wang and Dubois, 2010). In contrast, COX-derived lipid hydroperoxides have been largely ignored in spite of their importance as initial products of COX-mediated arachidonic acid metabolism (Lee et al., 2007).

Numerous studies of purified COX-1 and COX-2 enzymes from sheep, mouse and humans have shown that 11(*R*)-HETE, 15(*S*)-HETE, and 15(*R*)-HETE metabolites are formed in relatively high amounts (Lee et al., 2005). The HETEs arise from reduction of the corresponding HPETEs either through the peroxidase activity of COX enzymes or through the action of cytosolic peroxidases (Blair, 2008). We showed that 11(*R*)-HETE is a major eicosanoid secreted at early time-points by arachidonic acid-treated rat intestinal epithelial cells that stably express COX-2 (RIES cells) but that it is rapidly metabolized so that PGE₂ becomes the major metabolite at later time-points (Lee et al., 2007). The second most abundant metabolite (15(*S*)-HETE) is metabolized to 15-oxo-ETE as would be anticipated from its configuration at C-15 and the known substrate specificity of 15-PGDH (Wei et al., 2009). In our earlier study (Lee et al., 2007), we were unable to identify the metabolites of 11(*R*)-HETE that were secreted by the RIES cells. We have now synthesized 11-oxo-ETE and developed a LC-MRM/MS method for its analysis. This method was then used to determine whether 11-oxo-ETE is secreted from COX-2 expressing RIES cells and human Caco-2 cells (Lee et al., 2005; Kamitani et al., 1998) and to identify the dehydrogenase responsible for its formation.

3.3 Materials and Methods

3.3.1 Materials – Arachidonic acid (peroxide-free), [²H₆]-5-oxo-ETE, 11(*R,S*)-HETE, [²H₈]-12(*S*)-HETE, 15(*R,S*)-HETE, [²H₈]-15(*S*)-HETE, 15-oxo-ETE, 15-oxo-PGE₂, CAY10397, recombinant human 15-PGDH, murine COX-2 polyclonal antibody and horseradish peroxidase conjugated anti-rabbit monoclonal IgG (mIgG) were purchased from Cayman Chemical Co. (Ann Arbor, MI). The Dess-Martin reagent [periodinane; 1,1,1-Tris(acetyloxy)-1,1-dihydro-1,2-benziodoxol-3-(1*H*)-one], PFB bromide, Trizma-

HCl, lipoxidase from Glycine max (soybean), sodium borohydride, β -Nicotinamide adenine dinucleotide hydrate (NAD⁺) and FBS were purchased from Sigma-Aldrich (St. Louis, MO). RPMI-1640 media, Medium 199 (M199), D-glucose, L-glutamine, penicillin, streptomycin, pre-cast 4-12% NuPAGE Novex Bis-Tris gels, 0.45 μ M nitrocellulose membranes and protease inhibitor cocktail were supplied by Invitrogen (Carlsbad, CA). BCA protein assay reagent was obtained from Pierce Biotechnology (Rockford, IL). Caco-2 cells and Eagle's minimum essential medium (EMEM) were obtained from American Type Culture Collection (ATCC) (Manassas, VA). High performance LC grade water, hexane, methanol, isopropanol and dichloromethane were obtained from Fisher Scientific (Fair Lawn, NJ). Gases were supplied by BOC Gases (Lebanon, NJ). [¹³C₂₀]-AA was obtained from Spectra Stable Isotopes (Columbia, MD). Pure 15(*S*)-HPETE was prepared by soybean oxidation of AA using standard procedures. 11(*R*)-HPETE was a kind gift from Dr. Alan Brash (Vanderbilt University, Nashville, TN). RIES cells were a kind gift from Dr. Raymond N. DuBois (University of Texas M. D. Anderson Cancer Center, Houston, TX), and HCT-116 cells were a generous gift from Dr. Thomas Eling, National Institute of Environmental Health Sciences, NIH, Research Triangle Park, NC). The final concentration of ethanol in the culture media was less than 0.1 %. Cell numbers (typically 10⁶/plate) were counted by a hemocytometer.

3.3.2 Mass Spectrometry - The quantitative targeted lipidomics profile was obtained on a TSQ Quantum Ultra AM mass spectrometer (Thermo Scientific, San Jose, CA) as described in Chapter 2. The following MRM transitions were monitored with PFB-derivatized eicosanoids: 11-oxo-ETE (m/z 317 \rightarrow 165), 15-oxo-ETE (m/z 317 \rightarrow 113), [²H₆]-5-oxo-ETE (m/z 323 \rightarrow 279), 15-HETEs (m/z 319 \rightarrow 219), [²H₈]-15(*S*)-HETE (m/z

327 → 226), 11-HETEs (m/z 319 → 167), and [$^2\text{H}_8$]-12(*S*)-HETE (m/z 327 → 184). An ion trap LTQ mass spectrometer (Thermo Fisher, San Jose, CA) equipped with electrospray ionization (ESI) source was used to acquire the complete product ion spectra for structural confirmation of 11- and 15-oxo-ETE. Operating conditions were as follows: spray voltage at 4 kV and capillary temperature at 220 °C. Nitrogen was used as the sheath gas and auxiliary gas, set at 35 and 18 (in arbitrary units), respectively. The 11-oxo-ETE (m/z 341, $[\text{M}+\text{Na}]^+$), 15-oxo-ETE (m/z 341, $[\text{M}+\text{Na}]^+$) and $^{13}\text{C}_{20}$ -15-oxo-ETE (m/z 361, $[\text{M}+\text{Na}]^+$) were monitored in the full scan positive mode. For the analysis of sulfhydryl adducts formed in 11(*R,S*)-HETE-treated RIES cells, an ion-trap Finnigan LTQ XL mass spectrometer (Thermo Scientific, San Jose, CA) was equipped with an ESI source and operated in the positive ion mode. Operating conditions were as follows: The spray voltage was 5000 V, the capillary voltage was 46 V, the capillary temperature was 275 °C and the tube lens was at 50 V. Nitrogen was used for the sheath gas and auxiliary gas set at 30 and 10 (in arbitrary units), respectively. The MS/MS spectrum for 11-OEG was acquired by CID of MH^+ at m/z 626 (collision energy, 20 eV). Accurate mass measurements were obtained using ESI on a Thermo LTQ-FT mass spectrometer at a resolution of 100,000 and NMR spectra were obtained on a Bruker 500 MHz NMR instrument.

3.3.3 Liquid Chromatography - Normal phase chiral LC-ECAPCI/MS analyses for PFB-derivatized lipidomics profile were conducted using a Waters Alliance 2690 high performance LC system (Waters Corp., Milford, MA). A Chiralpak AD-H column (250 x 4.6-mm internal diameter (id), 5 μm ; Daicel Chemical Industries, West Chester, PA) was employed for LC system 1 with a flow rate of 1.0 ml/min. Solvent A was hexane, and

solvent B was methanol/isopropanol (1:1, v/v). The linear gradient for LC system 1 was as follows: 2 % B at 0 min, 2 % B at 3 min, 3.6 % B at 11 min, 8 % B at 15 min, 8 % B at 27 min, 50 % B at 30 min, 50 % B at 35 min, 2 % B at 37 min and 2 % B at 45 min. Separations were performed at 30 °C. Reversed phase LC-ESI/MS analyses were conducted using LC system 2 with a Waters Alliance 2690 high-performance LC system and a Chiralpak AD-RH column (150 x 4.6-mm id, 5 µm; Daicel Chemical Industries)) at a flow rate of 0.5 ml/min. Solvent A was 0.1 % formic acid in water, and solvent B was 0.1 % formic acid in methanol. LC system 2 was isocratic using a mobile phase of 95 % B for 15 min. LC-UV chromatography for synthetic 11-oxo-ETE purification was conducted using LC system 3 on a Hitachi L-6200A Intelligent Pump equipped with a Hitachi L4000 UV detector (Hitachi, San Jose, CA). The separation employed a Beckman ultrasphere normal phase column (250 x 10 mm id; 5µm). LC system 3 was isocratic with a mobile phase of hexane/isopropanol (197:3) containing 0.1 % acetic acid. Separations were conducted at a flow rate 2.5 ml/min and at ambient temperature. Reverse phase LC-ESI/MS analyses for GSH-adducts were conducted using LC system 4. This employed an Eksigent Express LCTM-100 high performance LC system coupled with CTC Analytics HTC PAL autosampler system (Leap Technologies, Carrboro, NC). Gradient elution of GSH-adducts was performed in the linear mode employing a YMC J'sphere M18S column (150 x 1.0-mm inner id, 4 µm; Phenomenex, Torrance, CA) at a flow rate of 20 µl/min. Solvent A was 10 mM ammonium acetate and 0.1% trifluoroacetic acid (TFA) in water, and solvent B was 10 mM ammonium acetate and 0.1% TFA in acetonitrile. LC system 4 was as follows: 20 % B at 0 min, 20 % B at 5

min, 60 % B at 10 min, 60 % B at 20 min, 90 % B at 22 min, 90 % B at 33 min, 20 % B at 35 min.

3.3.4 Eicosanoid Analyses – A portion of the cell media (3 ml) was transferred into a glass tube and adjusted to pH 3 with 2.5 N HCl. Lipids were extracted with diethyl ether (4 ml x 2) and the organic layer was then evaporated to dryness under nitrogen. Eicosanoids PFB derivatization was conducted by dissolving the residue in 100 μ l of acetonitrile, 100 μ l of PFB bromide in acetonitrile (1:19, v/v) and 100 μ l of DIPE in acetonitrile (1:9, v/v) and the solution was heated at 60 °C for 60 min. The solution was allowed to cool down, evaporated to dryness under nitrogen at room temperature, dissolved in 100 μ l of hexane/ethanol (97:3, v/v) and an aliquot of the final solution (20 μ l) was used for normal-phase chiral LC-ECAPCI/MS analysis using LC system 1. Blank media standards (3 ml) were prepared, spiked with the following amounts of authentic lipid standards [11(*R,S*)-HETEs, 15(*R,S*)-HETEs, 11-oxo-ETE, and 15-oxo-ETE]: 10, 20, 50, 100, 200, 500 and 1000 pg. A mixture of internal standards [$^2\text{H}_6$]-5-oxo-ETE, [$^2\text{H}_8$]-12(*S*)-HETE, and [$^2\text{H}_8$]-15(*S*)-HETE (1 ng of each) was added to cell supernatant samples and standard solutions. Calibration curves were obtained with linear regressions of analyte versus internal standard peak-area ratio 11(*R,S*)-HETEs/[$^2\text{H}_8$]-12(*S*)-HETE, 15(*R,S*)-HETE/[$^2\text{H}_8$]-15(*S*)-HETE, and 11-oxo-ETE and 15-oxo-ETE/[$^2\text{H}_6$]-5-oxo-ETE against analyte concentrations. Concentrations of HETEs and oxo-ETEs in the media supernatants were calculated by interpolation from the calculated regression lines. The limit of detection for each HETE and oxo-ETE was 0.1 nM.

3.3.5 Synthesis and Purification of 11-oxo-ETE – This was performed by Dr. Suhong Zhang in the Blair laboratory. Dess-Martin reagent (1 mg, 2.36 μ mol) was added to a

solution of 11(*R,S*)-HETE (2 mg, 6.2 mmol) in dichloromethane (0.5 ml) and stirred for 2 h at room temperature. Analysis by LC-MS after PFB derivatization using LC system 1 revealed there was no starting material left and that there was one major product corresponding to 11-oxo-EETE. The reaction mixture was centrifuged twice at 3,400 rpm (10 min) and the supernatant was evaporated ready for LC purification. The residue was dissolved in the mobile phase (200 μ l) and preparative LC separation conducted using LC system 3 monitoring the UV absorbance at 236 nm. The retention time for 11-oxo-EETE was 15.0 min and for 15-oxo-EETE was 12.7 min. High resolution electrospray ionization-MS of 11-oxo-EETE revealed accurate masses of m/z 319.2263 and m/z 341.2079 for the protonated and sodiated molecules, respectively [calculated accurate mass measurements for protonated ($C_{20}H_{31}O_3$) and sodiated ($C_{20}H_{30}O_3Na$) molecules, m/z 319.2273 and m/z 341.2093, respectively]. 500 MHz 1H -NMR (δ H, $CDCl_3$; Fig. 3.2) 7.55 (dd, $J_1 = 11.5$ Hz, $J_2 = 15.5$, 1H), 6.21(d, $J = 15.5$ Hz, 1H), 6.15-6.11 (m, 1H), 5.97-5.92 (m, 1H), 5.60-5.58 (m, 2H), 5.41-5.38 (m, 2H), 3.35 (d, $J = 4.5$ Hz, 2H), 2.83-2.81 (m, 2H), 2.38-2.31 (m, 4H), 2.17-2.12 (m, 2H), 1.74-1.25 (m, 8H), 0.89 (t, $J = 7.0$ Hz, 3H). Analysis of purified 11-oxo-EETE as its PFB derivative was conducted using LC system 1. A single peak was observed at a retention time of 7.5 min with an intense negative ion at m/z 317 corresponding to $[M-PFB]^-$. CID of $[M-PFB]^-$ (m/z 317) and MS/MS analysis revealed major product ions at m/z 123, 149, 165, 219, and 273 (Fig. 3.3a). The UV spectrum was consistent with the presence of a conjugated dienone with a UV λ_{max} at 279 nm and molecular extinction coefficient (ϵ) of $18,985 M^{-1}cm^{-1}$. 11-Oxo-EETE was identified previously as an endogenous fatty acid oxidation product that was present in human atherosclerotic plaques (Waddington et al., 2001).

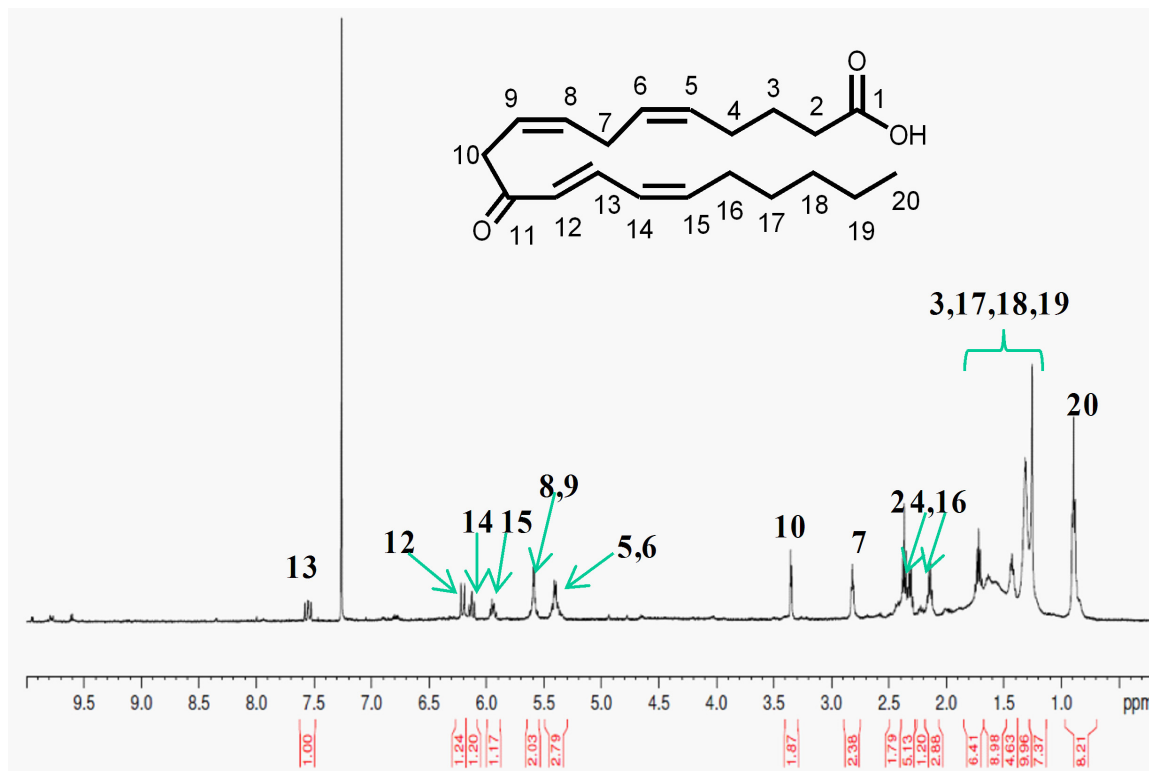


Figure 3.2 ¹H NMR spectrum for 11-oxo-ETE.

3.3.6 Preparation and Purification of 15(*S*)-HETE and 11(*R*)-HETE – This was performed by Dr. Suhong Zhang in the Blair laboratory. 15(*S*)-HPETE and 11(*R*)-HPETE were reduced in 4 ml methanol containing NaBH₄ (4 mg) at room temperature for 1 h to give rise to 15(*S*)-HETE and 11(*R*)-HETE. The reaction was quenched by adding 4 ml water on ice and adjusted pH to 3 with 3 N HCl. 15(*S*)-HETE and 11(*R*)-HETE were extracted by hexane (2 x 4 ml). The upper organic layer was taken and evaporated to dryness under nitrogen. The concentrations of 11(*R*)-HETE of 15(*S*)-HETE and were confirmed by UV spectroscopy (λ_{max} 236 nm, $\epsilon=27000 \text{ M}^{-1}\text{cm}^{-1}$). The purities of 11(*R*)-HETE and 15(*S*)-HETE were established as > 99 % by reversed-phase

chiral LC-electrospray ionization/MS analysis using LC system 2, eluting respectively at retention time of 6.1 min and 13.2 min with ammoniated molecules at m/z 338 ($[M+NH_4]^+$).

3.3.7 Preparation of $[^{13}C_{20}]$ -15-oxo-ETE - This was performed by Dr. Jasbir Arora in the Blair laboratory. $[^{13}C_{20}]$ -AA was converted to $[^{13}C_{20}]$ -15(*S*)-HPETE using soybean lipoxygenase. The labeled HPETE was then reduced to $[^{13}C_{20}]$ -15(*S*)-HETE with $NaBH_4$, which was then oxidized to $[^{13}C_{20}]$ -15-oxo-ETE using the Dess-Martin reagent as described above. There was < 0.5 % of $[^{12}C_{20}]$ -15-oxo-ETE present in the $[^{13}C_{20}]$ -15-oxo-ETE.

3.3.8 Preparation of 11-Oxo-ETE-Glutathione-Adduct (OEG) – This was performed by Dr. Jasbir Arora in the Blair laboratory. 11-oxo-ETE and glutathione (GSH) was converted to 11-OEG by incubating in 100 mM phosphate buffer (pH 6.5) for 5 h at 37 °C, or by incubating with glutathione-S-transferase (GST) in 100 mM phosphate buffer (pH 6.5) for 5 h at 37 °C. The reaction mixture was then spun to evaporate traces of ethanol in speed vac. 11-OEG extraction was performed by solid phase extraction (SPE) using pre-conditioned Waters Oasis HLB cartridges (6 ml, 200 mg). The cartridges were washed with 3 ml water and 11-oxo-ETE-GSH was eluted with 3 ml acetonitrile/water (80:20). The eluted extraction was evaporated under nitrogen to dryness and reconstituted in CH_3CN /water (20:80) for LC-MS analysis.

3.3.9 Cell Culture - RIES cells were cultured in RPMI 1640 media with 10 % FBS, 2 mM L-glutamine, 100,000 units/l penicillin and 100,000 μ g/l streptomycin. Before the treatment for lipidomics analysis, the culture media was replaced with serum-free RPMI 1640 media. Caco-2 cells were cultured in cell culture dishes precoated with FNC-

coating mix (AthenaES, Baltimore, MD) and maintained in EMEM supplemented with 10 % FBS, 100,000 units/l penicillin and 100,000 µg/l streptomycin. Before treatment, cell culture media were replaced with serum-free EMEM containing a balanced salt solution, non-essential amino acids, 2 mM L-glutamine, 1 mM sodium pyruvate, and 1500 mg/L sodium bicarbonate. HCT-116 cells were cultured in cell culture dishes precoated with FNC-coating mix (AthenaES, Baltimore, MD) and maintained in McCoy's 5A Medium supplemented with 10 % FBS, 100,000 units/l penicillin and 100,000 µg/l streptomycin.

3.3.10 Metabolism of Arachidonic Acid by RIES Cells - RIES cells were cultured as described above until 90% confluent. The media was replaced with serum-free RPMI 1640 and cells were treated with AA (10 µM final concentration). Incubations were then conducted for 5 min, 15 min, 30 min, 40 min, 1 h, 3 h and 6 h at 37 °C. Lipid extractions from cell culture media (3 ml) were performed as described above.

3.3.11 Inhibition of RIES cell 15-PGDH with CAY10397 – RIES cells were cultured as described above until 90% confluent. The media was replaced with serum-free RPMI-1640 containing CAY10397 (100 µM final concentration). Cells were then incubated for 4 h at 37 °C followed by incubation with AA (10 µM final concentration) for 10 min. In separate experiments the media was replaced with serum-free RPMI-1640 containing various doses of CAY10397 (0 µM, 5 µM, 10 µM, 15 µM, 25 µM, 50 µM, and 100 µM final concentration). Cells were then incubated for 4 h at 37 °C followed by incubation with additional 11(*R*)-HETE (50 nM final concentration) or AA (10 µM final concentration) for 10 min.

3.3.12 Western Blot Analysis of Caco-2 Cells and HCT-116 Cells – Cells were cultured as described above, and washed with PBS. Lysis buffer containing protease inhibitor cocktail were then added cells to lyse the cells. Cells were then collected and centrifuged at 13,000 rpm for 10 min. Protein concentration was determined by BCA assay. 12 micrograms of heat-inactivated protein were loaded and analyzed on 4-12% SDS/PAGE. For Western blot analysis fractionated proteins were electrotransferred onto a nitrocellulose membrane (Invitrogen, Carlsbad, CA) and unspecific binding was blocked with tris(hydroxymethyl)aminomethane (Tris)-buffered saline containing 10% non-fat milk powder and 0.1% Tween-20. A rabbit antibody against murine COX-2 (Cayman Chemical Co., Ann Arbor, MI) served as the primary antibody. The secondary antibody was conjugated with peroxidase (Jackson Immunoresearch Laboratories, West Grove, PA) and the antigen-antibody complex was detected with ECL Plus (Amersham Biosciences, Piscataway, NJ).

3.3.13 Metabolism of Arachidonic Acid by Caco-2 Cells – Caco-2 cells were cultured as described above until 90% confluent. The media was replaced with serum-free EMEM. AA (10 μ M final concentration) in ethanol was added to the media and cells were incubated for 5 min at 37 °C. In separate experiments, the media was replaced with serum-free EMEM containing CAY10397 (100 μ M final concentration). Cells were then incubated for 4 h at 37 °C followed by incubation with additional AA (10 μ M final concentration) for 10 min.

3.3.14 Analysis of 11-Oxo-ETE-Glutathione-Adduct (OEG) and its Cysteinylglycine Metabolite in 11(*R,S*)-HETE-Treated-RIES Cells – The media was replaced with serum-free RPMI-1640 containing 11(*R,S*)-HETE (1 μ M final concentration). Cells were

then incubated for 30 min at 37 °C. The cell culture medium was loaded on a solid phase extraction column (C₁₈, 3 ml), which was preconditioned with acetonitrile and water. After they were washed with 3 ml of water, OEG and the cysteinylglycine-adduct were eluted with 6 ml of 50 % acetonitrile in water. The solution was evaporated to dryness under nitrogen, and reconstituted in 100 µl methanol which was then diluted by 1000 times. An aliquot of 20 µl was used for reversed-phase LC-electrospray ionization/MS analysis using LC system 4.

3.3.15 Metabolism of 11(*R*)-HETE and 15(*S*)-HETE by 15-PGDH – This was performed by Ms. Xiaojing Liu in the Blair laboratory. Various concentrations of 11(*R*)-HETE (0, 2.3 µM, 4.6 µM, 6.9 µM, 9.2 µM and 23 µM) were incubated with 9.0 nM of recombinant 15-PGDH (50 ng, 1.8 pmol) and cofactor NAD⁺ (400 µM) in 50 mM Tris-Cl (pH 7.9) for 3.5 min at 37 °C. Similarly, various concentrations of 15(*S*)-HETE (0, 0.92 µM, 1.84 µM, 2.76 µM, 3.68 µM, 4.6 µM, 9.2 µM and 23 µM) were incubated with 2.25 nM (13 ng, 0.45 pmol) of recombinant 15-PGDH and cofactor NAD⁺ (400 µM) in 500 mM Tris-Cl (pH 7.9) for 3 min at 37 °C. Each total reaction volume was 200 µl. After a 3 min incubation, the enzymatic reaction was quenched with 400 µl of ice cold methanol and [¹³C₂₀]-15-oxo-ETE (8 ng) added as the internal standard. Eicosanoids were extracted with dichloromethane/methanol (1.2 ml; 8:1, v/v). The lower organic layer was then evaporated to dryness under nitrogen and reconstituted in methanol (100 µl). An aliquot (25 µl) was used for reversed-phase chiral LC-electrospray ionization/MS analysis using LC system 2. The retention times for 11-oxo-ETE and 15-oxo-ETE were 8.7 min and 9.3 min, respectively. In separate experiments, the formation

of 11-oxo-ETE and 15-oxo-ETE were found to be linear for the first 5 min. Eicosanoids were quantified by interpolation from a standard curve prepared with 15-oxo-ETE and 11-oxo-ETE using [$^{13}\text{C}_{20}$]-15-oxo-ETE as the internal standard.

3.3.16 Statistical Analyses – All experiments were conducted in triplicate. Statistical significance (p value < 0.05) was determined using a two-tailed unpaired t-test employing GraphPad Prism software (v 5.01, GraphPad Software Inc., La Jolla).

3.4 Results

3.4.1 LC-MS and MS/MS Analysis of 11-oxo-ETE and 15-oxo-ETE - RIES cells were incubated with 1 μM 11(*R*)-HETE for 5 min. LC-MS analysis of PFB derivatives of lipids extracted from the RIES cell media showed that there was a single major metabolite, which eluted at 7.4 min (data not shown). The full scan mass spectrum of this metabolite had only one major ion at m/z 317 corresponding to $[\text{M-PFB}]^+$. CID and MS/MS analysis revealed the formation of intense product ions at m/z 123, 149, 165, 219, and 273 (Fig. 3.3b). The MS/MS spectrum was identical with that obtained from authentic synthetic 11-oxo-ETE-PFB (Fig. 3.3a), which confirmed the identity of 11-oxo-ETE from RIES cells. In comparison, CID and MS/MS analysis of authentic 15-oxo-ETE-PFB standard showed major product ions at m/z 113, 139, 147, 219, and 273 (Fig. 3.3c). The product ion at m/z 165 in RIES cell-derived and synthetic 11-oxo-ETE-PFB corresponded to cleavage between C-9 and C-10 and m/z 123 was formed from cleavage between C-11 and C-12 (Figs. 3.3a and 3.3b). In contrast, the specific product ion of 15-oxo-ETE-PFB at m/z 113 was formed from the cleavage of the double bond between C-13 and C-14 (Fig. 3.3c).

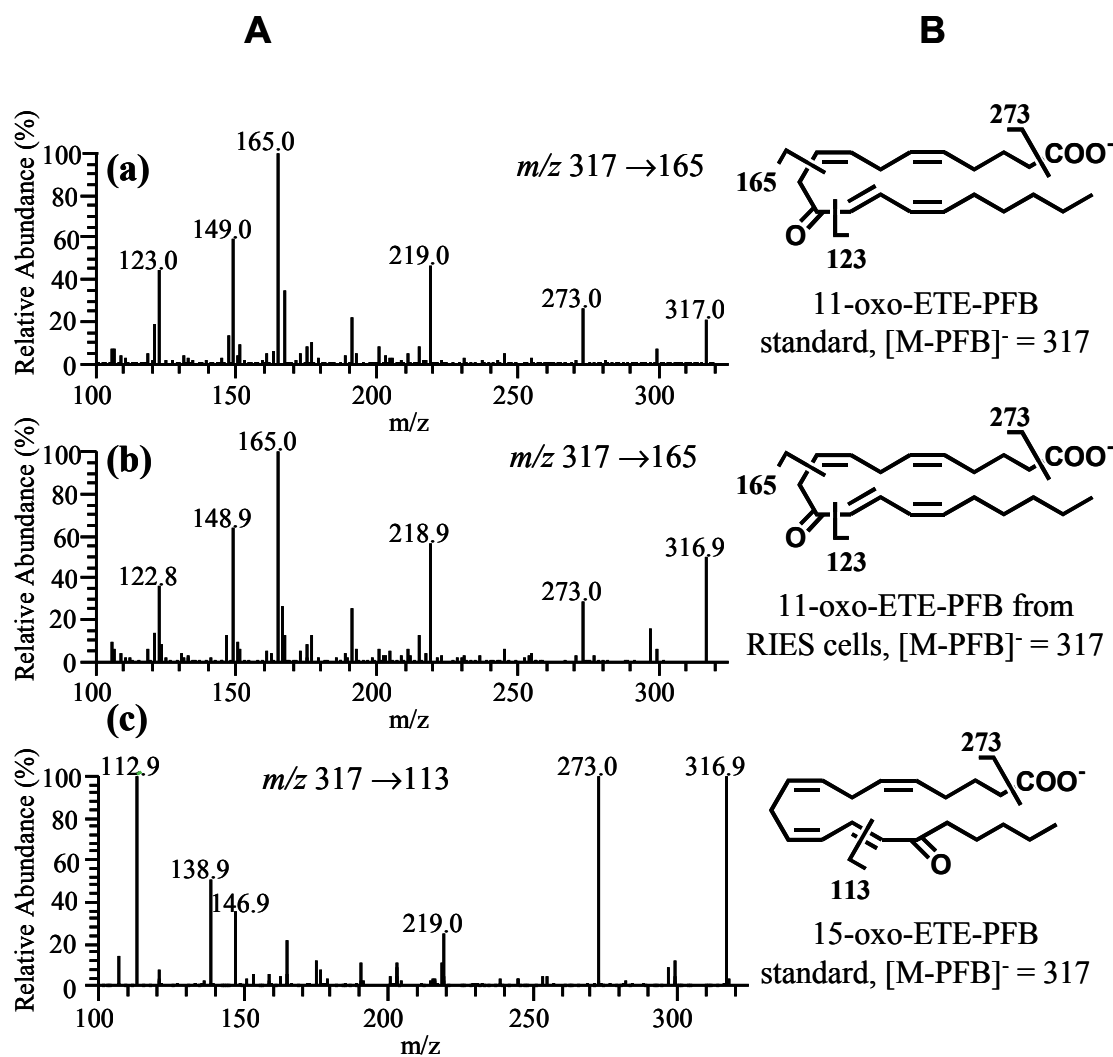


Figure 3.3 MS/MS analyses of 11-oxo-ETE and 15-oxo-ETE. **A.** Product ion spectra for (a) synthetic 11-oxo-ETE-PFB standard, (b) 15-PGDH-derived 11-oxo-ETE-PFB from RIES cells treated with 1 μ M 11(*R*)-HETE, and (c) synthetic 15-oxo-ETE-PFB standard. **B.** Structure of 11-oxo-ETE [(a) and (b)] and 15-oxo-ETE (c) along with the specific product ions observed by CID of [M-PFB]⁻ (m/z 317) and MS/MS analysis of 11- and 15-oxo-ETE-PFB.

3.4.2 Arachidonic Acid-Mediated Formation of HETEs in RIES Cells - RIES cells were incubated with 10 μ M AA for 6 h and RIES cell supernatants were analyzed by LC-

MS. This demonstrated the secretion of 11-oxo-EETE (retention time 7.4 min) and 11(*R*)-HETE (retention time, 10.4 min) within 5 min of AA addition (Figs. 3.4Aa and 3.4Af). The chromatograms also revealed the presence of 15-oxo-EETE (retention time, 7.5 min) as well as its potential precursors 15(*R*)-HETE (retention time, 11.7 min) and 15(*S*)-HETE (retention time, 15.2 min) (Figs. 3.4Ab and 3.4Ad). Quantification of 15(*R*)- and 15(*S*)-HETE revealed a 20 % enantiomeric excess of 15(*S*)-HETE (Fig. 3.4Ad). 11(*R*)-HETE was the most abundant metabolite of AA secreted by cells at the early time points (< 1 h), as we had observed previously (Lee et al., 2007). The maximum 11(*R*)-HETE concentrations was observed within 5-min of AA addition (Fig. 3.5A). 11(*R*)-HETE was then rapidly metabolized over 3 h (Fig. 3.5A). 11-Oxo-EETE in the cell media was also observed to peak within 5 min of AA addition and declined to a steady state after 3 h (Fig. 3.5B). Only trace amounts of 11(*S*)-HETE were observed after the addition of AA (Fig. 3.4Af) or 11(*R*)-HETE (data not shown) to the RIES cells. Pre-treatment with CAY10397 resulted in increased levels of 15(*S*)-HETE (Fig. 3.7A) and decreased levels of 15-oxo-EETE (Fig. 3.7B). This suggested that CAY10397-mediated inhibition of 15-PGDH led to a modest accumulation of 15(*S*)-HETE (Fig. 3.7A) and a simultaneous inhibition of 15-oxo-EETE formation (Fig. 3.7B). The level of 15(*R*)-HETE was almost identical after the addition of AA alone when compared with the presence of CAY10397 (Fig. 3.7A). Pre-treatment of CAY10397 also resulted in a substantial increase in 11(*R*)-HETE concentrations (Fig. 3.8A) together with a reduction in 11-oxo-EETE concentrations (Fig. 3.8B).

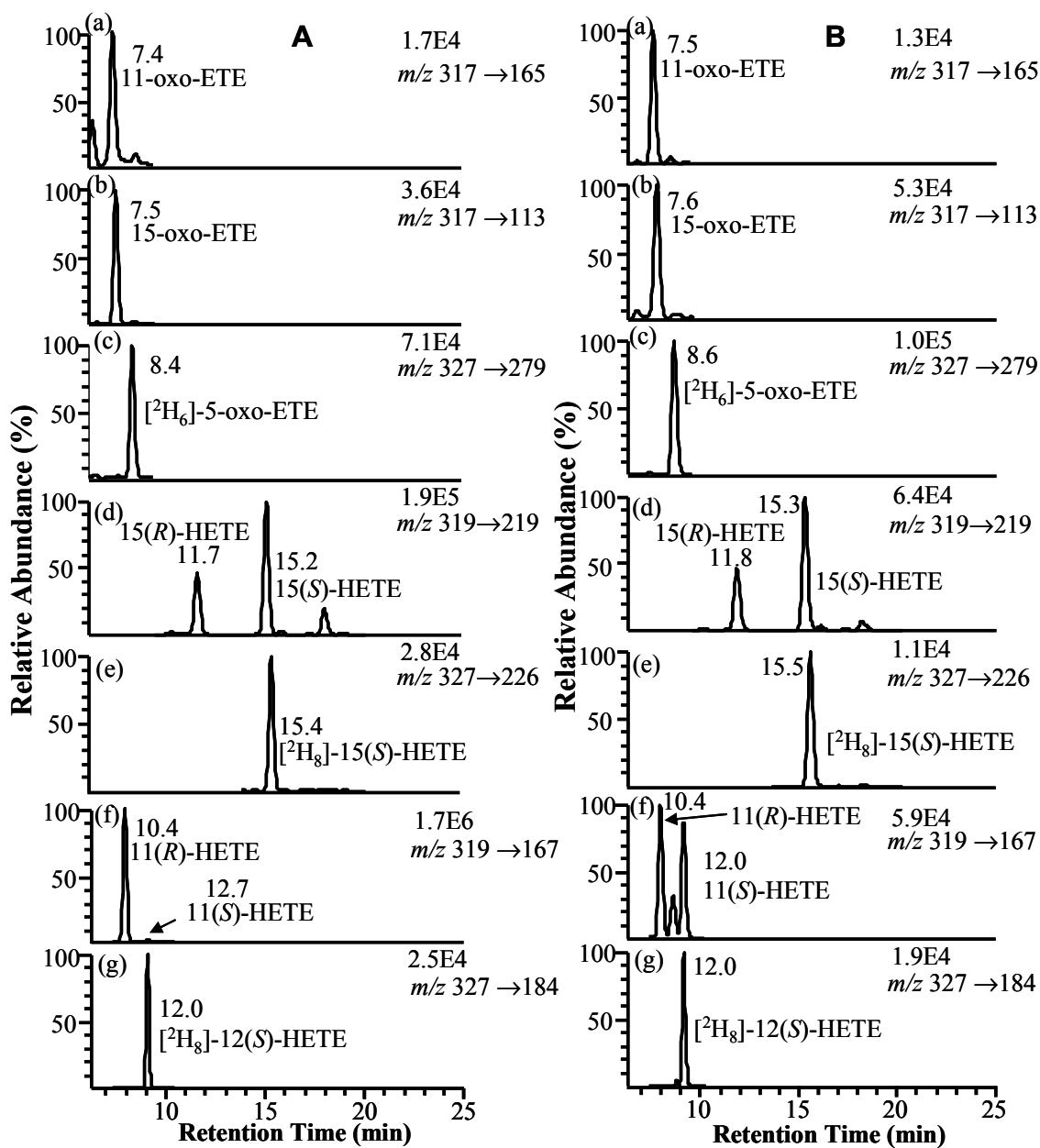


Figure 3.4 Targeted chiral lipidomics analysis of COX-2 derived AA metabolites from RIES and Caco-2 cells. MRM chromatograms are shown for (a) 11-oxo-EETE-PFB (m/z 317 \rightarrow 165), (b) 15-oxo-EETE-PFB (m/z 317 \rightarrow 113), (c) $[^2\text{H}_6]$ -5-oxo-EETE-PFB internal standard (m/z 326 \rightarrow 279), (d) 15-(*R,S*)-HETE-PFB (m/z 319 \rightarrow 219), (e) $[^2\text{H}_8]$ -

15(*S*)-HETE-PFB internal standard (m/z 327 \rightarrow 226), (f) 11(*R,S*)-HETE-PFB (m/z 319 \rightarrow 167), (g) [$^2\text{H}_8$]-12(*S*)-HETE-PFB internal standard (m/z 327 \rightarrow 184). (A) RIES cells. (B) Caco-2 cells.

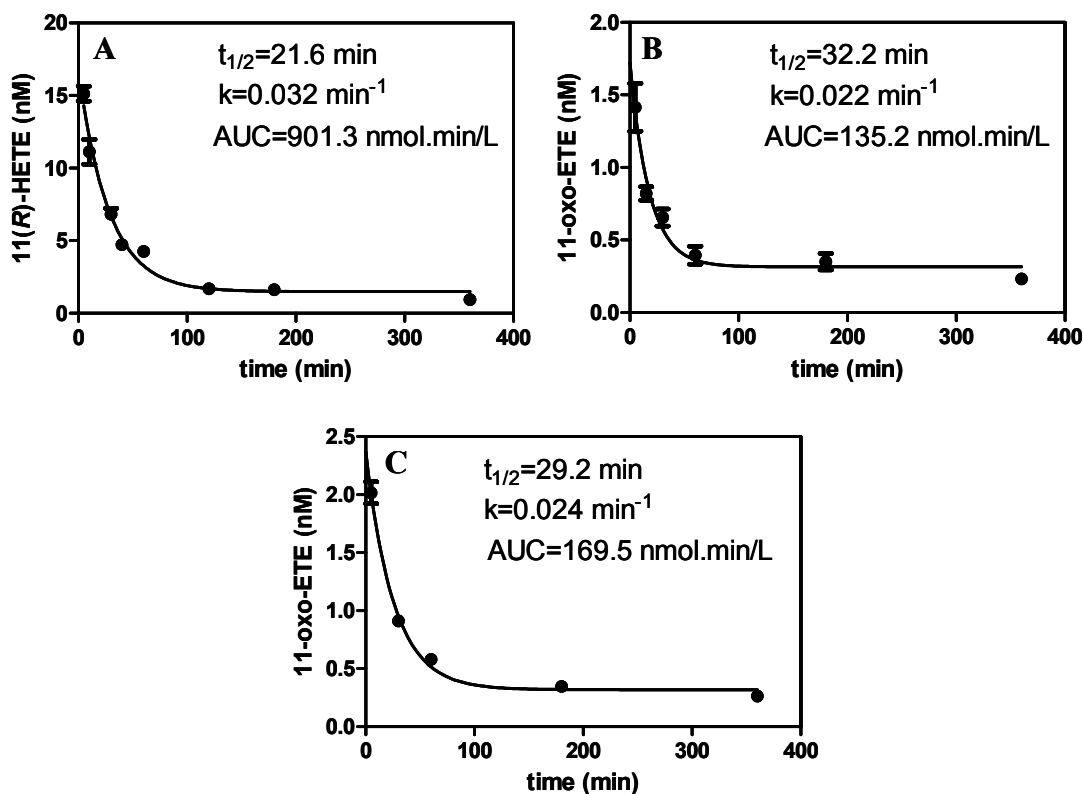


Figure 3.5 Kinetics of 11(*R*)-HETE and 11-oxo-EETE by RIES cells. RIES cells were incubated with AA (10 μM) or 11(*R*)-HETE (1 μM) for a period of 360 min. Supernatant was collected at different time points. Lipid metabolites [11(*R*)-HETE and 11-oxo-EETE] in the cell supernatant were extracted and derivatized with PFB and their concentrations were determined in triplicate (means \pm S.E.M.) by LC-ECAPCI/MRM/MS analysis. (A) Kinetic plot of 11(*R*)-HETE metabolism by RIES cells treated with AA (10 μM) ($t_{1/2}=21.6$ min and $k=0.0321$ min $^{-1}$); (B) Kinetic plot of 11-oxo-EETE metabolism by RIES

cells treated with AA (10 μM) ($t_{1/2}$ =32.2 min and k =0.0215 min^{-1}); (C) Kinetic plot of 11-oxo-ETE metabolism by RIES cells treated with 11(*R*)-HETE (1 μM) ($t_{1/2}$ =29.2 min and k =0.0237 min^{-1}).

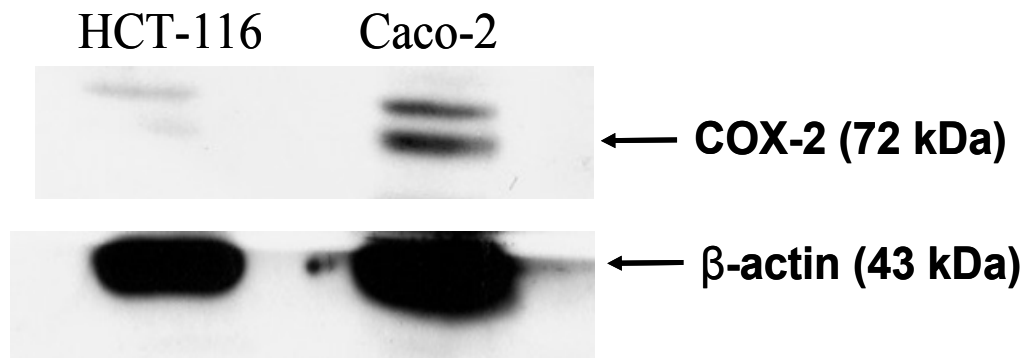


Figure 3.6 Western blot analysis of COX-2 in human epithelial colorectal adenocarcinoma cells (HCT-116 and Caco-2). Western blot analysis are shown for COX-2 (72 kDa) in HCT-116 cells and Caco-2 cells, with β -actin (43 kDa) as a loading control.

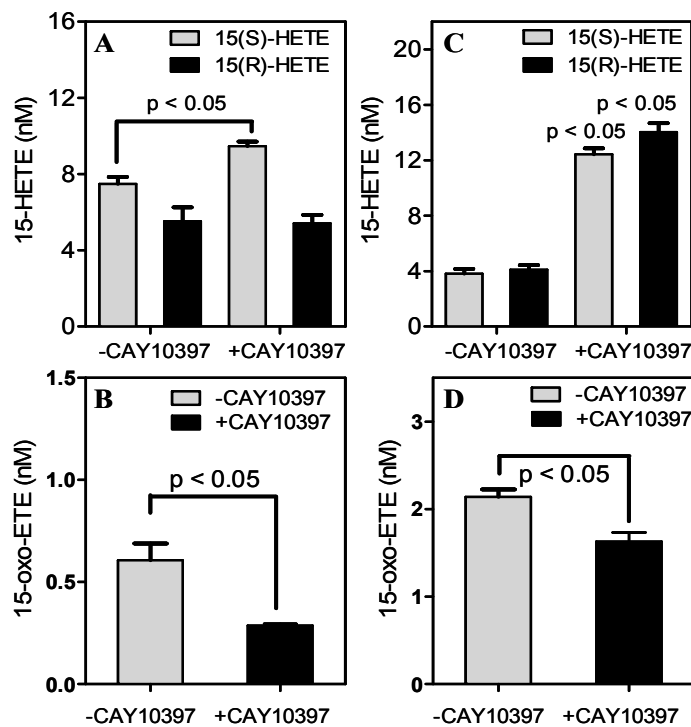


Figure 3.7 Inhibition of 15-HETE metabolism to 15-oxo-EETE by 15-PGDH inhibitor CAY 10397. (A) 15(*S*)-HETE and 15(*R*)-HETE formation by RIES cells that were treated with 10 μ M AA or pretreated with 100 μ M CAY10397 for 4 h before 10 μ M AA treatment. (B) 15-oxo-EETE formation by RIES cells that were treated with 10 μ M AA or pretreated with 100 μ M CAY10397 for 4 h before 10 μ M AA treatment. (C) 15(*S*)-HETE and 15(*R*)-HETE formation by Caco-2 cells that were treated with 10 μ M AA or pretreated with 100 μ M CAY10397 for 4 h before 10 μ M AA treatment. (D) 15-oxo-EETE formation by Caco-2 cells that were treated with 10 μ M AA or pretreated with 100 μ M CAY10397 for 4 h before 10 μ M AA treatment. Lipid metabolites in the cell media were extracted and derivatized with PFB. 11(*S*)-HETE, 11(*R*)-HETE, and 11-oxo-EETE concentrations were determined in triplicate by stable isotope dilution by LC-

ECAPCI/MRM/MS analysis of PFB derivatives. Values presented in bar graphs are means \pm S.E.M.

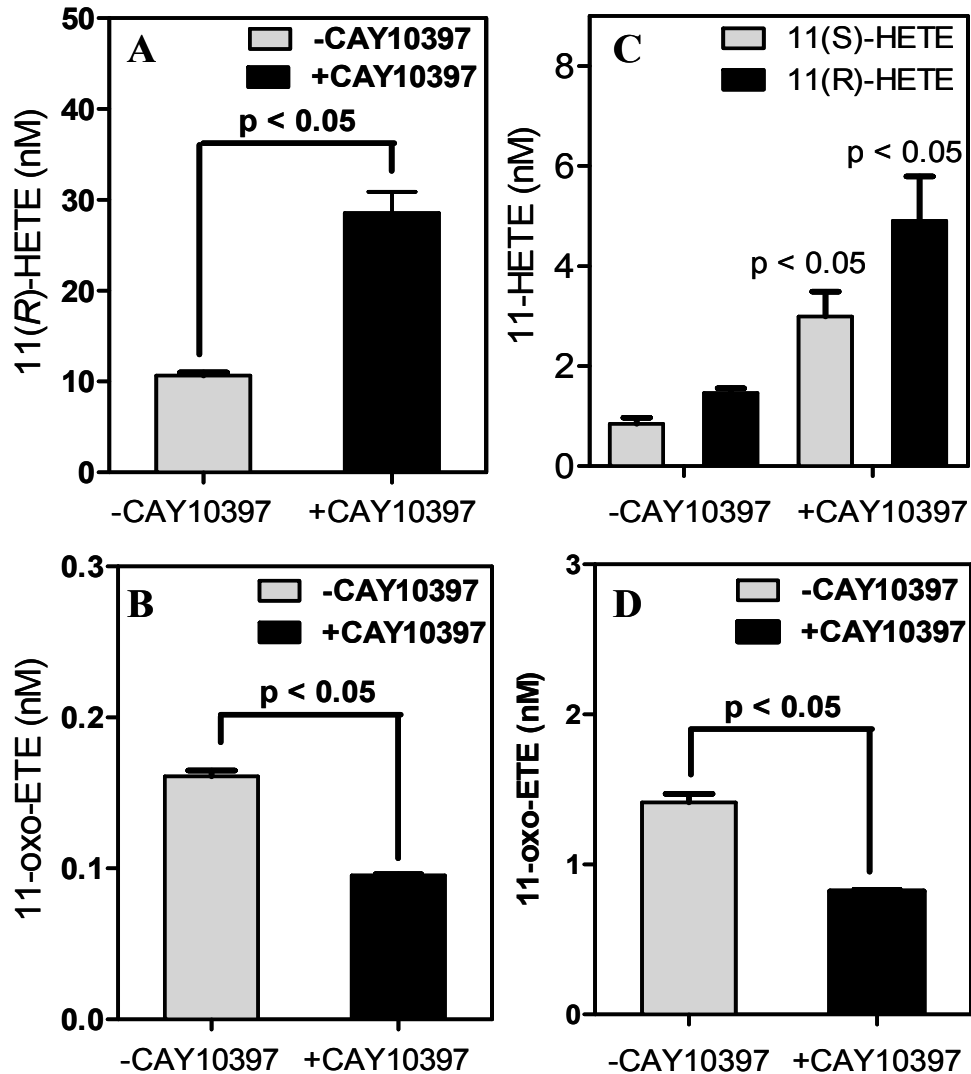


Figure 3.8 Inhibition of 11-HETE metabolism to 11-oxo-EETE by 15-PGDH inhibitor CAY 10397. (A) 11(R)-HETE formation by RIES cells that were treated with 10 μ M AA or pretreated with 100 μ M CAY10397 for 4 h before 10 μ M AA treatment. (B) 11-oxo-EETE formation by RIES cells that were treated with 10 μ M AA or pretreated with 100 μ M CAY10397 for 4 h before 10 μ M AA treatment. (C) 11(S)-HETE and (R)-

HETE formation by Caco-2 cells that were treated with 10 μ M AA or pretreated with 100 μ M CAY10397 for 4 h before 10 μ M AA treatment. **(D)** 11-oxo-EETE formation by Caco-2 cells that were treated with 10 μ M AA or pretreated with 100 μ M CAY10397 for 4 h before 10 μ M AA treatment. Lipid metabolites in the cell media were extracted and derivatized with PFB. 11(*S*)-HETE, 11(*R*)-HETE, and 11-oxo-EETE concentrations were determined in triplicate by stable isotope dilution by LC-ECAPCI/MRM/MS analysis of PFB derivatives. Values presented in bar graphs are means \pm S.E.M.

3.4.3 Dose-dependent Effect of CAY10397 on 11-oxo-EETE and 11(*R*)-HETE in RIES Cells - AA (10 μ M) was added to the RIES cells for 10 min, with or without the pre-treatment with various doses of CAY10397 (0-100 μ M) for 4 h. This resulted in a significant inhibition of 11-oxo-EETE formation (Fig. 3.9A) and a simultaneous accumulation of 11(*R*)-HETE in a dose-dependent manner (Fig. 3.9C). To confirm that 15-PGDH was the enzyme that oxidized 11(*R*)-HETE to 11-oxo-EETE, RIES cells were treated with 50 nM 11(*R*)-HETE for 10 min, with or without the pre-treatment with various doses of CAY10397 (0-100 μ M) for 4 h. Addition of 11(*R*)-HETE alone resulted in the formation of 11-oxo-EETE, whereas CAY10397 pre-treatment resulted in a dose dependent inhibition of 11-oxo-EETE formation (Fig. 3.9B). Inhibition of 11-oxo-EETE formation reached 70 % in the presence of 100 μ M CAY10397 (Fig. 3.9B). CAY10397 also caused a dose-dependent increase in 11(*R*)-HETE concentrations after the addition of exogenous 11(*R*)-HETE (Fig. 3.9D). In the absence of AA, CAY10397 did not lead to 11-oxo-EETE generation (data not shown), whereas there was significant inhibition of AA-

mediated (Fig. 3.9A) and 11(*R*)-HETE-mediated (Fig. 3.9B) formation of 11-oxo-ETE. The EC₅₀ for CAY10397-induced increase in AA-mediated 11(*R*)-HETE formation (Fig. 3.9C) was significantly higher than the IC₅₀ of CAY10397 on AA-mediated 11-oxo-ETE formation (Fig. 3.9C). In contrast, EC₅₀ for 11(*R*)-HETE concentration after the addition of exogenous 11(*R*)-HETE (Fig. 3.9D), which was similar to the IC₅₀ for inhibition of 11(*R*)-HETE-mediated 11-oxo-ETE formation (Fig. 3.9C). This is most likely because of the complexity of the pathways involved in AA-mediated 11-oxo-ETE formation compared with its direct formation from 11(*R*)-HETE.

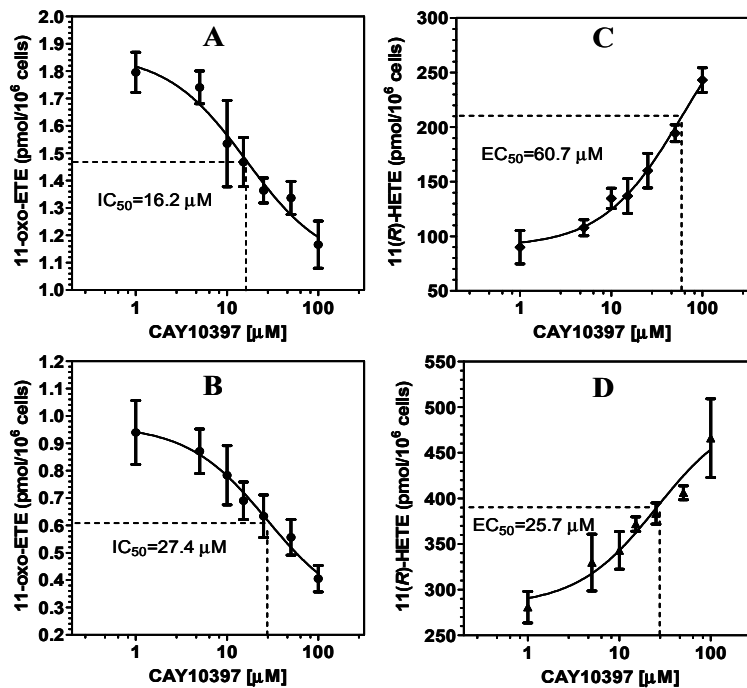


Figure 3.9 Dose-dependent effects of CAY 10397 on the levels of 11-oxo-ETE and 11-HETEs released by RIES cells. (A) Dose-dependent inhibition curve of CAY 10397 on 11-oxo-ETE released by RIES cells treated with 10 μ M AA for 10 min following the 4 h pretreatment with CAY 10397; (B) Dose-dependent inhibition curve of CAY 10397

on 11-oxo-ETE released by RIES cells treated with 50 nM 11(*R*)-HETE for 5 min following the 4 h pretreatment with CAY 10397; (C) Dose-dependent curve of CAY 10397 on 11(*R*)-HETE accumulation by RIES cells treated with 10 μ M AA for 10 min following the 4 h pretreatment with CAY 10397; (D) Dose-dependent curve of CAY 10397 on 11(*R*)-HETE accumulation by RIES cells treated with 50 nM 11(*R*)-HETE for 5 min following the 4 h pretreatment with CAY 10397. Cell supernatant was collected at each time point. Lipid metabolites in the cell supernatant were extracted and derivatized with PFB. Determinations were conducted in triplicate (means \pm S.E.M.) by stable isotope dilution LC-ECAPCI/MRM/MS analyses of PFB derivatives.

3.4.4 Formation of 11-OEG-adduct in RIES Cell Culture - Secretion of 11-OEG and its conversion to the corresponding cysteinylglycine-adduct were monitored in the media after the addition of 11(*R, S*)-HETE to the RIES cells. 11-OEG was detected by specific LC-MS monitoring as significant metabolites after 30 min incubation. The OEG (retention time = 13.1 min) (Fig. 3.10Ac) and its cysteinylglycine metabolite (11-oxo-ETE-cysteinylglycine-adduct) (data not shown) were also observed as intense peaks in the chromatogram when analyzed by LC system 4 coupled with electrospray ionization/MS. The 11-OEG observed from RIES cells shared the same chromatograms with the authentic 11-OEG synthesized with GST (Fig. 3.10Aa) or synthesized without GST at pH 6.5 (Fig. 3.10Ab). The full scan mass spectrum of this metabolite had only one major ion at m/z 626 corresponding to $[M+H]^+$. CID and MS/MS analysis revealed the formation of intense product ions at m/z 497, 479, 394, 319 and 301 (Fig. 3.10Bb).

The MS/MS spectrum was identical with that obtained from authentic synthetic 11-OEG (Fig. 3.10Ba and 3.10Bb), which confirmed the identity of 11-OEG from RIES cells.

3.4.5 Arachidonic acid-Mediated Formation of HETEs in Caco-2 Cells Analysis –

In order to examine the formation of COX-2-derived HETEs in human epithelial cells, the Caco-2 colorectal carcinoma cell line was employed. Caco-2 cells were reported previously to constitutively express COX-2 (Kamitani et al., 1998). This was confirmed by Western blot analysis before AA was added to the cells (Fig. 3.6). A very similar product and kinetic profile was observed as for the RIES cells (Figs. 3.4B and 3.5) with 11-oxo-EETE (Fig. 3.4Ba), 15-oxo-EETE (Fig. 3.4Bb), 15(*R*)-HETE (Fig. 3.4Bd), 15(*S*)-HETE (Fig. 3.4Bd), and 11(*R*)-HETE (Fig. 3.4Bf) as the major AA-derived metabolites. A significant amount of 11(*S*)-HETE was secreted from the cells (Fig. 3.4Bf). AA (10 μ M) was added to the Caco-2 for 10 min, with or without the pre-treatment with CAY10397 (100 μ M) for 4 h. Unlike the RIES cells, CAY10397 caused an increase of both 15(*S*)-HETE and 15(*R*)-HETE (Fig. 3.7C). There was a concomitant reduction in 15-oxo-EETE levels (Fig. 3.7D). This suggested that there was some inter-conversion between 15-oxo-EETE and 15(*R*)-HETE. Pre-treatment of CAY10397 also resulted in a substantial increase in 11(*R*)-HETE concentrations (Fig. 3.8C) together with a reduction in 11-oxo-EETE (Fig. 3.8D). Again, unlike the RIES cells, there was a substantial increase in 11(*S*)-HETE concentrations (Fig. 3.8C). This suggested that there was also some inter-conversion between 11-oxo-EETE and 11(*S*)-HETE in the Caco-2 cells.

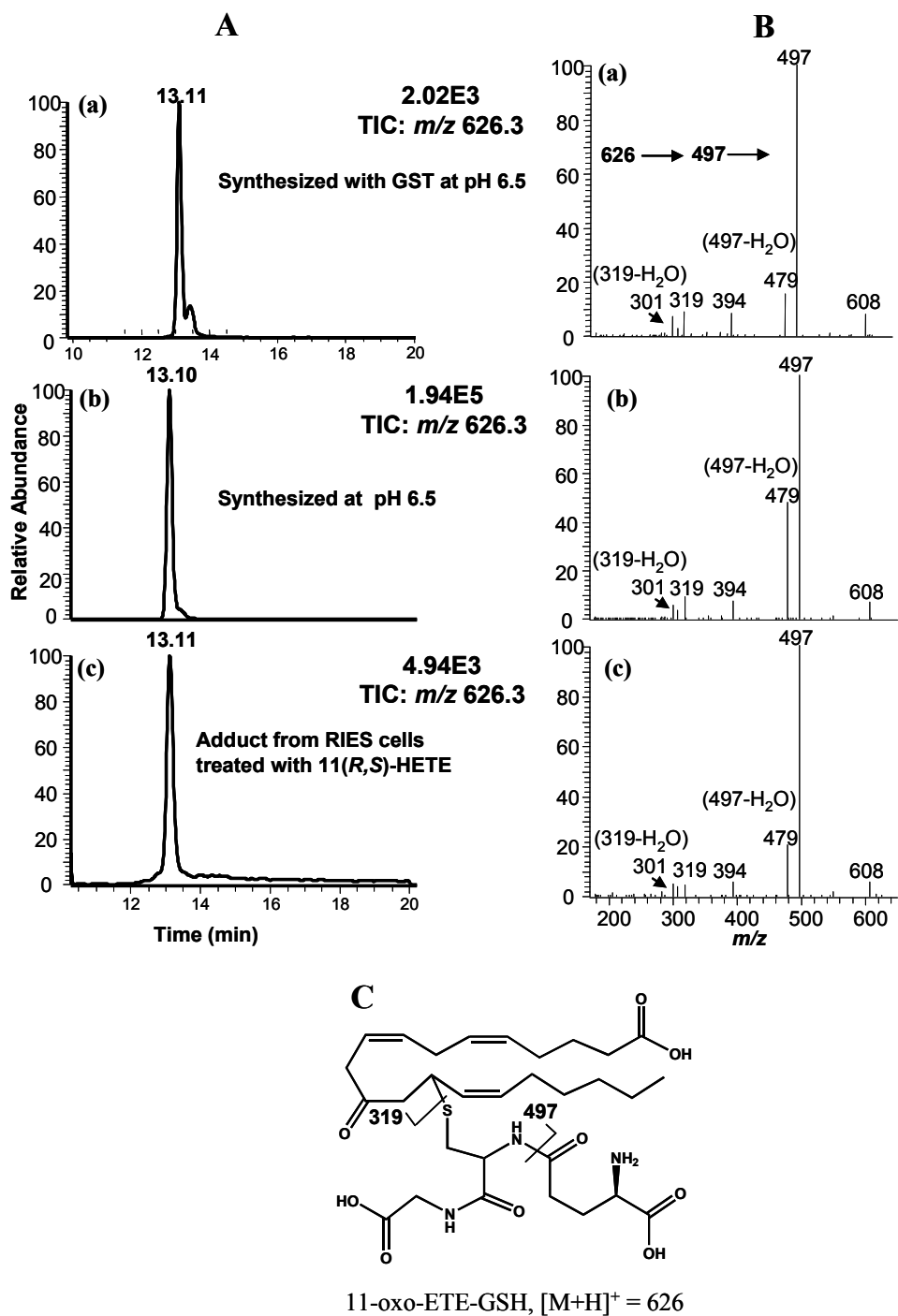


Figure 3.10 LC-MS analysis and MS/MS spectrums of the formation of 11-oxo-EETE-GSH adduct (11-OEG). (A) Representative LC-MS chromatograms of reaction products between 11-oxo-EETE and GSH incubated with 4 nM glutathione-S-transferases

(GST) (a), without GST in the chemical condition of pH 6.5 (b), and 11-OEG derived from 11(*R,S*)-HETE by RIES cells (c). The reconstituted ion chromatograms for MH^+ of the major adduct (m/z 626, 13.1 min) are shown. (B) Product ion spectra for (a) GST-mediated synthetic 11-OEG standard, (b) chemically synthetic 11-OEG standard without enzyme. (c) 11-OEG from RIES cells treated with 1 μ M 11(*R,S*)-HETE. (C) Structure of 11-OEG along with the specific product ions observed by CID of $[M+H]^+$ (m/z 626) and MS/MS analysis of 11-OEG.

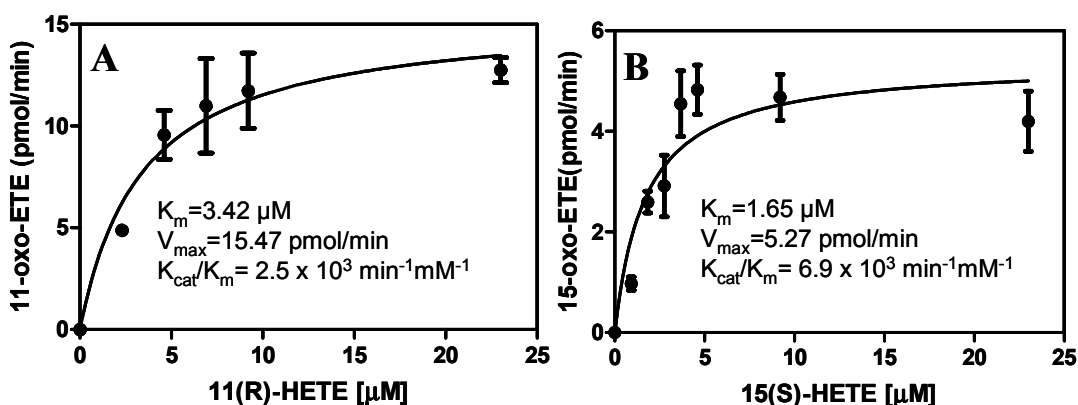


Figure 3.11 Kinetic plot of the formation of 11-oxo-EETE and 15-oxo-EETE by 15-PGDH. Various concentrations of (A) 11(*R*)-HETE or (B) 15(*S*)-HETE, were incubated with 4 nM 15-PGDH and cofactor NAD^+ . Determinations were conducted in triplicate (means \pm S.E.M.) by stable isotope dilution LC-ESI/MRM/MS analyses. (A) 11-oxo-EETE. (B) 15-oxo-EETE.

3.4.6 15-PGDH-Mediated Formation of 11-oxo-ETE and 15-oxo-ETE - Various concentrations of 11(*R*)-HETE and 15(*S*)-HETE were incubated with recombinant human 15-PGDH and NAD⁺ at 37 °C. A Michaelis-Menton kinetic analysis of 11-oxo-ETE formation revealed that the V_{\max} , K_m , and k_{cat} values for oxidation of 11(*R*)-HETE (Fig. 3.11A) and 15(*S*)-HETE (Fig. 3.11B) were similar. Therefore, the catalytic efficiency (K_{cat}/K_m) for 15-PGDH-mediated oxidation of 11(*R*)-HETE ($2.5 \times 10^3 \text{ min}^{-1}\text{mM}^{-1}$) and 15(*S*)-HETE were similar ($6.9 \times 10^3 \text{ min}^{-1}\text{mM}^{-1}$).

3.5 Discussion

Eicosanoids secreted from RIES and human Caco-2 cells were analyzed as PFB derivatives by chiral LC-ECAPCI/MS methodology (Lee and Blair, 2007; Mesaros et al., 2009). This revealed the presence of 11-oxo-ETE, 15-oxo-ETE, 15(*R*)-HETE, 15(*S*)-HETE, and 11(*R*)-HETE (Fig. 3.3). The product ion mass spectrum of 11-oxo-ETE secreted from the RIES cells was identical with the product ion mass spectrum of an authentic 11-oxo-ETE standard that we had synthesized (Fig. 3.3). Importantly, there were significant differences between the product ion spectra of 11-oxo-ETE and 15-oxo-ETE. The ions at m/z 113, 139, and 147 in 15-oxo-ETE were completely absent in the spectrum from 11-oxo-ETE. Conversely, ions at m/z 123, 149, and 165 in the spectrum from 11-oxo-ETE were completely absent in the spectrum from 15-oxo-ETE. This made it possible to analyze the two oxo-ETE PFB derivatives using specific LC-MRM/MS transitions even though their LC retention times were very similar (Fig. 3.3). These studies confirmed our previous finding that 11(*R*)-HETE was the major HETE secreted from RIES cells (Lee et al., 2007). They also showed that 11(*R*)-HETE was cleared rapidly ($t_{1/2}$ of 21.6 min, Fig. 3.5B). The 11-oxo-ETE that was formed from 11(*R*)-HETE

was metabolized at a similar rate (Fig. 3.5C). This was due in part to the rapid intracellular inactivation to 11-OEG through GST-mediated metabolism as we observed previously for 15-oxo-ETE (Lee et al., 2007). The inactive 11-OEG was then secreted and converted to the corresponding cysteinylglycine-adduct by γ -glutamyltranspeptidase analogous to 15-OEG (Lee et al., 2007). Similar results were obtained with Caco-2 cells, except that the 15-oxo-ETE and 11-oxo-ETE were converted to 15(*R*)-HETE and 11(*S*)-HETE, respectively (Fig. 3.4B). Formation of these HETEs became much more apparent when 15-PGDH was inhibited, which resulted in an almost three-fold increase in both 15(*R*)-HETE (Fig. 3.7C) and 11(*S*)-HETE (Fig. 3.8C) concentrations. This might arise from AKRs in the human Caco-2 cells which have increased activity when compared with the RIES cells (Penning and Byrns, 2009). Subsequent 15-PGDH-mediated oxo-ETE formation would lead to redox cycling between the oxo-ETEs and HETEs. AKR-mediated metabolism of the oxo-ETEs could then compete with GST-mediated 15-OEG formation (Fig. 3.12). This might explain why secreted 11-oxo-ETE concentrations reached a low steady state of 0.23 nM in the RIES cells rather than being completely metabolized to the corresponding 11-OEG (Figs. 3.5B and 3.5C). Reductive metabolism of the oxo-ETEs could also provide an endogenous pathway for decreasing the *in vivo* concentrations of anti-proliferative 11- and 15-oxo-ETE as has been suggested previously for 15d-PGJ₂ (Penning and Byrns, 2009).

15-PGDH catalyzes NAD⁺-mediated oxidation of the 15(*S*)-hydroxyl moiety of PGs and other eicosanoids (Fig. 3.1) (Wei et al., 2009). It is a key PG catabolism enzyme that converts PGE₂ and PGD₂ to inactive 15-oxo-metabolites (Figs. 3.1 and 3.13) (Backlund et al., 2005; Rangachari and Betti, 1993). Our previous studies established

that 15-oxo-ETE was formed from 15-LO-1-derived 15(*S*)-HETE in macrophages and monocytes and that its biosynthesis was reduced by CAY10397, a 15-PGDH inhibitor (Wei et al., 2009). Surprisingly, CAY10937 had even greater effects on the 11(*R*)-HETE pathway. Thus, there was an almost three-fold increase in 11(*R*)-HETE concentrations after CAY10937-mediated inhibition of 11-oxo-ETE formation in both RIES cells and human Caco-2 cells (Figs. 3.7A and 3.7C). There was also a significant decrease in 11-oxo-ETE levels (Figs. 3.7B and 3.7D). IC₅₀ values for inhibition of 15-PGDH-mediated 11-oxo-ETE formation by CAY10937 from either AA-derived 11(*R*)-HETE (Fig. 3.8A) or from added 11(*R*)-HETE (Fig. 3.8B) were similar. The corresponding EC₅₀ values for inhibition of 15-PGDH-mediated oxidation of AA-derived 11(*R*)-HETE (Fig. 3.8C) or added 11(*R*)-HETE (Fig. 3.8D) were similar to those found in mouse macrophages and human monocytes for inhibition of 15(*S*)-HETE oxidation (Wei et al., 2009). These results were very surprising in view of the lack of a 15(*S*)-hydroxyl group on 11(*R*)-HETE and suggested that perhaps the CAY10397 could be inhibiting another dehydrogenase. This was shown not to be the case because the catalytic activity of human 15-PGDH for oxidation of 11(*R*)-HETE was less than a factor of three lower than that observed for 15-oxo-ETE (Fig. 3.11). These data clearly show that 11(*R*)-HETE is an excellent substrate for 15-PGDH in spite of its lack of an appropriate functional group at C-15 and incorrect 11(*R*)-stereochemistry (Fig. 3.1).

We realized that when compared to 15-oxo-ETE, its isomer, 11-oxo-ETE, is very similar in structure to 15d-PGJ₂. It only differs in the lack of a C-8 to C-12 bond, in having a *cis*-8,9- rather than *cis*-9,10-double bond, and a *cis*- rather than *trans*-14,15-double bond (Fig. 3.1). This suggested that 11-oxo-ETE might be a more effective

inhibitor of HUVEC proliferation than 15-oxo-ETE (Wei et al., 2009) with a potency similar to that observed for 15d-PGJ₂ (Xin et al., 1999). Ground-breaking experiments conducted in 1994 by M. O'Reilly in the Folkman group had revealed that angiostatin, a kringle-containing internal fragment of plasminogen, was a potent inhibitor of endothelial cell proliferation (O'Reilly et al., 1994).

As noted above, inhibition of 15-PGDH resulted in significant decreases in 11-oxo-ETE formation in both RIES and human Caco-2 cells (Figs. 3.8B and 3.8D). 15-PGDH is down-regulated in numerous cancers (Celis et al., 2008; Tai et al., 2007; Pham et al., 2010; Thiel et al., 2009; Backlund et al., 2005; Tseng-Rogenski et al., 2010), which would cause a decrease in 11-oxo-ETE biosynthesis by preventing the *in vivo* conversion of 11(*R*)-HETE to 11-oxo-ETE (Fig. 3.1). This could potentially be devastating as COX-2 becomes up-regulated during tumorigenesis because the decreased 15-PGDH-mediated inactivation of PGE₂ through its conversion to 15-oxo-PGE₂ would result in increased in PGE₂-mediated pro-proliferative activity (Markowitz and Bertagnolli, 2009; Wang and Dubois, 2010) without the counter effect of anti-proliferative oxo-ETEs. Increased PGE₂ activity can also arise through up-regulation of the efflux ATP binding cassette (ABC) C4 transporter and down-regulation of the influx PG transporter - the organic anion transporter polypeptide (OATP) 2A1 (Fig. 3.12) (Holla et al., 2008; Meijerman et al., 2008).

Major metabolic pathways involved in 11-oxo-ETE inactivation involve GST-mediated formation of 11-OEG and a pathway that could involve AKRs (Fig. 3.12) (Penning and Byrns, 2009). Up-regulation of these metabolic pathways, which is often observed in cancer patients (Pompella et al., 2007; Meijerman et al., 2008; Penning and

Lerman, 2008), would reduce the amount of endogenous anti-proliferative 15-oxo-ETE and/or 11-oxo-ETE. Increased metabolism of 11-oxo-ETE and 15-oxo-ETE, together with reduced biosynthesis through down-regulation of 15-PGDH could then potentially result in increased endothelial cell proliferation (Bergers and Benjamin, 2003). The inhibition of endothelial cell proliferation could arise by a mechanism involving inhibition of the NF- κ B pathway as has been suggested for 15d-PGJ₂ (Scher and Pillinger, 2009). It is noteworthy that 11-oxo-ETE can activate the nuclear receptor PPAR γ (Waku et al., 2009). PPAR γ is a ligand-dependent transcription factor responsible for the regulation of a number of cellular events ranging from lipid metabolism to apoptosis (Wang and Dubois, 2008). 15d-PGJ₂ is also a PPAR γ agonist, which might account for its ability to inhibit endothelial cell proliferation (Forman et al., 1995; Xin et al., 1999). However, this effect is only observed with pharmacological amounts of 15d-PGJ₂ rather than endogenous concentrations (Ide et al., 2003). In view of the ability of COX-2/15-PGDH to rapidly metabolize AA to nM amounts of oxo-ETEs, together with the structural similarity of oxo-ETEs and 15d-PGJ₂ (Fig. 3.1), it will be important to determine which of these activities are shared by both classes of eicosanoids.

In summary, our studies have revealed that down-regulation of 15-PGDH inhibits the formation of 11-oxo-ETE and 15-oxo-ETE (an endogenous anti-proliferative eicosanoid). Therefore, 15-PGDH has two quite distinct properties; it can either inactivate PGs or activate HETEs to oxo-ETEs that potentially exert a paracrine effect on endothelial cells (Fig. 3.12). 11-oxo-ETE, a member of the oxo-ETE family, (O'Flaherty et al., 1994; Grant et al., 2009), was observed previously as an endogenously-derived lipid in human atherosclerotic plaques (Waddington et al., 2001). In that earlier study,

the biosynthesis of 11-oxo-EETE was not evaluated. Furthermore, there does not appear to be any subsequent reports of its formation either *in vitro* or *in vivo*. In this study, 11-oxo-EETE was identified to be derived from COX-2/15-PGDH-mediated AA metabolism, and it could potentially have similar activity as 15-oxo-EETE and 15d-PGJ₂ (Xin et al., 1999; Waku et al., 2009). There is some evidence 11-oxo-EETE is an activator of PPAR γ similar to 15d-PGJ₂ (Forman et al., 1995; Waku et al., 2009), which suggests it could have anti-proliferative activity similar to 15-oxo-EETE and 15d-PGJ₂ (Ondrey, 2009). Finally, biologically active stable analogs of 15-oxo-EETE, could potentially have efficacy as anti-cancer agents.

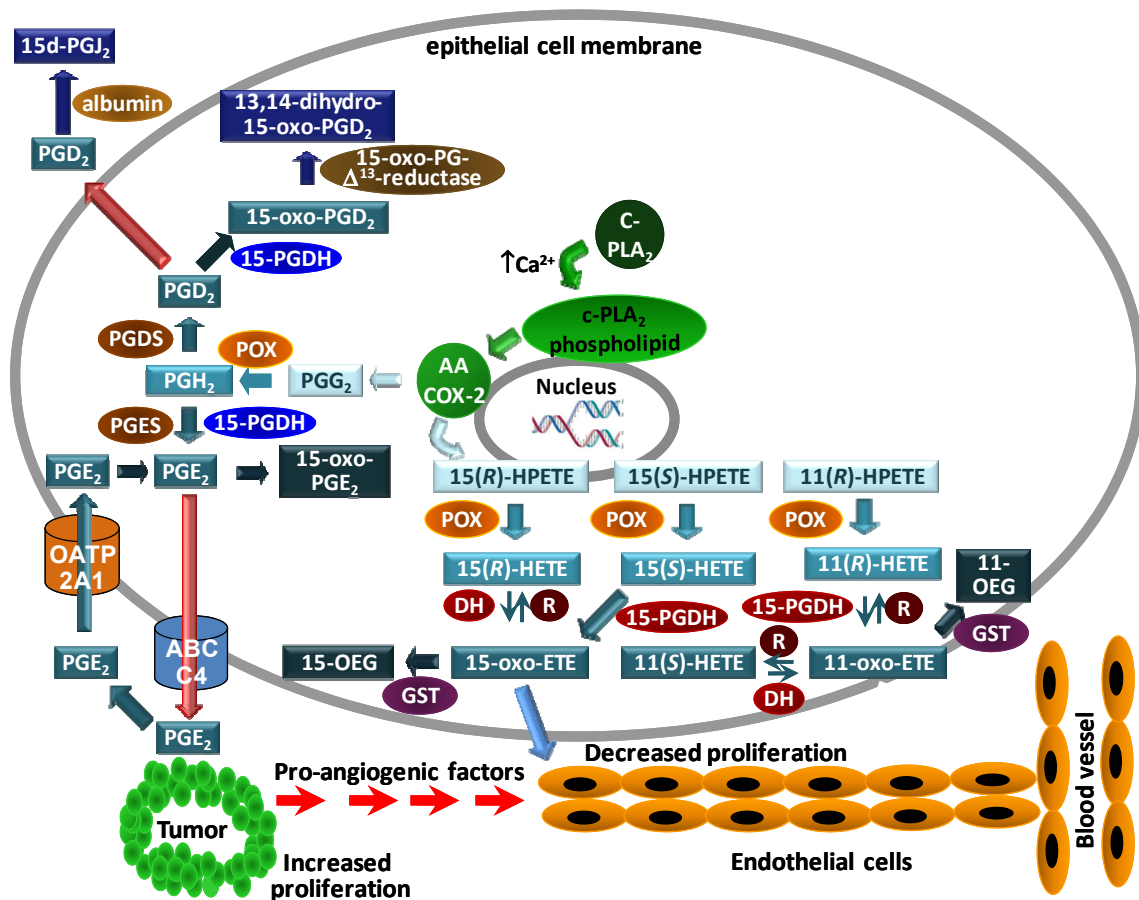


Figure 3.12 Formation and action of COX-2-derived eicosanoids in epithelial cell models. AA is released from membrane phospholipids by calcium-dependent cytosolic cPLA₂. The released AA undergoes COX-2-mediated metabolism to PGs or forms the LOX products 15(*R*)-HPETE, 15(*S*)-HPETE and 11(*R*)-HPETE, which are reduced to the corresponding HETEs. PGE₂ and PGD₂ are inactivated by 15-PGDH-mediated conversion to their 15-oxo-metabolites. PGE₂ released from the epithelial cells can initiate tumor cell proliferation. In contrast to PGE₂ and PGD₂, 15(*S*)-HETE and 11(*R*)-HETE are activated by 15-PGDH-mediated oxidation to 15-oxo-ETE and 11-oxo-ETE, respectively. 15(*R*)-HETE is oxidized by an unknown DH to 15-oxo-ETE. The oxo-ETEs are conjugated to form OEGs, which are secreted and hydrolyzed by γ -glutamyltranspeptidase to OECs. 15-oxo-ETE and 11-oxo-ETE are reduced back to HETEs in the mammalian epithelial cells (most likely by AKRs) and re-oxidized by DHs. Secreted 15-oxo-ETE can inhibit EC proliferation. Therefore, down-regulation of 15-PGDH would result in increased tumor cell proliferation and increased endothelial cell proliferation.

CHAPTER 4

Novel Aspirin Effect on COX-2-Mediated Formation and Metabolism of 15-Oxo-Eicosatetraenoic Acid and 11-Oxo-Eicosatetraenoic Acid

4.1 Abstract

COX-2 expression is upregulated in many cancers. Inhibition of COXs by nonsteroidal anti-inflammatory drugs (NSAIDs) such as aspirin has been recognized to reduce the risk of colon and breast cancers. However, the mechanism of the anti-tumorigenesis effect of aspirin is still uncertain. Our previous studies showed that aspirin significantly induced the production of 15(*R*)-HETE even after 24 h of treatment with AA. The present study was to determine the potential effect of aspirin on the formation and metabolic kinetics of AA metabolites in colorectal cancer cell models by LC-MS. Rat (RIES) and human epithelial cells (Caco-2) that expressed COX-2 were employed to study the effect of aspirin on the formation and metabolic kinetics of AA metabolites. RIES cells were treated with AA following the pretreatment with aspirin in comparison with no aspirin pretreatment, to determine the effect of aspirin on the production of 11-HETE, 15-HETE enantiomers, 15-oxo-ETE and 11-oxo-ETE formation and metabolism. Quantification of AA metabolites was performed using stable isotope dilution chiral LC coupled with ECAPCI/MS. The quantitative analysis revealed that aspirin pretreatment increased the 15(*R*)-HETE enantiomeric excess to 61%, comparing to the 15(*S*)-HETE enantiomeric excess of 19% with only AA treatment, indicating aspirin switched the 15(*S*)-lipoxygenase activity of COX-2 to 15(*R*)-lipoxygenase activity. The analysis also demonstrated that aspirin significantly accelerated the metabolism of 11(*R*)-HETE, 15(*S*), *R*)-HETEs, 11-oxo-ETE and 15-oxo-ETE. 15-oxo-ETE generation following 15(*R*)-

HETE treatment as well as 11-oxo-ETE generation following 11(*R*)-HETE treatment was also monitored by LC-EPAPCI/MS. The pretreatment of 11-hydroxysteroid-dehydrogenase (11-HSD) inhibitor, carbenoxolone, followed by AA treatment in RIES cells significantly inhibited the 15(*R*)-HETE-mediated production of 15-oxo-ETE in a dose-dependent manner, indicating 11-HSD is the enzyme catalyzing the metabolism of 15(*R*)-HETE to 15-oxo-ETE. These data also established that the formation of 15-oxo-ETE as a downstream metabolite of 15(*R*)-HETE in the AA metabolic pathway, and also suggests 11-HSD as the enzyme responsible for its biosynthesis from 15(*R*)-HETE. The formation of 15-oxo-ETE from 15(*R*)-HETE after aspirin treatment, through a pathway that does not involve 15-PGDH, could potentially help counteract the increased proliferative activity of PGE₂ in cancer.

4.2 Introduction

PUFAs such as AA and LA are present in many esterified lipid classes. Free AA and LA can be released from esterified lipid pools by the action of specific lipases. AA and LA, as free fatty acids or as esterified lipids, can be oxidized to lipid hydroperoxides either enzymatically by COXs (Blair, 2008) and LOs (Jian et al., 2009) or non-enzymatically by the action of ROS (Porter et al., 1995). The inducible COX isoenzyme, COX-2, is overexpressed in precursor lesions in colorectum (adenomatous polyps), breast (ductal carcinoma in situ), and lung (Eberhart et al., 1994; Hwang et al., 1998; Wolff et al., 1998; Half et al., 2002; Thun et al., 2002; Zhang and Sun, 2002; Brown and DuBois, 2005). Bioactive lipid mediators are increasingly being recognized as important endogenous regulators and biomarkers of cancer and cancer angiogenesis (Gonzalez-Periz and Claria, 2007; Marks et al., 2007; Wang and DuBois, 2007; Kim and Surh,

2008; Wang and Dubois, 2010). One of the major cascades of bioactive lipid mediator production involves the release of AA from membrane phospholipids followed by COX-2-mediated formation of eicosanoids, leading to the formation of bioactive prostaglandins (PGs) as well as HPETEs, HETEs and thromboxanes (Jones et al., 2003; Chen et al., 2006; Lee et al., 2007). Eicosanoids produced by COX-2 are thought to promote tumorigenesis by stimulating angiogenesis such as PGE₂ (Cha et al., 2006). The roles and the metabolism pathways of COX-2-mediated lipid hydroperoxide formation of HETEs as well as the novel bioactive family of oxo-ETEs in colon cancer progression have been largely ignored.

Although NSAIDs, which target COX enzymes, are still among the most promising chemopreventive agents for cancer, cardiovascular and gastrointestinal side effects have dampened enthusiasm for their use as chemopreventive agents (Wang and Dubois, 2010). Aspirin, also known as acetylsalicylic acid, is a widely used anti-inflammatory drug for more than 100 years, and is the only treatment combining the benefit of protection against cardiovascular disease with the potential to reduce the risk of some types of cancer (Cuzick et al., 2009). Aspirin is a non-selective COX-1/COX-2 inhibitor, which acetylates the enzymes and inhibits the conversion of AA to thromboxanes and PGs. Clinical studies showed that low dose aspirin (e.g. 100 mg) selectively inhibits thromboxane synthesis in platelets where COX-1 is constitutively expressed, and only small amounts of the drug survive reach the systemic circulation (Cuzick et al., 2009). Higher doses of aspirin (e. g. 500 mg) were shown to reach the systemic circulation and inhibit PGE₂ production in gastric epithelium and PGI₂ synthesis in vascular endothelial cells (Cuzick et al., 2009). A large body of evidence supports an

antitumor effect of aspirin on colorectal cancer (Cuzick et al., 2009), including two random trials of 300 mg, 500 mg, or 1200 mg daily, which showed a decrease in cancer incidence (Flossmann and Rothwell, 2007). Additionally, observational evidence of a chemopreventive effect of aspirin has been reported for esophageal, gastric, lung, breast, and prostate cancer (Schreinemachers and Everson, 1994; Bosetti et al., 2006). The aim of the present study was to determine whether could modulated the formation of HETEs and oxo-ETEs in rat and human colon cancer cell lines that expressed COX-2.

4.3 Materials and Methods

4.3.1 Materials – AA (peroxide-free), 15(*S*)-HPETE, 15(*S*)-HETE, 15-oxo-ETE, [²H₈]-15(*S*)-HETE, [²H₆]-5-oxo-AA (peroxide-free), 11(*R*)-HPETE, 11(*R*)-HETE, 15-oxo-ETE, [²H₈]-15(*S*)- HETE, [²H₆]-5-oxo-ETE, [²H₈]-12(*S*)-HETE, and [²H₄]-PGE₂ were purchased from Cayman Chemical Co. (Ann Arbor, MI). All chemicals, PFB bromide, aspirin, carbenoxolone disodium salt, and FBS were purchased from Sigma-Aldrich (St. Louis, MO). RPMI-1640 media, EMEM, D-glucose, L-glutamine, penicillin, and streptomycin were supplied by Invitrogen (Carlsbad, CA). High performance LC grade water, hexane, methanol, isopropanol and dichloromethane were obtained from Fisher Scientific (Fair Lawn, NJ). Gases were supplied by BOC Gases (Lebanon, NJ). Caco-2 cells were purchased from ATCC (Manassas, VA). RIES cells were a kind gift from Dr. Raymond N. DuBois (University of Texas M. D. Anderson Cancer Center, Houston, TX). Statistical analyses and kinetic plots were performed using GraphPad software (v5.01, GraphPad Software Inc., La Jolla, CA). BCA protein assay reagent was obtained from Pierce Biotechnology (Rockford, IL).

4.3.2 LC-MS Analysis of Eicosanoids - Normal phase chiral LC-ECAPCI/MS analyses for PFB-derivatized eicosanoids were conducted using a Finnigan TSQ Quantum Ultra AM spectrometer (Thermo Electron, San Jose, CA) as described in Chapter 2. The following MRM transitions were monitored with PFB-derivatized eicosanoids: 11-oxo-ETE (m/z 317 \rightarrow 165), 15-oxo-ETE (m/z 317 \rightarrow 113), [$^2\text{H}_6$]-5-oxo-ETE (m/z 323 \rightarrow 279), 15-HETEs (m/z 319 \rightarrow 219), [$^2\text{H}_8$]-15(*S*)-HETE (m/z 327 \rightarrow 226), 11-HETEs (m/z 319 \rightarrow 167), and [$^2\text{H}_8$]-12(*S*)-HETE (m/z 327 \rightarrow 184).

4.3.3 Cell Culture and Treatment - RIES cells and Caco-2 cells were cultured and maintained as described in Chapter 3.

4.3.4 AA Treatment of RIES cells – RIES cells were cultured as described above. The media was removed and replaced with serum-free RPMI 1640 containing peroxide-free AA (10 μM final concentration). The final concentration of ethanol in the culture media was less than 0.1 %. Cells were then incubated for 5 min, 15 min, 30 min, 40 min, 1 h, 3 h and 6 h at 37 $^\circ\text{C}$. After each incubation, the extraction, analysis and concentration calculations of eicosanoids were performed following the procedures as described in Chapter 3.

4.3.5 AA Treatment of RIES Cells with Aspirin - RIES cells were cultured as described above until almost confluent. The media was removed and replaced with serum-free RPMI-1640 containing aspirin (200 μM final concentration). The final concentration of ethanol in the culture media was less than 0.1 %. Cells were then incubated for 3 h at 37 $^\circ\text{C}$ followed by incubation with additional AA (10 μM final

concentration) for 5 min, 15 min, 30 min, 1 h, 3 h and 6 h at 37 °C. Lipid extractions from cell culture media (3 ml) were performed as described in Chapter 3.

4.3.6 15(*R*)-HETE Treatment of RIES Cells - RIES cells were cultured as described above until almost confluent. The media was removed and replaced with serum-free RPMI-1640 containing 15(*R*)-HETE (100 nM final concentration). The final concentration of ethanol in the culture media was less than 0.1 %. Cells were then incubated for 5 min, 15 min, 30 min, 1 h, 3 h and 6 h at 37 °C. Cells and media were then harvested for further analysis. Extraction and quantitation of 15(*R*)-HETE and 15-oxo-ETE from cell culture media (3 ml) were performed as described in Chapter 3.

4.3.7 15(*R*)-HETE of RIES Cells with 11-HSD Inhibitor Carbenoxolone - RIES cells were cultured as described above until almost confluent. The media was removed and replaced with serum-free RPMI-1640 containing various doses of carbenoxolone (0 µM, 10 µM or 100 µM final concentrations). Cells were then incubated for 3 h or 24 h at 37 °C followed by incubation with additional 15(*R*)-HETE (50 nM final concentration) for 10 min. Extraction and quantitation of 15(*R*)-HETE and 15-oxo-ETE from cell culture media (3 ml) were performed as described in Chapter 3.

4.3.8 AA or 11(*R*)-HETE Treatment of Caco-2 Cells - Caco-2 cells were cultured as described above. AA (10 µM final concentration) and 11(*R*)-HETE (50 nM final concentration) in ethanol was added to the media and cells were incubated for 5 min, 15 min, 30 min, 1 h, 3 h and 6 h at 37 °C. The final concentration of ethanol in the culture media was less than 0.1 %. Cells and media were then harvested for further analysis. A portion of cell supernatant (3 ml) was transferred into a glass tube and adjusted to pH 3 with 2.5 N HCl. Extraction of 15(*R,S*)-HETEs, 15-oxo-ETE, 11(*R,S*)-HETEs and 11-

oxo-ETE from cell culture media and LC-ECAPCI/MRM/MS analyses were performed as described in Chapter 3. Cell numbers were counted by a hemocytometer.

4.4 Results

4.4.1 Effect of Aspirin on AA-mediated Production of HETEs in RIES Cells - RIES

cells were incubated with 10 μ M AA for 6 h and LC-ECAPCI/MRM/MS analyses of the RIES cell supernatants was conducted. This demonstrated the secretion of 15-oxo-ETE (rt 7.7 min) as well as its potential precursors 15(*R*)-HETE (rt, 11.8 min) and 15(*S*)-HETE (rt, 15.1 min) within 5 min of AA treatment (Fig. 4.1A). The chromatograms also revealed the presence of 11-oxo-ETE (rt, 7.6 min) and 11(*R*)-HETE (rt, 10.6 min) (data not shown). When RIES cells were incubated with 10 μ M AA for a period of 6 h following 200 μ M aspirin pretreatment, the LC-ECAPCI/MRM/MS analyses of the RIES cell supernatants demonstrated the secretion of 15-oxo-ETE (rt 7.8 min) as well as its potential precursors 15(*R*)-HETE (rt, 11.9 min) and 15(*S*)-HETE (rt, 15.2 min) within 5 min of AA treatment (Fig. 4.1B). The chromatogram showed that the ratio of 15(*R*)-HETE to 15(*S*)-HETE in the cells with aspirin pretreatment was much higher than that in only AA treatment. The chromatograms also revealed the presence of 11-oxo-ETE (rt, 7.6 min) and 11(*R*)-HETE (rt, 10.6 min) (data not shown).

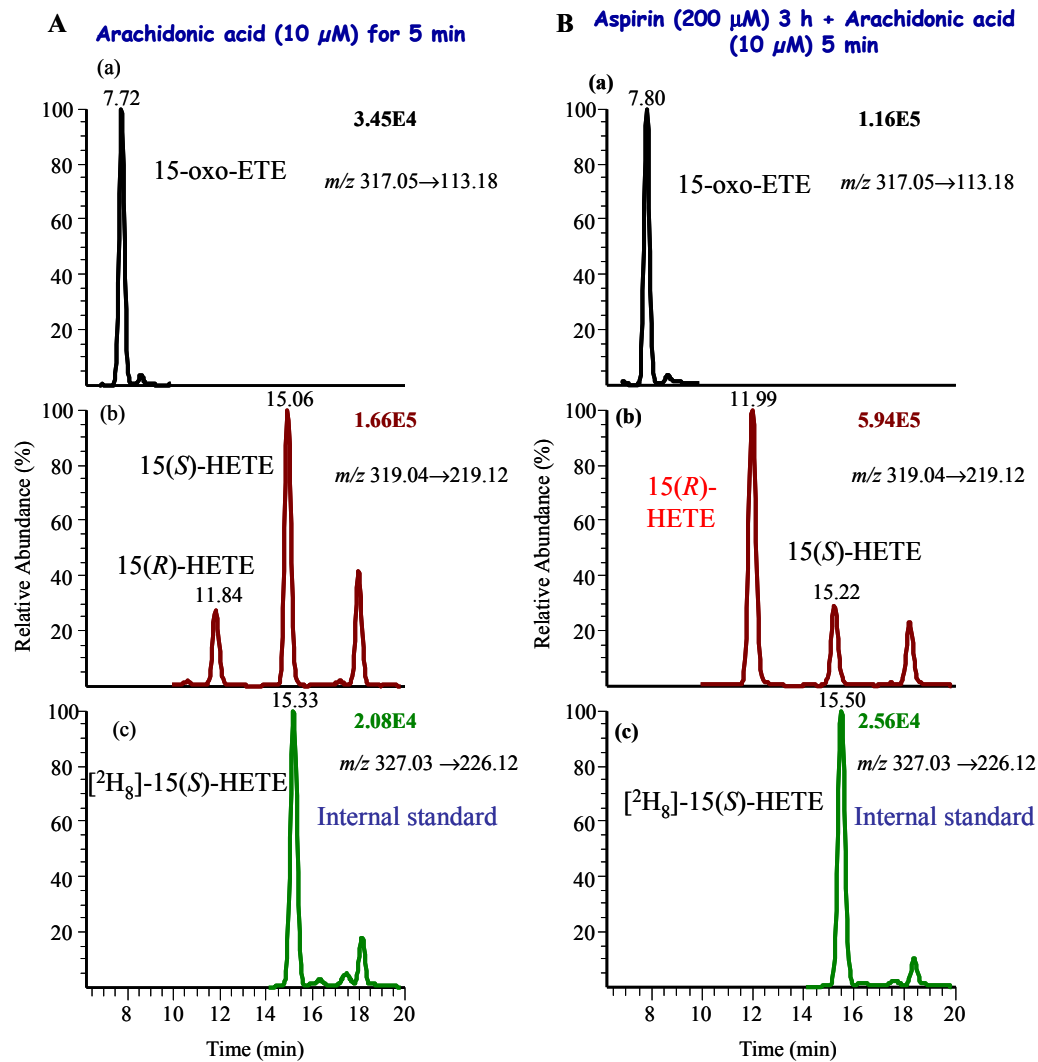


Figure 4.1 LC-MRM/MS analysis of 15(*R,S*)-HETE and 15-oxo-EETE derived from AA in RIES cells. (A) Representative chromatograms of COX-2-derived 15(*R,S*)-HETE and 15-oxo-EETE released by RIES cells after 5-min treatment with 10 μ M AA. (B) Representative chromatograms of 15(*R,S*)-HETE and 15-oxo-EETE released by RIES cells treated with 10 μ M AA for 5 min following the treatment with 200 μ M aspirin for 3 h. MRM chromatograms are shown for (a) 15-oxo-EETE-PFB (m/z 317 \rightarrow 113), (b) 15-

(*R,S*)-HETE-PFB (m/z 319 \rightarrow 219), and (c) [$^2\text{H}_8$]-15(*S*)-HETE-PFB internal standard (m/z 327 \rightarrow 226).

4.4.2 Kinetics of 15(*R, S*)-HETE and 15-oxo-ETE Metabolism by RIES Cells and

Aspirin-Treated RIES Cells - RIES cells were incubated with AA (10 μM) for 6 h.

15(*R, S*)-HETE was one of the abundant metabolites of AA released by cells, as we had observed previously (Lee et al., 2007). The maximum 15(*R,S*)-HETE concentrations was 15.73 (\pm 0.55) nM within 5-min treatment of AA (Fig. 4.2A). 15(*R, S*)-HETE was then rapidly metabolized over 6 h with a half-life ($t_{1/2}$) of 29.6 min and a pseudo first-order rate constant (k) of 0.0234 min^{-1} (Fig. 4.2A). The area under curve (AUC) of 15(*R, S*)-HETE metabolism was determined to be 1254.6 nmol.min/L (Fig. 4.2A). Concomitantly, 15-oxo-ETE in the cell media was observed to peak within 5 min of AA treatment with the concentration of 2.66 (\pm 0.03) nM, and a pseudo first-order rate constant (k) of 0.0235 min^{-1} and AUC of 196.0 nmol.min/L (Fig. 4.2B). Quantification of 15(*R*)- and 15(*S*)-HETE revealed a 19 % enantiomeric excess of 15(*S*)-HETE (Fig. 4.2A).

When RIES cells were incubated with AA (10 μM) for 6 h, with the pre-treatment with aspirin (200 μM) for 3 h, the maximum 15(*R*)-HETE concentrations was 38.69 (\pm 1.90) nM within 5-min treatment of AA (Fig. 4.2C). 15(*R*)-HETE was then rapidly metabolized over 3 h with a half-life ($t_{1/2}$) of 2.48 min and a pseudo first-order rate constant (k) of 0.2798 min^{-1} (Fig. 4.2C). The area under curve (AUC) of 15(*R*)-HETE metabolism was determined to be 1428.6 nmol.min/L (Fig. 4.2C). Concomitantly, 15-oxo-ETE in the cell media was observed to peak within 5 min of AA treatment with the concentration of 7.32 (\pm 0.37) nM, and declined to a steady state of 0.29 (\pm 0.05) nM

after 1 h (Fig. 4.2D). The half-life ($t_{1/2}$) of 15-oxo-ETE was determined to be 3.72 min and the pseudo first-order rate constant (k) was 0.1862 min^{-1} with AUC of $186.1 \text{ nmol}\cdot\text{min}/\text{L}$ (Fig. 4.2D). Aspirin significantly accelerated the initial rate of 15(*R,S*)-HETE and 15-oxo-ETE metabolism and made 15-oxo-ETE reach a steady concentration after 1 h. Quantification of 15(*R*)- and 15(*S*)-HETE revealed a 61 % enantiomeric excess of 15(*R*)-HETE in the aspirin-treated RIES cells (Fig. 4.2C), compared with 19 % enantiomeric excess of 15(*S*)-HETE in only AA-treated RIES cells (Fig. 4.2A).

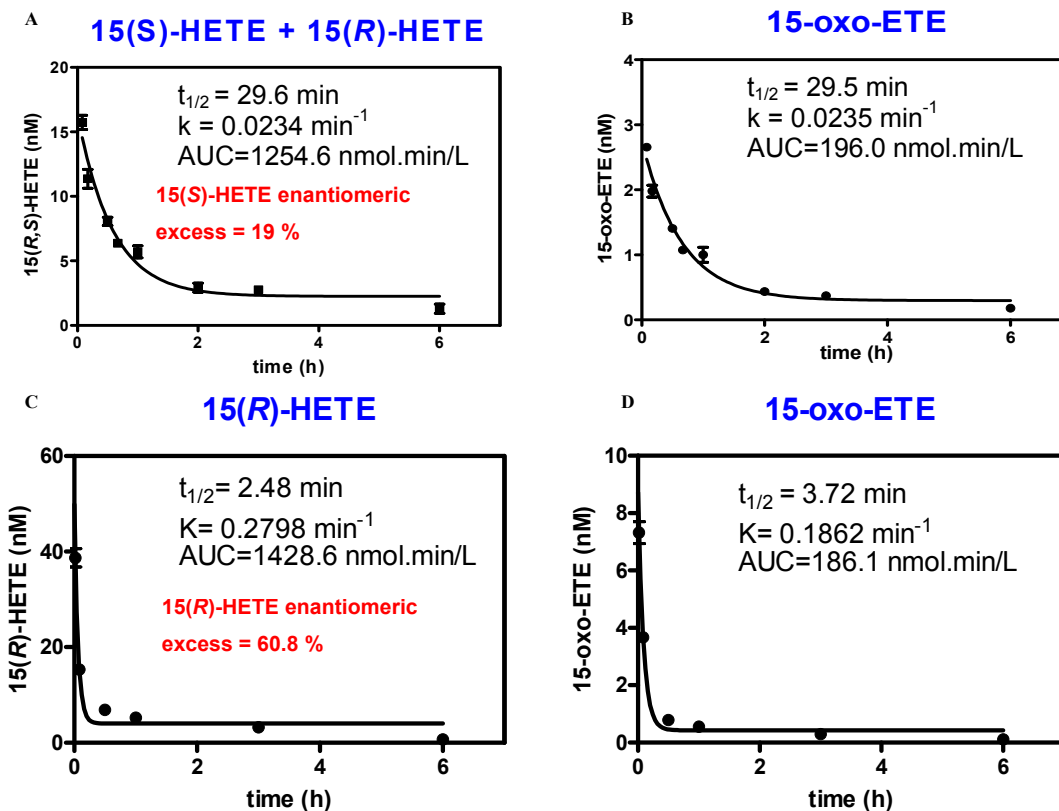


Figure 4.2 Kinetics of 15(*R, S*)-HETE and 15-oxo-ETE by RIES cells. RIES cells were incubated with $10 \mu\text{M}$ AA for a period of 360 min (A, B) or with $200 \mu\text{M}$ aspirin for 3 h followed by $10 \mu\text{M}$ AA treatment for a period of 360 min (C, D). The media were

collected at different time points. Secreted lipid metabolites present in the media were extracted, converted to PFB derivative, and their concentrations were determined in triplicate (means \pm S.E.M.) by stable isotope dilution chiral LC-ECAPCI/MRM/MS analysis. (A) Kinetic plot of 15(*S*, *R*)-HETE metabolism by RIES cells to which only AA was added ($t_{1/2}$ =29.6 min); (B) Kinetic plot of 15-oxo-ETE metabolism by only AA-treated RIES cells ($t_{1/2}$ =29.5 min); (C) Kinetic plot of 15(*R*)-HETE metabolism by aspirin treated-RIES cells followed by AA treatment ($t_{1/2}$ =2.48 min); (D) Kinetic plot of 15-oxo-ETE metabolism by aspirin treated-RIES cells followed by AA treatment ($t_{1/2}$ =3.72 min).

4.4.3 Kinetics of 11(*R*)-HETE and 11-oxo-ETE Metabolism by RIES Cells and Aspirin-Treated RIES Cells

RIES cells were incubated with AA (10 μ M) for 6 h. 11(*R*)-HETE was the most abundant metabolite of AA released by cells at the early time points (< 1 h), as we had observed previously (Lee et al., 2007). The maximum 11(*R*)-HETE concentrations was 15.13 (\pm 0.43) nM within 5-min treatment of AA (Fig. 4.3A). 11(*R*)-HETE was then rapidly metabolized over 3 h with a half-life ($t_{1/2}$) of 21.6 min and a pseudo first-order rate constant (k) of 0.0321 min^{-1} (Fig. 4.3A). The area under curve (AUC) of 11(*R*)-HETE metabolism was determined to be 904.8 nmol.min/L (Fig. 4.3A). Concomitantly, 11-oxo-ETE in the cell media was observed to peak within 5 min of AA treatment with the concentration of 1.42 (\pm 0.17) nM, and declined to a steady state of 0.23 (\pm 0.03) nM after 3 h (Fig. 4.3B). The half-life ($t_{1/2}$) of 11-oxo-ETE was determined to be 32.2 min and the pseudo first-order rate constant (k) was 0.0215 min^{-1} with AUC of 135.2 nmol.min/L (Fig. 4.3B). Only trace amounts of 11(*S*)-HETE were observed after the addition of AA (Fig. 3.4Af) or 11(*R*)-HETE (data not shown) to the RIES cells.

When RIES cells were incubated with AA (10 μ M) for 6 h, with the pre-treatment with aspirin (200 μ M) for 3 h, the maximum of 11(*R*)-HETE concentrations was 4.07 (\pm 0.16) nM within 5-min treatment of AA (Fig. 4.3C). 11(*R*)-HETE was then rapidly metabolized over 3 h with a half-life ($t_{1/2}$) of 3.72 min and a pseudo first-order rate constant (k) of 0.1862 min^{-1} (Fig. 4.3C). The area under curve (AUC) of 11(*R*)-HETE metabolism was determined to be 447.1 nmol.min/L (Fig. 4.3C). Concomitantly, 11-oxo-ETE in the cell media was observed to peak within 5 min of AA treatment with the concentration of 1.06 (\pm 0.34) nM, and declined to a steady state of 0.24 (\pm 0.03) nM after 1 h (Fig. 4.3D). The half-life ($t_{1/2}$) of 11-oxo-ETE was determined to be 10.72 min and the pseudo first-order rate constant (k) was 0.0647 min^{-1} with AUC of 110.1 nmol.min/L (Fig. 4.3D). These data suggested that besides the effect on 15(*R,S*)-HETE and 15-oxo-ETE metabolism, aspirin also caused significant acceleration of 11(*R*)-HETE and 11-oxo-ETE metabolism.

4.4.4 Kinetics of 15(*R*)-HETE to 15-oxo-ETE Metabolism by RIES Cells - RIES cells were incubated with 15(*R*)-HETE (100 nM) for 6 h. The $t_{1/2}$ of 15(*R*)-HETE metabolism in the cells was determined to be 42.5 min and the pseudo first-order rate constant (k) was 0.0163 min^{-1} with an AUC of 5455.8 nmol.min/L (Fig. 4.4A). Concomitantly, 15-oxo-ETE in the cell media was observed to peak within 5 min of 15(*R*)-HETE treatment with the concentration of 5.56 nM, and declined to a steady state of 0.51 nM after 6 h (Fig. 4.4B). The $t_{1/2}$ of 15-oxo-ETE derived from the addition of 15(*R*)-HETE to the cells was determined to be 40.0 min and k was 0.0173 min^{-1} with an AUC of 513.5 nmol.min/L (Fig. 4.4B). Only trace amounts of 15(*S*)-HETE were observed after the addition 15(*R*)-HETE to the RIES cells (data not shown).

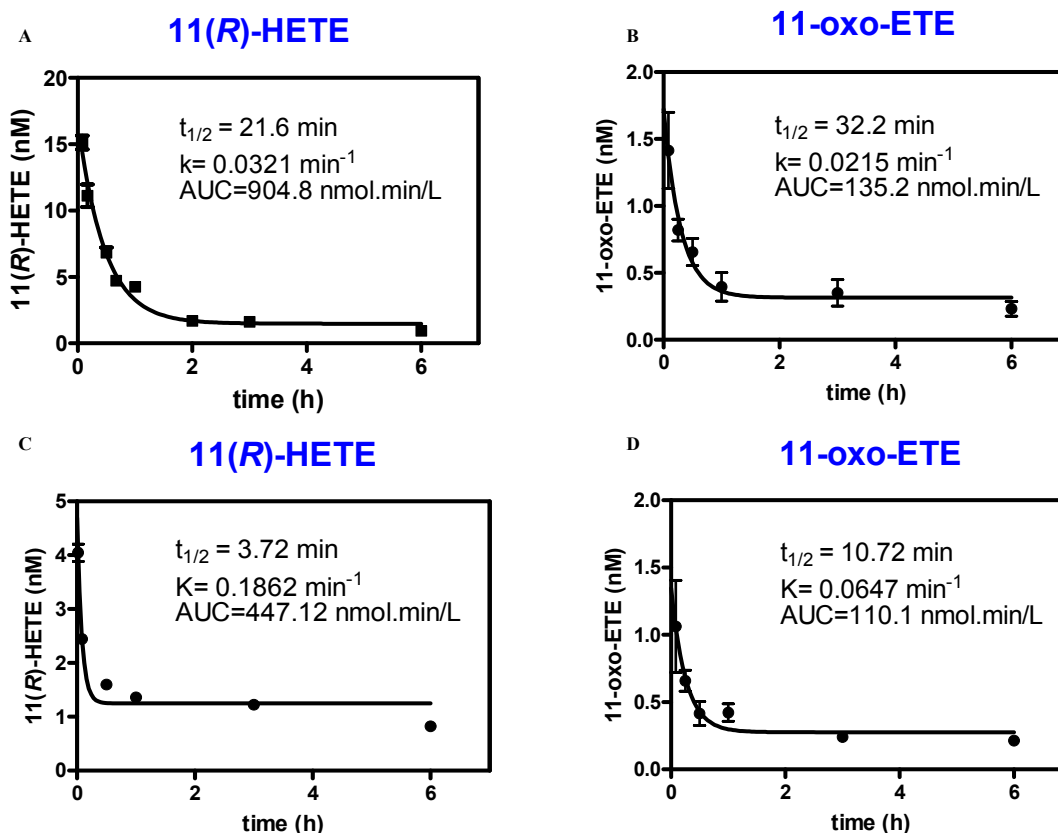


Figure 4.3 Kinetics of 11(R)-HETE and 11-oxo-EETE by RIES cells. RIES cells were incubated with 10 μM AA for a period of 360 min (**A**, **B**) or with 200 μM aspirin for 3 h followed by 10 μM AA treatment for a period of 360 min (**C**, **D**). The media were collected at different time points. Secreted lipid metabolites present in the media were extracted, converted to PFB derivative, and their concentrations were determined in triplicate (means \pm S.E.M.) by stable isotope dilution chiral LC-ECAPCI/MRM/MS analysis. (**A**) Kinetic plot of 11(R)-HETE metabolism by RIES cells only incubated with AA ($t_{1/2}=21.6 \text{ min}$); (**B**) Kinetic plot of 11-oxo-EETE metabolism by only AA-treated RIES cells ($t_{1/2}=32.2 \text{ min}$); (**C**) Kinetic plot of 11(R)-HETE metabolism by aspirin treated-RIES cells followed by AA treatment ($t_{1/2}=3.72 \text{ min}$); (**D**) Kinetic plot of 11-oxo-

ETE metabolism by aspirin treated-RIES cells followed by AA treatment ($t_{1/2}$ =10.72 min).

15(R)-HETE (100 nM) added to RIES cells

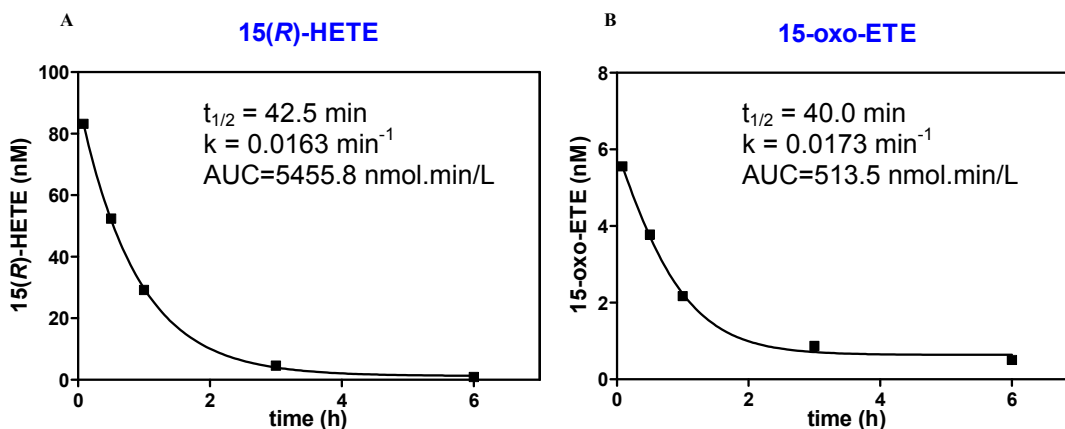


Figure 4.4 Metabolism of 15(R)-HETE to 15-oxo-ETE by RIES cells. RIES cells were incubated with 15(R)-HETE (100 nM) for a period of 360 min. The media was collected at different time points. Lipid metabolites [15(R)-HETE and 15-oxo-ETE] in the cell supernatant were extracted and derivatized with PFB and their concentrations were determined in triplicate (means \pm S.E.M.) by LC-ECAPCI/MRM/MS analysis. (A) Kinetic plot of 15(R)-HETE metabolism by RIES cells treated with 15(R)-HETE (100 nM) ($t_{1/2}$ =42.5 min and k =0.0163 min⁻¹); (B) Kinetic plot of 15-oxo-ETE metabolism by RIES cells treated with 15(R)-HETE (100 nM) ($t_{1/2}$ =40.0 min and k =0.0173 min⁻¹).

4.4.5 Effect of Carbenoxolone on 15(R)-HETE and 15-oxo-ETE in RIES Cells –

Carbenoxolone (CBX) is a selective inhibitor of the 11 β -HSD that oxidizes 11(S)-hydroxyl group of prostaglandins (PGs) and 11(S)-HETE to a 11-oxo-group (Duax et al., 2000). RIES cells were treated with 50 nM 15(R)-HETE for 10 min, with or without the pretreatment with various doses of CBX (10 μ M or 100 μ M) for 3 h or 24 h. The level of

15(*R*)-HETE was determined to be 18.48 (\pm 0.38) nM in the absence of carbenoxolone; whereas pre-treatment with 10 μ M or 100 μ M CBX for 24 h resulted in an increased level of 15(*R*)-HETE to 27.21 (\pm 1.46) nM or 32.67 (\pm 0.77) nM, respectively (Fig. 4.5A). Conversely, the level of 15-oxo-EETE was determined to be 0.86 (\pm 0.05) nM in the absence of CBX; whereas pre-treatment with CBX resulted in a decreased level of 15-oxo-EETE to 0.54 (\pm 0.08) nM for 10 μ M CBX and 0.33 (\pm 0.03) nM for 100 μ M CBX (Fig. 4.5B). This suggested CBX led to an increase of 15(*R*)-HETE (Fig. 4.5A) and a simultaneous inhibition of the production of 15-oxo-EETE (Fig. 4.5B), which was also observed when cells were pretreated with CBX for 3 h (Fig. 4.5C and D). These data revealed that 15(*R*)-HETE was oxidized to 11-oxo-EETE by 11 β -HSD in RIES cells.

4.4.6 AA-mediated Production of HETEs in Caco-2 cells - The Caco-2 cells were incubated with AA as described for the Caco-2 cells for 6 h (Fig. 4.6). A similar product profile was observed as for the RIES cells (Figs. 4.3A and 4.3B) with 11-oxo-EETE, 15-oxo-EETE, 15(*R*)-HETE, 15(*S*)-HETE and 11(*R*)-HETE as the major AA-derived metabolites in human Caco-2 cells (Fig. 4.6). However, unlike the RIES cells, a significant amount of 11(*S*)-HETE was secreted from the cells (Fig 4.6B). The $t_{1/2}$ of AA-derived 11(*S*)-HETE metabolism in Caco-2 cells was 62.0 min and the pseudo first-order rate constant (k) was 0.0164 min^{-1} with AUC of 128.2 nmol.min/L (Fig. 4.6B). The $t_{1/2}$ of 11-oxo-EETE metabolism in Caco-2 cells was 21.1 min and k was 0.0328 min^{-1} with AUC of 69.1 nmol.min/L (Fig. 4.6C). The $t_{1/2}$ (=39.2 min) of AA-derived 11(*R*)-HETE metabolism in Caco-2 cells (Fig. 4.6A) was longer than that in RIES cells (Fig. 4.3A). The k was 0.0258 min^{-1} and the AUC of 11(*R*)-HETE was 286.0 nmol.min/L (Fig. 4.3A).

4.4.7 Kinetic Analysis of 11(*R*)-HETE to 11-oxo-ETE Metabolism by Caco-2 Cells -

Caco-2 cells were incubated with 11(*R*)-HETE (50 nM) as described above for 6 h. The $t_{1/2}$ of 11(*R*)-HETE metabolism in the cells was determined to be 27.6 min and k was 0.00254 min^{-1} with AUC of 1884.0 nmol.min/L (Fig. 4.7A). Concomitantly, 11-oxo-ETE in the cell media was observed to peak within 5 min of 11(*R*)-HETE treatment with the concentration of 0.10 nM, and declined to a steady state of 0.031 nM after 6 h (Fig. 4.4B). The $t_{1/2}$ of 11-oxo-ETE derived from the addition of 11(*R*)-HETE to the cells was determined to be 19.3 min and k was 0.0360 min^{-1} with an AUC of 13.9 nmol.min/L (Fig. 4.7C). 11(*S*)-HETE was also observed after the addition 11(*R*)-HETE to the Caco-2 cells. The maximum of 11(*S*)-HETE production was 2.5 nM at 5 min after addition of 11(*R*)-HETE (Fig. 4.7B). The $t_{1/2}$ of 11(*S*)-HETE to the cells was determined to be 28.0 min and k was 0.0248 min^{-1} with an AUC of 121.1 nmol.min/L (Fig. 4.7B). These data suggested that there was a conversion of 11-oxo-ETE to 11(*S*)-HETE during the 6-h-time-course in human epithelial colorectal adenocarcinoma Caco-2 cells.

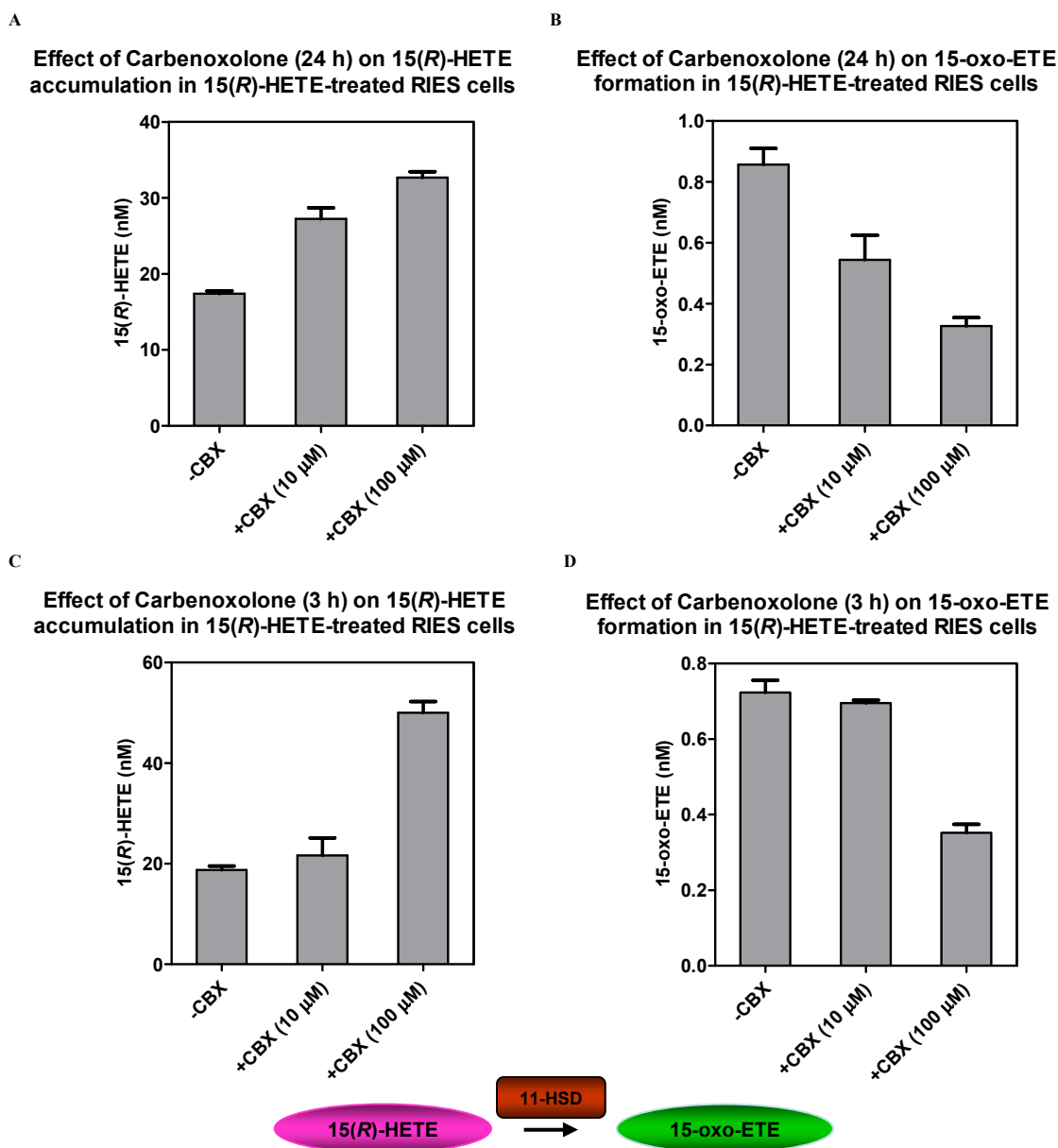


Figure 4.5 Inhibition of 15(*R*)-HETE metabolism to 15-oxo-EETE by 11-HSD inhibitor carbenoxolone (CBX) in RIES cells. (A) Increased 15(*R*)-HETE level by RIES cells that were pretreated with 10 μ M or 100 μ M CBX for 24 h before the addition of 15(*R*)-HETE (50 nM) for 10 min. (B) Inhibition of 15-oxo-EETE formation by RIES cells that were pretreated with 10 μ M or 100 μ M CBX for 24 h before the addition of

15(*R*)-HETE (50 nM) for 10 min. (C) Increased 15(*R*)-HETE level by RIES cells that were pretreated with 10 μ M or 100 μ M CBX for 3 h before the addition of 15(*R*)-HETE (50 nM) for 10 min. (D) Inhibition of 15-oxo-EETE formation by RIES cells that were pretreated with 10 μ M or 100 μ M CBX for 3 h before the addition of 15(*R*)-HETE (50 nM) for 10 min. Lipid metabolites in the cell media were extracted and derivatized with PFB. 15(*R*)-HETE and 15-oxo-EETE concentrations were determined in triplicate by stable isotope dilution by LC-ECAPCI/MRM/MS analysis of PFB derivatives. Values presented in bar graphs are means \pm S.E.M.

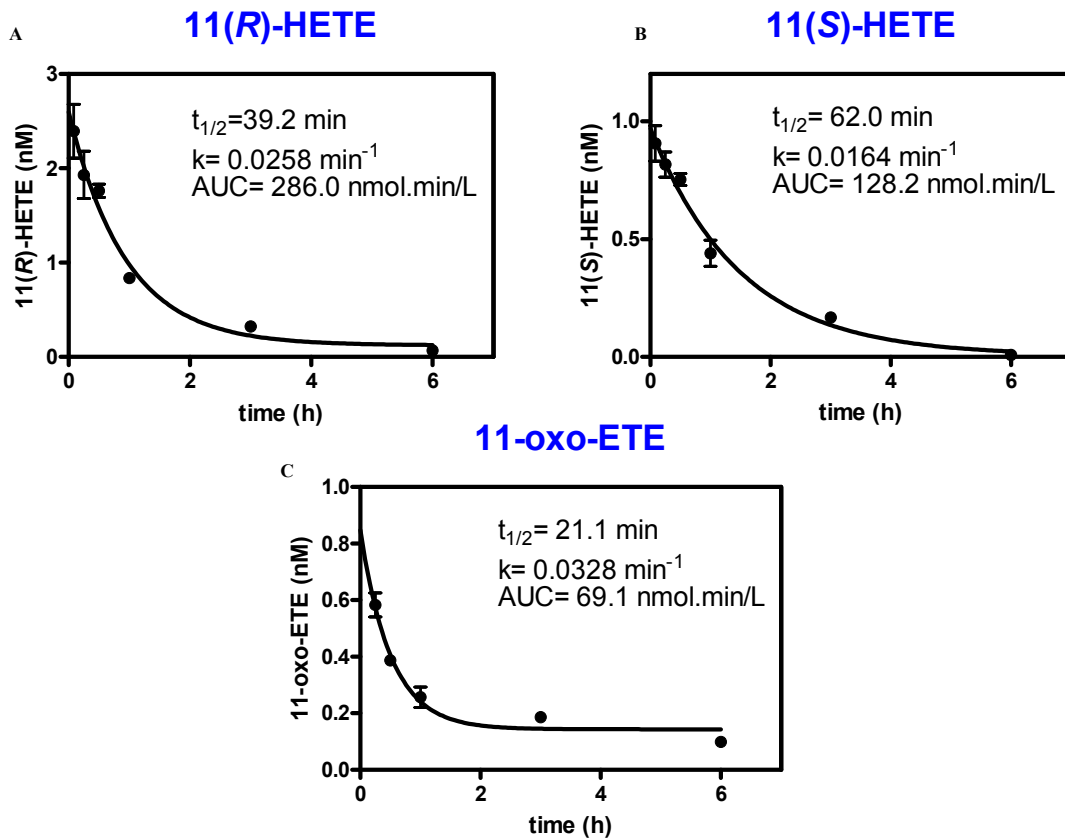


Figure 4.6 Metabolism of AA to 11(*R,S*)-HETE and 11-oxo-ETE by Caco-2 cells.

(A) 11(*R*)-HETE formation by cells that were treated with 10 μM AA for a period of 6 h.

(B) 11(*S*)-HETE formation by cells that were treated with 10 μM AA for a period of 6 h.

(C) 11-Oxo-ETE formation by cells that were treated with 10 μM AA for a period of 6 h.

Lipid metabolites in the cell media were extracted and derivatized with PFB. 11-Oxo-ETE and 11(*R,S*)-HETE concentrations were determined in triplicate by stable isotope dilution LC-ECAPCI/MRM/MS analyses of PFB derivatives. Values presented in bar graphs are means \pm S.E.M.

11(*R*)-HETE (50 nM) added to Caco-2 cells

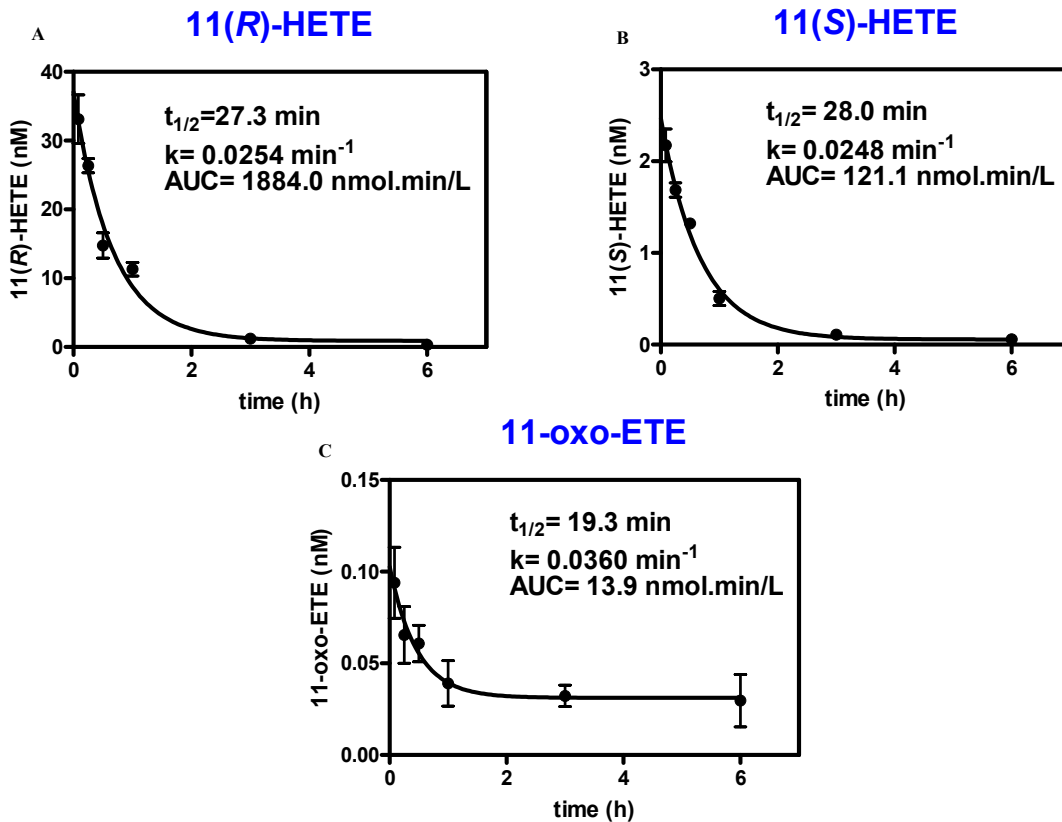


Figure 4.7 Kinetics of 11(*R, S*)-HETE and 11-oxo-EETE by Caco-2 cells. Caco-2 cells were incubated with 11(*R*)-HETE (50 nM) for a period of 6 h. (A) Kinetic plot of 11(*R*)-HETE metabolism by Caco-2 cells treated with 11(*R*)-HETE (100 nM) ($t_{1/2}=27.3$ min and $k=0.0163$ min⁻¹); (B) Formation and metabolism of 11(*S*)-HETE metabolism by Caco-2 cells treated with 11(*R*)-HETE (50 nM) ($t_{1/2}=28$ min and $k=0.0248$ min⁻¹); (C) Kinetic plot of 11-oxo-EETE metabolism by Caco-2 cells treated with 11(*R*)-HETE (50 nM) ($t_{1/2}=19.3$ min and $k=0.0360$ min⁻¹). Lipid metabolites in the cell media were extracted and derivatized with PFB. 11(*R,S*)-HETE and 11-oxo-EETE concentrations were determined in triplicate by stable isotope dilution by LC-ECAPCI/MRM/MS analysis of PFB derivatives. Values presented in bar graphs are means \pm S.E.M.

4.5 Discussion

COX-2 is the enzyme responsible for the formation of PGs *in vivo*. However, it also has 15-LO activity for 15(*R,S*)-HETE biosynthesis and 11-LO activity for the biosynthesis of 11(*R*)-HETE (Lee et al., 2007). The enzyme expression is elevated in most human colorectal cancer (CRC) and is associated with worse survival among CRC patients (Wang and Dubois, 2010). In addition, numerous studies have implicated the COX-2 pathway as an important mediator in inflammation, cardiovascular diseases, and neurological diseases, but very little studies have been focused on the effect of NSAIDs on COX-2-mediated lipid hydroperoxides. Our recent studies on lipid peroxidation suggested that eicosanoids formed from COX-2- and 15-LO-1-mediated AA metabolism could modulate cell proliferation and might be involved in inflammatory pathways (Lee et al., 2007; Wei et al., 2009). We hypothesized that aspirin as one of NSAIDs which

inhibited COX-2 activity would modulate the formation and metabolism of AA-derived 15-oxo-ETE. This could in principle confer a beneficial therapeutic effect because 15-oxo-ETE is an anti-proliferative eicosanoid (Wei et al. 2009).

AA-derived eicosanoids released from RIES cells with aspirin pretreatment followed with AA or with only AA treatment were analyzed by chiral LC-ECAPCI/MS methodology (Lee and Blair, 2007; Mesaros et al., 2009). This revealed 15(*R*)-HETE and 15-oxo-ETE as the major products in aspirin-pretreated cells (Fig. 4.1 and 4.2). Aspirin caused a significant chirality switch of 15-HETE from 15(*S*)-HETE to 15(*R*)-HETE (Fig. 4.1), with the enantiomeric excess of 15(*R*)-HETE up to 61% compared to the 19% enantiomeric excess of 15(*S*)-HETE in only AA-treated RIES cells (Fig. 4.2A and C). In addition, 15-oxo-ETE levels released from aspirin-treated RIES cells were 3 times higher than with only AA treatment (Fig. 4.2B and D). Aspirin-pretreated RIES cells were found to significantly increase the rate of metabolism of 15(*R*)-HETE, 15-oxo-ETE, 11(*R*)-HETE and 11-oxo-ETE by 12 times, 8 times, 6 times and 3 times, respectively.

15(*R*)-HETE added to RIES cells was converted to 15-oxo-ETE as expected (Fig. 4.4). After addition of 15(*R*)-HETE (100 nM) to RIES cells, the half-life of 15(*R*)-HETE and 15-oxo-ETE was slightly longer than that of AA-derived 15(*R*)-HETE and 15-oxo-ETE (Fig. 4.2 and 4.4). That 15-PGDH inhibitor CAY10397 inhibited the conversion of 15(*S*)-HETE to 15-oxo-ETE but did not inhibit the metabolism of 15(*R*)-HETE (Wei et al., 2009). Therefore, 15-PGDH is not involved in the oxidation of 15(*R*)-HETE to 15-oxo-ETE.

The present study demonstrated that 11 β -HSD inhibitor carbenoxolone caused a decreased in the formation of 15-oxo-ETE (Fig. 4.5B) and a simultaneous increase of 15(*R*)-HETE in a dose-dependent manner in RIES cells (Fig. 4.5). In human, There are two isoforms of 11 β -HSD, 11 β -hydroxysteroid dehydrogenase type 1 (11 β -HSD I) and 11 β -hydroxysteroid dehydrogenase type 2 (11 β -HSD II) (Seckl, 1997). Both types of 11 β -HSD catalyzes the conversion of inert 11-oxo-steroids (cortisone) to active 11-oxo-steroids (cortisol), or vice versa (Seckl and Walker, 2001), thus regulating the access of glucocorticoids to their steroid receptors. It was observed that human renal 11 β -HSDI appears to function as a dehydrogenase with no significant "reverse" reductase activity (Gong et al., 2008). The study in kidney by using immuno-histochemistry and Western blot analysis showed that 11 β -HSDI was found to co-localize with COX-2 in proximal tubule cells, while COX-2 was not observed co-localizing with 11 β -HSDII in cortical collecting duct (Gong et al., 2008). The COX-2 mRNA response to IL-1 α was associated with an approximate 18-fold increase in mRNA levels of 11 β -HSDI in human ovarian surface epithelial cells which was considered as a compensatory anti-inflammatory component to the process of COX-2-mediated inflammation (Rae et al., 2004). Interestingly, the expression of 11 β -HSD II was up-regulated in human colonic and Apc^{+/*min*} mouse intestinal adenomas, and inhibition of 11 β -HSD II suppressed colon carcinogenesis in mice and humans (Zhang et al., 2009). Further studies need to be performed in order to confirm which specific type of 11 β -HSD (I or II) involved in conversion of 15(*R*)-HETE to 15-oxo-ETE.

Our studies have demonstrated that aspirin-mediated conversion of COX-2 into a 15(*R*)-lipoygenase results in increased formation of 15-oxo-ETE (Fig. 4.8). In contrast

to 15(*S*)-HETE, 15(*R*)-HETE is converted to 15-oxo-EETE through a pathway that does not involve 15-PGDH. Most likely the oxidation of 15(*R*)-HETE is mediated through an 11 β -HSD. The formation of 11(*R*)-HETE and 11-oxo-EETE was much lower than that observed before aspirin treatment. The oxo-EETs are conjugated to form OEGs, which are secreted and hydrolyzed by γ -glutamyltranspeptidase to OECs. 15-oxo-EETE and 11-oxo-EETE are reduced back to HETEs in human epithelial cells (most likely by AKRs) and re-oxidized by DHs. Secreted 15-oxo-EETE is potentially anti-angiogenic through inhibition of EC proliferation. 11-oxo-EETE could have similar activity as 15-oxo-EETE, although additional studies will be required to test this possibility. Therefore, down-regulation of 15-PGDH would result in decreased anti-proliferative 15-oxo-EETE, increased pro-proliferative PGE₂ and so the potential for concomitant increased tumor and EC proliferation. The formation of 15-oxo-EETE from 15(*R*)-HETE after aspirin treatment, through a pathway that does not involve 15-PGDH, could potentially help counteract the increased pro-proliferative activity of PGE₂.

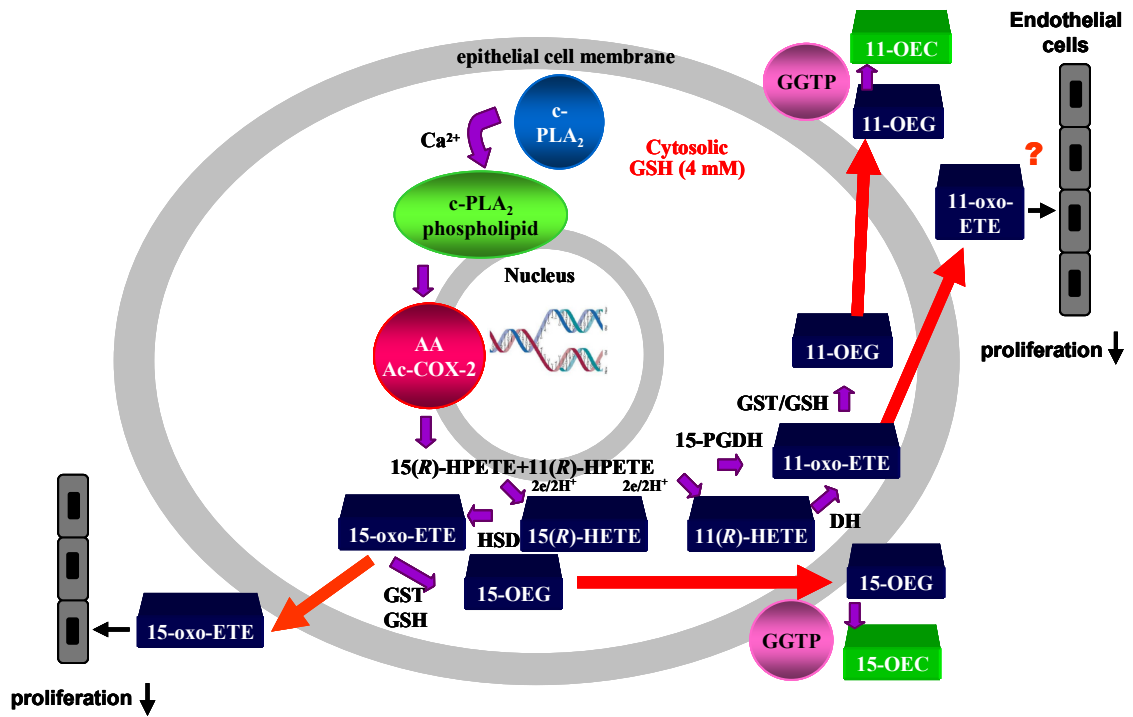


Figure 4.8 Formation of eicosanoids and inhibition of endothelial proliferation by aspirin-treated COX-2 in epithelial cell models. AA is released from membrane phospholipids by calcium-dependent cPLA₂. Aspirin acetylates COX-2 enzyme and inhibits PGs and 15(*S*)-HPETE formation which are derived from the released AA by COX-2 mediated metabolism, and this only leaves the LOX products 15(*R*)-HPETE and 11(*R*)-HPETE as the major AA metabolites, which are reduced to the corresponding HETEs. In contrast 15(*S*)-HETE, 15(*R*)-HETE is activated by 11-HSD (most likely 11-HSD I) -mediated oxidation to 15-oxo-ETE. 11(*R*)-HETE is activated by 15-PGDH-mediated oxidation to 11-oxo-ETE. The oxo-ETEs are conjugated to form OEGs, which are secreted and hydrolyzed by γ -glutamyltranspeptidase to OECs. 15-oxo-ETE and 11-oxo-ETE are reduced back to HETEs in the human epithelial cells (most likely by AKRs) and re-oxidized by DHs. Secreted 15-oxo-ETE is potentially anti-angiogenic through

inhibition of EC proliferation. 11-oxo-ETE could also be able to inhibit EC proliferation, which needs to be confirmed. Therefore, down-regulation of 15-PGDH would result in increased tumor cell proliferation and increased angiogenesis.

CHAPTER 5

General Discussion and Conclusions

5.1 Conclusions

The research reported in this thesis leads to a number of conclusions:

1. From 15-LO-1-expressing mouse macrophages and primary human monocytes, 15-oxo-ETE and 15-OEG were identified and quantified. 15-oxo-ETE was characterized as a metabolite of 15-PGDH. The novel bioactivity of 15-oxo-ETE was identified as inhibiting HUVEC proliferation.
2. A novel metabolite of COX-2 and 15-PGDH, 11-oxo-ETE, as well as its further metabolite 11-OEG were identified by LC-MS/MS analysis and targeted lipidomics studies. 11-oxo-ETE was quantified as AA-derived metabolite in both rat and human epithelial cells that expressed COX-2.
3. Aspirin was observed to significantly stimulate the production of 15(*R*)-HETE instead of 15(*S*)-HETE, as well as the production of 15-oxo-ETE in COX-2 expressing rat intestinal epithelial cells. Aspirin was also found to accelerate the metabolism of 11(*R*)-HETE, 15(*R*)-HETE, 11-oxo-ETE and 15-oxo-ETE. It was observed that an 11 β -HSD inhibitor reduced the conversion of 15(*R*)-HETE to 15-oxo-ETE in COX-2 expressing rat intestinal epithelial cells. This suggested that an 11 β -HSD isoform is responsible for the conversion of 15(*R*)-HETE to 11-oxo-ETE. The formation of 15-oxo-ETE from 15(*R*)-HETE after aspirin treatment, through a pathway that does not involve 15-PGDH, could potentially help counteract the increased pro-proliferative activity of PGE₂ when 15-PGDH is down-regulated during tumor progression and carcinogenesis.

5.2 Discussion and Future Directions

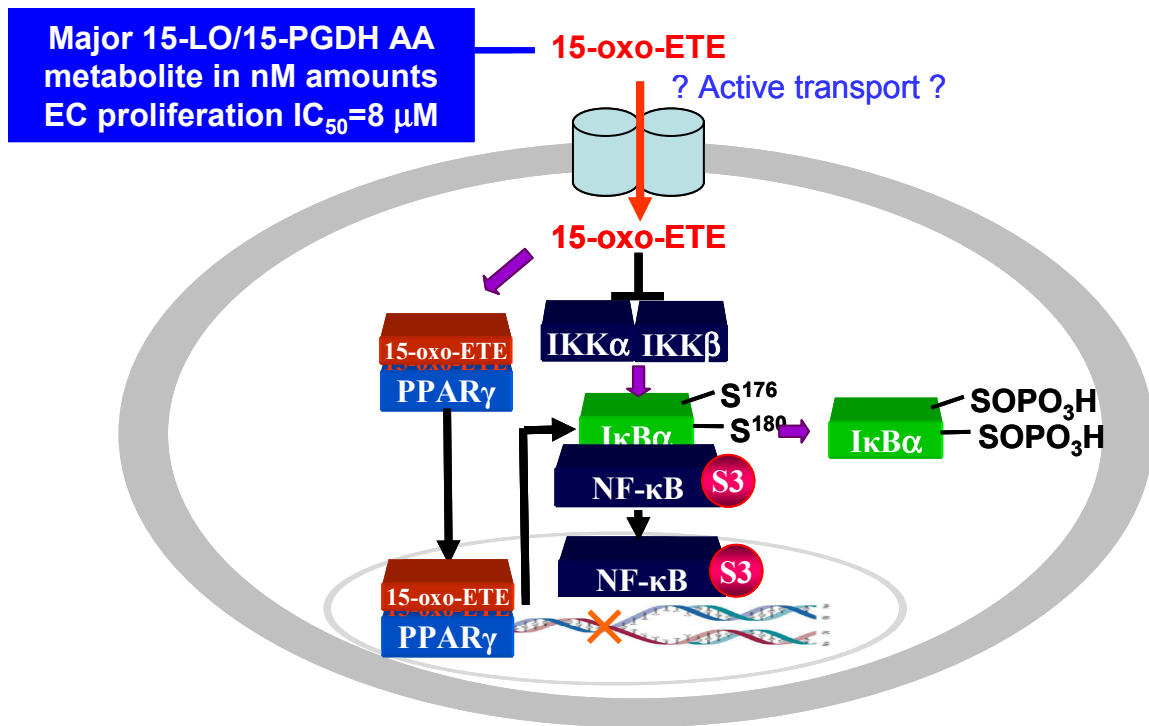
15-Oxo-ETE was shown to arise from rabbit lung 15-PGDH-mediated oxidation of 15(*S*)-HETE over twenty years ago (Bergholte et al., 1987). Recently, our group identified 15-oxo-ETE as a metabolite of COX-2-mediated AA metabolism in mouse epithelial cell model (Lee et al., 2007). The current study by employing targeted lipidomic analysis revealed the formation of 15-oxo-ETE as a 15-LO-1-mediated metabolite from endogenous AA in primary human monocytes and mouse macrophages (R15L cells). R15L cells are a mouse macrophage cell line RAW264.7 stably transfected with human 15-LO-1. It showed stable expression of 15-LO level over several passages with Western blot analysis (data not shown). Stable isotope-labeled internal standards were added in the followed cellular experiments to facilitate the quantification of 15-oxo-ETE as well as its upstream 15(*S*)-HETE metabolite. The targeted lipidomics studies of cell culture medium showed a greater than 100 fold increase in the production of 15(*S*)-HETE and 15-oxo-ETE. However, this interesting AA metabolite has remained a pharmacological curiosity for years.

The endothelium lining the vascular lumen plays a crucial role in cancer angiogenesis as well as controlling thrombosis and inflammation. HUVECs form a spindle monolayer, which is characteristic of endothelial cells. The cells stably express endothelial-specific markers, such as platelet-endothelial cell adhesion molecule-1 (PECAM-1) and intracellular adhesion molecule-1 (ICAM-1). Therefore, they have been widely used as model of ECs that can readily be maintained in culture (Muro et al., 2003). This thesis study demonstrated for the first time that 15-oxo-ETE which is released from macrophages can inhibit HUVEC proliferation, which could further

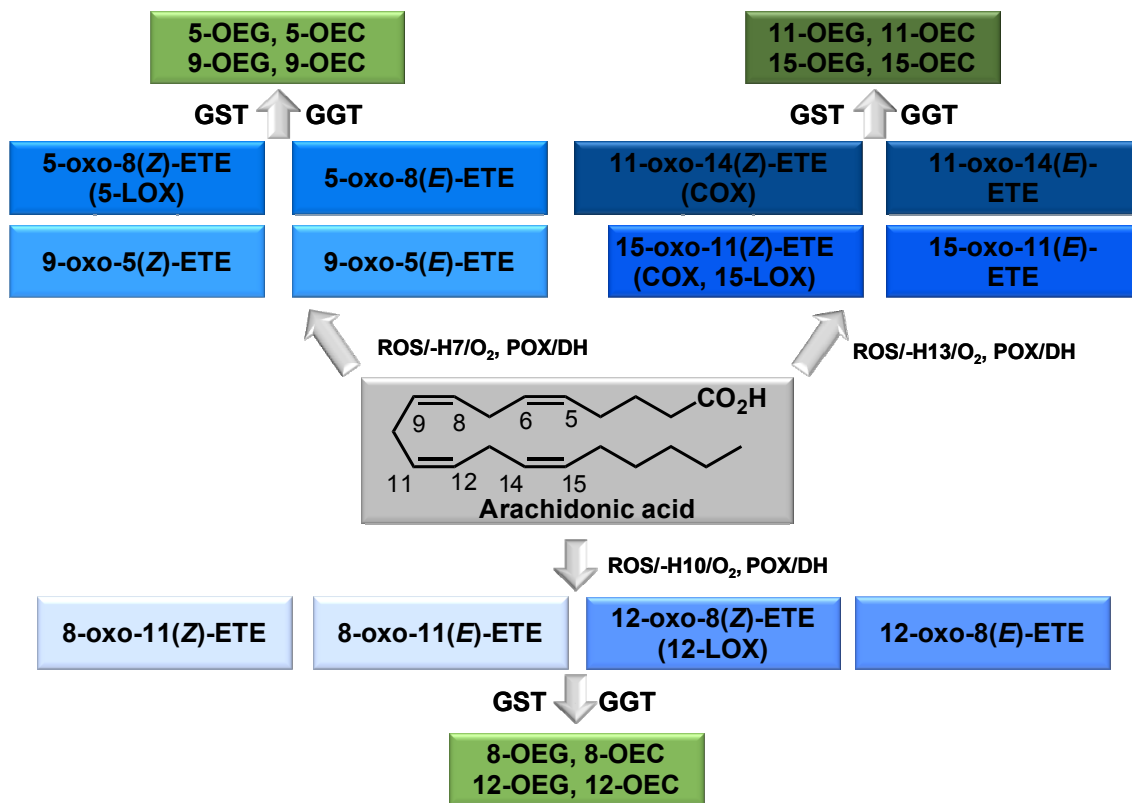
prevent endothelial growth and that in turn could lead to the inhibition of angiogenesis. Rapid 15-oxo-ETE uptake in these cells was verified to confirm that these biological effects are indeed due to 15-oxo-ETE. It was demonstrated that the expression of 15-PGDH is down-regulated in colon cancer (Backlund et al., 2005). In the absence of 15-PGDH, no 15-oxo-ETE would be formed from 15(*S*)-HETE and therefore its anti-proliferative activity on endothelial cells would be lost. This could then in turn lead to increased tumor growth and metastasis. Moreover, it is known that GSTs are up-regulated in cancer so that 15-oxo-ETE-GSH-adduct formation would increase with a concomitant loss of macrophage-derived 15-oxo-ETE, reducing a factor that could be involved in preventing EC proliferation. Therefore, identification of 15-oxo-ETE as a biologically active mediator in the macrophage-HUVEC model suggests that it could be a potential endogenous inhibitor of EC proliferation and serve to modulate tumor cell-mediated angiogenesis.

Both PGD₂ and its dehydration end product 15d-PGJ₂ are involved in the regulation of inflammation, via both receptor-dependent (PGD₂ receptors DP1 and DP2) and receptor-independent mechanisms (Scher and Pillinger, 2009). Intracellular effects of PGD₂ and 15d-PGJ₂ that may suppress inflammation include inhibition of nuclear factor-kappaB (NF-κB) by multiple mechanisms (IkappaB kinase inhibition and blockade of NF-κB nuclear binding) and activation of peroxisome proliferator-activated receptor-gamma (PPARγ) (Scher and Pillinger, 2009). Based on the similar chemical structure characteristics, we hypothesize that the biological activity of 15-oxo-ETE on endothelial cell inhibition could also be mediated by NF-κB and PPARγ (Scheme 5.1). In addition, it was recently demonstrated that the synthetic oxo-ETE family including 5-, 9-, 11-, 12-,

and 15-oxo-EETE induced PPAR γ activation by covalent modification (Waku et al., 2009) (Scheme 5.2). And very recently, it was reported that the reduction in 15-LO activity with decreased levels of 15(S)-HETE and 13(S)-HODE resulting in the decreased PPAR γ activity were observed in human lung cancer tissue and also contributed to the development of lung tumors induced by tobacco smoking (Yuan et al., 2010). This could be attributed to the decrease of 15(S)-HETE metabolite 15-oxo-EETE which inhibits endothelial cell proliferation further leading to inhibition of new vessel formation.



Scheme 5.1 Further proposed mechanisms of oxo-ETEs on the inhibition of EC proliferation (Modified from Scher JU and Pillinger MH. *J Investig Med.* 2009;57:703).



Scheme 5.2 Oxo-ETE family and their GSH-adducts. (*Z*)-ETEs are produced from enzyme-mediated lipid peroxidation which may have potential bioactivities, while (*E*)-ETEs are from the ROS (reactive oxygen species).

A novel metabolite of COX-2 and 15-PGDH, 11-oxo-ETE, was identified as secreted eicosanoids of rat and human colorectal adenocarcinoma epithelial cells (RIES cells and Caco-2 cells) in this study. Quantitative studies demonstrated that 11-oxo-ETE was a metabolite of AA-derived 11(*R*)-HETE and that it was secreted into the cell media at nM concentrations. It will be very intriguing to study the biological activity of 11-oxo-ETE because of its structural similarity to 15-oxo-ETE and 15d-PGJ₂. Preliminary

studies have suggested that it can bind to PPAR γ and that it can induce transcriptional regulation. 15-oxo-EETE and 11-oxo-EETE are rapidly cleared from the cells, indicating that 15-oxo-EETE and 11-oxo-EETE undergo further metabolism. LC-ESI/MS analysis revealed the formation of 15-OEG and 15-OEC adducts as the further metabolites of 15-oxo-EETE in R15L cells. Similarly, 11-OEG and 11-OEC adducts were identified derived from 11-oxo-EETE. However, whether 11-/15-OEG adducts and/or 11-/15-OEC adducts have any biological activity is not known yet. Previous studies have shown that GSH adducts of AA-derived metabolites can arise and some of these GSH-adducts such as LTC₄ and 5-oxo-7-glutathionyl-8,11,14-eicosatrienoic acid (FOG₇) have potent biological effects (Murphy and Zarini, 2002; Blair, 2006). These GSH-adducts can interact with cysteinyl LT receptors CysLT₁ and CysLT₂, and thus, LTC₄ can stimulate pro-inflammatory activities including endothelial cell adherence and chemokine production (Bowers et al., 2000). Similarly, FOG₇ is a highly potent stimulator of eosinophil and neutrophil chemotaxis, which is also capable of initiating actin polymerization (Zarini and Murphy, 2003). Therefore, it is plausible to speculate that GSH-adducts of 15-oxo-EETE and 11-oxo-EETE could have significant biological activities. Further work will also be conducted to quantify 11-/15-OEG and 11-/15-OEC derived from 15-LO-1-expressing macrophages as well as COX-2-expressing epithelial cells (Scheme 5.2). In addition, OEGs could be used as a read-out of increased lipid peroxidation in both 15-LO-1- and COX-2- expressing cells.

Studies on 5-oxo-EETE indicated its receptor is coupled by a Gi/o-protein (Grant et al., 2009). The oxo-EETE analog 15d-PGJ₂ can engage DP1 and DP2 as its receptors, but its main receptors seem to be active transporters (Scher and Pillinger, 2009). It will be

important to identify the receptors and/or active transporters for the oxo-ETE family and to reveal endogenous or exogenous agonists or antagonists of oxo-ETE receptors, which would shed light on its intracellular mechanism. Oxo-ETEs could also be tested for their anti-angiogenic effects on the capillary endothelial cells which could be induced to form three-dimensional networks *in vitro*. Furthermore, animal models could be employed to investigate the *in vivo* anti-angiogenic effect of oxo-ETEs including studying endothelial tube formation.

Aspirin switched the chirality of the 15(*S*)-LO activity of COX-2 to 15(*R*)-LO activity, giving significantly high production of 15(*R*)-HETE and 15-oxo-ETE, and accelerated the metabolism of AA and its metabolites. A more complete study on the effects of aspirin mechanism as well as the acceleration of PUFA metabolism could lead to more in depth understanding of aspirin some 100 years after it was discovered.

APPENDIX

HPETE-Mediated DNA Damage by Forming DNA-Adducts

A.1 Background

PUFAs can be converted into lipid hydroperoxides by the action of LOs (Brash 1999), COXs (Laneuville, Breuer et al. 1995) or ROS (Porter et al., 1995). Lipid hydroperoxides undergo homolytic decomposition into bifunctional electrophiles, which react with DNA bases to form DNA-adducts such as heptanone-1, N^6 -etheno-2'-deoxyadenosine (H- ϵ dAdo), heptanone-3, N^4 -etheno-2'-deoxycytidine (H- ϵ dCyd) and heptanone-1, N^2 -etheno-2'-deoxyguanosine (H- ϵ dGuo) (Fig. A.1A) (Blair, 2010) (Jian 2009). These DNA modifications are proposed to be involved in the etiology of cancer, cardiovascular disease, and neurodegeneration (Spiteller, 2001; Blair, 2010). In previous studies, the homolytic decomposition of 13(*S*)-HPODE and 5(*S*)-HPETE were examined (Jian 2009) (Fig. A.1A). The major decomposition products were identified as HPNE, ONE, HNE, and EDE (Lee et al., 2000; Lee et al., 2001). ONE was responsible for the formation of and H- ϵ dGuo (Lee et al., 2000; Rindgen et al., 2000; Lee et al., 2002). HPNE and EDE were the precursors in the formation of E-dAdo and E-dGuo adducts (Lee et al., 2002; Lee et al., 2005). On the basis of structure similarities of the HPETEs, 11(*R,S*)-HPETE, 12(*R,S*)-HPETE and/or 15(*R,S*)-HPETE could also under go hemolytic decomposition leading to DNA-adduct formtion(Figs. A.1A and A.1B). As mentioned in Chapter 2 and 3, AA is an essential fatty acid and a precursor of HETEs and oxo-ETEs, which are potential potent inhibitors in angiogenesis. The first step of biosynthesis of HETEs and oxo-ETEs is conversion of AA into 11-HPETE and/or 15-HPETE by COX-2

and 15-LO. In this study, the H- ϵ dAdo, H- ϵ dCyd, and H- ϵ dGuo adducts produced from the reaction between calf thymus DNA and 11-HPETE, 12-HPETE or 15-HPETE in the presence of vitamin C were identified and analyzed by LC-MS.

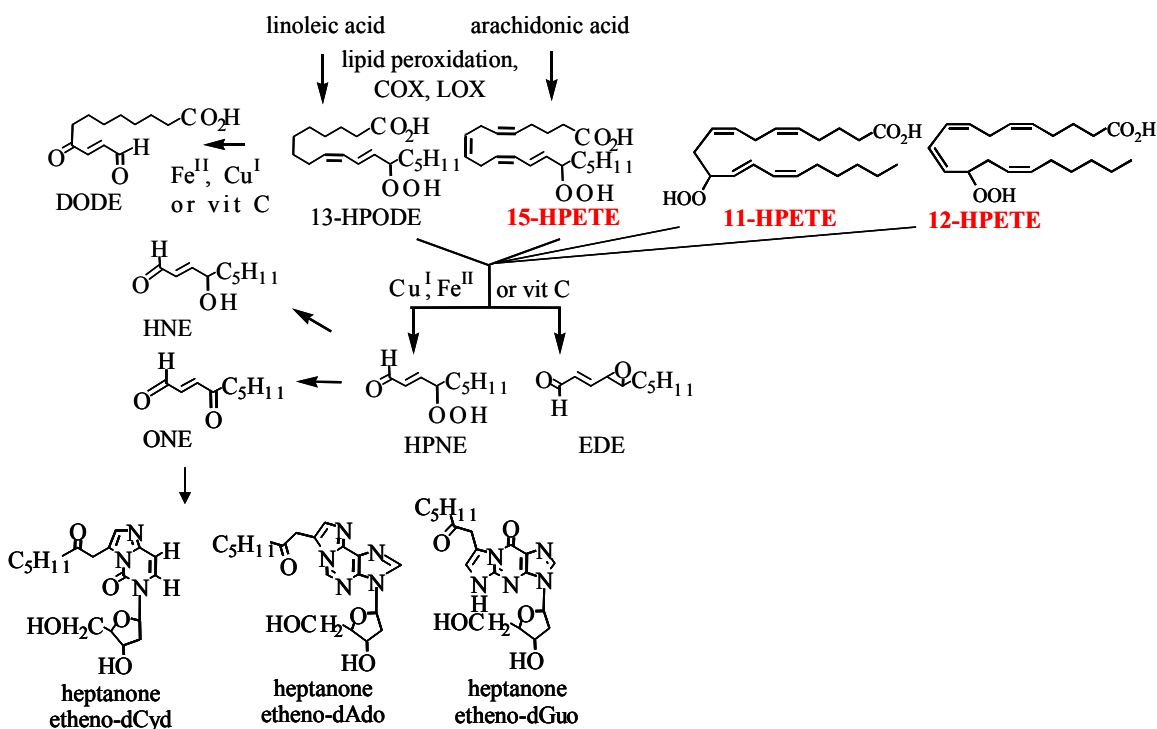


Figure A.1 HPETE-mediated DNA damage.

A.2 Experimental Procedure

A.2.1 Vitamin C-Mediated Decomposition of 11-HPETE, 12-HPETE, and 15-

HPETE in the Presence of Calf Thymus DNA –A solution of 11-HPETE, 12-HPETE or 15-HPETE (each 50 μ g, 149 nmol) in ethanol (10 μ L) and vitamin C (157.4 μ g, 894 nmol) in water (10 μ L) were added to calf thymus DNA (295 μ g, 894 nmol) in Chelex-treated 100 mM MOPS containing 150 mM NaCl (pH 7.4, 180 μ L). The reaction mixture was sonicated for 15 min at room temperature, incubated at 60 $^{\circ}$ C for 24 h.

DNA-adducts from the reaction mixture was precipitated and DNA hydrolysis was performed. DNA was dissolved in 300 μ L of 10 mM MOPS and 100 mM $MgCl_2$, pH 7.4 (chelex-treated). DNase I (2.5 μ g) was added, the samples were incubated at 37 $^{\circ}C$ for 1.5 h. At the end of the incubation, 45 μ L chelex-treated 0.2 M glycine buffer (pH 10) and phosphodiesterase (0.5 units) were added, and the samples were incubated at 37 $^{\circ}C$ for 2 h. Then 45 μ L Tris-HCl (50 mM, pH 7.4) and shrimp alkaline phosphatase (15 units) were added, and the samples were incubated for 2 h. An aliquot (100 μ L) of the hydrolyzed DNA was taken for LC-UV base analysis. DNA hydrolysis products were analyzed with LC gradient system A.1 by monitoring the UV absorbance at 260 nm. The quantitation of DNA bases was achieved through constructing standard curves of known amounts of H- ϵ dGuo, H- ϵ dAde and H- ϵ dCyd in the range of 0.005 mg/mL to 0.25 mg/mL. Blank reaction solution (pH 7.4, 200 μ L) was prepared, spiked with the following amounts of authentic DNA-adducts standards (H- ϵ dAdo, H- ϵ dCyd and H- ϵ dGuo): 10, 20, 50, 100, 200, 500 and 1000 pg. A mix of internal standards [$^{15}N_5$]-H- ϵ dAdo, [$^{15}N_3$]-H- ϵ dCyd and [$^{15}N_5$]-H- ϵ dGuo, 2 ng each, was added to each reaction and blank sample. The samples were then loaded onto Supelclean LC-18 SPE columns (0.5 g) that had been preconditioned with ACN (7.5 mL) followed by water (7.5 mL). The columns were then washed with water (2.5 mL) and methanol/water mixture (0.5 mL, 5:95 v/v). Adducts were eluted with ACN/water mixture (3 mL, 1:1 v/v). The eluted samples were evaporated to dryness under nitrogen and reconstituted in 100 μ L water/acetonitrile (94:6). An aliquot of the sample (20 μ L) was injected into LC-MRM/MS system for analysis.

A.2.2 LC-MS Analysis of HPETE-Mediated DNA-adducts – LC-UV DNA base analysis and LC-ESI/MRM/MS analysis for DNA adduct were conducted on Hitachi L-2200 Autosamplers equipped with Hitachi L-2130 Pump (Hitachi, San Jose, CA). For LC gradient system A.1 for DNA base analysis, solvent A was water and solvent B was ACN. The gradient condition was as follows: 0 % B at 0 min, 0 % B at 3 min, 13% B at 15 min, 100 % B at 20 min, 100 % B at 22 min, 0 % B at 25 min, followed by equilibration for 5 min, employing a Phenomenex Luna C8 column (250 mm × 4.6 mm i.d., 5 µm; Phenomenex, Inc., Torrance, CA) with a flow rate of 1 mL/min. The separation for LC-MS analysis employed a Luna C18 column (150 × 4.6 mm i.d., 3 µm; Phenomenex, Torrance, CA). For LC-ESI/MRM/MS analysis for DNA adduct, solvent A was 5 mM ammonium acetate in water and solvent B was 5 mM ammonium acetate in acetonitrile. The flow rate was 0.3 mL/min and the gradient was as follows: 6 % B at 0 min, 6 % B at 2 min, 9% B at 12 min, 55 % B at 22 min, 80 % B at 30 min, 80 % B at 35 min, 6 % B at 37 min, and 6 % B at 47 min. Gradient elution was conducted in linear mode and the separation was performed at ambient temperature. For DNA adduct analysis, mass spectrometry was conducted with a Thermo Finnigan TSQ Quantum Ultra AM Triple Quadrupole mass spectrometer (Thermo Electron, San Jose, CA) equipped with ESI source in positive mode. Operating conditions for the instrument was as follows: vaporizer temperature at 550 °C, heated capillary temperature at 180 °C, with the corona discharge needle set at 18 µA. The sheath gas (nitrogen), auxiliary gas (nitrogen) and ion sweep gas (nitrogen) were 30, 3 and 0 (arbitrary units), respectively. Source CID collision energy was -5 eV. CID was performed using argon as the collision gas in the RF-only quadrupole. LC-ESI/MRM/MS analysis was conducted and the following

MRM transitions were monitored: H- ϵ dAdo m/z 388 \rightarrow 272 (collision energy, 20 eV); [$^{15}\text{N}_5$]-H- ϵ dAdo, m/z 393 \rightarrow 277 (collision energy, 20 eV); H- ϵ dCyd m/z 364 \rightarrow 248 (collision energy, 20 eV); [$^{15}\text{N}_3$]-H- ϵ dCyd, m/z 367 \rightarrow 251 (collision energy, 20 eV); H- ϵ dGuo, m/z 404 \rightarrow 288 (collision energy, 20 eV); and [$^{15}\text{N}_5$]-H- ϵ dGuo, m/z 409 \rightarrow 293 (collision energy, 20 eV).

A.3 Result and Discussion

LC-MS analysis of the reaction of calf thymus DNA and 11-HPETE, 12-HPETE or 15-HPETE in the presence of vitamin C showed three types formation of heptonone-etheno adduct (H- ϵ dAdo, H- ϵ dCyd, and H- ϵ dGuo) for each reaction (Fig. A.2). The chromatograms from LC-ESI/MRM/MS analyses demonstrated the formation of H- ϵ dAdo (rt, 28.7 min), H- ϵ dCyd (rt, 29.0 min) and H- ϵ dGuo (rt, 27.8 min) from the reactions between 11-HPETE with DNA (Figs. A.2Aa, A.2Ac and A.2Ae), 12-HPETE with DNA (Figs. A.1Ba, c and e), and 15-HPETE with DNA (Figs. A.2Ca, A.2Cc and A.2Ce). The signal intensities of 11-HPETE- and 15-HPETE-mediated H- ϵ dAdo was approximately 3-fold higher (1.10×10^5 and 9.30×10^4) (Figs. A.2Aa and A.2Ca) than the intensity of 12-HPETE-mediated H- ϵ dAdo (3.24×10^4) (Fig. A.2Ba). Similarly, the signal intensities of 11-HPETE- and 15-HPETE-mediated H- ϵ dCyd were higher (9.90×10^5 and 7.51×10^5) (Figs. A.2Ac and A.2Cc) than that of 12-HPETE-mediated H- ϵ dCyd (2.57×10^5) (Fig. A.2Bc), while the intensities of 11-HPETE- and 15-HPETE-mediated H- ϵ dGuo (6.41×10^3 and 5.15×10^3) (Figs. A.2Ae and A.2Ce) were lower than that of 12-HPETE-mediated H- ϵ dCyd (8.56×10^3) (Fig. A.2Be).

The quantitative analyses revealed that 11-HPETE, 12-HPETE and 15-HPETE led to H- ϵ dAdo formation of 2.6 adducts/ 10^5 bases, 0.4 adducts/ 10^5 bases and 3.4

adducts/ 10^5 bases respectively, H- ϵ dCyd formation up to 7.5 adducts/ 10^5 bases, 2 adducts/ 10^5 bases and 12.1 adducts/ 10^5 bases respectively, and H- ϵ dGuo formation of 0.6 adducts/ 10^5 bases, 0.6 adducts/ 10^5 bases and 1.6 adducts/ 10^5 bases respectively (Fig. A.3).

These observations combined with the data from previous chapters indicated HPETE metabolism could generate DNA-adducts leading to further mutagenesis or undergo reduction and further oxidation to form oxo-ETEs inhibiting endothelial cell proliferation resulting in anti-angiogenesis (Wei et al. 2009) (Fig. A.4).

The preliminary conclusion of this study needs to be further confirmed by analyzing the DNA-adduct formation of 11-HPETE, 12-HPETE and 15-HPETE reacted with individual DNA nucleotides (dAdo, dCyd and dGuo). And the levels of DNA-adduct formation of specific 11(*R*)-HPETE, 15(*R*)-HPETE and 15(*S*)-HPETE should also be determined, since they could play very important role in COX-2-mediated DNA damage. In addition, the formation of the heptanone-etheno-DNA-adducts can server as biomarkers for oxidative stress. A quantitative LC-MS method is being developed and will be employed to analyze the heptanone-etheno-DNA-adducts in human urine and plasma with high sensitivity and high specificity.

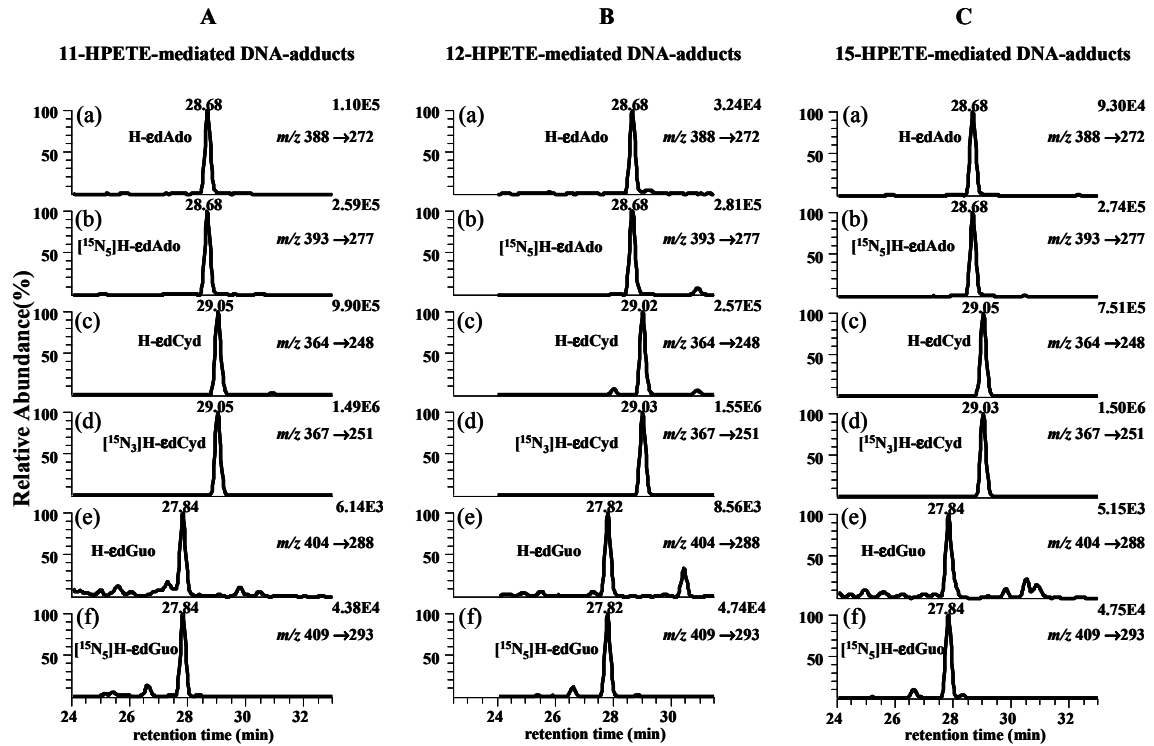
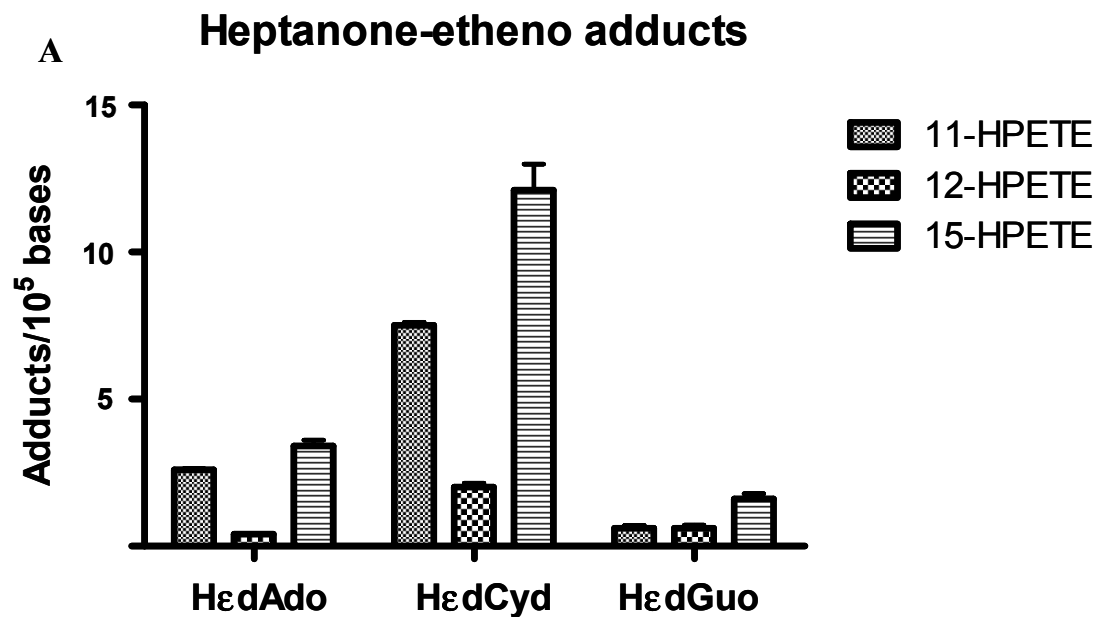


Figure A.2 Quantitative analysis of DNA-adducts formed from 11-HPETE (A), 12-HPETE (B) and 15-HPETE (C).



B

Summary		11-HPETE	12-HPETE	15-HPETE
adducts/10 ⁵ bases	H-εdAdo	2.6	0.4	3.4
	H-εdCyd	7.5	2	12.1
	H-εdGuo	0.6	0.6	1.6

Figure A.3 Quantitative analysis of DNA-adducts formed from 11-, 12- and 15-HPETE.

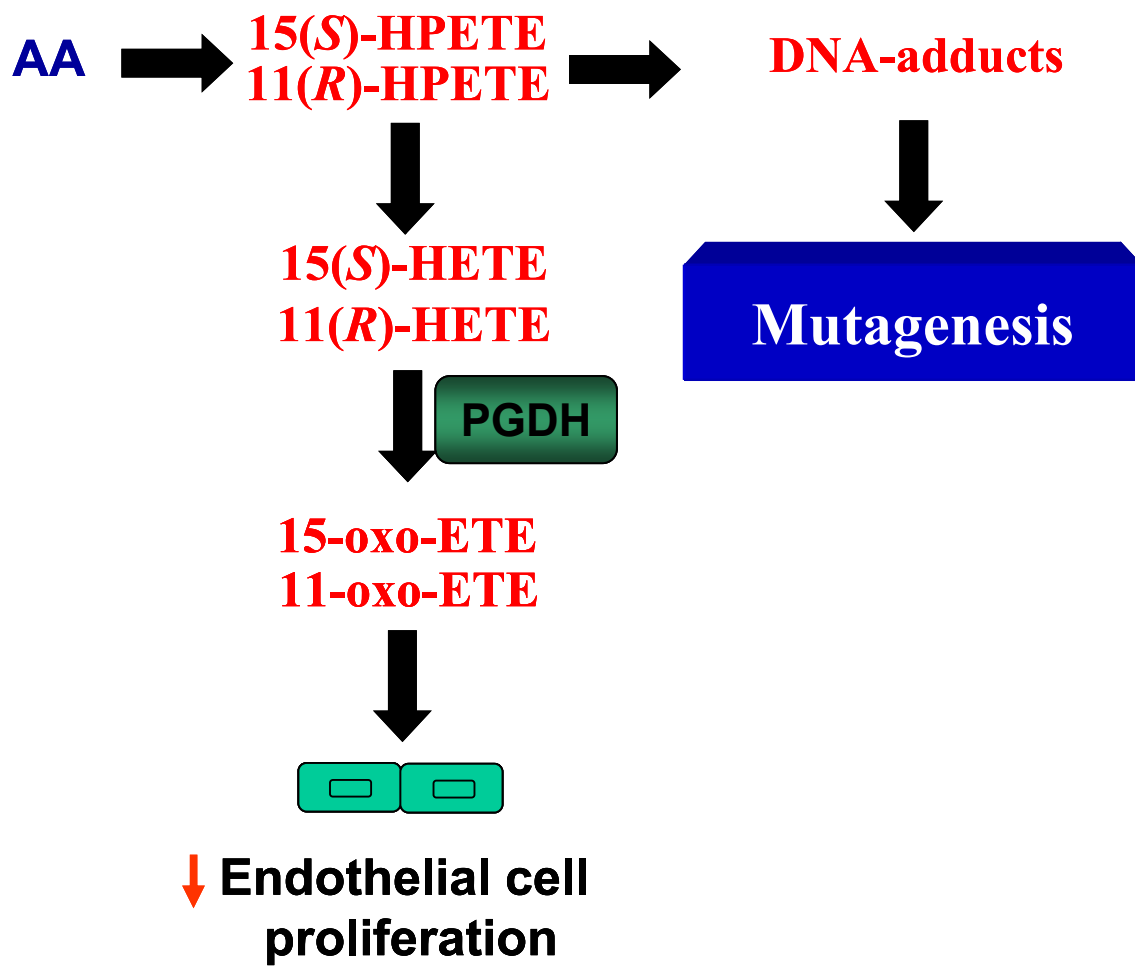


Figure A.4 The potential role of COX-2-derived eicosanoids in mutagenesis and proliferation.

BIBLIOGRAPHY

- Abuja, P. M. and Albertini, R. (2001). "Methods for monitoring oxidative stress, lipid peroxidation and oxidation resistance of lipoproteins." *Clin Chim Acta* 306(1-2): 1-17.
- Aldini, G., Carini, M., Beretta, G., Bradamante, S. and Facino, R. M. (2002). "Carnosine is a quencher of 4-hydroxy-nonenal: through what mechanism of reaction?" *Biochem Biophys Res Commun* 298(5): 699-706.
- Aldini, G., Granata, P. and Carini, M. (2002). "Detoxification of cytotoxic alpha,beta-unsaturated aldehydes by carnosine: characterization of conjugated adducts by electrospray ionization tandem mass spectrometry and detection by liquid chromatography/mass spectrometry in rat skeletal muscle." *J Mass Spectrom* 37(12): 1219-1228.
- Ames, B. N., Shigenaga, M. K. and Hagen, T. M. (1993). "Oxidants, antioxidants, and the degenerative diseases of aging." *Proc Natl Acad Sci U S A* 90(17): 7915-7922.
- Arthur, J. R. (2000). "The glutathione peroxidases." *Cell Mol Life Sci* 57(13-14): 1825-1835.
- Aviram, M. (1996). "Interaction of oxidized low density lipoprotein with macrophages in atherosclerosis, and the antiatherogenicity of antioxidants." *Eur J Clin Chem Clin Biochem* 34(8): 599-608.
- Awasthi, Y. C., Sharma, R., Cheng, J. Z., Yang, Y., Sharma, A., Singhal, S. S. and Awasthi, S. (2003). "Role of 4-hydroxynonenal in stress-mediated apoptosis signaling." *Mol Aspects Med* 24(4-5): 219-230.
- Awasthi, Y. C., Yang, Y., Tiwari, N. K., Patrick, B., Sharma, A., Li, J. and Awasthi, S. (2004). "Regulation of 4-hydroxynonenal-mediated signaling by glutathione S-transferases." *Free Radic Biol Med* 37(5): 607-619.
- Backlund, M. G., Mann, J. R., Holla, V. R., Buchanan, F. G., Tai, H. H., Musiek, E. S., Milne, G. L., Katkuri, S. and DuBois, R. N. (2005). "15-Hydroxyprostaglandin dehydrogenase is down-regulated in colorectal cancer." *J Biol Chem* 280(5): 3217-3223.
- Baker, C. S., Hall, R. J., Evans, T. J., Pomerance, A., Maclouf, J., Creminon, C., Yacoub, M. H. and Polak, J. M. (1999). "Cyclooxygenase-2 is widely expressed in atherosclerotic lesions affecting native and transplanted human coronary arteries and colocalizes with inducible nitric oxide synthase and nitrotyrosine particularly in macrophages." *Arterioscler Thromb Vasc Biol* 19(3): 646-655.
- Baker, P. R., Lin, Y., Schopfer, F. J., Woodcock, S. R., Groeger, A. L., Batthyany, C., Sweeney, S., Long, M. H., Iles, K. E., Baker, L. M., Branchaud, B. P., Chen, Y. E. and Freeman, B. A. (2005). "Fatty acid transduction of nitric oxide signaling: multiple nitrated unsaturated fatty acid derivatives exist in human blood and urine and serve as endogenous peroxisome proliferator-activated receptor ligands." *J Biol Chem* 280(51): 42464-42475.

- Ballatori, N., Hammond, C. L., Cunningham, J. B., Krance, S. M. and Marchan, R. (2005). "Molecular mechanisms of reduced glutathione transport: role of the MRP/CFTR/ABCC and OATP/SLC21A families of membrane proteins." *Toxicol Appl Pharmacol* 204(3): 238-255.
- Belkner, J., Wiesner, R., Rathman, J., Barnett, J., Sigal, E. and Kuhn, H. (1993). "Oxygenation of lipoproteins by mammalian lipoxygenases." *Eur J Biochem* 213(1): 251-261.
- Bergers, G. and Benjamin, L. E. (2003). "Tumorigenesis and the angiogenic switch." *Nat Rev Cancer* 3(6): 401-410.
- Bergholte, J. M., Soberman, R. J., Hayes, R., Murphy, R. C. and Okita, R. T. (1987). "Oxidation of 15-hydroxyeicosatetraenoic acid and other hydroxy fatty acids by lung prostaglandin dehydrogenase." *Arch Biochem Biophys* 257(2): 444-450.
- Berry, C. N., Hoult, J. R., Peers, S. H. and Agback, H. (1983). "Inhibition of prostaglandin 15-hydroxydehydrogenase by sulphasalazine and a novel series of potent analogues." *Biochem Pharmacol* 32(19): 2863-2871.
- Bertagnolli, M. M. (2007). "Chemoprevention of colorectal cancer with cyclooxygenase-2 inhibitors: two steps forward, one step back." *Lancet Oncol* 8(5): 439-443.
- Bishop-Bailey, D. and Hla, T. (1999). "Endothelial cell apoptosis induced by the peroxisome proliferator-activated receptor (PPAR) ligand 15-deoxy-Delta12, 14-prostaglandin J2." *J Biol Chem* 274(24): 17042-17048.
- Blair, I. A. (2006). "Endogenous glutathione adducts." *Curr Drug Metab* 7(8): 853-872.
- Blair, I. A. (2008). "DNA adducts with lipid peroxidation products." *J Biol Chem* 283(23): 15545-15549.
- Blair, I. A. (2010). "Analysis of endogenous glutathione-adducts and their metabolites." *Biomed Chromatogr* 24(1): 29-38.
- Blair, I. A. (2010). "Analysis of estrogens in serum and plasma from postmenopausal women: past present, and future." *Steroids* 75(4-5): 297-306.
- Bolton, J. L., Trush, M. A., Penning, T. M., Dryhurst, G. and Monks, T. J. (2000). "Role of quinones in toxicology." *Chem Res Toxicol* 13(3): 135-160.
- Bonazzi, A., Bolla, M., Buccellati, C., Hernandez, A., Zarini, S., Vigano, T., Fumagalli, F., Viappiani, S., Ravasi, S., Zannini, P., Chiesa, G., Folco, G. and Sala, A. (2000). "Effect of endogenous and exogenous prostaglandin E(2) on interleukin-1 beta-induced cyclooxygenase-2 expression in human airway smooth-muscle cells." *Am J Respir Crit Care Med* 162(6): 2272-2277.
- Borst, P., Evers, R., Kool, M. and Wijnholds, J. (2000). "A family of drug transporters: the multidrug resistance-associated proteins." *J Natl Cancer Inst* 92(16): 1295-1302.

- Bosetti, C., Gallus, S. and La Vecchia, C. (2006). "Aspirin and cancer risk: an updated quantitative review to 2005." *Cancer Causes Control* 17(7): 871-888.
- Boveris, A. and Chance, B. (1973). "The mitochondrial generation of hydrogen peroxide. General properties and effect of hyperbaric oxygen." *Biochem J* 134(3): 707-716.
- Bowers, R. C., Hevko, J., Henson, P. M. and Murphy, R. C. (2000). "A novel glutathione containing eicosanoid (FOG7) chemotactic for human granulocytes." *J Biol Chem* 275(39): 29931-29934.
- Brash, A. R. (1999). "Lipoxygenases: occurrence, functions, catalysis, and acquisition of substrate." *J Biol Chem* 274(34): 23679-23682.
- Breen, E. C. (2007). "VEGF in biological control." *J Cell Biochem* 102(6): 1358-1367.
- Brinckmann, R., Heydeck, D., Kolde, G. and Kuhn, H. (1997). "Subcellular localization of the 15-lipoxygenase in mammalian cells." *Adv Exp Med Biol* 407: 27-32.
- Brinckmann, R., Schnurr, K., Heydeck, D., Rosenbach, T., Kolde, G. and Kuhn, H. (1998). "Membrane translocation of 15-lipoxygenase in hematopoietic cells is calcium-dependent and activates the oxygenase activity of the enzyme." *Blood* 91(1): 64-74.
- Brown, J. R. and DuBois, R. N. (2005). "COX-2: a molecular target for colorectal cancer prevention." *J Clin Oncol* 23(12): 2840-2855.
- Bryant, R. W., Bailey, J. M., Schewe, T. and Rapoport, S. M. (1982). "Positional specificity of a reticulocyte lipoxygenase. Conversion of arachidonic acid to 15-S-hydroperoxy-eicosatetraenoic acid." *J Biol Chem* 257(11): 6050-6055.
- Burcham, P. C. (1998). "Genotoxic lipid peroxidation products: their DNA damaging properties and role in formation of endogenous DNA adducts." *Mutagenesis* 13(3): 287-305.
- Cagen, L. M. and Pisano, J. J. (1979). "The glutathione conjugate of prostaglandin A1 is a better substrate than prostaglandin E for partially purified avian prostaglandin E 9-ketoreductase." *Biochim Biophys Acta* 573(3): 547-551.
- Capraro, M. A. and Hughey, R. P. (1985). "Use of acivicin in the determination of rate constants for turnover of rat renal gamma-glutamyltranspeptidase." *J Biol Chem* 260(6): 3408-3412.
- Carini, M., Aldini, G. and Facino, R. M. (2004). "Mass spectrometry for detection of 4-hydroxy-trans-2-nonenal (HNE) adducts with peptides and proteins." *Mass Spectrom Rev* 23(4): 281-305.
- Carmeliet, P. (2005). "Angiogenesis in life, disease and medicine." *Nature* 438(7070): 932-936.
- Cathcart, M. K. and Folcik, V. A. (2000). "Lipoxygenases and atherosclerosis: protection versus pathogenesis." *Free Radic Biol Med* 28(12): 1726-1734.
- Celis, J. E., Gromov, P., Cabezon, T., Moreira, J. M., Friis, E., Jirstrom, K., Llombart-Bosch, A., Timmermans-Wielenga, V., Rank, F. and Gromova, I. (2008). "15-prostaglandin dehydrogenase

expression alone or in combination with ACSM1 defines a subgroup of the apocrine molecular subtype of breast carcinoma." *Mol Cell Proteomics* 7(10): 1795-1809.

Cernuda-Morollon, E., Pineda-Molina, E., Canada, F. J. and Perez-Sala, D. (2001). "15-Deoxy-Delta 12,14-prostaglandin J2 inhibition of NF-kappaB-DNA binding through covalent modification of the p50 subunit." *J Biol Chem* 276(38): 35530-35536.

Cha, Y. I., Solnica-Krezel, L. and DuBois, R. N. (2006). "Fishing for prostanoids: deciphering the developmental functions of cyclooxygenase-derived prostaglandins." *Dev Biol* 289(2): 263-272.

Chaitidis, P., Schewe, T., Sutherland, M., Kuhn, H. and Nigam, S. (1998). "15-Lipoxygenation of phospholipids may precede the sn-2 cleavage by phospholipases A2: reaction specificities of secretory and cytosolic phospholipases A2 towards native and 15-lipoxygenated arachidonoyl phospholipids." *FEBS Lett* 434(3): 437-441.

Chandrasekharan, N. V., Dai, H., Roos, K. L., Evanson, N. K., Tomsik, J., Elton, T. S. and Simmons, D. L. (2002). "COX-3, a cyclooxygenase-1 variant inhibited by acetaminophen and other analgesic/antipyretic drugs: cloning, structure, and expression." *Proc Natl Acad Sci U S A* 99(21): 13926-13931.

Chatila, T. A. (2004). "Interleukin-4 receptor signaling pathways in asthma pathogenesis." *Trends Mol Med* 10(10): 493-499.

Chaudhary, A. K., Nokubo, M., Marnett, L. J. and Blair, I. A. (1994). "Analysis of the malondialdehyde-2'-deoxyguanosine adduct in rat liver DNA by gas chromatography/electron capture negative chemical ionization mass spectrometry." *Biol Mass Spectrom* 23(8): 457-464.

Chaudhary, A. K., Nokubo, M., Reddy, G. R., Yeola, S. N., Morrow, J. D., Blair, I. A. and Marnett, L. J. (1994). "Detection of endogenous malondialdehyde-deoxyguanosine adducts in human liver." *Science* 265(5178): 1580-1582.

Chen, H. J., Wu, C. F., Hong, C. L. and Chang, C. M. (2004). "Urinary excretion of 3,N4-etheno-2'-deoxycytidine in humans as a biomarker of oxidative stress: association with cigarette smoking." *Chem Res Toxicol* 17(7): 896-903.

Chen, N. G. and Han, X. (2001). "Dual function of troglitazone in ICAM-1 gene expression in human vascular endothelium." *Biochem Biophys Res Commun* 282(3): 717-722.

Chen, X., Sood, S., Yang, C. S., Li, N. and Sun, Z. (2006). "Five-lipoxygenase pathway of arachidonic acid metabolism in carcino-genesis and cancer chemoprevention." *Curr Cancer Drug Targets* 6(7): 613-622.

Chen, X. S. and Funk, C. D. (2001). "The N-terminal "beta-barrel" domain of 5-lipoxygenase is essential for nuclear membrane translocation." *J Biol Chem* 276(1): 811-818.

Chen, Y. Q., Duniec, Z. M., Liu, B., Hagmann, W., Gao, X., Shimoji, K., Marnett, L. J., Johnson, C. R. and Honn, K. V. (1994). "Endogenous 12(S)-HETE production by tumor cells and its role in metastasis." *Cancer Res* 54(6): 1574-1579.

- Chen, Z. S., Furukawa, T., Sumizawa, T., Ono, K., Ueda, K., Seto, K. and Akiyama, S. I. (1999). "ATP-Dependent efflux of CPT-11 and SN-38 by the multidrug resistance protein (MRP) and its inhibition by PAK-104P." *Mol Pharmacol* 55(5): 921-928.
- Cho, H., Ueda, M., Tamaoka, M., Hamaguchi, M., Aisaka, K., Kiso, Y., Inoue, T., Ogino, R., Tatsuoka, T., Ishihara, T. and et al. (1991). "Novel caffeic acid derivatives: extremely potent inhibitors of 12-lipoxygenase." *J Med Chem* 34(4): 1503-1505.
- Chou, W. L., Chuang, L. M., Chou, C. C., Wang, A. H., Lawson, J. A., FitzGerald, G. A. and Chang, Z. F. (2007). "Identification of a novel prostaglandin reductase reveals the involvement of prostaglandin E2 catabolism in regulation of peroxisome proliferator-activated receptor gamma activation." *J Biol Chem* 282(25): 18162-18172.
- Ciccimaro, E. and Blair, I. A. (2010). "Stable-isotope dilution LC-MS for quantitative biomarker analysis." *Bioanalysis* 2(2): 311-341.
- Cohen, G. and Hochstein, P. (1963). "Glutathione Peroxidase: the Primary Agent for the Elimination of Hydrogen Peroxide in Erythrocytes." *Biochemistry* 2: 1420-1428.
- Cole, S. P. C., Sparks, K. E., Fraser, K., Loe, D. W., Grant, C. E., Wilson, G. M. and Deeley, R. G. (1994). "Pharmacological Characterization of Multidrug-Resistant Mrp-Transfected Human Tumor-Cells." *Cancer Research* 54(22): 5902-5910.
- Cornicelli, J. A. and Trivedi, B. K. (1999). "15-Lipoxygenase and its inhibition: a novel therapeutic target for vascular disease." *Curr Pharm Des* 5(1): 11-20.
- Cuzick, J., Otto, F., Baron, J. A., Brown, P. H., Burn, J., Greenwald, P., Jankowski, J., La Vecchia, C., Meyskens, F., Senn, H. J. and Thun, M. (2009). "Aspirin and non-steroidal anti-inflammatory drugs for cancer prevention: an international consensus statement." *Lancet Oncol* 10(5): 501-507.
- Dalton, T. P., Chen, Y., Schneider, S. N., Nebert, D. W. and Shertzer, H. G. (2004). "Genetically altered mice to evaluate glutathione homeostasis in health and disease." *Free Radic Biol Med* 37(10): 1511-1526.
- Di Mascio, P., Murphy, M. E. and Sies, H. (1991). "Antioxidant defense systems: the role of carotenoids, tocopherols, and thiols." *Am J Clin Nutr* 53(1 Suppl): 194S-200S.
- Dickinson, D. A. and Forman, H. J. (2002). "Cellular glutathione and thiols metabolism." *Biochem Pharmacol* 64(5-6): 1019-1026.
- Diestra, J. E., Condom, E., Del Muro, X. G., Scheffer, G. L., Perez, J., Zurita, A. J., Munoz-Segui, J., Vignes, F., Scheper, R. J., Capella, G., Germa-Lluch, J. R. and Izquierdo, M. A. (2003). "Expression of multidrug resistance proteins P-glycoprotein, multidrug resistance protein 1, breast cancer resistance protein and lung resistance related protein in locally advanced bladder cancer treated with neoadjuvant chemotherapy: biological and clinical implications." *J Urol* 170(4 Pt 1): 1383-1387.

- Doss, G. A. and Baillie, T. A. (2006). "Addressing metabolic activation as an integral component of drug design." *Drug Metab Rev* 38(4): 641-649.
- DuBois, R. N., Radhika, A., Reddy, B. S. and Entingh, A. J. (1996). "Increased cyclooxygenase-2 levels in carcinogen-induced rat colonic tumors." *Gastroenterology* 110(4): 1259-1262.
- Eberhart, C. E., Coffey, R. J., Radhika, A., Giardiello, F. M., Ferrenbach, S. and DuBois, R. N. (1994). "Up-regulation of cyclooxygenase 2 gene expression in human colorectal adenomas and adenocarcinomas." *Gastroenterology* 107(4): 1183-1188.
- Enoiu, M., Herber, R., Wennig, R., Marson, C., Bodaud, H., Leroy, P., Mitrea, N., Siest, G. and Wellman, M. (2002). "gamma-Glutamyltranspeptidase-dependent metabolism of 4-hydroxynonenal-glutathione conjugate." *Arch Biochem Biophys* 397(1): 18-27.
- Esterbauer, H., Striegl, G., Puhl, H. and Rotheneder, M. (1989). "Continuous monitoring of in vitro oxidation of human low density lipoprotein." *Free Radic Res Commun* 6(1): 67-75.
- Farrow, B. and Evers, B. M. (2002). "Inflammation and the development of pancreatic cancer." *Surg Oncol* 10(4): 153-169.
- Feinmark, S. J. and Cornicelli, J. A. (1997). "Is there a role for 15-lipoxygenase in atherogenesis?" *Biochem Pharmacol* 54(9): 953-959.
- Fierro, I. M., Kutok, J. L. and Serhan, C. N. (2002). "Novel lipid mediator regulators of endothelial cell proliferation and migration: aspirin-triggered-15R-lipoxin A(4) and lipoxin A(4)." *J Pharmacol Exp Ther* 300(2): 385-392.
- Fitzpatrick, F. A. and Wynalda, M. A. (1983). "Albumin-catalyzed metabolism of prostaglandin D2. Identification of products formed in vitro." *J Biol Chem* 258(19): 11713-11718.
- Flossmann, E. and Rothwell, P. M. (2007). "Effect of aspirin on long-term risk of colorectal cancer: consistent evidence from randomised and observational studies." *Lancet* 369(9573): 1603-1613.
- Folkman, J. (1995). "Angiogenesis in cancer, vascular, rheumatoid and other disease." *Nat Med* 1(1): 27-31.
- Folkman, J. (2007). "Angiogenesis: an organizing principle for drug discovery?" *Nat Rev Drug Discov* 6(4): 273-286.
- Forman, B. M., Tontonoz, P., Chen, J., Brun, R. P., Spiegelman, B. M. and Evans, R. M. (1995). "15-Deoxy-delta 12, 14-prostaglandin J2 is a ligand for the adipocyte determination factor PPAR gamma." *Cell* 83(5): 803-812.
- Forman, H. J. and Torres, M. (2001). "Redox signaling in macrophages." *Mol Aspects Med* 22(4-5): 189-216.
- Fujita, Y., Abe, R. and Shimizu, H. (2008). "Clinical approaches toward tumor angiogenesis: past, present and future." *Curr Pharm Des* 14(36): 3820-3834.

Fukai, M., Hayashi, T., Yokota, R., Shimamura, T., Suzuki, T., Taniguchi, M., Matsushita, M., Furukawa, H. and Todo, S. (2005). "Lipid peroxidation during ischemia depends on ischemia time in warm ischemia and reperfusion of rat liver." *Free Radic Biol Med* 38(10): 1372-1381.

Funk, C. D. (2001). "Prostaglandins and leukotrienes: advances in eicosanoid biology." *Science* 294(5548): 1871-1875.

Furstenberger, G., Krieg, P., Muller-Decker, K. and Habenicht, A. J. (2006). "What are cyclooxygenases and lipoxygenases doing in the driver's seat of carcinogenesis?" *Int J Cancer* 119(10): 2247-2254.

Gallasch, B. A. and Spiteller, G. (2000). "Synthesis of 9,12-dioxo-10(Z)-dodecenoic acid, a new fatty acid metabolite derived from 9-hydroperoxy-10,12-octadecadienoic acid in lentil seed (*Lens culinaris* Medik.)." *Lipids* 35(9): 953-960.

Goetzl, E. J., An, S. and Smith, W. L. (1995). "Specificity of expression and effects of eicosanoid mediators in normal physiology and human diseases." *FASEB J* 9(11): 1051-1058.

Gong, R., Latif, S., Morris, D. J. and Brem, A. S. (2008). "Co-localization of glucocorticoid metabolizing and prostaglandin synthesizing enzymes in rat kidney and liver." *Life Sci* 83(21-22): 725-731.

Gonzalez-Periz, A. and Claria, J. (2007). "New approaches to the modulation of the cyclooxygenase-2 and 5-lipoxygenase pathways." *Curr Top Med Chem* 7(3): 297-309.

Grant, G. E., Rokach, J. and Powell, W. S. (2009). "5-Oxo-ETE and the OXE receptor." *Prostaglandins Other Lipid Mediat* 89(3-4): 98-104.

Griffith, O. W., Bridges, R. J. and Meister, A. (1978). "Evidence that the gamma-glutamyl cycle functions in vivo using intracellular glutathione: effects of amino acids and selective inhibition of enzymes." *Proc Natl Acad Sci U S A* 75(11): 5405-5408.

Gulliksson, M., Brunnstrom, A., Johannesson, M., Backman, L., Nilsson, G., Harvima, I., Dahlen, B., Kumlin, M. and Claesson, H. E. (2007). "Expression of 15-lipoxygenase type-1 in human mast cells." *Biochim Biophys Acta* 1771(9): 1156-1165.

Gupta, S., Srivastava, M., Ahmad, N., Sakamoto, K., Bostwick, D. G. and Mukhtar, H. (2001). "Lipoxygenase-5 is overexpressed in prostate adenocarcinoma." *Cancer* 91(4): 737-743.

Half, E., Tang, X. M., Gwyn, K., Sahin, A., Wathen, K. and Sinicrope, F. A. (2002). "Cyclooxygenase-2 expression in human breast cancers and adjacent ductal carcinoma in situ." *Cancer Res* 62(6): 1676-1681.

Hamberg, M. (1998). "Stereochemistry of oxygenation of linoleic acid catalyzed by prostaglandin-endoperoxide H synthase-2." *Arch Biochem Biophys* 349(2): 376-380.

- Hammarberg, T., Provost, P., Persson, B. and Radmark, O. (2000). "The N-terminal domain of 5-lipoxygenase binds calcium and mediates calcium stimulation of enzyme activity." *J Biol Chem* 275(49): 38787-38793.
- Hampton, M. B., Kettle, A. J. and Winterbourn, C. C. (1998). "Inside the neutrophil phagosome: oxidants, myeloperoxidase, and bacterial killing." *Blood* 92(9): 3007-3017.
- Hansen-Petrik, M. B., McEntee, M. F., Jull, B., Shi, H., Zemel, M. B. and Whelan, J. (2002). "Prostaglandin E(2) protects intestinal tumors from nonsteroidal anti-inflammatory drug-induced regression in Apc(Min/+) mice." *Cancer Res* 62(2): 403-408.
- Harats, D., Ben-Shushan, D., Cohen, H., Gonen, A., Barshack, I., Goldberg, I., Greenberger, S., Hodish, I., Harari, A., Varda-Bloom, N., Levanon, K., Grossman, E., Chaitidis, P., Kuhn, H. and Shaish, A. (2005). "Inhibition of carcinogenesis in transgenic mouse models over-expressing 15-lipoxygenase in the vascular wall under the control of murine preproendothelin-1 promoter." *Cancer Lett* 229(1): 127-134.
- Harris, R. E., Beebe-Donk, J., Doss, H. and Burr Doss, D. (2005). "Aspirin, ibuprofen, and other non-steroidal anti-inflammatory drugs in cancer prevention: a critical review of non-selective COX-2 blockade (review)." *Oncol Rep* 13(4): 559-583.
- Hayes, J. D., Flanagan, J. U. and Jowsey, I. R. (2005). "Glutathione transferases." *Annu Rev Pharmacol Toxicol* 45: 51-88.
- Hecker, M. and Ullrich, V. (1989). "On the mechanism of prostacyclin and thromboxane A2 biosynthesis." *J Biol Chem* 264(1): 141-150.
- Hecker, M., Ullrich, V., Fischer, C. and Meese, C. O. (1987). "Identification of novel arachidonic acid metabolites formed by prostaglandin H synthase." *Eur J Biochem* 169(1): 113-123.
- Hedrick, C. C., Kim, M. D., Natarajan, R. D. and Nadler, J. L. (1999). "12-Lipoxygenase products increase monocyte:endothelial interactions." *Adv Exp Med Biol* 469: 455-460.
- Hennig, R., Ding, X. Z., Tong, W. G., Schneider, M. B., Standop, J., Friess, H., Buchler, M. W., Pour, P. M. and Adrian, T. E. (2002). "5-Lipoxygenase and leukotriene B(4) receptor are expressed in human pancreatic cancers but not in pancreatic ducts in normal tissue." *Am J Pathol* 161(2): 421-428.
- Hinchman, C. A. and Ballatori, N. (1994). "Glutathione conjugation and conversion to mercapturic acids can occur as an intrahepatic process." *J Toxicol Environ Health* 41(4): 387-409.
- Holla, V. R., Backlund, M. G., Yang, P., Newman, R. A. and DuBois, R. N. (2008). "Regulation of prostaglandin transporters in colorectal neoplasia." *Cancer Prev Res (Phila Pa)* 1(2): 93-99.
- Homolya, L., Varadi, A. and Sarkadi, B. (2003). "Multidrug resistance-associated proteins: Export pumps for conjugates with glutathione, glucuronate or sulfate." *Biofactors* 17(1-4): 103-114.

- Honn, K. V., Tang, D. G., Gao, X., Butovich, I. A., Liu, B., Timar, J. and Haggmann, W. (1994). "12-lipoxygenases and 12(S)-HETE: role in cancer metastasis." *Cancer Metastasis Rev* 13(3-4): 365-396.
- Hsi, L. C., Wilson, L. C. and Eling, T. E. (2002). "Opposing effects of 15-lipoxygenase-1 and -2 metabolites on MAPK signaling in prostate. Alteration in peroxisome proliferator-activated receptor gamma." *J Biol Chem* 277(43): 40549-40556.
- Hsi, L. C., Xi, X., Lotan, R., Shureiqi, I. and Lippman, S. M. (2004). "The histone deacetylase inhibitor suberoylanilide hydroxamic acid induces apoptosis via induction of 15-lipoxygenase-1 in colorectal cancer cells." *Cancer Res* 64(23): 8778-8781.
- Huang, M. T., Lysz, T., Ferraro, T., Abidi, T. F., Laskin, J. D. and Conney, A. H. (1991). "Inhibitory effects of curcumin on in vitro lipoxygenase and cyclooxygenase activities in mouse epidermis." *Cancer Res* 51(3): 813-819.
- Hughes, D., Otani, T., Yang, P., Newman, R. A., Yantiss, R. K., Altorki, N. K., Port, J. L., Yan, M., Markowitz, S. D., Mazumdar, M., Tai, H. H., Subbaramaiah, K. and Dannenberg, A. J. (2008). "NAD⁺-dependent 15-hydroxyprostaglandin dehydrogenase regulates levels of bioactive lipids in non-small cell lung cancer." *Cancer Prev Res (Phila Pa)* 1(4): 241-249.
- Huo, Y., Zhao, L., Hyman, M. C., Shashkin, P., Harry, B. L., Burcin, T., Forlow, S. B., Stark, M. A., Smith, D. F., Clarke, S., Srinivasan, S., Hedrick, C. C., Pratico, D., Witztum, J. L., Nadler, J. L., Funk, C. D. and Ley, K. (2004). "Critical role of macrophage 12/15-lipoxygenase for atherosclerosis in apolipoprotein E-deficient mice." *Circulation* 110(14): 2024-2031.
- Hwang, D., Scollard, D., Byrne, J. and Levine, E. (1998). "Expression of cyclooxygenase-1 and cyclooxygenase-2 in human breast cancer." *J Natl Cancer Inst* 90(6): 455-460.
- Ide, T., Egan, K., Bell-Parikh, L. C. and FitzGerald, G. A. (2003). "Activation of nuclear receptors by prostaglandins." *Thromb Res* 110(5-6): 311-315.
- Ischiropoulos, H., Zhu, L. and Beckman, J. S. (1992). "Peroxynitrite formation from macrophage-derived nitric oxide." *Arch Biochem Biophys* 298(2): 446-451.
- Itoh, T., Fairall, L., Amin, K., Inaba, Y., Szanto, A., Balint, B. L., Nagy, L., Yamamoto, K. and Schwabe, J. W. (2008). "Structural basis for the activation of PPARgamma by oxidized fatty acids." *Nat Struct Mol Biol* 15(9): 924-931.
- Jakobsson, P. J., Thoren, S., Morgenstern, R. and Samuelsson, B. (1999). "Identification of human prostaglandin E synthase: a microsomal, glutathione-dependent, inducible enzyme, constituting a potential novel drug target." *Proc Natl Acad Sci U S A* 96(13): 7220-7225.
- Jang, J. H. and Surh, Y. J. (2005). "Beta-amyloid-induced apoptosis is associated with cyclooxygenase-2 up-regulation via the mitogen-activated protein kinase-NF-kappaB signaling pathway." *Free Radic Biol Med* 38(12): 1604-1613.

- Ji, C., Amarnath, V., Pietenpol, J. A. and Marnett, L. J. (2001). "4-hydroxynonenal induces apoptosis via caspase-3 activation and cytochrome c release." *Chem Res Toxicol* 14(8): 1090-1096.
- Jian, W., Lee, S. H., Arora, J. S., Silva Elipse, M. V. and Blair, I. A. (2005). "Unexpected formation of etheno-2'-deoxyguanosine adducts from 5(S)-hydroperoxyeicosatetraenoic acid: evidence for a bis-hydroperoxide intermediate." *Chem Res Toxicol* 18(3): 599-610.
- Jian, W., Lee, S. H., Williams, M. V. and Blair, I. A. (2009). "5-Lipoxygenase-mediated endogenous DNA damage." *J Biol Chem* 284(25): 16799-16807.
- Jones, R., Adel-Alvarez, L. A., Alvarez, O. R., Broaddus, R. and Das, S. (2003). "Arachidonic acid and colorectal carcinogenesis." *Mol Cell Biochem* 253(1-2): 141-149.
- Kabe, Y., Ando, K., Hirao, S., Yoshida, M. and Handa, H. (2005). "Redox regulation of NF-kappaB activation: distinct redox regulation between the cytoplasm and the nucleus." *Antioxid Redox Signal* 7(3-4): 395-403.
- Kamitani, H., Geller, M. and Eling, T. (1998). "Expression of 15-lipoxygenase by human colorectal carcinoma Caco-2 cells during apoptosis and cell differentiation." *J Biol Chem* 273(34): 21569-21577.
- Karin, M. (2006). "Nuclear factor-kappaB in cancer development and progression." *Nature* 441(7092): 431-436.
- Kawamori, T., Uchiya, N., Sugimura, T. and Wakabayashi, K. (2003). "Enhancement of colon carcinogenesis by prostaglandin E2 administration." *Carcinogenesis* 24(5): 985-990.
- Kelavkar, U. P., Glasgow, W., Olson, S. J., Foster, B. A. and Shappell, S. B. (2004). "Overexpression of 12/15-lipoxygenase, an ortholog of human 15-lipoxygenase-1, in the prostate tumors of TRAMP mice." *Neoplasia* 6(6): 821-830.
- Kelavkar, U. P., Nixon, J. B., Cohen, C., Dillehay, D., Eling, T. E. and Badr, K. F. (2001). "Overexpression of 15-lipoxygenase-1 in PC-3 human prostate cancer cells increases tumorigenesis." *Carcinogenesis* 22(11): 1765-1773.
- Kim, E. H. and Surh, Y. J. (2008). "The role of 15-deoxy-delta(12,14)-prostaglandin J(2), an endogenous ligand of peroxisome proliferator-activated receptor gamma, in tumor angiogenesis." *Biochem Pharmacol* 76(11): 1544-1553.
- Kinder, M., Wei, C., Shelat, S. G., Kundu, M., Zhao, L., Blair, I. A. and Pure, E. (2010). "Hematopoietic stem cell function requires 12/15-lipoxygenase-dependent fatty acid metabolism." *Blood*.
- Kliwer, S. A., Lehmann, J. M. and Willson, T. M. (1999). "Orphan nuclear receptors: shifting endocrinology into reverse." *Science* 284(5415): 757-760.

- Kliwer, S. A., Lenhard, J. M., Willson, T. M., Patel, I., Morris, D. C. and Lehmann, J. M. (1995). "A prostaglandin J2 metabolite binds peroxisome proliferator-activated receptor gamma and promotes adipocyte differentiation." *Cell* 83(5): 813-819.
- Kockx, M. M. and Herman, A. G. (2000). "Apoptosis in atherosclerosis: beneficial or detrimental?" *Cardiovasc Res* 45(3): 736-746.
- Kruh, G. D., Zeng, H., Rea, P. A., Liu, G., Chen, Z. S., Lee, K. and Belinsky, M. G. (2001). "MRP subfamily transporters and resistance to anticancer agents." *J Bioenerg Biomembr* 33(6): 493-501.
- Kuhn, H. and Borchert, A. (2002). "Regulation of enzymatic lipid peroxidation: the interplay of peroxidizing and peroxide reducing enzymes." *Free Radic Biol Med* 33(2): 154-172.
- Kuhn, H. and Chan, L. (1997). "The role of 15-lipoxygenase in atherogenesis: pro- and antiatherogenic actions." *Curr Opin Lipidol* 8(2): 111-117.
- Kuhn, H., Heydeck, D., Hugou, I. and Gniwotta, C. (1997). "In vivo action of 15-lipoxygenase in early stages of human atherogenesis." *J Clin Invest* 99(5): 888-893.
- Kuhn, H. and O'Donnell, V. B. (2006). "Inflammation and immune regulation by 12/15-lipoxygenases." *Prog Lipid Res* 45(4): 334-356.
- Kuhn, H., Walther, M. and Kuban, R. J. (2002). "Mammalian arachidonate 15-lipoxygenases structure, function, and biological implications." *Prostaglandins Other Lipid Mediat* 68-69: 263-290.
- Ladner, J. E., Parsons, J. F., Rife, C. L., Gilliland, G. L. and Armstrong, R. N. (2004). "Parallel evolutionary pathways for glutathione transferases: structure and mechanism of the mitochondrial class kappa enzyme rGSTK1-1." *Biochemistry* 43(2): 352-361.
- Laneuville, O., Chang, M., Reddy, C. C., Corey, E. J. and Pace-Asciak, C. R. (1990). "Isozyme specificity in the conversion of hepoxilin A3 (HxA3) into a glutathionyl hepoxilin (HxA3-C) by the Yb2 subunit of rat liver glutathione S-transferase." *J Biol Chem* 265(35): 21415-21418.
- Le Bras, M., Clement, M. V., Pervaiz, S. and Brenner, C. (2005). "Reactive oxygen species and the mitochondrial signaling pathway of cell death." *Histol Histopathol* 20(1): 205-219.
- Lee, S. H. and Blair, I. A. (2007). "Targeted chiral lipidomics analysis by liquid chromatography electron capture atmospheric pressure chemical ionization mass spectrometry (LC-ECAPCI/MS)." *Methods Enzymol* 433: 159-174.
- Lee, S. H. and Blair, I. A. (2009). "Targeted chiral lipidomics analysis of bioactive eicosanoid lipids in cellular systems." *BMB Rep* 42(7): 401-410.
- Lee, S. H., Oe, T. and Blair, I. A. (2001). "Vitamin C-induced decomposition of lipid hydroperoxides to endogenous genotoxins." *Science* 292(5524): 2083-2086.

- Lee, S. H., Oe, T. and Blair, I. A. (2002). "4,5-Epoxy-2(E)-decenal-induced formation of 1,N(6)-etheno-2'-deoxyadenosine and 1,N(2)-etheno-2'-deoxyguanosine adducts." *Chem Res Toxicol* 15(3): 300-304.
- Lee, S. H., Rangiah, K., Williams, M. V., Wehr, A. Y., DuBois, R. N. and Blair, I. A. (2007). "Cyclooxygenase-2-mediated metabolism of arachidonic acid to 15-oxo-eicosatetraenoic acid by rat intestinal epithelial cells." *Chem Res Toxicol* 20(11): 1665-1675.
- Lee, S. H., Rindgen, D., Bible, R. H., Jr., Hajdu, E. and Blair, I. A. (2000). "Characterization of 2'-deoxyadenosine adducts derived from 4-oxo-2-nonenal, a novel product of lipid peroxidation." *Chem Res Toxicol* 13(7): 565-574.
- Lee, S. H., Williams, M. V., DuBois, R. N. and Blair, I. A. (2003). "Targeted lipidomics using electron capture atmospheric pressure chemical ionization mass spectrometry." *Rapid Commun Mass Spectrom* 17(19): 2168-2176.
- Lee, S. H., Williams, M. V., Dubois, R. N. and Blair, I. A. (2005). "Cyclooxygenase-2-mediated DNA damage." *J Biol Chem* 280(31): 28337-28346.
- Levine, R. L., Miller, H., Grollman, A., Ohashi, E., Ohmori, H., Masutani, C., Hanaoka, F. and Moriya, M. (2001). "Translesion DNA synthesis catalyzed by human pol eta and pol kappa across 1,N6-ethenodeoxyadenosine." *J Biol Chem* 276(22): 18717-18721.
- Levine, R. L., Yang, I. Y., Hossain, M., Pandya, G. A., Grollman, A. P. and Moriya, M. (2000). "Mutagenesis induced by a single 1,N6-ethenodeoxyadenosine adduct in human cells." *Cancer Res* 60(15): 4098-4104.
- Li, A. C., Binder, C. J., Gutierrez, A., Brown, K. K., Plotkin, C. R., Pattison, J. W., Valledor, A. F., Davis, R. A., Willson, T. M., Witztum, J. L., Palinski, W. and Glass, C. K. (2004). "Differential inhibition of macrophage foam-cell formation and atherosclerosis in mice by PPARalpha, beta/delta, and gamma." *J Clin Invest* 114(11): 1564-1576.
- Li, N., Sood, S., Wang, S., Fang, M., Wang, P., Sun, Z., Yang, C. S. and Chen, X. (2005). "Overexpression of 5-lipoxygenase and cyclooxygenase 2 in hamster and human oral cancer and chemopreventive effects of zileuton and celecoxib." *Clin Cancer Res* 11(5): 2089-2096.
- Li, Y., Zhang, J., Schopfer, F. J., Martynowski, D., Garcia-Barrio, M. T., Kovach, A., Suino-Powell, K., Baker, P. R., Freeman, B. A., Chen, Y. E. and Xu, H. E. (2008). "Molecular recognition of nitrated fatty acids by PPAR gamma." *Nat Struct Mol Biol* 15(8): 865-867.
- Lieberman, M. W., Barrios, R., Carter, B. Z., Habib, G. M., Lebovitz, R. M., Rajagopalan, S., Sepulveda, A. R., Shi, Z. Z. and Wan, D. F. (1995). "gamma-Glutamyl transpeptidase. What does the organization and expression of a multipromoter gene tell us about its functions?" *Am J Pathol* 147(5): 1175-1185.
- Limor, R., Sharon, O., Knoll, E., Many, A., Weisinger, G. and Stern, N. (2008). "Lipoxygenase-derived metabolites are regulators of peroxisome proliferator-activated receptor gamma-2 expression in human vascular smooth muscle cells." *Am J Hypertens* 21(2): 219-223.

- Liu, R. M., Hu, H., Robison, T. W. and Forman, H. J. (1996). "Differential enhancement of gamma-glutamyl transpeptidase and gamma-glutamylcysteine synthetase by tert-butylhydroquinone in rat lung epithelial L2 cells." *Am J Respir Cell Mol Biol* 14(2): 186-191.
- Liu, W., Kato, M., Akhand, A. A., Hayakawa, A., Suzuki, H., Miyata, T., Kurokawa, K., Hotta, Y., Ishikawa, N. and Nakashima, I. (2000). "4-hydroxynonenal induces a cellular redox status-related activation of the caspase cascade for apoptotic cell death." *J Cell Sci* 113 (Pt 4): 635-641.
- Lovett, B. D., Strumberg, D., Blair, I. A., Pang, S., Burden, D. A., Megonigal, M. D., Rappaport, E. F., Rebbeck, T. R., Osheroff, N., Pommier, Y. G. and Felix, C. A. (2001). "Etoposide metabolites enhance DNA topoisomerase II cleavage near leukemia-associated MLL translocation breakpoints." *Biochemistry* 40(5): 1159-1170.
- Lu, S. C. (2000). "Regulation of glutathione synthesis." *Curr Top Cell Regul* 36: 95-116.
- Mahipal, S. V., Subhashini, J., Reddy, M. C., Reddy, M. M., Anilkumar, K., Roy, K. R., Reddy, G. V. and Reddanna, P. (2007). "Effect of 15-lipoxygenase metabolites, 15-(S)-HPETE and 15-(S)-HETE on chronic myelogenous leukemia cell line K-562: reactive oxygen species (ROS) mediate caspase-dependent apoptosis." *Biochem Pharmacol* 74(2): 202-214.
- Mancini, J. A., Blood, K., Guay, J., Gordon, R., Claveau, D., Chan, C. C. and Riendeau, D. (2001). "Cloning, expression, and up-regulation of inducible rat prostaglandin e synthase during lipopolysaccharide-induced pyresis and adjuvant-induced arthritis." *J Biol Chem* 276(6): 4469-4475.
- Mangal, D., Vudathala, D., Park, J. H., Lee, S. H., Penning, T. M. and Blair, I. A. (2009). "Analysis of 7,8-dihydro-8-oxo-2'-deoxyguanosine in cellular DNA during oxidative stress." *Chem Res Toxicol* 22(5): 788-797.
- Markowitz, S. D. and Bertagnolli, M. M. (2009). "Molecular origins of cancer: Molecular basis of colorectal cancer." *N Engl J Med* 361(25): 2449-2460.
- Marks, F., Furstenberger, G. and Muller-Decker, K. (2007). "Tumor promotion as a target of cancer prevention." *Recent Results Cancer Res* 174: 37-47.
- Marra, F., DeFranco, R., Grappone, C., Parola, M., Milani, S., Leonarduzzi, G., Pastacaldi, S., Wenzel, U. O., Pinzani, M., Dianzani, M. U., Laffi, G. and Gentilini, P. (1999). "Expression of monocyte chemoattractant protein-1 precedes monocyte recruitment in a rat model of acute liver injury, and is modulated by vitamin E." *J Investig Med* 47(1): 66-75.
- Marx, N., Mach, F., Sauty, A., Leung, J. H., Sarafi, M. N., Ransohoff, R. M., Libby, P., Plutzky, J. and Luster, A. D. (2000). "Peroxisome proliferator-activated receptor-gamma activators inhibit IFN-gamma-induced expression of the T cell-active CXC chemokines IP-10, Mig, and I-TAC in human endothelial cells." *J Immunol* 164(12): 6503-6508.
- Maskrey, B. H., Bermudez-Fajardo, A., Morgan, A. H., Stewart-Jones, E., Dioszeghy, V., Taylor, G. W., Baker, P. R., Coles, B., Coffey, M. J., Kuhn, H. and O'Donnell, V. B. (2007). "Activated platelets and monocytes generate four hydroxyphosphatidylethanolamines via lipoxygenase." *J Biol Chem* 282(28): 20151-20163.

- McCord, J. M. and Edeas, M. A. (2005). "SOD, oxidative stress and human pathologies: a brief history and a future vision." *Biomed Pharmacother* 59(4): 139-142.
- McCoull, K. D., Rindgen, D., Blair, I. A. and Penning, T. M. (1999). "Synthesis and characterization of polycyclic aromatic hydrocarbon o-quinone depurinating N7-guanine adducts." *Chem Res Toxicol* 12(3): 237-246.
- McGeer, P. L., McGeer, E. G. and Yasojima, K. (2002). "Expression of COX-1 and COX-2 mRNAs in atherosclerotic plaques." *Exp Gerontol* 37(7): 925-929.
- Mehrabian, M. and Allayee, H. (2003). "5-lipoxygenase and atherosclerosis." *Curr Opin Lipidol* 14(5): 447-457.
- Meijerman, I., Beijnen, J. H. and Schellens, J. H. (2008). "Combined action and regulation of phase II enzymes and multidrug resistance proteins in multidrug resistance in cancer." *Cancer Treat Rev* 34(6): 505-520.
- Merched, A. J., Ko, K., Gotlinger, K. H., Serhan, C. N. and Chan, L. (2008). "Atherosclerosis: evidence for impairment of resolution of vascular inflammation governed by specific lipid mediators." *Faseb J* 22(10): 3595-3606.
- Mesaros, C., Lee, S. H. and Blair, I. A. (2009). "Targeted quantitative analysis of eicosanoid lipids in biological samples using liquid chromatography-tandem mass spectrometry." *J Chromatogr B Analyt Technol Biomed Life Sci* 877(26): 2736-2745.
- Middleton, M. K., Zukas, A. M., Rubinstein, T., Jacob, M., Zhu, P., Zhao, L., Blair, I. and Pure, E. (2006). "Identification of 12/15-lipoxygenase as a suppressor of myeloproliferative disease." *J Exp Med* 203(11): 2529-2540.
- Minekura, H., Kumagai, T., Kawamoto, Y., Nara, F. and Uchida, K. (2001). "4-Hydroxy-2-nonenal is a powerful endogenous inhibitor of endothelial response." *Biochem Biophys Res Commun* 282(2): 557-561.
- Morrow, J. D., Awad, J. A., Boss, H. J., Blair, I. A. and Roberts, L. J., 2nd (1992). "Non-cyclooxygenase-derived prostanoids (F2-isoprostanes) are formed in situ on phospholipids." *Proc Natl Acad Sci U S A* 89(22): 10721-10725.
- Morrow, J. D., Hill, K. E., Burk, R. F., Nammour, T. M., Badr, K. F. and Roberts, L. J., 2nd (1990). "A series of prostaglandin F2-like compounds are produced in vivo in humans by a non-cyclooxygenase, free radical-catalyzed mechanism." *Proc Natl Acad Sci U S A* 87(23): 9383-9387.
- Morrow, J. D. and Roberts, L. J., 2nd (1994). "Mass spectrometry of prostanoids: F2-isoprostanes produced by non-cyclooxygenase free radical-catalyzed mechanism." *Methods Enzymol* 233: 163-174.

- Mulcahy, R. T. and Gipp, J. J. (1995). "Identification of a putative antioxidant response element in the 5'-flanking region of the human gamma-glutamylcysteine synthetase heavy subunit gene." *Biochem Biophys Res Commun* 209(1): 227-233.
- Muro, S., Wiewrodt, R., Thomas, A., Koniaris, L., Albelda, S. M., Muzykantov, V. R. and Koval, M. (2003). "A novel endocytic pathway induced by clustering endothelial ICAM-1 or PECAM-1." *J Cell Sci* 116(Pt 8): 1599-1609.
- Murphy, R. C., Hammarstrom, S. and Samuelsson, B. (1979). "Leukotriene C: a slow-reacting substance from murine mastocytoma cells." *Proc Natl Acad Sci U S A* 76(9): 4275-4279.
- Murphy, R. C. and Zarini, S. (2002). "Glutathione adducts of oxyeicosanoids." *Prostaglandins Other Lipid Mediat* 68-69: 471-482.
- Mutoh, M., Watanabe, K., Kitamura, T., Shoji, Y., Takahashi, M., Kawamori, T., Tani, K., Kobayashi, M., Maruyama, T., Kobayashi, K., Ohuchida, S., Sugimoto, Y., Narumiya, S., Sugimura, T. and Wakabayashi, K. (2002). "Involvement of prostaglandin E receptor subtype EP(4) in colon carcinogenesis." *Cancer Res* 62(1): 28-32.
- Nair, J., Furstenberger, G., Burger, F., Marks, F. and Bartsch, H. (2000). "Promutagenic etheno-DNA adducts in multistage mouse skin carcinogenesis: correlation with lipoxygenase-catalyzed arachidonic acid metabolism." *Chem Res Toxicol* 13(8): 703-709.
- Nie, D. (2007). "Cyclooxygenases and lipoxygenases in prostate and breast cancers." *Front Biosci* 12: 1574-1585.
- Nita, D. A., Nita, V., Spulber, S., Moldovan, M., Popa, D. P., Zagrean, A. M. and Zagrean, L. (2001). "Oxidative damage following cerebral ischemia depends on reperfusion - a biochemical study in rat." *J Cell Mol Med* 5(2): 163-170.
- O'Flaherty, J. T., Cordes, J. F., Lee, S. L., Samuel, M. and Thomas, M. J. (1994). "Chemical and biological characterization of oxo-eicosatetraenoic acids." *Biochim Biophys Acta* 1201(3): 505-515.
- O'Flaherty, J. T., Rogers, L. C., Paumi, C. M., Hantgan, R. R., Thomas, L. R., Clay, C. E., High, K., Chen, Y. Q., Willingham, M. C., Smitherman, P. K., Kute, T. E., Rao, A., Cramer, S. D. and Morrow, C. S. (2005). "5-Oxo-ETE analogs and the proliferation of cancer cells." *Biochim Biophys Acta* 1736(3): 228-236.
- O'Reilly, M. S., Holmgren, L., Shing, Y., Chen, C., Rosenthal, R. A., Cao, Y., Moses, M., Lane, W. S., Sage, E. H. and Folkman, J. (1994). "Angiostatin: a circulating endothelial cell inhibitor that suppresses angiogenesis and tumor growth." *Cold Spring Harb Symp Quant Biol* 59: 471-482.
- Oe, T., Arora, J. S., Lee, S. H. and Blair, I. A. (2003). "A novel lipid hydroperoxide-derived cyclic covalent modification to histone H4." *J Biol Chem* 278(43): 42098-42105.

- Okada, K., Wangpoengtrakul, C., Osawa, T., Toyokuni, S., Tanaka, K. and Uchida, K. (1999). "4-Hydroxy-2-nonenal-mediated impairment of intracellular proteolysis during oxidative stress. Identification of proteasomes as target molecules." *J Biol Chem* 274(34): 23787-23793.
- Ondrey, F. (2009). "Peroxisome proliferator-activated receptor gamma pathway targeting in carcinogenesis: implications for chemoprevention." *Clin Cancer Res* 15(1): 2-8.
- Ozer, M. K., Parlakpınar, H., Cigremis, Y., Ucar, M., Vardi, N. and Acet, A. (2005). "Ischemia-reperfusion leads to depletion of glutathione content and augmentation of malondialdehyde production in the rat heart from overproduction of oxidants: can caffeic acid phenethyl ester (CAPE) protect the heart?" *Mol Cell Biochem* 273(1-2): 169-175.
- Pace-Asciak, C. R., Laneuville, O., Chang, M., Reddy, C. C., Su, W. G. and Corey, E. J. (1989). "New products in the hepxilin pathway: isolation of 11-glutathionyl hepxilin A3 through reaction of hepxilin A3 with glutathione S-transferase." *Biochem Biophys Res Commun* 163(3): 1230-1234.
- Palinski, W., Rosenfeld, M. E., Yla-Herttuala, S., Gurtner, G. C., Socher, S. S., Butler, S. W., Parthasarathy, S., Carew, T. E., Steinberg, D. and Witztum, J. L. (1989). "Low density lipoprotein undergoes oxidative modification in vivo." *Proc Natl Acad Sci U S A* 86(4): 1372-1376.
- Pathak, S. K., Sharma, R. A., Steward, W. P., Mellon, J. K., Griffiths, T. R. and Gescher, A. J. (2005). "Oxidative stress and cyclooxygenase activity in prostate carcinogenesis: targets for chemopreventive strategies." *Eur J Cancer* 41(1): 61-70.
- Penning, T. M. and Byrns, M. C. (2009). "Steroid hormone transforming aldo-keto reductases and cancer." *Ann N Y Acad Sci* 1155: 33-42.
- Penning, T. M. and Lerman, C. (2008). "Genomics of smoking exposure and cessation: lessons for cancer prevention and treatment." *Cancer Prev Res (Phila Pa)* 1(2): 80-83.
- Peters-Golden, M. and Brock, T. G. (2001). "Intracellular compartmentalization of leukotriene synthesis: unexpected nuclear secrets." *FEBS Lett* 487(3): 323-326.
- Pham, H., Chen, M., Li, A., King, J., Angst, E., Dawson, D. W., Park, J., Reber, H. A., Hines, O. J. and Eibl, G. (2010). "Loss of 15-hydroxyprostaglandin dehydrogenase increases prostaglandin E2 in pancreatic tumors." *Pancreas* 39(3): 332-339.
- Pompella, A., Corti, A., Paolicchi, A., Giommarelli, C. and Zunino, F. (2007). "Gamma-glutamyltransferase, redox regulation and cancer drug resistance." *Curr Opin Pharmacol* 7(4): 360-366.
- Porter, N. A., Caldwell, S. E. and Mills, K. A. (1995). "Mechanisms of free radical oxidation of unsaturated lipids." *Lipids* 30(4): 277-290.
- Powell, W. S. and Rokach, J. (2005). "Biochemistry, biology and chemistry of the 5-lipoxygenase product 5-oxo-ETE." *Prog Lipid Res* 44(2-3): 154-183.

- Pratico, D., Barry, O. P., Lawson, J. A., Adiyaman, M., Hwang, S. W., Khanapure, S. P., Iuliano, L., Rokach, J. and FitzGerald, G. A. (1998). "IPF2alpha-I: an index of lipid peroxidation in humans." *Proc Natl Acad Sci U S A* 95(7): 3449-3454.
- Pratico, D., Iuliano, L., Mauriello, A., Spagnoli, L., Lawson, J. A., Rokach, J., Maclouf, J., Violi, F. and FitzGerald, G. A. (1997). "Localization of distinct F2-isoprostanes in human atherosclerotic lesions." *J Clin Invest* 100(8): 2028-2034.
- Pratico, D., Rokach, J., Lawson, J. and FitzGerald, G. A. (2004). "F2-isoprostanes as indices of lipid peroxidation in inflammatory diseases." *Chem Phys Lipids* 128(1-2): 165-171.
- Quidville, V., Segond, N., Lausson, S., Frenkian, M., Cohen, R. and Jullienne, A. (2006). "15-Hydroxyprostaglandin-dehydrogenase is involved in anti-proliferative effect of non-steroidal anti-inflammatory drugs COX-1 inhibitors on a human medullary thyroid carcinoma cell line." *Prostaglandins Other Lipid Mediat* 81(1-2): 14-30.
- Rae, M. T., Niven, D., Critchley, H. O., Harlow, C. R. and Hillier, S. G. (2004). "Antiinflammatory steroid action in human ovarian surface epithelial cells." *J Clin Endocrinol Metab* 89(9): 4538-4544.
- Rangachari, P. K. and Betti, P. A. (1993). "Biological activity of metabolites of PGD2 on canine proximal colon." *Am J Physiol* 264(5 Pt 1): G886-894.
- Rappa, G., Lorico, A., Flavell, R. A. and Sartorelli, A. C. (1997). "Evidence that the multidrug resistance protein (MRP) functions as a co-transporter of glutathione and natural product toxins." *Cancer Res* 57(23): 5232-5237.
- Rashid, R., Langfinger, D., Wagner, R., Schuchmann, H. P. and von Sonntag, C. (1999). "Bleomycin versus OH-radical-induced malonaldehydic-product formation in DNA." *Int J Radiat Biol* 75(1): 101-109.
- Raso, E., Dome, B., Somlai, B., Zacharek, A., Hagmann, W., Honn, K. V. and Timar, J. (2004). "Molecular identification, localization and function of platelet-type 12-lipoxygenase in human melanoma progression, under experimental and clinical conditions." *Melanoma Res* 14(4): 245-250.
- Ribatti, D. (2009). "Endogenous inhibitors of angiogenesis: a historical review." *Leuk Res* 33(5): 638-644.
- Richman, P. G. and Meister, A. (1975). "Regulation of gamma-glutamyl-cysteine synthetase by nonallosteric feedback inhibition by glutathione." *J Biol Chem* 250(4): 1422-1426.
- Ricote, M., Li, A. C., Willson, T. M., Kelly, C. J. and Glass, C. K. (1998). "The peroxisome proliferator-activated receptor-gamma is a negative regulator of macrophage activation." *Nature* 391(6662): 79-82.
- Rigas, B., Goldman, I. S. and Levine, L. (1993). "Altered eicosanoid levels in human colon cancer." *J Lab Clin Med* 122(5): 518-523.

- Rindgen, D., Lee, S. H., Nakajima, M. and Blair, I. A. (2000). "Formation of a substituted 1,N(6)-etheno-2'-deoxyadenosine adduct by lipid hydroperoxide-mediated generation of 4-oxo-2-nonenal." *Chem Res Toxicol* 13(9): 846-852.
- Rioux, N. and Castonguay, A. (1998). "Inhibitors of lipoxygenase: a new class of cancer chemopreventive agents." *Carcinogenesis* 19(8): 1393-1400.
- Ritter, C. A., Jedlitschky, G., Meyer zu Schwabedissen, H., Grube, M., Kock, K. and Kroemer, H. K. (2005). "Cellular export of drugs and signaling molecules by the ATP-binding cassette transporters MRP4 (ABCC4) and MRP5 (ABCC5)." *Drug Metab Rev* 37(1): 253-278.
- Rittner, H. L., Hafner, V., Klimiuk, P. A., Szweda, L. I., Goronzy, J. J. and Weyand, C. M. (1999). "Aldose reductase functions as a detoxification system for lipid peroxidation products in vasculitis." *J Clin Invest* 103(7): 1007-1013.
- Robinson, A., Huttley, G. A., Booth, H. S. and Board, P. G. (2004). "Modelling and bioinformatics studies of the human Kappa-class glutathione transferase predict a novel third glutathione transferase family with similarity to prokaryotic 2-hydroxychromene-2-carboxylate isomerases." *Biochem J* 379(Pt 3): 541-552.
- Rosenfeld, M. E., Palinski, W., Yla-Herttuala, S., Butler, S. and Witztum, J. L. (1990). "Distribution of oxidation specific lipid-protein adducts and apolipoprotein B in atherosclerotic lesions of varying severity from WHHL rabbits." *Arteriosclerosis* 10(3): 336-349.
- Rossi, A., Kapahi, P., Natoli, G., Takahashi, T., Chen, Y., Karin, M. and Santoro, M. G. (2000). "Anti-inflammatory cyclopentenone prostaglandins are direct inhibitors of I κ B kinase." *Nature* 403(6765): 103-108.
- Ruef, J., Moser, M., Bode, C., Kubler, W. and Runge, M. S. (2001). "4-hydroxynonenal induces apoptosis, NF-kappaB-activation and formation of 8-isoprostane in vascular smooth muscle cells." *Basic Res Cardiol* 96(2): 143-150.
- Salomon, R. G., Kaur, K., Podrez, E., Hoff, H. F., Krushinsky, A. V. and Sayre, L. M. (2000). "HNE-derived 2-pentylpyrroles are generated during oxidation of LDL, are more prevalent in blood plasma from patients with renal disease or atherosclerosis, and are present in atherosclerotic plaques." *Chem Res Toxicol* 13(7): 557-564.
- Schafer, F. Q. and Buettner, G. R. (2001). "Redox environment of the cell as viewed through the redox state of the glutathione disulfide/glutathione couple." *Free Radic Biol Med* 30(11): 1191-1212.
- Scher, J. U. and Pillinger, M. H. (2009). "The anti-inflammatory effects of prostaglandins." *J Invest Med* 57(6): 703-708.
- Schnurr, K., Brinckmann, R. and Kuhn, H. (1999). "Cytokine induced regulation of 15-lipoxygenase and phospholipid hydroperoxide glutathione peroxidase in mammalian cells." *Adv Exp Med Biol* 469: 75-81.

- Schopfer, F. J., Baker, P. R., Giles, G., Chumley, P., Batthyany, C., Crawford, J., Patel, R. P., Hogg, N., Branchaud, B. P., Lancaster, J. R., Jr. and Freeman, B. A. (2005). "Fatty acid transduction of nitric oxide signaling. Nitrolinoleic acid is a hydrophobically stabilized nitric oxide donor." *J Biol Chem* 280(19): 19289-19297.
- Schreinemachers, D. M. and Everson, R. B. (1994). "Aspirin use and lung, colon, and breast cancer incidence in a prospective study." *Epidemiology* 5(2): 138-146.
- Seckl, J. R. (1997). "11beta-Hydroxysteroid dehydrogenase in the brain: a novel regulator of glucocorticoid action?" *Front Neuroendocrinol* 18(1): 49-99.
- Seckl, J. R. and Walker, B. R. (2001). "Minireview: 11beta-hydroxysteroid dehydrogenase type 1- a tissue-specific amplifier of glucocorticoid action." *Endocrinology* 142(4): 1371-1376.
- Segui, J., Gironella, M., Sans, M., Granell, S., Gil, F., Gimeno, M., Coronel, P., Pique, J. M. and Panes, J. (2004). "Superoxide dismutase ameliorates TNBS-induced colitis by reducing oxidative stress, adhesion molecule expression, and leukocyte recruitment into the inflamed intestine." *J Leukoc Biol* 76(3): 537-544.
- Serhan, C. N., Chiang, N. and Van Dyke, T. E. (2008). "Resolving inflammation: dual anti-inflammatory and pro-resolution lipid mediators." *Nat Rev Immunol* 8(5): 349-361.
- Shannon, V. R., Stenson, W. F. and Holtzman, M. J. (1993). "Induction of epithelial arachidonate 12-lipoxygenase at active sites of inflammatory bowel disease." *Am J Physiol* 264(1 Pt 1): G104-111.
- Sharma, R. A., Gescher, A., Plastaras, J. P., Leuratti, C., Singh, R., Gallacher-Horley, B., Offord, E., Marnett, L. J., Steward, W. P. and Plummer, S. M. (2001). "Cyclooxygenase-2, malondialdehyde and pyrimidopurinone adducts of deoxyguanosine in human colon cells." *Carcinogenesis* 22(9): 1557-1560.
- Shen, J., Herderick, E., Cornhill, J. F., Zsigmond, E., Kim, H. S., Kuhn, H., Guevara, N. V. and Chan, L. (1996). "Macrophage-mediated 15-lipoxygenase expression protects against atherosclerosis development." *J Clin Invest* 98(10): 2201-2208.
- Shureiqi, I., Jiang, W., Zuo, X., Wu, Y., Stimmel, J. B., Leesnitzer, L. M., Morris, J. S., Fan, H. Z., Fischer, S. M. and Lippman, S. M. (2003). "The 15-lipoxygenase-1 product 13-S-hydroxyoctadecadienoic acid down-regulates PPAR-delta to induce apoptosis in colorectal cancer cells." *Proc Natl Acad Sci U S A* 100(17): 9968-9973.
- Shureiqi, I., Wojno, K. J., Poore, J. A., Reddy, R. G., Moussalli, M. J., Spindler, S. A., Greenson, J. K., Normolle, D., Hasan, A. A., Lawrence, T. S. and Brenner, D. E. (1999). "Decreased 13-S-hydroxyoctadecadienoic acid levels and 15-lipoxygenase-1 expression in human colon cancers." *Carcinogenesis* 20(10): 1985-1995.
- Siems, W. and Grune, T. (2003). "Intracellular metabolism of 4-hydroxynonenal." *Mol Aspects Med* 24(4-5): 167-175.

- Six, D. A. and Dennis, E. A. (2000). "The expanding superfamily of phospholipase A(2) enzymes: classification and characterization." *Biochim Biophys Acta* 1488(1-2): 1-19.
- Smith, W. L., DeWitt, D. L. and Garavito, R. M. (2000). "Cyclooxygenases: structural, cellular, and molecular biology." *Annu Rev Biochem* 69: 145-182.
- Smyth, E. M., Grosser, T., Wang, M., Yu, Y. and FitzGerald, G. A. (2009). "Prostanoids in health and disease." *J Lipid Res* 50 Suppl: S423-428.
- Sonoshita, M., Takaku, K., Sasaki, N., Sugimoto, Y., Ushikubi, F., Narumiya, S., Oshima, M. and Taketo, M. M. (2001). "Acceleration of intestinal polyposis through prostaglandin receptor EP2 in Apc(Delta 716) knockout mice." *Nat Med* 7(9): 1048-1051.
- Sozzani, S., Zhou, D., Locati, M., Bernasconi, S., Luini, W., Mantovani, A. and O'Flaherty, J. T. (1996). "Stimulating properties of 5-oxo-eicosanoids for human monocytes: synergism with monocyte chemotactic protein-1 and -3." *J Immunol* 157(10): 4664-4671.
- Spanbroek, R., Grabner, R., Lotzer, K., Hildner, M., Urbach, A., Ruhling, K., Moos, M. P., Kaiser, B., Cohnert, T. U., Wahlers, T., Zieske, A., Plenz, G., Robenek, H., Salbach, P., Kuhn, H., Radmark, O., Samuelsson, B. and Habenicht, A. J. (2003). "Expanding expression of the 5-lipoxygenase pathway within the arterial wall during human atherogenesis." *Proc Natl Acad Sci U S A* 100(3): 1238-1243.
- Spiteller, G. (2001). "Lipid peroxidation in aging and age-dependent diseases." *Exp Gerontol* 36(9): 1425-1457.
- Stamler, J. S., Singel, D. J. and Loscalzo, J. (1992). "Biochemistry of nitric oxide and its redox-activated forms." *Science* 258(5090): 1898-1902.
- Steele, V. E., Holmes, C. A., Hawk, E. T., Kopelovich, L., Lubet, R. A., Crowell, J. A., Sigman, C. C. and Kelloff, G. J. (1999). "Lipoxygenase inhibitors as potential cancer chemopreventives." *Cancer Epidemiol Biomarkers Prev* 8(5): 467-483.
- Steinberg, D., Parthasarathy, S., Carew, T. E., Khoo, J. C. and Witztum, J. L. (1989). "Beyond cholesterol. Modifications of low-density lipoprotein that increase its atherogenicity." *N Engl J Med* 320(14): 915-924.
- Straus, D. S., Pascual, G., Li, M., Welch, J. S., Ricote, M., Hsiang, C. H., Sengchanthalangsy, L. L., Ghosh, G. and Glass, C. K. (2000). "15-deoxy-delta 12,14-prostaglandin J2 inhibits multiple steps in the NF-kappa B signaling pathway." *Proc Natl Acad Sci U S A* 97(9): 4844-4849.
- Suzuki, H. and Sugiyama, Y. (1998). "Excretion of GSSG and glutathione conjugates mediated by MRP1 and cMOAT/MRP2." *Semin Liver Dis* 18(4): 359-376.
- Tai, H. H., Tong, M. and Ding, Y. (2007). "15-hydroxyprostaglandin dehydrogenase (15-PGDH) and lung cancer." *Prostaglandins Other Lipid Mediat* 83(3): 203-208.
- Tanabe, T. and Tohnai, N. (2002). "Cyclooxygenase isozymes and their gene structures and expression." *Prostaglandins Other Lipid Mediat* 68-69: 95-114.

- Tanaka, T., Kondo, S., Iwasa, Y., Hiai, H. and Toyokuni, S. (2000). "Expression of stress-response and cell proliferation genes in renal cell carcinoma induced by oxidative stress." *Am J Pathol* 156(6): 2149-2157.
- Thiel, A., Ganesan, A., Mrena, J., Junnila, S., Nykanen, A., Hemmes, A., Tai, H. H., Monni, O., Kokkola, A., Haglund, C., Petrova, T. V. and Ristimaki, A. (2009). "15-hydroxyprostaglandin dehydrogenase is down-regulated in gastric cancer." *Clin Cancer Res* 15(14): 4572-4580.
- Thun, M. J. (1996). "NSAID use and decreased risk of gastrointestinal cancers." *Gastroenterol Clin North Am* 25(2): 333-348.
- Thun, M. J., Henley, S. J. and Patrono, C. (2002). "Nonsteroidal anti-inflammatory drugs as anticancer agents: mechanistic, pharmacologic, and clinical issues." *J Natl Cancer Inst* 94(4): 252-266.
- Thun, M. J., Namboodiri, M. M. and Heath, C. W., Jr. (1991). "Aspirin use and reduced risk of fatal colon cancer." *N Engl J Med* 325(23): 1593-1596.
- Thuresson, E. D., Lakkides, K. M. and Smith, W. L. (2002). "PGG2, 11R-HPETE and 15R/S-HPETE are formed from different conformers of arachidonic acid in the prostaglandin endoperoxide H synthase-1 cyclooxygenase site." *Adv Exp Med Biol* 507: 67-72.
- Tontonoz, P., Nagy, L., Alvarez, J. G., Thomazy, V. A. and Evans, R. M. (1998). "PPARgamma promotes monocyte/macrophage differentiation and uptake of oxidized LDL." *Cell* 93(2): 241-252.
- Tseng-Rogenski, S., Gee, J., Ignatoski, K. W., Kunju, L. P., Bucheit, A., Kintner, H. J., Morris, D., Tallman, C., Evron, J., Wood, C. G., Grossman, H. B., Lee, C. T. and Liebert, M. (2010). "Loss of 15-hydroxyprostaglandin dehydrogenase expression contributes to bladder cancer progression." *Am J Pathol* 176(3): 1462-1468.
- Tuomisto, T. T., Korkeela, A., Rutanen, J., Viita, H., Brasen, J. H., Riekkinen, M. S., Rissanen, T. T., Karkola, K., Kiraly, Z., Kolble, K. and Yla-Herttuala, S. (2003). "Gene expression in macrophage-rich inflammatory cell infiltrates in human atherosclerotic lesions as studied by laser microdissection and DNA array: overexpression of HMG-CoA reductase, colony stimulating factor receptors, CD11A/CD18 integrins, and interleukin receptors." *Arterioscler Thromb Vasc Biol* 23(12): 2235-2240.
- Turrens, J. F. (1997). "Superoxide production by the mitochondrial respiratory chain." *Biosci Rep* 17(1): 3-8.
- Viita, H., Markkanen, J., Eriksson, E., Nurminen, M., Kinnunen, K., Babu, M., Heikura, T., Turpeinen, S., Laidinen, S., Takalo, T. and Yla-Herttuala, S. (2008). "15-lipoxygenase-1 prevents vascular endothelial growth factor A- and placental growth factor-induced angiogenic effects in rabbit skeletal muscles via reduction in growth factor mRNA levels, NO bioactivity, and downregulation of VEGF receptor 2 expression." *Circ Res* 102(2): 177-184.

- Volkel, W., Alvarez-Sanchez, R., Weick, I., Mally, A., Dekant, W. and Pahler, A. (2005). "Glutathione conjugates of 4-hydroxy-2(E)-nonenal as biomarkers of hepatic oxidative stress-induced lipid peroxidation in rats." *Free Radic Biol Med* 38(11): 1526-1536.
- Waddell, W. R., Ganser, G. F., Cerise, E. J. and Loughry, R. W. (1989). "Sulindac for polyposis of the colon." *Am J Surg* 157(1): 175-179.
- Waddington, E., Sienuarine, K., Puddey, I. and Croft, K. (2001). "Identification and quantitation of unique fatty acid oxidation products in human atherosclerotic plaque using high-performance liquid chromatography." *Anal Biochem* 292(2): 234-244.
- Waku, T., Shiraki, T., Oyama, T., Fujimoto, Y., Maebara, K., Kamiya, N., Jingami, H. and Morikawa, K. (2009). "Structural insight into PPAR γ activation through covalent modification with endogenous fatty acids." *J Mol Biol* 385(1): 188-199.
- Walther, M., Wiesner, R. and Kuhn, H. (2004). "Investigations into calcium-dependent membrane association of 15-lipoxygenase-1. Mechanistic roles of surface-exposed hydrophobic amino acids and calcium." *J Biol Chem* 279(5): 3717-3725.
- Wang, D. and Dubois, R. N. (2006). "Prostaglandins and cancer." *Gut* 55(1): 115-122.
- Wang, D. and DuBois, R. N. (2007). "Measurement of eicosanoids in cancer tissues." *Methods Enzymol* 433: 27-50.
- Wang, D. and Dubois, R. N. (2010). "Eicosanoids and cancer." *Nat Rev Cancer* 10(3): 181-193.
- Wang, D. and Dubois, R. N. (2010). "The role of COX-2 in intestinal inflammation and colorectal cancer." *Oncogene* 29(6): 781-788.
- Wang, D., Wang, H., Shi, Q., Katkuri, S., Walhi, W., Desvergne, B., Das, S. K., Dey, S. K. and DuBois, R. N. (2004). "Prostaglandin E(2) promotes colorectal adenoma growth via transactivation of the nuclear peroxisome proliferator-activated receptor delta." *Cancer Cell* 6(3): 285-295.
- Wang, M. T., Honn, K. V. and Nie, D. (2007). "Cyclooxygenases, prostanoids, and tumor progression." *Cancer Metastasis Rev* 26(3-4): 525-534.
- Ward, C., Dransfield, I., Murray, J., Farrow, S. N., Haslett, C. and Rossi, A. G. (2002). "Prostaglandin D2 and its metabolites induce caspase-dependent granulocyte apoptosis that is mediated via inhibition of I kappa B alpha degradation using a peroxisome proliferator-activated receptor-gamma-independent mechanism." *J Immunol* 168(12): 6232-6243.
- Warner, D. S., Sheng, H. and Batinic-Haberle, I. (2004). "Oxidants, antioxidants and the ischemic brain." *J Exp Biol* 207(Pt 18): 3221-3231.
- Watanabe, K., Kawamori, T., Nakatsugi, S., Ohta, T., Ohuchida, S., Yamamoto, H., Maruyama, T., Kondo, K., Ushikubi, F., Narumiya, S., Sugimura, T. and Wakabayashi, K. (1999). "Role of the prostaglandin E receptor subtype EP1 in colon carcinogenesis." *Cancer Res* 59(20): 5093-5096.

- Wei, C., Zhu, P., Shah, S. J. and Blair, I. A. (2009). "15-oxo-Eicosatetraenoic acid, a metabolite of macrophage 15-hydroxyprostaglandin dehydrogenase that inhibits endothelial cell proliferation." *Mol Pharmacol* 76(3): 516-525.
- Weibel, G. L., Joshi, M. R., Alexander, E. T., Zhu, P., Blair, I. A. and Rothblat, G. H. (2009). "Overexpression of human 15(S)-lipoxygenase-1 in RAW macrophages leads to increased cholesterol mobilization and reverse cholesterol transport." *Arterioscler Thromb Vasc Biol* 29(6): 837-842.
- Weibel, G. L., Joshi, M. R., Wei, C., Bates, S. R., Blair, I. A. and Rothblat, G. H. (2009). "15(S)-Lipoxygenase-1 associates with neutral lipid droplets in macrophage foam cells: evidence of lipid droplet metabolism." *J Lipid Res* 50(12): 2371-2376.
- Werz, O. (2002). "5-lipoxygenase: cellular biology and molecular pharmacology." *Curr Drug Targets Inflamm Allergy* 1(1): 23-44.
- Wild, A. C. and Mulcahy, R. T. (2000). "Regulation of gamma-glutamylcysteine synthetase subunit gene expression: insights into transcriptional control of antioxidant defenses." *Free Radic Res* 32(4): 281-301.
- Williams, C. S. and DuBois, R. N. (1996). "Prostaglandin endoperoxide synthase: why two isoforms?" *Am J Physiol* 270(3 Pt 1): G393-400.
- Williams, M. V., Lee, S. H. and Blair, I. A. (2005). "Liquid chromatography/mass spectrometry analysis of bifunctional electrophiles and DNA adducts from vitamin C mediated decomposition of 15-hydroperoxyeicosatetraenoic acid." *Rapid Commun Mass Spectrom* 19(6): 849-858.
- Williams, M. V., Lee, S. H., Pollack, M. and Blair, I. A. (2006). "Endogenous lipid hydroperoxide-mediated DNA-adduct formation in min mice." *J Biol Chem* 281(15): 10127-10133.
- Wittwer, J. and Hersberger, M. (2007). "The two faces of the 15-lipoxygenase in atherosclerosis." *Prostaglandins Leukot Essent Fatty Acids* 77(2): 67-77.
- Wolff, H., Saukkonen, K., Anttila, S., Karjalainen, A., Vainio, H. and Ristimäki, A. (1998). "Expression of cyclooxygenase-2 in human lung carcinoma." *Cancer Res* 58(22): 4997-5001.
- Woods, J. W., Evans, J. F., Ethier, D., Scott, S., Vickers, P. J., Hearn, L., Heibin, J. A., Charleson, S. and Singer, II (1993). "5-lipoxygenase and 5-lipoxygenase-activating protein are localized in the nuclear envelope of activated human leukocytes." *J Exp Med* 178(6): 1935-1946.
- Xin, X., Yang, S., Kowalski, J. and Gerritsen, M. E. (1999). "Peroxisome proliferator-activated receptor gamma ligands are potent inhibitors of angiogenesis in vitro and in vivo." *J Biol Chem* 274(13): 9116-9121.
- Yang, Y., Sharma, R., Sharma, A., Awasthi, S. and Awasthi, Y. C. (2003). "Lipid peroxidation and cell cycle signaling: 4-hydroxynonenal, a key molecule in stress mediated signaling." *Acta Biochim Pol* 50(2): 319-336.

Yla-Herttuala, S., Palinski, W., Rosenfeld, M. E., Parthasarathy, S., Carew, T. E., Butler, S., Witztum, J. L. and Steinberg, D. (1989). "Evidence for the presence of oxidatively modified low density lipoprotein in atherosclerotic lesions of rabbit and man." *J Clin Invest* 84(4): 1086-1095.

Yla-Herttuala, S., Rosenfeld, M. E., Parthasarathy, S., Glass, C. K., Sigal, E., Witztum, J. L. and Steinberg, D. (1990). "Colocalization of 15-lipoxygenase mRNA and protein with epitopes of oxidized low density lipoprotein in macrophage-rich areas of atherosclerotic lesions." *Proc Natl Acad Sci U S A* 87(18): 6959-6963.

Yocum, A. K., Oe, T., Yergey, A. L. and Blair, I. A. (2005). "Novel lipid hydroperoxide-derived hemoglobin histidine adducts as biomarkers of oxidative stress." *J Mass Spectrom* 40(6): 754-764.

Yuan, H., Li, M. Y., Ma, L. T., Hsin, M. K., Mok, T. S., Underwood, M. J. and Chen, G. G. (2010). "15-Lipoxygenases and its metabolites 15(S)-HETE and 13(S)-HODE in the development of non-small cell lung cancer." *Thorax* 65(4): 321-326.

Zarini, S. and Murphy, R. C. (2003). "Biosynthesis of 5-oxo-6,8,11,14-eicosatetraenoic acid from 5-hydroperoxyeicosatetraenoic acid in the murine macrophage." *J Biol Chem* 278(13): 11190-11196.

Zhang, B., Cao, H. and Rao, G. N. (2005). "15(S)-hydroxyeicosatetraenoic acid induces angiogenesis via activation of PI3K-Akt-mTOR-S6K1 signaling." *Cancer Res* 65(16): 7283-7291.

Zhang, H. and Sun, X. F. (2002). "Overexpression of cyclooxygenase-2 correlates with advanced stages of colorectal cancer." *Am J Gastroenterol* 97(4): 1037-1041.

Zhang, M. Z., Xu, J., Yao, B., Yin, H., Cai, Q., Shrubsole, M. J., Chen, X., Kon, V., Zheng, W., Pozzi, A. and Harris, R. C. (2009). "Inhibition of 11beta-hydroxysteroid dehydrogenase type II selectively blocks the tumor COX-2 pathway and suppresses colon carcinogenesis in mice and humans." *J Clin Invest* 119(4): 876-885.

Zhou, X., Taghizadeh, K. and Dedon, P. C. (2005). "Chemical and biological evidence for base propenals as the major source of the endogenous M1dG adduct in cellular DNA." *J Biol Chem* 280(27): 25377-25382.

Zhu, P., Oe, T. and Blair, I. A. (2008). "Determination of cellular redox status by stable isotope dilution liquid chromatography/mass spectrometry analysis of glutathione and glutathione disulfide." *Rapid Commun Mass Spectrom* 22(4): 432-440.